Beyond The Standard Model Physics: Grand Unification & Otherwise

A THESIS

submitted for the Award of Ph.D. degree of

MOHANLAL SUKHADIA UNIVERSITY

BY

Ketankumar Patel

FACULTY OF SCIENCE

MOHANLAL SUKHADIA UNIVERSITY

UDAIPUR

Year of submission: 2011

There is a fine line between wrong & visionary.
Unfortunately, one has to be a visionary to see it.

Dr. Sheldon Cooper (*fictitious character*)
[The Big Bang Theory: Season 3, Episode 04]

DECLARATION

I **Mr. Ketankumar Patel**, S/o Mr. Mohanbhai Patel, resident of C/426, Vivekanand nagar society, Maninagar, Ahmedabad 380 008, hereby declare that the research work incorporated in the present thesis entitled, **"Beyond The Standard Model Physics: Grand Unification & Otherwise"** is my own work and is original. This work (in part or in full) has not been submitted to any University for the award of a Degree or a Diploma. I have properly acknowledged the material collected from secondary sources wherever required. I solely own the responsibility for the originality of the entire content.

Date:

Ketankumar Patel

(Author)

CERTIFICATE

I feel great pleasure in certifying that the thesis entitled, **"Beyond The Standard Model Physics: Grand Unification & Otherwise"** by Mr. Ketankumar Patel under my guidance. He has completed the following requirements as per Ph.D regulations of the University.

(a) Course work as per the university rules.

(b) Residential requirements of the university.

(c) Regularly submitted six monthly progress reports.

(d) Presented his work in the departmental committee.

(e) Published minimum of one research papers in a referred research journal.

I recommend the submission of thesis.

Date:

Dr. Namit Mahajan
(Thesis Supervisor)
Reader, Theoretical Physics Division,
Physical Research Laboratory,
Ahmedabad - 380 009.

Countersigned by

Head of the Department

ACKNOWLEDGEMENTS

The work reported in this thesis has been carried out under the guidance of Prof. Anjan Joshipura. I express my most sincere and deep gratitude to him for his invaluable guidance, encouragement and support throughout the course of this work. I am immensely benefited from his insight and expertise in the subject. His enthusiasm, kind nature and positive outlook have made the years working with him pleasant and memorable. I consider myself very fortunate to have been able to work with him. I am very grateful to my thesis supervisor Dr. Namit Mahajan who has always helped me in several problems whenever I approached him. I thank him for his continuous encouragement, concerns, and very useful advises. His helps in physics and administrative formalities and his dedicated efforts in upgrading the computer facilities in the division have made my work very easy and enjoyable.

I would like to thank my collaborators Sudhir Vempati, Bhavik Kodrani, Pankaj Sharma, Stefano Morisi and Eduardo Peinado for providing me opportunities to work with them. Working with all of them was a great learning experience in my career. Especially, sharing ideas with Bhavik and Pankaj has provided me a good insight of the subject and has cleared many of my doubts. I also thank Prof. Jose Valle for arranging my visit to University of Valencia in Spain which gave me an opportunity to interact and work with his group members.

I warmly thank: Prof. Saurabh Rindani for useful comments, Prof. Utpal Sarkar for motivating me to pursue my career in high energy physics, Prof. Subhendra Mohanty, Dr. Dilip K. Ghosh, Dr. Srubabati Goswami, Dr. R. Rangarajan, Prof. P. K. Panigrahi and Dr. Dilip K. Angom for teaching useful courses, Santosh K. Singh for helping me in learning Group Theory, Bhavik for teaching me the software packages for the numerical optimization and perhaps more importantly for helping me to understand how PRL administration works, Pankaj for several useful discussions on the subject and for clarifying my doubts, Vimal for making things difficult to understand, Arvind Singh for helping me in understanding Vimal's concepts, Vineet for setting up brain teasers in lunch and tea breaks, Amzad for listening me and Vineet patiently, Suman for helping me whenever I got stuck in Linux operations, Bhaswar and Pravin for being nice companions during several trips to Udaipur, my batch mates JRF-07 for making coursework enjoyable and some of my senior and younger colleagues for sharing some memorable time with me in PRL.

The kind of support, encouragement, love, care and conducive environment that I have been receiving from my parents since I was born are something beyond acknowledgements. I must thank my younger sister for making me little organized. Finally, I am indebted to Manisha for her immense understanding and being actively involved in family even though staying away from us.

Ketan M. Patel

ABSTRACT

Grand unified theories (GUTs) which unify strong and electroweak interactions also provide a constrained and unified description of all the fermions. In particular, the renormalizable versions of GUTs based on $SO(10)$ gauge group are considered as excellent platforms to study the peculiar patterns of quark and lepton masses and mixing angles observed in nature. In this thesis, we examine many such $SO(10)$ models for their viability or otherwise in explaining all the fermion masses and mixing angles. The different $SO(10)$ models, which we study in this work, can be divided in three main categories: (i) the supersymmetric $SO(10)$ models (ii) the sypersymmetric $SO(10)$ models with flavor symmetries and (iii) the non-supersymmetric $SO(10)$ models.

First we carry out an exhaustive analysis of supersymmetric models with minimal ($10_H + \overline{126}_H$) and non-minimal ($10_H + \overline{126}_H + 120_H$) Higgs content. Extensive numerical fits to fermion masses and mixing are carried out in each case assuming dominance of type-II or type-I seesaw mechanism. We use data corresponding to different values of $\tan\beta$ and with or without appreciable finite supersymmetric threshold corrections. All the cases studied provide quite good fits if the type-I seesaw mechanism dominates. This is not the case in the minimal model based on several data sets and type-II seesaw mechanism. This can be traced to the absence of the b-τ unification at the GUT scale in these cases. In contrast, the type-II seesaw mechanism works uniformly well in all the non-minimal model. Required scale of the $B - L$ breaking is identified in each case. In the case of type-I seesaw dominance in both the minimal and non-minimal models, it is observed that the $B-L$ breaking scale inferred from neutrino masses lies closer to the GUT scale compared to the type-II seesaw mechanism.

In $SO(10)$ models, it is not clear if the exact tribimaximal mixing (TBM) among leptons would be consistent with a precise description of the quark masses and mixing. We address this question by developing a novel formalism which allows determination of most general structures of the neutrino and charged lepton mixing matrices consistent with tribimaximal mixing. These

are then integrated into an $SO(10)$ model within which detailed fits to fermion masses and mixing angles are given. It is shown that one can obtain excellent fits to all the fermion masses and quark mixing angles keeping tri-bimaximal leptonic mixing intact. Various perturbations to tri-bimaximal mixing which can arise in the model are considered and their impact on the predictions of the reactor mixing angle θ_{13} is numerically discussed.

In the second part of this thesis, we study some interesting consequences of different flavor symmetries when integrated with supersymmetric $SO(10)$ frameworks. First we integrate the μ-τ symmetry in the non-minimal supersymmetric $SO(10)$ model. This scenario is shown to lead to a generalized CP invariance of the mass matrices and vanishing CP violating phases if the Yukawa couplings are invariant under the μ-τ symmetry. Small explicit breaking of the μ-τ symmetry is then shown to provide a very good understanding of all the fermion masses and mixing. Second we propose a specific ansatz for the structure of Yukawa matrices in $SO(10)$ models which differ from its generic expectations of hierarchical neutrinos and lead to quasi degenerate neutrino masses through the type-I seesaw mechanism. Consistency of this ansatz is demonstrated through a detailed fits to fermion masses and mixing angles all of which can be explained with reasonable accuracy in a model which uses the most general Yukawa Higgs sector of $SO(10)$. The proposed ansatz is shown to follow from an extended model based on the three generations of the vector like fermions and an $O(3)$ flavour symmetry. Large neutrino mixing angles emerge as a consequence of neutrino mass degeneracy in this model. In the last section in this category, we propose a discrete symmetry $S_4 \times Z_n$ when suitably integrated with $SO(10)$ provides a viable framework to obtain an interesting empirical relation called Quark-Lepton Complementarity (QLC), namely $\theta_{12}^l \sim \pi/4 - \theta_C$. Consistency of this model is discussed through detailed analysis of fermion masses and mixing angles. The model leads to the lepton mixing matrix that is dominantly bimaximal with $\mathcal{O}(\theta_C)$ corrections related to quark mixings which generically predicts the large reactor angle $\theta_{13}^l \sim \theta_C/\sqrt{2}$.

In the last part of this thesis, we carry out a detailed study of some non-

supersymmetric $SO(10)$ models. The non-supersymmetric $SO(10)$ models with a global $U(1)_{PQ}$ symmetry lead to the similar Yukawa sum-rules predicted in the supersymmetric models. Detailed numerical fits to fermion masses and mixing are carried out in each case assuming dominance of type-II or type-I seesaw mechanism. It is shown that the minimal non-supersymmetric model with type-I seesaw dominance gives excellent fits. In the presence of a 45_H and an intermediate scale, the model can also account for the gauge coupling unification making it potentially interesting model for the complete unification. Structure of the Yukawa coupling matrices obtained numerically in this specific case is shown to follow from a very simple $U(1)$ symmetry and a Froggatt-Nielsen singlet. The non-minimal model with type-I seesaw also provides an excellent fit to entire fermion spectrum while the model with $120_H + \overline{126}_H$ fails badly in this task. It is observed that type-II seesaw dominance is disfavored in all the models because of non-unification of b quark and τ masses at the GUT scale in the absence of supersymmetry.

LIST OF PUBLICATIONS

A. Publications related to the thesis work

1. **"Fermion Masses and Mixings in a μ-τ symmetric $SO(10)$"**
   A. S. Joshipura, B. P. Kodrani and K. M. Patel
   Phys. Rev. D **79**, 115017 (2009) [arXiv:0903.2161 [hep-ph]]

2. **"Quasi-degenerate neutrinos in $SO(10)$"**
   A. S. Joshipura and K. M. Patel
   Phys. Rev. D **82** (Rapid Communication), 031701 (2010) [arXiv:1005.0045 [hep-ph]]

3. **"An $SO(10) \times S_4$ Model of Quark-Lepton Complementarity"**
   K. M. Patel
   Phys. Lett. B **695**, 225 (2011) [arXiv:1008.5061 [hep-ph]]

4. **"Fermion Masses in $SO(10)$ Models"**
   A. S. Joshipura and K. M. Patel
   Phys. Rev. D **83**, 095002 (2011) [arXiv:1102.5148 [hep-ph]]

5. **"Viability of the exact tri-bimaximal mixing at M_{GUT} in $SO(10)$"**
   A. S. Joshipura and K. M. Patel
   JHEP **1109**, 137 (2011) [arXiv:1105.5943 [hep-ph]]

B. Other Publications

1. **"Type I seesaw mechanism for quasi degenerate neutrinos"**
   A. S. Joshipura, K. M. Patel and S. K. Vempati
   Phys. Lett. B **690**, 289 (2010) [arXiv:0911.5618 [hep-ph]]

2. **"Forward-backward asymmetry in top quark production from light colored scalars in $SO(10)$ model"**
   K. M. Patel and P. Sharma
   JHEP **1104**, 085 (2011) [arXiv:1102.4736 [hep-ph]]

3. **"Model for T2K indication with maximal atmospheric angle and tri-maximal solar angle"**
   S. Morisi, K. M. Patel and E. Peinado
   Phys. Rev. D **84**, 053002 (2011) [arXiv:1107.0696 [hep-ph]]

C. Conference Proceedings

1. **"Unified description of fermion masses with quasi-degenerate neutrinos in SO(10)"**
   A. S. Joshipura and K. M. Patel
   AIP Conf. Proc. **1382**, 115 (2011)
   Presented at 12th International Workshop on Neutrino Factories, Super Beams and Beta Beams, Mumbai, India, 20-25 Oct 2010

ABBREVIATIONS

BSM	Beyond the Standard Model
CDM	Cold Dark Matter
CG	Clebsch-Gordan
CKM	Cabibbo-Kobayashi-Maskawa
EW	Electroweak
EWSB	Electroweak Symmetry Breaking
FG	Froggatt-Nielsen
GUT	Grand Unified Theory
GWS	Glashow-Weinberg-Salam
LHC	Large Hadron Collider
MSGUT	Minimal Supersymmetric $SO(10)$ Model
MSSM	Minimal Supersymmetric Standard Model
PMNS	Pontecorvo-Maki-Nakagawa-Sakata
PS	Pati-Salam
QCD	Quantum Chromodynamics
QED	Quantum Electrodynamics
QLC	Quark Lepton Complementarity
RG	Renormalization Group
RH	Right Handed
SM	Standard Model
SSB	Spontaneous Symmetry Breaking
SUSY	Supersymmetry
TBM	Tribimaximal Mixing
VEV	Vacuum Expectation Value

Contents

List of Tables

List of Figures

Chapter 1

Introduction

The last four decades or so has witnessed a tremendous advance in our understanding of the elementary particles and their interactions. One of the great triumphs of physics in these years has been the development of a theory of the strong, weak and electromagnetic interactions - the Standard Model (SM) - which is now universally accepted [1, 2, 3]. The standard model is considered to be a substantially correct and fundamental description of all interactions except gravity. Moreover, many experimental evidences like the discoveries of the charm and neutral current interactions in seventies, the direct production of the intermediate gauge bosons in the middle of eighties, discovery of top quark in the middle of nineties and the two decades of extensive precision tests have confirmed the relevance of the standard model to such an extend that it is often called the *Standard Theory* of elementary particle interactions rather than just a "model".

It is an impressive fact that the SM originated from the need to overcome the issues of the Feynman-Gellmann [4] and Sudarshan-Marshak [5] model of weak interactions formulated as a description of the physics in the hundred MeV range. However the validity of SM is not compromised even stretching the probed energy span up to the hundred GeV scale. At present, the SM is undergoing the TeV scale experimental tests through the Large Hadron Collider (LHC) at CERN. Assuming that the SM correctly describes all low-energy (*i.e.* energies that have been explored to date) physics, one must still ask whether

the SM is the entire story or whether it is just the low energy limit of a bigger theory. The difficulty with the first point of view is that the SM leaves an uncomfortable number of important questions unanswered. For example, there is no explanation or prediction of the number of elementary fields. The SM contains 19 arbitrary parameters (26 if one allows the neutrinos to have masses). Furthermore, the strong, weak and electromagnetic interactions are basically independent of each other in the SM. The attempt to understand and to answer some of these questions has led to the development of Grand Unified Theories (GUTs). The main idea behind such theory is that the observed interactions are merely the low energy manifestation of an underlying unified theory. It is possible that this underlying theory possesses additional structure that may constrain some of the quantities that appear arbitrary at the level of the SM.

A basic introduction to the main motivations behind such unified theories is the main topic of this chapter. We begin by giving a very brief overview of the SM in the next section. We particularly focus on the gauge structure of the SM and discuss the fundamental interactions allowed by it. The symmetry breaking mechanism and the origin of masses of different particles in the SM will be mentioned briefly. Few questions which remain unanswered in the SM will also be outlined. In Section 1.2, we describe the basic idea of the grand unification and discuss its advantages over the SM. Finally, the outline of the rest of the chapters in the thesis will be given in the last section.

1.1 The standard model & its limitations

The standard model is the combination of the Glashow-Weinberg-Salam (GWS) model [1, 2, 3] of electroweak interactions and the theory of strong interactions known as the Quantum Chromodynamics (QCD) developed by Fritzsch and Gell-Mann [6, 7]. The gauge group of the SM is a direct product of three different local gauge symmetries, $G_{SM} \equiv SU(3)_c \times SU(2)_L \times U(1)_Y$. The $SU(3)_c$ corresponds to the gauge symmetry which governs the strong inter-

actions while $SU(2)_L \times U(1)_Y$ is a symmetry of the electroweak interactions. The fundamental quantum fields which appear in the SM are of four types. These fields and their representations under $SU(3)_c \times SU(2)_L \times U(1)_Y$ are

	Fields	$SU(3)_c \times SU(2)_L \times U(1)_Y$ representations
Quarks	$Q_L \equiv \begin{pmatrix} u^\alpha \\ d^\alpha \end{pmatrix}_L, \begin{pmatrix} c^\alpha \\ s^\alpha \end{pmatrix}_L, \begin{pmatrix} t^\alpha \\ b^\alpha \end{pmatrix}_L$	$(3,\ 2,\ \frac{1}{3})$
	$u_R^\alpha,\ c_R^\alpha,\ t_R^\alpha$	$(3,\ 1,\ -\frac{4}{3})$
	$d_R^\alpha,\ s_R^\alpha,\ b_R^\alpha$	$(3,\ 1,\ \frac{2}{3})$
Leptons	$L_L \equiv \begin{pmatrix} \nu_e \\ e \end{pmatrix}_L, \begin{pmatrix} \nu_\mu \\ \mu \end{pmatrix}_L, \begin{pmatrix} \nu_\tau \\ \tau \end{pmatrix}_L$	$(1,\ 2,\ -1)$
	$e_R,\ \mu_R,\ \tau_R$	$(1,\ 1,\ 2)$
Gauge bosons	G_β^α (gluons)	$(8,\ 1,\ 0)$
	$W^\pm,\ W^3$	$(1,\ 3,\ 0)$
	B	$(1,\ 1,\ 0)$
Scalar	$\phi \equiv \begin{pmatrix} \varphi^0 \\ \varphi^- \end{pmatrix}$	$(1,\ 2,\ -1)$

Table 1.1: The fundamental quantum fields which appear in the standard model and their representations under the standard model gauge group $SU(3)_c \times SU(2)_L \times U(1)_Y$. The superscript $\alpha = r, g, b$ denote the color degree of freedom.

shown in Table 1.1 where $SU(2)_L$ doublets are shown in a column vector and $SU(3)_c$ triplets are indicated by the color indices $\alpha = r, g, b$. The gauge or vector bosons mediate the various interactions. The photon γ is responsible for electromagnetic interactions, while the intermediate vector bosons $W^\pm$ and Z mediate charged and neutral current weak interactions respectively (We will see later in this chapter that the γ and Z boson arise due to mixing between W^3 and B after the electroweak symmetry breaking). The strong interactions are ultimately due to the exchange of eight gluons G_α^β. The basic fermions are the leptons, or non-strongly interacting particles, and the quarks, which interact strongly and are believed to be the constituents of the hadrons. Each quark comes in three color states. The spin-0 scalar fields are introduced into the SM to break the symmetry spontaneously and to give masses to all the fermions and weak gauge bosons, $W^\pm$ and Z.

1.1.1 The $SU(3)_c \times SU(2)_L \times U(1)_Y$ theory

The fundamental interactions of all the SM fields can be described by the Lorentz invariant and renormalizable Lagrangian which is also invariant under the local gauge transformations of $SU(3)_c \times SU(2)_L \times U(1)_Y$ group. As already mentioned, such a Lagrangian can be written as a combination of the strong and electroweak interactions.

$$\mathcal{L}_{SM} \equiv \mathcal{L}_{QCD} + \mathcal{L}_{EW} \tag{1.1}$$

Let us briefly review the important features of the basic interactions described by $\mathcal{L}_{QCD}$ and $\mathcal{L}_{EW}$. The $\mathcal{L}_{QCD}$ represents the interactions of QCD which is a gauge theory based on the group $SU(3)_c$. The quark fields q^α of a definite flavor transform according to the fundamental triplet representation of $SU(3)_c$. The leptons are of course $SU(3)_c$ singlets and hence do not participate in the strong interactions. The $SU(3)_c$ has eight generators which correspond to the same number of the gauge fields G^a required for the local gauge invariance. The $SU(3)_c$ symmetry is assumed unbroken and therefore the eight gluons are massless. The QCD Lagrangian in Eq.(1.1) can be written as

$$\mathcal{L}_{QCD} = \sum_i \overline{q}_i \gamma^\mu \left(\partial_\mu - i g_s \frac{\lambda^a}{2} G^a_\mu \right) q_i - \frac{1}{4} \mathcal{G}^a_{\mu\nu} \mathcal{G}^{\mu\nu a}, \tag{1.2}$$

where $q_i = (q_i^r, q_i^g, q_i^b)$, for three colors and $i = u, c, t, d, s, b$ represents different flavors. λ^a are Gell-Mann's matrices for $SU(3)_c$ generators and $\mathcal{G}^a_{\mu\nu}$ are the field strength tensors defined as

$$\mathcal{G}^a_{\mu\nu} = \partial_\mu G^a_\nu - \partial_\nu G^a_\mu + g_s f_{abc} G^b_\mu G^c_\nu. \tag{1.3}$$

The above Lagrangian is independent of flavor and is non-chiral. The gauge coupling constant g_s determine the strength of the strong interactions between two colored quarks. In this theory, g_s has the property of asymptotic freedom [8, 9], *i.e.* $g_s(Q^2) \to 0$ for $Q^2 \to \infty$, which was confirmed in the deep inelastic scattering experiments. Here Q is the energy scale at which the experiment is

performed.

The $\mathcal{L}_{EW}$ represents the gauge theory based on the group $SU(2)_L \times U(1)$, which is also known as GWS model of electroweak interactions. Such Lagrangian is completely dictated by the requirements of gauge invariance and renormalizability and can be written as

$$\mathcal{L}_{EW} = \mathcal{L}_F + \mathcal{L}_G + \mathcal{L}_\phi - V(\phi) + \mathcal{L}_Y \tag{1.4}$$

where

$$\begin{aligned} \mathcal{L}_F &= \overline{\psi}_L \gamma^\mu \left(\partial_\mu - i\frac{g_L}{2}\tau^a W_\mu^a - i\frac{g_Y}{2}B_\mu\right)\psi_L \\ &+ \overline{\psi}_R \gamma^\mu \left(\partial_\mu - i\frac{g_Y}{2}B_\mu\right)\psi_R \end{aligned} \tag{1.5}$$

is the gauge invariant kinetic term of the fermion fields. In the above expression, the color and generation indices are suppressed and are summed over. $\psi_L \equiv Q_L, L_L$ and $\psi_R \equiv u_R, d_R, e_R$ are the left handed and right handed fermions of the SM respectively. The kinetic term for the gauge boson fields will be

$$\mathcal{L}_G = -\frac{1}{4}\mathcal{W}^{a\mu\nu}\mathcal{W}^a_{\mu\nu} - \frac{1}{4}\mathcal{B}^{\mu\nu}\mathcal{B}_{\mu\nu} \tag{1.6}$$

where $\mathcal{W}^a_{\mu\nu}$ and $\mathcal{B}_{\mu\nu}$ are field strength tensors for the vector fields of $SU(2)_L$ and $U(1)_Y$ respectively and can be defined similarly as that of $SU(3)_c$ shown in Eq. (1.3). The $\mathcal{L}_\phi$ represents the gauge invariant kinetic term of the scalar field which can be written as

$$\mathcal{L}_\phi = |\left(\partial_\mu\phi - i\frac{g_L}{2}\tau^a W_\mu^a\phi - i\frac{g_Y}{2}B_\mu\phi\right)|^2 \tag{1.7}$$

The Yukawa interactions term in the SM is

$$\mathcal{L}_Y = \sum_{i,j}\left(Y_d^{ij}\overline{Q}_{Li}\phi d_{Rj} + Y_u^{ij}\overline{Q}_{Li}\tilde{\phi}u_{Rj} + Y_l^{ij}\overline{L}_{Li}\phi e_{Rj}\right) \tag{1.8}$$

where $\tilde{\phi} = i\tau_2\phi^*$ and $i, j = 1, 2, 3$ stand for three generations of fermions. $Y^{ij}_{d,u,l}$

are complex Yukawa couplings.

Electroweak symmetry breaking and generation of the gauge boson masses

Let us briefly study the breakdown of $SU(2)_L \times U(1)_Y$ symmetry to $U(1)_{em}$, which is the only observed exact local symmetry in nature. Consider the following $SU(2)_L \times U(1)_Y$ invariant Higgs potential in Eq. (1.4)

$$V(\phi) = -\mu^2 \phi^\dagger \phi + \lambda (\phi^\dagger \phi)^2. \tag{1.9}$$

For $\mu^2 > 0$, it is easy to see that the minimum of V corresponds to

$$\langle \phi \rangle = \frac{1}{\sqrt{2}} \begin{pmatrix} 0 \\ \upsilon \end{pmatrix}, \tag{1.10}$$

where $\upsilon = \mu/\sqrt{\lambda}$. It is easily checked that

$$\frac{1}{2}(\tau_3 + Y)\langle \phi \rangle = 0, \tag{1.11}$$

which is the unbroken generator. The symmetry corresponds to this generator can be identified with the $U(1)_{em}$ and one get the following formula for the "electric charge".

$$Q = I_3 + \frac{Y}{2}. \tag{1.12}$$

It is important to note that Y is a free parameter of the theory and one can adjust it appropriately so that the electric charges of the quarks and leptons come out correctly. This becomes possible due to the fact that $\Delta Q = \Delta I_3 = 1$ for all doublets of fermions.

Since all the other electroweak generators are broken by the vacuum, the gauge bosons corresponding to those generators become massive. The masses of these generators can be obtained by substituting Eq. (1.10) in the kinetic

term (1.7) of the scalar field which leads to

$$\mathcal{L}^{W,Z}_{mass} = -\frac{1}{4}g_L^2 \upsilon^2 W^{+\mu}W^-_\mu - \frac{1}{8}\upsilon^2(g_L W_{3\mu} - g_Y B_\mu)^2. \tag{1.13}$$

This implies that

$$m_W = \frac{1}{2}g_L \upsilon, \tag{1.14}$$

and one linear combination of the two neutral gauge bosons, *i.e.*,

$$Z_\mu \equiv \frac{1}{\sqrt{g_L^2 + g_Y^2}}(g_L W_{3\mu} - g_Y B_\mu) \tag{1.15}$$

picks up the mass

$$m_Z = \frac{1}{2}\sqrt{g_L^2 + g_Y^2}\upsilon. \tag{1.16}$$

The other massless combination

$$A_\mu \equiv \frac{1}{\sqrt{g_L^2 + g_Y^2}}(g_Y W_{3\mu} + g_L B_\mu) \tag{1.17}$$

associated with the unbroken generator Q can be identified as the photon field. It can also be checked that $m_A = 0$. The gauge coupling associated with A_μ is the electric charge which can be expressed in terms of g_L and g_Y as follows.

From Eq. (1.5), the gauge interactions involving only W_3 and B vector boson can be extracted out and written as

$$\mathcal{L}_F(W_{3\mu}, Z_\mu) = \overline{\psi}_L \gamma^\mu \left(i\frac{g_L}{2}\tau^3 W^3_\mu - i\frac{g_Y}{2}B_\mu \right) \psi_L. \tag{1.18}$$

Using Eqs. (1.15) and (1.17) one can rewrite the above expression as follows:

$$\mathcal{L}_F(W_{3\mu}, Z_\mu) = \overline{\psi}_L \gamma^\mu \left(\frac{g_L^2 \tau_3/2 - (g_Y^2/2)Y}{\sqrt{g_L^2 + g_Y^2}} Z_\mu + \frac{g_L g_Y}{\sqrt{g_L^2 + g_Y^2}} Q A_\mu \right) \psi_L. \tag{1.19}$$

The first term predicts the structure of the neutral current interactions while the second term in Eq. (1.19) implies that the magnitude of the electric charge

of the positron is

$$e = \frac{g_L g_Y}{\sqrt{g_L^2 + g_Y^2}} \tag{1.20}$$

It is convenient to introduce a reparametrization of g_L and g_Y in terms of an angle θ_W (also known as the Weinberg angle) and the electric charge of the positron:

$$g_L \equiv \frac{e}{\sin\theta_W}, \tag{1.21}$$

$$g_Y \equiv \frac{e}{\cos\theta_W}. \tag{1.22}$$

$$\Rightarrow \tan\theta_W = g_Y/g_L. \tag{1.23}$$

The W- and Z- masses can be written as

$$m_W = \frac{ev}{2\sin\theta_W}, \quad m_Z = \frac{ev}{2\sin\theta_W\cos\theta_W}. \tag{1.24}$$

Using the above equations in the first term of Eq. (1.19), *i.e.* the neutral current interaction involving the Z-boson can be written as

$$\mathcal{L}_{N.C.} = -i\frac{e}{\sin\theta_W\cos\theta_W} Z_\mu \overline{\psi}_L \gamma^\mu \left(I_{3W} - \sin^2\theta_W Q\right)\psi_L. \tag{1.25}$$

From this we can read off the neutral-current interaction of any particle. This is an important prediction of the $SU(2)_L \times U(1)_Y$ model and has been confirmed to a great degree of accuracy by neutral-current experiments.

The kinetic energy term $\mathcal{L}_F$ also generates the conventional charged-current weak interactions, which has the following form:

$$\mathcal{L}_{C.C.} = -i\frac{g}{2\sqrt{2}} W_\mu^+ [\overline{u}_L \gamma^\mu d_L + \overline{\nu}_L \gamma^\mu e_L] + h.c. \tag{1.26}$$

In the above equation, the mixing between the various generations is not displayed. This will be addressed in the next paragraph.

Fermion masses and mixing

The bare mass terms for fermions violate $SU(2)_L$ gauge invariance and therefore cannot be included in the SM Lagrangian shown in Eq. (1.1). However, it is possible to generate masses for the fermions using the same Higgs field ϕ which is used to break the gauge symmetries. Recall that Eq. (1.8) enables the fermions to interact with the Higgs doublet through the gauge invariant Yukawa interactions. Subsequent to the spontaneous breakdown of the gauge symmetry, $\mathcal{L}_Y$ leads to the following mass terms for fermions:

$$\mathcal{L}^F_{mass} = \overline{d}_{Li} M^d_{ij} d_{Rj} + \overline{u}_{Li} M^u_{ij} u_{Rj} + \overline{e}_{Li} M^l_{ij} e_{Rj}, \tag{1.27}$$

where $M^f = Y^f \upsilon/\sqrt{2}$ with $f = u, d, l$ denoting the mass matrices for down- and up-quarks and charged leptons respectively. Note that neutrinos are massless and will never acquire mass in higher orders because its chiral partner ν_R does not exist in the SM and the Majorana mass term for ν_L breaks the lepton number.

The above mass matrices mix the weak eigenstates of different generations and give rise to mixing between the different flavors of up- and down-type quarks. The mass eigenstates which are the true eigenstates of the Hamiltonian can be obtained by diagonalizing the mass matrices by means of biunitary transformations:

$$U^{f\dagger}_L M^f U^f_R = M^f_{diag.} = \text{Diag.}(m_{f1}, m_{f2}, m_{f3}), \tag{1.28}$$

where m_{fi} are the masses of i^{th} generation of f-type fermion. From the above expression, the mass eigenstates denoted by f' can be written as

$$f'_{L,R} \equiv U^{f\dagger}_{L,R} f_{L,R}. \tag{1.29}$$

If we now rewrite the gauge boson interactions given in Eqs. (1.25) and (1.26) in the mass eigenstates, we find that the neutral current interaction of the Z boson remains diagonal, *i.e.* different flavors do not mix. This is an extremely

desirable feature of the SM because it implies that any neutral-current process that changes flavor can arise only at loop level and, therefore, must be suppressed. This agrees with observations such as the suppression of $K_L^0 \to \mu\overline{\mu}$ decay, $K_L - K_S$ mass difference, etc.

In the mass eigenstates, the charged-current interaction term (1.26) can be rewritten as

$$\mathcal{L}_{C.C.} = -i\frac{g}{2\sqrt{2}} W_\mu^+ \overline{u'}_L \gamma^\mu U_L^{u\dagger} U_L^d d'_L + h.c. \tag{1.30}$$

One can define

$$V_{CKM} \equiv U_L^{u\dagger} U_L^d \tag{1.31}$$

as the matrix that mixes different generations and is responsible for such phenomena as flavor changing weak processes. Such matrix is known as Cabbibo-Kobayashi-Maskawa (CKM) matrix. The V_{CKM} is a unitary matrix and in general, it can be parametrized in terms of $n(n-1)/2$ angles and $n(n+1)/2$ phases for n generations of fermions. However in the case of Dirac fermions, it is always possible to remove $2n-1$ phases by absorbing them in the fermion fields and therefore only $(n-1)(n-2)/2$ phases are physical. For example, the V_{CKM} can be parametrized in terms of 3 angles and a phase for three generations of fermions. The expression of V_{CKM} in its standard parametrization is given in Appendix A. Before we end this subsection, two important points must be noted about the mixing.

- The mixing matrices corresponding to U_R does not appear in the final theory involving flavor eigenstates.

- The left-handed mixing matrix for the charged leptons is also not observable because, in the charged current, one can redefine the neutrino states and absorb U_L^l in them. Since neutrinos are massless, all rotated basis are equivalent.

As described above, the standard model is remarkably successful in correlating all observed low-energy data in terms of a very few parameters. Moreover, all the particles predicted by the SM have been observed at particle

colliders except the Higgs boson. However most of the successes of the SM pertain only to the gauge sector of the theory where, with the help of only few parameter, numerous neutral-current data are successfully understood. But in the fermionic sector, all masses and mixing are unexplained. In the next subsection, we give a list of some of the major puzzles of the SM.

1.1.2 Problems with the standard model

Despite being the most successful theory of particle physics to date, the standard model is not perfect. There are number of questions for which the standard model does not give adequate explanations. Some of the unexplained features and unanswered questions are:

Neutrino masses and mixing

Perhaps the strongest motivation to go beyond the SM stems from the neutrino physics. In the last two decades or so, a significant amount of experimental information about neutrino masses and lepton mixing was accumulated. The solar and atmospheric neutrino anomalies found a successful theoretical description within the framework of the neutrino oscillations. The neutrino oscillations imply that neutrinos (at least two of them) are massive and they mix with each other. From the theoretical point of view, the neutrinos are strictly massless in the SM unlike other fermions. As already mentioned before, this difference arise due to the absence of the right-handed components of the neutrinos that would allow a Dirac mass term for them. The convincing evidences for neutrino mass imply that one certainly need an extension of the SM.

The flavor problem

This is one of the most unsatisfactory aspects of the SM. First of all, what dictates that the fermions must be assigned to doublets, except for a posteriori justification that it fits data? Second, why are there three generations?

Furthermore, the fermion masses and mixing angles seem to exhibit a strong hierarchical pattern. This stems from the fact that the symmetry of the model does not impose any constraints on the flavor structure of these couplings and thus there is no way to correlate the different Yukawa couplings from first principle.

The gauge problem

The pattern of groups and representations is complicated and arbitrary. For example, why should the gauge group be a direct product of three different factors which lead to three different gauge coupling constant? In a more satisfactory theory, one should have a way of not only understanding the three gauge groups but also the origin of the three gauge couplings.

The hierarchy problem

One of the problem in the SM is the so called hierarchy problem stemming from the fact that the Higgs mass is not protected by the gauge symmetry from receiving large radiative corrections from the physics at very high energies. This calls for a tremendous amount of fine-tunning order by order in the perturbation theory to make the Higgs mass stable and so the electroweak symmetry breaking scale.

Quantization of the electric charge

Electric charge is not quantized in the SM. That is, in the electric charge operator (1.12), the hypercharge assignment can be made independently for each representation. The only group theoretic constraint is that the charge differs by one unit between the fields that are associated in a doublet. However, the charges of leptons, quarks and Higgs scalars need not be related by simple factors like one or three.

In addition, the standard model does not provide an explanation of gravity. Also, it does not account for the dark matter, dark energy and matter-antimatter asymmetry found in the nature. It is obvious that one must go

beyond the SM to address these questions. The grand unified theories, to which I turn now, are motivated in part by the desire to answer some of these questions.

1.2 Grand unified theories

1.2.1 General description

One way to constrain or determine some of the features that are arbitrary in the standard model is to consider models with more symmetry. Especially promising are grand unified theories, in which the basic idea is that if $SU(3)_c \times SU(2)_L \times U(1)_Y$ is embedded in a larger underlying group G then the additional symmetries may restrict some of the features that were arbitrary in the standard model. A typical consequence of this embedding is that the new symmetry generators and their associated gauge bosons involve both flavor and color. The new interactions mediated by such gauge bosons lead to baryon number violating interaction like proton decay. However such an interaction is not found in the nature so far. The current experimental limit on the proton lifetime τ_p $(p \to \pi^0 e^+) > 8.2 \times 10^{33}$ years [10] requires that the baryon number violating interactions must be extremely weak. For models in which the proton can decay via the exchange of a single gauge boson X, the lifetime limit typically requires that $M_X > 10^{15.5}$ GeV. An unfortunate consequence of this extreme weakness is that the signature of the new interactions, other than proton decay, are beyond our experimental reach.

The most popular GUT schemes are based on the simple Lie groups which basically means that the group is not a direct product of factors. The famous examples are the groups $SU(5)$, $SO(10)$ and E_6. One can completely unify the strong and electroweak interactions in this class of GUTs. If any such theory is probed at momenta Q^2 large compared to M_X^2, where all the spontaneous symmetry breaking effects can be ignored, then the strong, weak, electromagnetic and baryon number violating interactions all look basically similar and there is a single coupling constant. Some of these GUTs also

unify the quarks and leptons which are placed together in the same representation of G. It is only for $Q < M_X^2$ that SSB becomes important and the running coupling constants g_s, g_L and g_Y become different. The strong, weak and electromagnetic interactions observed at the low energy are therefore simply the result of the pattern of SSB of the underlying gauge group G. Partial unification can also be achieved imposing for instance the Pati-Salam (PS) symmetry $SU(4)_c \times SU(2)_L \times SU(2)_R$ that treats the lepton as a "fourth color". Some other examples of such kind of symmetries are $SU(3)_c \times SU(2)_L \times SU(2)_R \times U(1)_{B-L}$ and the $SU(5) \times U(1)$. The choice of the unified gauge group is driven by the requirements of minimality and by the need of complex representations to account for chiral fermion. For example, the $SU(5)$ group has a fundamental representation $\overline{5}$ and 10-dimensional anti-symmetric representation which accommodate all the SM fermions preserving the chiral structure of the effective $SU(3)_c \times SU(2)_L \times U(1)_Y$ model. In the case of $SO(10)$, this can be achieved using its 16 dimensional irreducible spinorial representation which predicts an extra fermion per family. Similarly, E_6 has 27-dimensional representation which is chiral and it predicts extra 11 fermions per family

1.2.2 Aspects of the grand unification

As we have already discussed, the neutrinos are massless in the SM. One can extend the SM by introducing right handed neutrino which will generate the Dirac mass term ($M_D \overline{\nu}_L \nu_R$, where $M_D = Y^D v/\sqrt{2}$) for neutrinos like other fermions. However the smallness of neutrino masses cannot be understood in this way. A simplest way would be to break lepton number (or $B - L$) symmetry and add Majorana mass for the right-handed neutrino $M_R \nu_R^T C^{-1} \nu_R$. Thus both the terms lead to the Majorana neutrino mass matrix (in the basis $(\nu_L, \nu_R^c)^T$)

$$\mathcal{M} = \begin{pmatrix} 0 & M_D \\ M_D^T & M_R \end{pmatrix}. \tag{1.32}$$

In the limit $M_R \gg M_D$, the effective light neutrino masses can be given by

$$\mathcal{M}_{\nu_L} \approx -M_D M_R^{-1} M_D^T. \tag{1.33}$$

Clearly, the left handed neutrino masses are much smaller than typical charged fermion masses as long as $M_R \gg \upsilon$. This is also known as type-I seesaw mechanism [11]. Interestingly, if we take the Dirac Yukawa couplings of the order one then atmospheric neutrino data requires that $M_R \sim 10^{12-15}$ GeV. This value is very close to the conventional GUT scale of 10^{16} GeV. Hence it is possible that the seesaw mechanism naturally arises in GUTs and the small neutrino masses are consequences of heavy GUT scale in the theory. Moreover, a GUT based on $SO(10)$ gauge group automatically predicts the existence of the right handed neutrinos which makes the seesaw mechanism more plausible.

One of the interesting aspects of GUTs is a natural explanation of the fractional quark charges. In the Cartan algebra of the unified group, the electric charge operator can be identified with a combination of generators. The eigenvalues of such generators are subject to strong constraints arising from the nonabelian nature of the GUT group. For example, in the simplest $SU(5)$ GUT the electric charge operator must be traceless and thus the charges of the quarks and leptons residing in $\overline{5}$ must sum up to zero [12]. This implies that the three down-type antiquarks must equilibrate the electric charge of an electron which leads to the relation

$$3Q_{d^c} + Q_e = 0. \tag{1.34}$$

Hence GUT can address the problem of the electric charge quantization which is not answered in the SM.

Another aspect of the GUTs, which is the main theme of this thesis, is that it addresses the so called flavor problem of the SM. Such a problem arise in the SM due to the fact that each family of quarks and leptons resides in five different multiplets of $SU(3)_c \times SU(2)_L \times U(1)_Y$ and up to three independent Yukawa structures are needed to construct the masses for charged fermions as

shown in Eq. (1.8). The way this issue can be (at least partially) addresses in unified theories is clear. Since the number of different fermion representations are reduced considerably once the SM multiplets are accommodated within irreducible representations of higher symmetry group, the number of independent contractions needed to generate the Yukawa terms are smaller.

Like in the SM, GUTs neither constraints the number of fermion families nor correlate the fermions of different families. However, enhancing the communication among the multiplets in the "vertical" direction, *i.e.* within each generation of the SM multiplet, the GUTs can also lead to valuable clues on the flavor textures. For example, such correlations can arise as a consequence of various flavor symmetries acting on the generation indices of fermions. In this way, the GUTs severely restrict the structure of the "horizontal" symmetries.

In some GUTs, neutrino resides in the same GUT multiplet with the quarks and leptons. This provides a unique opportunity to study the structure of the seesaw mechanism(s) [11]. For example, the tight correlations among the effective Yukawa couplings of quarks and leptons arising from the same GUT origin can give rise to nontrivial constraints on the structure of leptonic Dirac and/or Majorana mass matrices which can subsequently uncover the patterns of the parameters governing the neutrino physics. The neutrinos differ from their charged partners in mass hierarchies and also the flavor mixing patterns observed in the quark and lepton sector are widely different. Clearly, this puzzle cannot be addressed in the SM because of the fact the quarks and leptons are treated differently in the SM. However any GUT which unifies quarks and leptons must explain the origin of such differences.

The potential qualitative influence of the GUTs on the puzzle of fermion masses was known since the time when GUTs were proposed. However in the last decade, several informations obtained from the the neutrino oscillation experiments and the precision measurements of the fermion masses and mixing parameters has inspired many quantitative studies of fermion masses in the GUT models. As a result of this, for the first time we are able to test some of the GUT models using the fermion mass data. As we will see later, of

particular interest are the models based on the $SO(10)$ gauge symmetry in which neutrinos are in close connections with the charged fermions. This is the main motivation behind the studies presented in this thesis. We focus our attention on the models based on $SO(10)$ group, in particular, those which are based on the renormalizable Yukawa sector. The specific objectives of our studies are:

- To do a general analysis of different versions of $SO(10)$ GUT and examine them for their viability or otherwise in explaining all the fermion masses and mixing angles.

- To study the applications of some flavor symmetries on $SO(10)$ and its consequences on fermion masses and mixing.

- To understand and categorize ways of obtaining large mixing among leptons and small mixing between quarks in spite of the fact that both are treated identically before $SO(10)$ breaking.

- To derive the predictions for the unknown parameters in the neutrino sector like the reactor angle, CP phases and etc. in the predictive frameworks built in $SO(10)$ GUTs.

1.3 Outline of the thesis

The thesis is organized in the following manner: In the second chapter, we review some general aspects of quarks and lepton masses in grand unified theories. We first discuss the prototype GUT based on $SU(5)$ gauge symmetry. The basic features of supersymmetric $SU(5)$ model constructed using minimal choice of Higgs fields are outlined and shortcomings of the model are pointed-out in brief. The most promising GUTs based on $SO(10)$ gauge group are also discussed in the same chapter. The origin of neutrino masses through the seesaw mechanisms and their close links with charged fermion masses are outlined.

Chapter 3 is devoted to the detailed studies of fermion masses in SUSY $SO(10)$ models. The extensive analysis of fermion masses and mixing angles is carried out in the case of minimal and non-minimal SUSY $SO(10)$ models. Several observations made from such studies will be outlined. The close connections between b-τ Yukawa unification and maximal atmospheric mixing angle in case of type-II seesaw dominance are discussed at quantitative level. In Chapter 4, we investigate the possibility of obtaining the exact tri-bimaximal pattern in lepton mixing in $SO(10)$ GUTs. We first derive the most general way to obtain the exact tribimaximal mixing in any framework. Using it, we check the viability of such mixing in the context of $SO(10)$ model. All the possible origins of perturbations in such mixing pattern are also discussed.

In Chapter 5, we investigate a role of some flavor symmetries in $SO(10)$ models. Viabilities of such approaches are discussed with detailed investigations of fermion spectrum in each case. Some interesting consequences arising in $SO(10)$ models due to different flavor symmetries are discussed. Chapter 6 is devoted to the nonsupersymmetric $SO(10)$ models. We investigate different possible choices of Higgs fields available in the renormalizable versions of non-SUSY $SO(10)$ in order to obtain realistic fermion mass spectrum. Merits and demerits of each model will be discussed. We conclude our studies in Chapter 7. Finally, a set of Appendices is added for the details of technical points in the main text.

Chapter 2

Grand Unified Theories and Fermion Masses

In this chapter, we start by briefly introducing the most attractive GUTs based on $SU(5)$ and $SO(10)$ gauge group and discussing their salient features in view of the possible predictive power in Yukawa sector. The introductory discussions and few observations that we make in this chapter will be very helpful in understanding the correlations among quark and lepton masses and mixing studied in the subsequent chapters.

2.1 $SU(5)$ GUT and fermion masses

The first realistic attempt to embed the three distinct sector of the standard model in a unified framework was made by Georgi-Glashow [13] in 1974 when they proposed a simple grand unified theory based on an $SU(5)$ gauge symmetry. The theory was capable of providing an understanding of the electric charge quantization and predicted weak mixing angle θ_W in rough agreement with the contemporary experimental data. Moreover, the different multiplets accommodating the SM matter fields of each generation were embedded into just two irreducible representations of $SU(5)$. The theory turned out to be very robust and compelling. Later, it was upgraded by further theoretical and phenomenological developments, in particular, supersymmetry was invoked

[14, 15] to solve the gauge hierarchy problem and to cure the mismatch of the running gauge couplings at the GUT scale. As a results of these efforts, an interesting GUT model known as the minimal SUSY $SU(5)$ [14] has emerged which is still considered a prototype of a potentially realistic grand unified framework.

To appreciate the power of the unification idea and to explain the motivations behind even larger GUT groups in subsequent chapters, let us first discuss some of the interesting consequences of the $SU(5)$ theory paying particular attention to the masses and mixing pattern arising in the quark and lepton sectors.

2.1.1 $SU(5)$ gauge symmetry and fermion fields

$SU(5)$ is the smallest group of rank four that can unify the SM gauge group [13]. In fact, it is actually the minimal group that unifies the $SU(2)_L$ and $SU(3)_c$ of the SM and which automatically accommodates an extra $U(1)$ symmetry that can be identified as the hypercharge. Three smallest irreducible representations of $SU(5)$ are of 5 (fundamental), 10 (two-index antisymmetric) and 15 (two-index symmetric) dimensions. Their decomposition under $SU(3)_c \times SU(2)_L \times U(1)_Y$ subgroup can be written as

$$\begin{aligned} 5 &= (3,1,1/3) \oplus (1,2,-1/2) \\ 10 &= (\overline{3},1,-2/3) \oplus (3,2,1/6) \oplus (1,1,1) \\ 15 &= (6,1,-2/3) \oplus (3,2,1/6) \oplus (1,3,1) \end{aligned} \tag{2.1}$$

In the SM, we have 15 Weyl fermion fields and the most natural way to unify them would be to put them in a 15 dimensional representation of $SU(5)$. However one can see from the above decompositions that 15-plet contains color sextet and weak triplet components which rule out this possibility. Interestingly, all the SM fermions can be accommodated in $\bar{5}$ and 10 dimensional multiplets

which has correct quantum numbers. One can identify

$$\bar{5}_F \equiv \begin{pmatrix} d_r^c \\ d_g^c \\ d_b^c \\ e \\ -\nu_e \end{pmatrix}_L \quad \text{and} \quad 10_F \equiv \frac{1}{\sqrt{2}} \begin{pmatrix} 0 & u_b^c & -u_g^c & u_r & d_r \\ -u_b^c & 0 & u_r^c & u_g & d_g \\ u_g^c & -u_r^c & 0 & u_b & d_b \\ -u_r & -u_g & -u_b & 0 & e^c \\ -d_r & -d_g & -d_b & -e^c & 0 \end{pmatrix}_L \tag{2.2}$$

Note that in $\bar{5}_F$, a negative sign convention for the ν_e field is used to ensure that $(e \ -\nu_e)^T$ transforms like $(\nu_e \ e)^T$ under the subgroup $SU(2)_L$. Moreover, the position of various fields in the corresponding multiplets are dictated by the way the fundamental triplet of $SU(3)_c$ and the doublet of $SU(2)_L$ are placed in the fundamental 5-plet of $SU(5)$. In our notation, the triplet is spanned over the first three indices of 5 while the doublet resides in the remaining pair. The structure of 10_F is then obtained by inspecting the distribution of the SM quantum numbers in the antisymmetric subspace of 5×5.

Note that the quarks and leptons reside in a single multiplet of $SU(5)$ and therefore they transform among each other via gauge interactions. As result, the baryon and lepton numbers are violated in the gauge interactions mediated through the new gauge bosons. This give rise to a variety of new phenomena, as for instance the proton decay or the neutron-antineutron oscillations.

2.1.2 The Higgs sector and Yukawa interactions

The $SU(5)$ decompositions of the three different matter bilinears constructed from $\bar{5}_F$ and 10_F are:

$$\begin{aligned} \bar{5} \times \bar{5} &= \overline{10} + \overline{15}, \\ \bar{5} \times 10 &= 5 + \overline{45}, \\ 10 \times 10 &= \overline{5} + 45 + 50. \end{aligned} \tag{2.3}$$

There is no singlet in the above equation and therefore the fermion masses must be generated by the Higgs mechanism as in the SM case. Note that $\bar{5}_F$ contains only one chiral component of matter fields residing in it so the matter bilinear $\bar{5}_F \times \bar{5}_F$ cannot provide Dirac masses for the fermions. However, it can be used to generate Majorana masses for neutrinos as we will see later in details. The second term $\bar{5}_F \times 10_F$ contains both of the chiral components of the down quarks and charged leptons and thus can be used to write Yukawa interactions for these fields. Similarly, the third bilinear term $10_F \times 10_F$ can do the same job for the up-type quarks.

Restricting to the minimal choices of Higgs fields, the Dirac masses of all quarks and charged leptons can be generated by only 5-plet Higgs. In the supersymmetric version of $SU(5)$, a pair $5_H + \bar{5}_H$ is needed due to holomorphic nature of superpotential. As it can be seen from Eq. (2.3), $\bar{5}_H$ give rise to the masses of charged leptons and down-type quarks while 5_H to the up-type quarks. The relevant part of the superpotential can be written as:

$$W_Y = Y_{\bar{5}}^{ij} \bar{5}_F^i 10_F^j \bar{5}_H + Y_5^{ij} 10_F^i 10_F^j 5_H \tag{2.4}$$

where the Yukawa coupling matrix Y_5 is symmetric in generation space due to the symmetry properties of the $10_F^i 10_F^j$ bilinear term. The 5_H and $\bar{5}_H$ contains the respective MSSM Higgs doublets H^u and H^d in them which break the electroweak symmetry by acquiring a nonzero VEV. The charged fermion mass matrices generated after the symmetry breaking then read

$$M_d = M_l^T = Y_{\bar{5}} \langle \bar{5}_H \rangle; \qquad M_u = Y_5 \langle 5_H \rangle. \tag{2.5}$$

We will discuss the phenomenological implications of the above mass relations in the next subsection.

Let us now discuss the symmetry breaking pattern in $SU(5)$. It is obvious that the 5_H (or $\bar{5}_H$) is not sufficient to break $SU(5)$ symmetry down to the $SU(3)_c \times SU(2)_L \times U(1)_Y$ as there is no SM singlet in it. Since both $SU(5)$ and $SU(3)_c \times SU(2)_L \times U(1)_Y$ are rank 4 groups, the adjoint of $SU(5)$ (a 24-

dimensional multiplet) is the smallest Higgs representation that can be used for this purpose. Under the $SU(3)_c \times SU(2)_L \times U(1)_Y$, the 24_H can be decomposed as

$$24_H \;=\; (8,1,0) \oplus (1,3,0) \oplus (3,2,-5/6) \oplus (\bar{3},2,5/6) \oplus (1,1,0). \quad (2.6)$$

The (1, 1, 0) component can acquire a GUT scale VEV and can break $SU(5)$ into the $SU(3)_c \times SU(2)_L \times U(1)_Y$ group of the SM. An alternate candidate which can break $SU(5)$ in to the SM is 75-dimensional Higgs multiplet that allows for an implementation of the so-called "missing partner mechanism" addressing the generic doublet-triplet splitting problem in unified schemes [16].

As discussed here, one needs atleast two Higgs fields to break $SU(5)$ completely in to the $SU(3)_c \times U(1)_{em}$ group. Of course, more than two fields can also be used for the same purpose. However, the choice of minimum Higgs content allows one to construct a simple and predictive model which can potentially be tested on the ground of its phenomenological implications. In the next subsection, we will discuss one such model which provide a very good example of the GUT framework constructed on the basis of minimality.

2.1.3 Minimal supersymmetric $SU(5)$ model & its shortcomings

The minimal SUSY $SU(5)$ model contains the 5_H, $\bar{5}_H$ and 24_H in its Higgs content. The role of each of these fields is discussed in the previous subsection. It is also assumed that model respects the R-parity. The Higgs superpotential of the model is

$$W_H = M_5 \bar{5}_H 5_H + M_{24} 24_H 24_H + \lambda 24_H 24_H 24_H + \eta \bar{5}_H 24_H 5_H \quad (2.7)$$

and the Yukawa part is given by Eq. (2.4). There are 4 complex couplings in the Higgs superpotential, that upon redefinition of two of the Higgs fields leave 6 real parameters. In the Yukawa sector, there are 6 complex parameters in

the symmetric matrix Y_5 and 9 complex parameters in $Y_{\bar{5}}$. Not all of them are physical and one can select a basis in which $Y_{\bar{5}}$ is real and diagonal. Having done that there is no more freedom in the up-quark coupling up to a phase which can be absorbed in 5_H. Together with the gauge coupling g, there are total 21 real parameters in the minimal SUSY $SU(5)$ model. Hence it turned out to be more predictive when compared to the the MSSM in which the total number of free parameters are 26. Of course we do not count the soft SUSY terms here which can be taken universal (as generally done in the potentially realistic SUSY models).

Though the minimal SUSY $SU(5)$ model seems to be a promising candidate for the simplest realistic GUT theory, it suffers from several drawbacks that require additional assumptions and extensions. Like in the SM, neutrinos remain massless in the minimal SUSY $SU(5)$. There are three different ways to solve this problem:

1. The most straightforward solution consists in adding $SU(5)$ singlet containing the right-handed neutrino component $1_F \equiv (\nu_L)^c$ and invoking the standard Yukawa interaction and the singlet Majorana mass term:

$$W_Y \ni Y_D^{ij} \bar{5}_F^i 1_F^j 5_H + M_R^{ij} 1_F^i 1_F^j. \tag{2.8}$$

   After the electroweak symmetry breaking, such term induces the masses for neutrinos through type-I seesaw mechanism. However, the number of real physical parameters one has to add are 21 (3 in M_R + 18 in Y_D). This doubles the parameters of the minimal model.

2. Another option could be to generate neutrino masses by adding a 15-plet of Higgs which interacts with $\bar{5}_F$ through the term

$$W_Y \ni Y_\nu^{ij} \bar{5}_F^i \bar{5}_F^j 15_H \tag{2.9}$$

   This is in a complete analogy with the type-II seesaw mechanism in which the neutrino masses are generated through $SU(2)_L$ triplet Higgs. The

15_H contains the similar submultiplet (2.1) in it. In this approach, the number of new real parameters is reduced to just 12 (arise from a real symmetric Y_ν). Note that one also needs a $\overline{15}_H$ to preserve supersymmetry at the High scale.

3. The third option is to allow R-parity violating couplings like $\bar{5}_F 5_H 24_H$ [17]. However, such R-parity violating couplings introduce many new parameters in the theory and some of them lead to the very short lifetime for the proton which is phenomenologically not viable.

Clearly, any of the above extensions come with considerable number of new parameters and the total number exceeds the number of real parameters in the MSSM.

The second serious problem in the minimal SUSY $SU(5)$ is with its predictions for the fermion masses and mixing angles. As we have seen in the previous subsection, the $SU(5)$ gauge symmetry yields $M_d = M_l^T$ at the renormalizable level. This is a nontrivial prediction that the down quark and the charged lepton spectra are identical at the GUT scale. In case of the third generation this relation is nicely satisfied in terms of the b-τ Yukawa unification acquired around the GUT scale. However, to get the right prediction for y_s and y_μ one would rather need roughly $y_\mu \sim 3y_s$ at M_{GUT} while for the first generation $3y_e \sim y_d$. Therefore the light fermion masses call for an extension of the minimal $SU(5)$, either by coupling additional Higgs multiplets (45_H for example) to the matter bilinears or emphasizing the role of the nonrenormalizable terms.

Another issue of the minimal SUSY $SU(5)$ model comes from the predictions for the proton lifetime. In supersymmetric GUTs, the new colored scalars (superpartners of fermions) give rise to a set of $d = 5$ baryon and lepton number violating operators [18, 19]. This usually leads to a strong enhancement of the proton decay amplitudes in comparison to the non-SUSY models where such operators usually appear at $d = 6$ level. In the minimal SUSY $SU(5)$, $d = 5$ operators are generated upon integrating out the heavy colored triplet $H_C \equiv (3, 1, -2/3)$ ($\bar{H}_C \equiv (\bar{3}, 1, +2/3)$) residing in 5_H ($\bar{5}_H$). The structure of

the coefficients of these operators is dictated by the Yukawa interactions of 5_H and $\bar{5}_H$ with matter fermions encoded in Eq. (2.4), namely

$$W_Y \ni Y_d^{ij} d_L^{c\,i} u_L^{c\,j} \bar{H}_C + Y_d^{ij} Q_L^i L_L^j \bar{H}_C + Y_u^{ij} Q_L^i L_L^j H_C + ... \tag{2.10}$$

In this scenario, the strength of proton decay operators is typically $\sim Y_u Y_d / M_{H_C}$. As a result, these type of operators give a stringent lower bound on the proton decay lifetime of roughly $\tau_p \sim 10^{32}$ years, see for instance [18, 19] and references therein. This should be compared to the present SuperKamiokande experimental bounds [10] of roughly $\tau_p \sim 8.2 \times 10^{33}$ years. This observation often leads to the claims that the minimal SUSY $SU(5)$ is excluded [19, 20]. However, it was pointed out in [21, 22, 23] that there still can be room in the parametric space that remain compatible with experimental limits if the effective operators are invoked and/or the effects of GUT scale Yukawa mismatch are taken into account. Therefore, though the minimal SUSY $SU(5)$ is clearly in troubles with proton decay, it still cannot be excluded completely on this ground

2.1.4 Non-SUSY $SU(5)$ model with adjoint fermions

As we have just discussed, the minimal SUSY $SU(5)$ successfully leads to the gauge coupling convergence while it badly suffers due to the predictions of fast proton decay. Both these features arise in the model due to supersymmetry. On the other hand, the minimal $SU(5)$ model [13], in the absence of low energy supersymmetry, does not provide the gauge coupling unification. One need a minimal extension that care this problem and also generate the viable neutrino masses. It does not suffice to add right-handed neutrinos as they are gauge singlet and do not help in achieving the gauge coupling unification. In other words type-I seesaw fails in minimal $SU(5)$. As noted in the previous subsection, one can add 15_H scalar and generate the neutrino masses through type-II seesaw mechanism. 15_H can also contribute in the running of gauge couplings and unification can be achieved if the mass of 15_H is adjusted accordingly.

This has been studied in [24, 25] and it is shown that the constraints coming from the unification of gauge interactions (up to two-loop level) predict light scalar leptoquarks that reside in 15_H.

The other interesting possibility is to add the adjoint fermions 24_F in the minimal non-SUSY $SU(5)$ model. This cures both the unification problem and accounts for realistic neutrino mass spectrum [26, 27]. The reason for the latter is that 24_F contains both triplet and singlet fermions (see below), and thus utilizing type-III seesaw [28, 29] gives also type-I as a bonus. The 24 dimensional adjoint representation of $SU(5)$ can be decomposed under $SU(3)_c \times SU(2)_L \times U(1)_Y$ as

$$24 = (1,1,0) \oplus (1,3,0) \oplus (3,2,-5/6) \oplus (\bar{3},2,5/6) \oplus (8,1,0). \tag{2.11}$$

The type-III seesaw can be implemented using the 5_H and 24_F in the following manner. The additional Yukawa interactions arising in the model due to 24_F can be written as

$$\begin{aligned} -\mathcal{L}_Y^{\rm new} &= y_0^i \bar{5}_F^i 24_F 5_H \\ &+ \frac{1}{\Lambda}\bar{5}_F^i[y_1^i 24_F 24_H + y_2^i 24_H 24_F + y_3^i Tr(24_H 24_F)]5_H + h.c. \end{aligned} \tag{2.12}$$

Note that the higher dimensional operators are required in order to correct the charged fermion masses which otherwise lead to unwanted relation like $M_d = M_l^T$. After the $SU(5)$ breaking one obtains the following physically relevant Yukawa interactions for neutrinos with the triplet $T_F \equiv T_F^i \sigma^i$ and singlet S_F fermions.

$$-\mathcal{L}_Y^{\rm new} = L_i(y_T^i T_F + y_S^i S_F)H + \frac{1}{2} m_S S_F S_F + \frac{1}{2} m_T T_F T_F + h.c. \tag{2.13}$$

where y_T^i, y_S^i are two different linear combinations of y_0^i and $y_a^i v_{\rm GUT}/\Lambda$ (with $a = 1,2,3$), L_i are the lepton doublets and H is the SM Higgs doublet. It is clear from the above formula that besides the new appearance of the triplet fermion, the singlet fermion in 24_F acts precisely as the right-handed neutrino.

After the electroweak symmetry breaking, one obtains in the usual manner the light neutrino mass matrix upon integrating out S_F and T_F

$$m_\nu^{ij} = v^2 \left(\frac{y_T^i y_T^j}{m_T} + \frac{y_S^i y_S^j}{m_S} \right) \tag{2.14}$$

with $m_T < 1$ TeV (determined from the requirement of the gauge coupling unification) and m_S undetermined. One important prediction emerges from the above formula is that only two light neutrinos get mass. This can be understood because the Yukawas are vectors and they can be rotated away in one direction, say 3rd direction. Thus only one light neutrino effectively couples to the triplet, *i.e.* only one neutrino gets the mass through this coupling. Obviously, the same can be said about the singlet and thus only two massive light neutrinos.

It is shown in [26, 27] that the combination of proton decay and unification constraints predicts the mass of the triplet fermion in 24_F and the mass of the triplet scalar in 24_H below TeV. The stability of the proton prefers these particles to lie as close as possible to M_Z. However, in order to keep these states light, the theory require substantial fine-tuning in parameters. Also the observations from the atmospheric neutrinos requires very small $y_T \approx 10^{-4}$-10^{-5} due to light seesaw scale.

In this section, we discussed two prototype GUTs based on $SU(5)$ group. As we have seen in these models, the grouping of SM multiplets within few irreducible representations of $SU(5)$ group leads to correlations among the various Yukawa couplings. The remainder of this chapter is devoted to a similar analysis of the other very popular class of the unified schemes, the $SO(10)$ GUTs.

2.2 Fermion masses in $SO(10)$ GUT models

The possibility of $SO(10)$ as a grand unification group of the SM was first noted by Georgi [30] and Fritzsch and Minkowski [31]. Unlike $SU(5)$, $SO(10)$

is a group of rank 5 with an extra $U(1)_{B-L}$ symmetry as in the left-right symmetric groups. The advantages of $SO(10)$ over $SU(5)$ grand unification are:

1. A family of fermions is entirely unified in an irreducible 16-dimensional spinorial representation of $SO(10)$. This predicts the existence of right-handed neutrino.

2. The left-right symmetry is a finite gauge transformation in the form of charge conjugation. This is because of both left-handed and right-handed fermions reside in the same representation, namely 16_F. As a result of this, the gauge interactions in $SO(10)$ conserve parity thus making it a part of a continuous symmetry:

3. Besides $SU(5) \times U(1)$, its other maximal subgroup is $SU(4)_c \times SU(2)_L \times SU(2)_R$ symmetry of Pati-Salam [32]. It therefore explains somewhat mysterious relations $m_d = m_e/3$ of $SU(5)$.

4. The unification of gauge couplings can be achieved with or without supersymmetry.

5. In the supersymmetric version, matter parity $M = (-1)^{B-L}$, equivalent to the R-parity $R = M(-1)^{2S}$, is a gauge transformation [33]. It is possible to keep R-parity exact at all energies if the $SO(10)$ gauge symmetry is broken properly.

In order to understand some of these points, and in order to understand the construction of the theory, we turn now to the brief discussions on $SO(10)$ GUT emphasizing its fermion mass sector in particular.

2.2.1 $SO(10)$ gauge symmetry & fermions

In general, $SO(2N)$ is the group of real orthogonal transformations, $O^T O = OO^T = \mathbf{I}$, with $Det(O) = 1$. The algebra of $SO(2N)$ group has been discussed in different ways in [34, 35, 36, 37, 38, 39]. One of the more convenient way

using the spinor $SU(N)$ basis is discussed in [35]. The different representations of $SO(10)$ and their decompositions in various subgroups are listed in [39, 40]. Here, we omit such discussions on the group theory of $SO(10)$ and focus our attention to the phenomenological consequences of $SO(10)$ symmetry. The reader is advised to refer to the above references for details of $SO(10)$ algebra.

One of the interesting result emerging from the $SO(10)$ algebra is that all the SM matter multiplets of one generation fit neatly within 16-dimensional chiral spinor of $SO(10)$. Under the $SU(3)_c \times SU(2)_L \times U(1)_Y$, the 16-plet fermion can be decomposed as

$$16_F = (3, 2, 1/3) \oplus (1, 2, -1) \oplus (\bar{3}, 1, -4/3) \oplus (\bar{3}, 1, 2/3) \oplus (1, 1, 2) \oplus (1, 1, 0). \tag{2.15}$$

These different components can be identified as Q_L, L_L, u_L^c, d_L^c, e_L^c and the SM singlet ν_L^c respectively. Equivalently, one can write

$$16_F = \bar{5}_F \oplus 10_F \oplus 1_F. \tag{2.16}$$

at the $SU(5)$ level. This immediately brings two important benefits from the fermion mass point of view.

The right handed neutrinos are automatically present and the structure and the scale of Majorana masses are dictated by the Yukawa couplings, spontaneous symmetry breaking pattern and the requirement of gauge-coupling unification. Secondly, since the gauge symmetry does not distinguish among the components of the decomposition (2.15) there are tight correlations among the effective Yukawa couplings that originate from a common source. As a result, the number of independent parameters determining the $SO(10)$ textures of the effective quark and lepton masses and mixing matrices can be reduced considerably. This will be discussed in some details later.

2.2.2 Higgs sector & symmetry breaking

As in any realistic GUT framework, the Higgs sector of a general $SO(10)$ GUT must satisfy two basic requirements: (1) It must allow for a proper spontaneous symmetry breaking of $SO(10)$ down to $SU(3)_c \times SU(2)_L \times U(1)_Y$ of the SM (or MSSM in case of SUSY $SO(10)$) and (2) through Yukawa interactions, it must be compatible with the current data on quark and lepton masses and mixing. The $SO(10)$ representations that are capable to act in both these role are particularly interesting. In this subsection, we mainly discuss the Higgs sector responsible for gauge symmetry breaking. The Higgs sector for viable Yukawa interactions will be discussed in the next subsection.

The important difference with respect to $SU(5)$ case comes from the fact that $SO(10)$ is a rank-5 group. Therefore, many different symmetry breaking chains are available which leads to the rank-4 gauge group of the SM. To break $SO(10)$ properly along the desired chain one must make sure that at each intermediate scale there live Higgs multiplets capable to break the considered symmetry down to a subsequent one. In addition, the components acquiring VEVs must be singlet under the desired lower intermediate symmetry groups. Looking at the decomposition of the basic $SO(10)$ representations with respect to the physically interesting subgroups, it is easy to see that only some combinations of the $SO(10)$ irreducible representations are suitable for such purpose. For more clear understanding, let's first decompose relevant representations of $SO(10)$ in to the Pati-Salam group, *i.e.* $SU(4)_c \times SU(2)_L \times SU(2)_R$ (see [40]

for the full list).

$$
\begin{aligned}
10 &= (6,1,1) \oplus (1,2,2) \\
16 &= (4,2,1) \oplus (\bar{4},1,2) \\
45 &= (15,1,1) \oplus (6,2,2) \oplus (1,3,1) \oplus (1,1,3) \\
54 &= (6,2,2) \oplus (20,1,1) \oplus (1,3,3) \oplus (1,1,1) \\
120 &= (15,2,2) \oplus (6,3,1) \oplus (6,1,3) \oplus (10,1,1) \oplus (\overline{10},1,1) \oplus (1,2,2) \\
126 &= (15,2,2) \oplus (10,3,1) \oplus (\overline{10},1,3) \oplus (6,1,1) \\
\overline{126} &= (15,2,2) \oplus (\overline{10},3,1) \oplus (10,1,3) \oplus (6,1,1) \\
210 &= (15,1,3) \oplus (15,3,1) \oplus (\overline{10},2,2) \oplus (10,2,2) \oplus \\
&\quad (6,2,2) \oplus (15,1,1) \oplus (1,1,1)
\end{aligned}
\tag{2.17}
$$

The most common $SO(10)$ breaking chains and different submultiplets that can be used to break the intermediate symmetries at each step are given Fig. 2.1.

Interestingly, inspecting Fig. 2.1 and Eq. (2.17) one can see that at least two (and three in the SUSY case) Higgs representations acquiring VEVs are needed to break $SO(10)$ down to the low energy $SU(3)_c \times U(1)_{em}$ gauge symmetry. For instance, the breaking of $SU(2)_L \times SU(2)_R$ subgroup of $SO(10)$ can be governed by only two multiplets that contains the SM singlets - 16_H or 126_H. However, the SM singlet components of none of these multiplets can break $SU(5)$ subgroup of $SO(10)$. This can be easily seen in the case of 16_H in which only the $SU(5)$ singlet is also a singlet under the SM. Therefore, to break $SO(10)$ through the left-right subgroups avoiding the $SU(5)$ intermediate step, additional Higgs representations are needed on the top of 16_H or 126_H. The adjoint 45_H can play this role in the non-supersymmetric $SO(10)$ models. In supersymmetric versions of $SO(10)$, 45_H turned out to be insufficient because it does not develop a SUSY-preserving VEV [17] and so the usual choice is $45_H + 54_H$. Another option is to replace these two representations by one, namely 210_H.

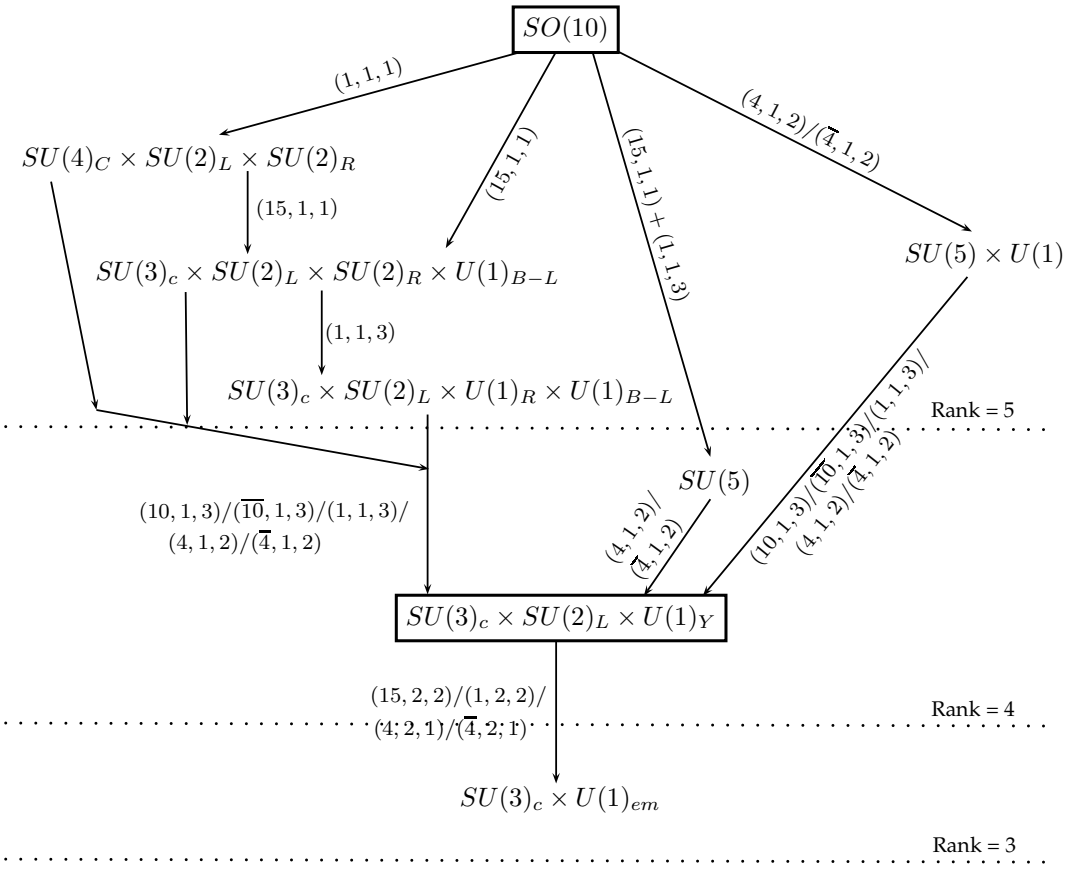

Figure 2.1: The physically viable breaking chains of $SO(10)$ down to the SM gauge symmetry. Different scalar multiplets which drive the breaking are shown in the Pati-Salam representations.

Finally, one must look for a representation that breaks the SM down to $SU(3)_c \times U(1)_{em}$. This can be achieved by SM like Higgs residing in the $SO(10)$ Higgs. Although there are already such submultiplets in 16_H or 126_H, usually additional multiplet(s) are also added to get viable Yukawa sector as we will discuss in the next subsection. In most cases, the 10_H vector representation and/or the three-index antisymmetric tensor 120_H is added to account for this.

2.2.3 Yukawa sector

The dimensions of the Higgs representation that can couple to the matter fermions of the SM are given by the group theoretical properties of the bilinear [40]

$$16 \times 16 = 10 + 126 + 120 \tag{2.18}$$

therefore, at the renormalizable level there are three types of $SO(10)$ Higgs multiplets that can give masses to the matter fermions. These are 10-dimensional vector representation 10_H, the 126-dimensional anti-self dual 5-index anti-symmetric tensor $\overline{126}_H$ and the 120-dimensional 3-index antisymmetric tensor 120_H. However, at the level of effective operators, any combination of Higgs representation containing at least one of these three structures as a part of its decomposition, can be used. In the renormalizable SUSY $SO(10)$ theories, the fermion masses arise from the following Yukawa interactions

$$-\mathcal{L}_Y = 16_F^i[Y_{10}^{ij}10_H + Y_{126}^{ij}\overline{126}_H + Y_{120}^{ij}120_H]16_F^j + h.c., \qquad (2.19)$$

where Y_{10} and Y_{126} are complex symmetric matrices while Y_{120} is a complex anti-symmetric matrix in the generation indices ij. The symmetric or anti-symmetric nature of Yukawa matrices arises from the group theoretical properties of corresponding bilinear couplings [34]. In the non-SUSY case one can have two additional Yukawa matrices since the conjugate fields 10_H^* and 120_H^* can also couple to the fermions. Let us now discuss in general the origin of Dirac and Majorana masses of fermions arise due to the above Yukawa interactions.

Dirac masses of fermions

The origin of fermion masses can be best understood in the language of Pati-Salam decompositions of 16_F, 10_H, $\overline{126}_H$ and 120_H already given in Eq. (2.17). Note that 10_H and $\overline{126}_H$ contain a SM like Higgs doublet in $(1,2,2) \in 10_H$ and $(15,2,2) \in \overline{126}_H$ while 120_H contains both of these multiplets. Moreover, the multiplets that do not couple directly to the fermionic bilinears may also contain similar submultiplets (for example, $(10,2,2) \in 210_H$). After the GUT-scale symmetry breaking, all these $SU(2)_L$ doublet components with equal SM quantum numbers can mix and enter in the formulae for the effective SM light Higgs doublet acquiring the electroweak VEV. In general, if there exist such n submultiplets, the spectrum of these submultiplets is encoded in the $n \times n$

Higgs masses matrix M_H. By minimal fine-tunning (enforcing $\mathrm{Det}(M_H) = 0$) one obtains a light electroweak Higgs doublet as an admixture of all these components:

$$H = V_{1j}\phi_j \tag{2.20}$$

where ϕ is n-dimensional vector made up of $SU(2)_L$ doublet components coming from different scalar multiplets in given $SO(10)$ model and V is a unitary mixing matrix. When the light Higgs doublet receive an electroweak VEV, due to the mixing in Eq. (2.20) the following VEVs are generated on the relevant $SO(10)$ components:

$$\begin{aligned} \langle(1,2,1)_{10_H}\rangle &= (V^\dagger)_{11}\langle H\rangle \equiv \upsilon_{10} \\ \langle(1,2,1)_{\overline{126}_H}\rangle &= (V^\dagger)_{21}\langle H\rangle \equiv \upsilon_{\overline{126}} \\ .. &= \ldots\ \ldots \end{aligned} \tag{2.21}$$

Thus, in general, there are n distinct complex VEV parameters that generate the fermion masses when electroweak symmetry is broken. In the supersymmetric versions of $SO(10)$, one needs two light Higgs doublets H_u and H_d and therefore it requires two fine-tunning conditions. Therefore, in such models, one gets $2n$ VEVs that contributes in the fermion masses. Depending on the actual Higgs content in the theory, one gets correlations between the mass matrices of different fermions. This will be discussed in more details in the subsequent chapters.

Majorana masses of neutrinos and seesaw mechanisms

As it is clear from the decompositions given in Eq. (2.17), the Majorana part of the neutrino sector is entirely governed by the VEVs of $\overline{126}_H$ (or $\overline{16}_H$ in the case of nonrenormalizable Yukawa interactions). The right handed neutrinos

get masses when the $(10,1,3) \in \overline{126}_H$ acquires a VEV:

$$\begin{aligned} Y_{126} 16_F 16_F \langle \overline{126}_H \rangle &\rightarrow Y_{126} (\overline{4},1,2)_{16} (\overline{4},1,2)_{16} \langle (10,1,3)_{\overline{126}} \rangle \quad \text{(under PS)} \\ &\rightarrow Y_{126} (1,1,0)_{16} (1,1,0)_{16} \langle (1,1,0)_{\overline{126}} \rangle \quad \text{(under SM)} \\ &\equiv M_R N_L^{cT} C^{-1} N_L^c \end{aligned} \tag{2.22}$$

Moreover, one can see that there is also a small VEV induced on the left-right mirror component of this triplet, namely $\langle (10,3,1) \rangle \in \overline{126}_H$. This naturally arises as a consequence of the Higgs potential minimization which approximately leads to the condition

$$\langle (10,3,1)_{\overline{126}} \rangle \, \langle (10,1,3)_{\overline{126}} \rangle = \frac{\upsilon_{\rm EW}^2}{\gamma} \tag{2.23}$$

where γ is a parameter in the Higgs potential which is of $\mathcal{O}(1)$ and $\upsilon_{\rm EW}$ is an electroweak VEV. Clearly, the VEV of $(10,3,1)_{\overline{126}}$ is naturally strongly suppressed. Since the $SU(2)_R$ breaking VEV must be close to the GUT scale, the $SU(2)_L$ triplet VEV giving rise to the Majorana masses to the left-handed neutrino

$$\begin{aligned} Y_{126} 16_F 16_F \langle \overline{126}_H \rangle &\rightarrow Y_{126} (4,2,1)_{16} (4,2,1)_{16} \langle (\overline{10},3,1)_{\overline{126}} \rangle \quad \text{(under PS)} \\ &\rightarrow Y_{126} (1,2,-1)_{16} (1,2,-1)_{16} \langle (1,3,2)_{\overline{126}} \rangle \quad \text{(under SM)} \\ &\equiv M_L L_L^T C^{-1} L_L \end{aligned} \tag{2.24}$$

falls approximately to the right range to provide a significant correction to the traditional (singlet) seesaw formula for the light neutrinos. Note that, in agreement with expectations, both the Majorana mass matrices are symmetric in the generation indices because of the symmetry properties of the Y_{126} matrix [34]. Combining, Eqs. (2.22), (2.24) and Dirac masses for neutrinos, one can construct a 6×6 Majorana neutrino mass matrix

$$\mathcal{M}_\nu = \begin{pmatrix} M_L & M_D \\ M_D^T & M_R \end{pmatrix} \tag{2.25}$$

which is when block-diagonalized in the limit of $M_L \ll M_D \ll M_R$ gives the effective light neutrino mass term

$$M_\nu = M_L - M_D M_R^{-1} M_D^T \equiv M_\nu^{II} + M_\nu^I \tag{2.26}$$

We will identify the first (second) term of the above equation as type-II (type-I) seesaw mechanism. Unlike in conventional bottom-up approaches, here the neutrino mass matrix is closely related with the charged fermion mass matrices. The detailed investigations of such relations is the main subject of the subsequent chapters in this thesis.

One can see the overlap of the sets of the multiplets equipped by the renormalizable Yukawa couplings - 10_H, $\overline{126}_H$ and 120_H - and those capable to break GUT scale symmetries (see Fig. 2.1) is actually very small. Apart of 10_H that can not play any role in the high scale symmetry breaking mechanism, only $\overline{126}_H$ contains colorless $SU(2)_L$ doublets that can give rise to Dirac masses of the matter fermions, and $SU(2)_R$ triplet capable to participate in the breaking of $SO(10)$ and also it can generate the small neutrino masses through seesaw mechanisms. From this point of view, $\overline{126}_H$ can be viewed as a crucial ingredient of a class of economical $SO(10)$ models. An important representative of this kind of model - the minimal renormalizable supersymmetric $SO(10)$ model - is the subject of the next chapter.

2.2.4 Proton decay in supersymmetric $SO(10)$ models

Before we end this chapter, let us briefly comment on the proton decay in SUSY $SO(10)$ models. The situation is almost similar to that of the minimal $SU(5)$ discussed briefly in Section 2.1.3. However, the structure of the effective operators that was very constrained in the $SU(5)$ case can be relaxed and the upper bound on τ_p can be pushed well above the experimental limits in some situations. This arise due to the fact that the colored Higgs triplets governing the rise of $d = 5$ effective operators can be found in different $SO(10)$ representations and mix once the GUT scale symmetries are broken.

Therefore, the relevant expressions for the Wilson coefficients typically contain elements of the mixing parameterizing the projections of the $SO(10)$ basis on the triplet mass eigenstates. As a result, one can often suppress the proton decay rate below the observable limit by adjusting properly the color triplet mixing. However, such spreading of the Higgs multiplets can affect the gauge coupling unification pattern. Further, in order to accommodate the realistic Yukawa textures arising from fermion masses and mixing data studied in the subsequent chapters, the Wilson coefficients cannot be made arbitrarily small and there are still rather stringent limits on the proton decay in realistic SUSY $SO(10)$ models, see [41, 42, 43, 44] for examples.

Chapter 3

Fermion Masses in Supersymmetric $SO(10)$ Models

Among the variety of grand unified frameworks, a particular attention should be naturally paid to the simplest schemes which has the maximum predictive power. On quantitative level, it is always the amount of predictability that qualifies a particular scheme (and the assumptions behind it) as experimentally testable and capable to draw conclusions about the beyond Standard Model physics. The elegant idea of grand unification can be tested only in such schemes which are unbiased by additional assumptions and powered by the concept of minimality. In this chapter, we investigate two such frameworks for their viability to explain the low energy observables.

3.1 The minimal model with $10 + \overline{126}$ Higgs

The minimal renormalizable supersymmetric $SO(10)$ (MSGUT) model is a very interesting example of a concise framework constructed on the principle of the grand unification. The basic structure of the minimal $SO(10)$ was first considered by Clark, Kuo and Nakagawa [45] and Aulakh and Mohapatra [46]. The most interesting feature of this framework that separates it out from the other unified theories is the minimal choice of the Higgs sector that allows only small number of free parameters and thus makes the model extremely

predictive. Both the renormalizability and supersymmetry play an important role in restricting the parameter space of theory while the latter also helps in achieving the gauge coupling unification and solving the hierarchy problem.

3.1.1 The minimal supersymmetric $SO(10)$ model

As we discussed in the previous chapter, the SM matter fields and a right handed neutrino resides in the three copies of 16-dimensional spinorial representation 16^i_F. Let us now discuss in detail the Higgs content, symmetry breaking pattern and Yukawa interactions in the minimal supersymmetric $SO(10)$ model.

The Higgs sector and symmetry breaking

The Higgs sector is strongly constrained by the requirement of minimality, renormalizability and supersymmetry. It is clear that such a theory must have $\overline{126}_H$ Higgs as it is indispensable to generate the masses of the right handed neutrino and hence the seesaw mechanism. However the VEV of $\overline{126}_H$ leads to non-vanishing D-term which breaks the supersymmetry at high scale. Supersymmetry can be preserved upto the TeV scale by adding the 126_H and assuming $\langle 126_H \rangle = \langle \overline{126}_H \rangle$. The VEVs of $\overline{126}_H$ leave $SU(5)$ unbroken so an additional 210_H Higgs is required for the consistent $SO(10)$ breaking upto the SM [46]. The other alternatives of the 210_H Higgs are 45_H and 54_H but none of them can do this job alone at the renormalizable level and both are needed [17]. However this leads to more number of parameters and the minimal choice would naturally be the 210_H Higgs. As we will see later in this chapter, the Yukawa interactions of 16^i_F fermions with only $\overline{126}_H$ Higgs gives incorrect masses of first and second generation charged fermions and also cannot generate CKM mixing in the quark sector. Therefore an additional 10_H Higgs is added to achieve the viable fermion spectrum in the model. In short, the MSGUT consists of 10_H, $\overline{126}_H$, 126_H and 210_H. The Higgs part of the

superpotential of the model can be written as [47]

$$\begin{aligned} W_H &= m_{10}10_H^2 + \frac{m_{210}}{4!}210_H^2 + \frac{m_{126}}{5!}126_H\overline{126}_H + \frac{\lambda}{4!}210_H^3 \\ &+ \frac{\eta}{4!}210_H126_H\overline{126}_H + \frac{1}{4!}210_H10_H(\alpha 126_H + \beta\overline{126}_H) \end{aligned} \tag{3.1}$$

and it has only 7 independent complex parameters. For the discussion that follows it is convenient to use the decomposition of the $SO(10)$ Higgs representations under the $SU(4)_{PS} \times SU(2)_L \times SU(2)_R$. Such decompositions is already given in Eq. (2.17).

The consistent breaking of $SO(10)$ down to the MSSM can be achieved by allowing the MSSM singlets to take a VEV. Since 10_H does not contain any MSSM singlet, it does not take part in the $SO(10)$ breaking. The physically allowed VEVs are [47]

$$p = \langle(1,1,1)_{210_H}\rangle; \quad a = \langle(15,1,1)_{210_H}\rangle; \quad \omega = \langle(15,1,3)_{210_H}\rangle$$

$$\sigma = \langle(\overline{10},1,3)_{210_H}\rangle; \quad \bar{\sigma} = \langle(10,1,3)_{\overline{126}_H}\rangle \tag{3.2}$$

As we have already discussed, the D-term flatness conditions implies $|\sigma| = |\bar{\sigma}|$. With this configuration of VEVs, the detailed calculations for the flatness conditions for the F and D-terms are carried out in [48]. The result of such analysis shows that if the VEVs of 210_H components are spread enough, there could be a cascade of intermediate steps. For example, $a \gg p, \omega, \sigma$ leads to the following breaking chain with left-right symmetry at intermediate scale.

$$SO(10) \xrightarrow{M_G} SU(3)_c \times SU(2)_L \times SU(2)_R \times U(1)_{B-L} \xrightarrow{M_I} SM$$

Similarly, the condition $p \gg a, \omega, \sigma$ allows the Pati-Salam symmetry at the intermediate scale.

$$SO(10) \xrightarrow{M_G} SU(4)_{PS} \times SU(2)_L \times SU(2)_R \xrightarrow{M_I} SM$$

In contrast, the successful gauge coupling unification in MSSM strongly favors a single step breaking with all the rank-5 subgroups broken at around $M_I \sim M_G$. The small uncertainty in the values of the couplings at M_Z allows M_I an order or two of magnitude away from M_G. However, the lowering of intermediate scale also brings the GUT scale lower and such possibility is discarded [48] by the existing proton lifetime bounds. So there is no room for intermediate scale in MSGUT (except $M_I \sim M_G$) concerning the gauge coupling unification and proton decay constraints and only a single step breaking of $SO(10)$ down to the MSSM is allowed.

One of the important feature of the MSGUT model is the automatic R-parity conservation along the symmetry breaking chains. The R-parity is defined as

$$R = (-1)^{3(B-L)+2S}$$

Note that the $B-L$ breaking is achieved by the VEVs of $(\overline{10}, 1, 3)$ component of the $\overline{126}_H$. This implies that the $B-L$ charge gets changed always by 2 units leaving R-parity exact. This automatically makes the lightest neutralino stable which may be the viable candidate of the cold dark matter (CDM).

Yukawa interactions and fermion masses

The Yukawa interactions responsible for fermion masses in the model are

$$W_Y \;=\; 16^i_F(Y^{ij}_{10}10_H + Y^{ij}_{126}\overline{126}_H)16^j_F \tag{3.3}$$

As already mentioned in Chapter 2, each of the representations 10_H, 126_H, $\overline{126}_H$ and 210_H contains one set of the MSSM like Higgs doublets H_u and H_d. After the $SO(10)$ breaking into the MSSM, the various doublets of the same MSSM quantum numbers mix with each other due to terms proportional to α, β and η in the superpotential shown in Eq. (3.1). This leads to 4×4 mass Higgs doublet matrix. In order to arrange the right spectrum in low energy theory, one has to impose the minimal fine-tuning condition [48] *i.e.* the determinant of the mass matrix of the doublets vanishes in the first approximation leaving

one massless linear combination of these doublets. Thus, in general, for each MSSM hypercharge there are 4 different multiplets that mix to give rise to the light Higgs doublets H_u and H_d which are identified with the standard MSSM doublets. The electroweak symmetry is then broken by the VEVs of H_u and H_d denoted by v_u and v_d respectively. The direction of these VEVs in the space of the various doublet components is distributed among all the relevant $SO(10)$ components. Two of these components 10_H and $\overline{126}_H$ which couple to matter fields through Yukawa interactions shown in Eq. (3.3) give rise to effective Yukawa sum rule [46]

$$\begin{aligned} M_d &= v_d^{10} Y_{10} + v_d^{126} Y_{126} \\ M_u &= v_u^{10} Y_{10} + v_u^{126} Y_{126} \\ M_l &= v_d^{10} Y_{10} - 3 v_d^{126} Y_{126} \\ M_D &= v_u^{10} Y_{10} - 3 v_u^{126} Y_{126} \end{aligned} \tag{3.4}$$

As it has already been discussed in previous chapter, the $\overline{126}_H$ representation contains the scalar multiplets $(10, 3, 1) \oplus (\overline{10}, 1, 3)$ under the Pati-Salam subgroup and their VEVs $v_L = \langle (10, 3, 1) \rangle$ and $v_R = \langle (\overline{10}, 1, 3) \rangle$ generate mass matrices for the left and right handed neutrino fields respectively.

$$\begin{aligned} M_L &= v_L Y_{126} \\ M_R &= v_R Y_{126} \end{aligned} \tag{3.5}$$

The effective mass matrix of the light neutrinos get contributions from both type-I and type-II seesaw mechanisms.

$$M_\nu = M_L - M_D M_R^{-1} M_D^T \tag{3.6}$$

Equations (3.4), (3.5) and (3.6) provide an excellent framework to study the relations between fermion masses and mixing and it is the main subject of a detailed analysis in this section.

For more details on other interesting features and issues that have been avoided in this brief description of the minimal SUSY $SO(10)$ scenario, the interested readers are advised to refer [45, 46, 48, 49] and in references therein.

3.1.2 b-τ unification & large atmospheric mixing

It was first pointed out by Babu and Mohapatra [50] in 1992 that the fermion mass relations (3.4), (3.5) and (3.6) in the MSGUT can provide a viable spectrum of fermion masses. Not only this, it establishes the deep connection between quark and lepton mixing angles and provide the information about the neutrino spectrum. Based on the relations given above, a very interesting connection between the atmospheric mixing angle and b-τ Yukawa unification was found a decade later in [51, 52]. In the case of type-II seesaw dominance, it is clear from Eqs. (3.4), (3.6) that

$$M_\nu \propto M_d - M_l \tag{3.7}$$

In the diagonal basis of the charged leptons and for the small down quark mixing, the 2-3 block of the neutrino mass matrix becomes

$$M_\nu \approx \begin{pmatrix} \epsilon & \epsilon \\ \epsilon & \frac{m_b - m_\tau}{m_b} \end{pmatrix} \tag{3.8}$$

where ϵ is a small parameter of the order of $\mathcal{O}(\lambda^2)$ and λ can be identified with Cabbibo angle. Clearly, one gets large (near maximal) atmospheric mixing angle when $m_b \approx m_\tau$. In fact the GUT extrapolated values of observed masses of the bottom quark and tau lepton show the approximate b-τ unification. Hence the maximality of atmospheric mixing angle can naturally be explained by linking it to the b-τ unification in this class of models. Following this simplified picture, the more detailed analysis including the first generation was carried out in [53, 54]. It was observed that the assumption of type II seesaw mechanism for small neutrino masses coupled with b-τ mass unification in MSGUT model leads not only to a natural understanding of large atmospheric

mixing angle among neutrinos but also to large solar angle and a small $U_{e3} \sim 0.16$ as required to fit observations.

In this chapter, we will see that this interesting connection has significant role to play whenever type-II dominated scenarios are considered in not only the minimal model but also in the simple extension of the minimal model with 120_H. Moreover, we will see in chapter 5 that this simple connection disfavors the the type-II dominance in non-supersymmetric GUT models due to non unification of bottom and tau masses.

3.1.3 Fermion masses and mixing: Numerical analysis

As it was argued in the first chapter, understanding the pattern of fermion masses and mixing is one of the longstanding challenges in particle physics. The standard approaches to establish the correlations among the quark and lepton masses and mixing parameters consists in imposing additional assumptions on the flavor structure through a class of the horizontal symmetries. In contrast, the construction of MSGUT is such that it naturally can be accountable for potentially realistic description of the fermion masses and mixing patterns. After some redefinitions of parameters, the Eqs. (3.4) and (3.5) can be rewritten as

$$\begin{aligned} M_d &= H + F, \\ M_u &= r(H + sF), \\ M_l &= H - 3F, \\ M_D &= r(H - 3sF), \\ M_L &= r_L F\ , \\ M_R &= r_R^{-1} F. \end{aligned} \tag{3.9}$$

where $H(= \upsilon_d^{10} Y_{10})$, $F(= \upsilon_d^{126} Y_{126})$ are complex symmetric matrices. r, s, r_L, r_R are dimensionless complex parameters of which r, r_L, r_R can be chosen real without lose of generality. H can be made diagonal with real and positive

eigenvalues by rotating the original 16_F fermions in generation space. Hence all the mass matrices are determined by 19 real parameters if only type-II or type-I seesaw dominates. These parameters are determined using 18 observable quantities. In spite of the number of observables being less than the parameters, not all observables can be fitted with required precision due to non-linear nature of Eq. (3.9). These fermion mass relations are fitted to the observed fermion parameters in various papers [53, 54, 55, 56, 57]. The most general minimization is performed by Bertolini *et al* [57] allowing for arbitrary combination of both the type-I and II seesaw contributions to neutrino masses. The input values for quark and the charged lepton masses used in this analysis is taken from [58] and correspond to $\tan\beta = 10$. It is found that the best fits are obtained in a mixed scenario, type-I gives slightly worse and type-II scenario is unable to reproduce all the observables within 1σ.

It is important to note that

1. All these existing analysis of fermion masses are based on simple extrapolation of fermion masses presented in [58] ignoring the effects of soft supersymmetry breaking. Clearly, the threshold effects introduced through susy breaking can have non negligible impact on the first and second generation fermion masses.

2. If type-II seesaw dominates then one needs b-τ unification at the GUT scale in order to reproduce large atmospheric mixing angle. In contrast, the extrapolated values [58] used in the analysis do not show complete b-τ unification. This results in a poor fit to the atmospheric mixing angle at the minimum. Threshold effects can play important role in achieving the b-τ unification and improves the fit to fermion masses.

Motivated by these reasons, we perform the numerical analysis to check the viability of Eqs. (3.9) with the updated data extrapolated at the GUT scale with and without threshold corrections. We perform the χ^2 minimization to fit the free parameters of the model. The details of extracting the physical observables from Eq. (3.9), the definition of the χ^2 function and details of

its minimization are discussed in Appendix A. Our input values of the quark masses and mixing angles at the GUT scale are based on the analysis in [59]. This uses the updated values of the b and t quark masses and the CKM parameters. More importantly, finite threshold corrections induced by sparticles are included in this analysis. Analysis in [59] proceeds in two steps. First, the quark masses and mixing angles are determined by fitting the available low energy data and evolving them to the supersymmetry braking scale M_S. In the second step, finite sparticle induced corrections are included and then evolution is performed up to the GUT scale M_{GUT}. We reproduce their table of values so obtained as Table 3.1 for convenience of the reader.

	A	**B**	**C**	**D**	**C1**	**C2**
$\tan\beta$	1.3	10	38	50	38	38
γ_b	0	0	0	0	-0.22	$+0.22$
γ_d	0	0	0	0	-0.21	$+0.21$
γ_t	0	0	0	0	0	-0.44
$y^t(M_X)$	6^{+1}_{-5}	0.48(2)	0.49(2)	0.51(3)	0.51(2)	0.51(2)
$y^b(M_X)$	$0.0113^{+0.0002}_{-0.01}$	0.051(2)	0.23(1)	0.37(2)	0.34(3)	0.34(3)
$y^\tau(M_X)$	0.0114(3)	0.070(3)	0.32(2)	0.51(4)	0.34(2)	0.34(2)
Observables	GUT scale values with propagated uncertainty					
(m_u/m_c)	0.0027(6)	0.0027(6)	0.0027(6)	0.0027(6)	0.0026(6)	0.0026(6)
(m_d/m_s)	0.051(7)	0.051(7)	0.051(7)	0.051(7)	0.051(7)	0.051(7)
(m_e/m_μ)	0.0048(2)	0.0048(2)	0.0048(2)	0.0048(2)	0.0048(2)	0.0048(2)
(m_c/m_t)	$0.0009^{+0.001}_{-0.00006}$	0.0025(2)	0.0024(2)	0.0023(2)	0.0023(2)	0.0023(2)
(m_s/m_b)	0.014(4)	0.019(2)	0.017(2)	0.016(2)	0.018(2)	0.010(2)
(m_μ/m_τ)	0.059(2)	0.059(2)	0.054(2)	0.050(2)	0.054(2)	0.054(2)
(m_b/m_τ)	$1.00^{+0.04}_{-0.4}$	0.73(3)	0.73(3)	0.73(4)	1.00(4)	1.00(4)
$\sin\theta^q_{12}$	0.227(1)	0.227(1)	0.227(1)	0.227(1)	0.227(1)	0.227(1)
$\sin\theta^q_{23}$	$0.0289^{+0.0179}_{-0.00073}$	0.0400(14)	0.0386(14)	0.0371(13)	0.0376(19)	0.0237(18)
$\sin\theta^q_{13}$	$0.0026^{+0.0022}_{-0.00045}$	0.0036(7)	0.0035(7)	0.0033(7)	0.0034(7)	0.0021(5)
$\delta_{CKM}[^\circ]$	56.31 ± 10.24	56.31 ± 10.24	56.31 ± 10.22	56.31 ± 10.22	56.31 ± 10.27	56.31 ± 10.25

Table 3.1: The input values of various observables of quark sector and charged lepton masses obtained at GUT-scale M_{GUT} for various values of $\tan\beta$ and threshold corrections $\gamma_{t,b,d}$ assuming an effective SUSY scale $M_S = 500$ GeV (see [59] for details). The numbers in the brackets denote the errors in the last digits of given quantities.

In the Table 3.1, column (A)-(D) show the evolved values of quark mass ratios and mixing angles in the absence of threshold corrections for various values of $\tan\beta$. One clearly sees the absence of the b-τ unification at the GUT scale except for the low value of $\tan\beta$. This changes with the inclusion of threshold corrections. These corrections are parameterized by $\gamma_{d,u,b,t}$ which are defined in the following manner. The down quark mass matrix is determine

by the term $QY_d d^c H_d$ in the minimal supersymmetric standard model. The corresponding term $QY'_d d^c H_u^*$ involving the second doublet H_u^* is not allowed in the superpotential by SUSY but it can be radiatively generated after the SUSY breaking. Since $\tan\beta \equiv \frac{\langle H_u^0 \rangle}{\langle H_d^0 \rangle}$, such terms give significant corrections to the tree level values for large $\tan\beta$ and should be included in evolving fermion masses and mixing from low energy scale to the M_X. The corrected down quark matrix is parameterized in [59] by

$$U_L^{d\dagger}(1 + \Gamma^d + V_{CKM}^\dagger \Gamma_u V_{CKM}) Y_{\rm diag}^d U_R^d$$

where $U_{L,R}^d$ and V_{CKM} are the (diagonal) down quark mass and the CKM matrix before the radiative corrections. The loops involving down squark-gaugino generate the second term and the loop with up squark-chargino generate the second term. $\Gamma_{d,u}$ are diagonal in the approximation of taking diagonal squark masses in the basis with diagonal quarks. Assuming equality of the first two generation squark masses, the diagonal elements $\Gamma_d = (\gamma_d, \gamma_d, \gamma_b)$ correct the down quark masses and $\Gamma_u = (\gamma_u, \gamma_u, \gamma_t)$ correct the CKM matrix in addition. The SUSY threshold corrections are included through these parameters and their best fit values corresponding to three classical GUT predictions namely $m_b = m_\tau$, $m_\mu = 3m_s$ and $\frac{m_d}{3m_e} = 1$ are determined. Last two columns correspond to different values of γ's determined this way. Comparison of column C with C1, C2 shows that threshold corrections change significantly the b quark mass as well as $\theta_{23}^q, \theta_{13}^q$. The neutrino masses and mixing that we use are the updated low scale values [60] but the effects of the evolution to M_{GUT} on the ratio of the solar to atmospheric mass scale and on the mixing angles are known to be small for the normal hierarchical spectrum that we obtain here.

We now discuss detailed fits to fermion masses and mixing based on the input values in Table 3.1. It is assumed that either the type-I or the type-II seesaw term in the neutrino mass matrix dominates and analysis is carried out separately in each of these two cases. It turns out to be convenient to express

H and F in terms of M_l and M_d, and substituting them in Eqs. (3.9) we get

$$\begin{aligned} M_u &= rm_\tau \left(\frac{3+s}{4}\tilde{M}_d + \frac{1-s}{4}\tilde{M}_l \right), \\ M_D &= rm_\tau \left(\frac{3(1-s)}{4}\tilde{M}_d + \frac{1+3s}{4}\tilde{M}_l \right), \\ M_L &= \frac{r_L m_\tau}{4}(\tilde{M}_d - \tilde{M}_l), \\ M_R &= \frac{r_R^{-1} m_\tau}{4}(\tilde{M}_d - \tilde{M}_l). \end{aligned} \tag{3.10}$$

We have chosen the basis with a diagonal M_l and introduced $\tilde{M}_{d,l} = \frac{1}{m_\tau} M_{d,l}$. Thus

$$\tilde{M}_l = Diag.(m_e/m_\tau, m_\mu/m_\tau, 1)$$

Hence all the quantities in the bracket in the above equation depend on the known ratios of charged lepton masses. $\tilde{M}_d$ is a complex symmetric matrix with 12 real parameters. Since we are fitting the ratios of different mass eigenvalues and mixing angles, the parameter r remains free and it can be fixed by m_t. r_L (r_R) in the case of type-II (type-I) seesaw dominance is determined from the atmospheric mass scale. There are total 14 real parameters (12 in $\tilde{M}_d$ and complex s) which are fitted over 14 observables. Four unknown observables in lepton sector (θ_{13}^l and three CP violating phases) get determined at the minimum. Results of numerical analysis carried out separately for the type-II and the type-I dominated seesaw mechanisms are shown in Table 3.2 and Table 3.3 respectively.

The main outcomes of this analysis are the following.

- The best fit in the type-II case is obtained at low $\tan\beta = 1.3$. The corresponding set of fitted parameters are given in Appendix B.1. This case has b-τ unification and threshold corrections are not very significant. On the other hand, cases B, C, D with relatively large $\tan\beta$ but without inclusion of threshold correction give quite bad fit. There is a clear correlation between the overall fit and the presence or absence of the b-τ unification in type-II models. Cases corresponding to the absence

	A	**B**	**C**	**D**	**C1**	**C2**
Observables	Pulls obtained for best fit solution					
(m_u/m_c)	-0.00668428	0.0276825	0.0259467	0.120767	-0.0212532	0.0356043
(m_c/m_t)	0.56521	0.157569	0.0201093	0.0730136	0.130288	0.320944
(m_d/m_s)	-1.21642	-0.891034	-0.27664	-1.36265	-1.04724	-1.57673
(m_s/m_b)	0.112798	0.440678	0.163272	0.752408	0.884723	0.789053
(m_e/m_μ)	0.0590249	-0.00627804	0.3944	0.0396087	0.0297987	0.0555931
(m_μ/m_τ)	0.182548	0.103214	0.821485	0.0192305	0.26316	0.121145
(m_b/m_τ)	0.87282	2.20829	2.79368	2.34331	0.26656	0.407798
$\left(\frac{\Delta m^2_{sol}}{\Delta m^2_{atm}}\right)$	0.256292	0.116314	-0.14908	0.230056	0.0188227	-0.0140039
$\sin\theta^q_{12}$	0.0730813	0.0702755	0.0399788	0.105989	0.0779176	0.127757
$\sin\theta^q_{23}$	-0.0311676	-0.172792	-0.471738	-0.0960437	-0.757038	-0.945821
$\sin\theta^q_{13}$	1.33502	-0.0354198	0.494732	0.606606	0.890741	1.17758
$\sin^2\theta^l_{12}$	0.00836789	-0.106439	-0.599727	-0.27881	-0.63356	-0.510182
$\sin^2\theta^l_{23}$	-1.53367	-4.97038	-4.95673	-4.70944	-2.56294	-1.84412
$\delta_{\rm CKM}[^\circ]$	-0.345931	-0.163765	-0.600814	-0.214459	-0.650554	-0.75885
χ^2_{min}	**6.9367**	**30.70**	**34.52**	**30.68**	**10.804**	**9.3559**
Observables	Corresponding Predictions at GUT scale					
$\sin^2\theta^l_{13}$	0.0226508	0.0190847	0.0206716	0.0196974	0.0239619	0.0209208
$\delta_{\rm MNS}[^\circ]$	19.9399	18.9784	19.5619	11.92	358.789	1.78569
$\alpha_1[^\circ]$	337.171	346.627	344.795	350.595	12.4786	349.711
$\alpha_2[^\circ]$	147.364	151.912	146.886	161.702	194.023	168.156
$r_L m_\tau$[GeV]	8.37×10^{-10}	6.0×10^{-10}	6.49×10^{-10}	6.94×10^{-10}	7.15×10^{-10}	9.1×10^{-10}

Table 3.2: Best fit solutions for fermion masses and mixing obtained assuming the type-II seesaw dominance in the minimal SUSY $SO(10)$ model. Pulls of various observables and predictions obtained at the minimum are shown for six different data sets.

of the b-τ unification cannot reproduce the atmospheric mixing angle and results in relatively poor fits. Inclusion of threshold corrections improves the fit but still $\frac{m_d}{m_s}$ and the atmospheric mixing angle cannot be reproduced within 1σ. The fit for $\tan\beta = 10$ obtained here with inputs from [59, 60] is poor compared to the corresponding fit presented in [57] which uses input from [58]. Compared to data in [58], the result from [59] display larger deviation from the b-τ unification and also errors in more recent input that we use for $\sin^2\theta^l_{23}$ are smaller. Both these features combine to give larger pulls for the ratio $\frac{m_b}{m_\tau}$ and $\sin^2\theta^l_{23}$ and results in poor fit.

- In contrast to the type-II case, the fits obtained in type-I case are uniformly better. Here one does not expect correlation between the atmospheric mixing angle and b-τ unification. Thus the cases B, C, D with large $\tan\beta$ also give quite good fits. Even in these cases (except D) main contribution to χ^2 comes from the pull in the atmospheric mixing

	A	**B**	**C**	**D**	**C1**	**C2**
Observables	Pulls obtained for best fit solution					
(m_u/m_c)	0.0486938	−0.180782	0.0653101	0.0053847	0.0467579	−0.0119661
(m_c/m_t)	1.22599	0.130589	0.246294	0.146932	0.297256	0.273346
(m_d/m_s)	−0.229546	−0.730641	0.223201	−0.748148	−2.2904	−0.689684
(m_s/m_b)	−0.932536	−0.886438	−0.977249	−1.05766	0.735548	0.000467775
(m_e/m_μ)	0.0340323	0.442759	0.103692	−0.476364	0.0649144	−0.0648856
(m_μ/m_τ)	0.310305	−0.526529	0.881934	0.938701	0.705648	0.0178824
(m_b/m_τ)	−0.486477	−0.194215	0.0172182	−0.34079	0.789868	−0.734937
$\left(\frac{\Delta m^2_{sol}}{\Delta m^2_{atm}}\right)$	0.122267	−0.10063	−0.00563647	−0.120429	−0.180164	0.158557
$\sin\theta^q_{12}$	0.0432634	0.227948	0.0186715	0.084149	0.130301	0.0922391
$\sin\theta^q_{23}$	−0.281221	−0.0401177	−0.167224	0.0649082	−0.273222	−1.17651
$\sin\theta^q_{13}$	1.37864	−0.275689	0.926186	0.559003	1.48675	0.248759
$\sin^2\theta^l_{12}$	−0.0528379	−0.0598219	−0.38133	−0.172148	−0.746107	0.0694831
$\sin^2\theta^l_{23}$	−1.22555	−1.27077	−1.43475	0.0548963	−1.99485	−0.946001
$\delta_{\rm CKM}[^\circ]$	−0.291137	0.397159	−0.350422	−0.755859	−0.956628	−0.3197
χ^2_{min}	**6.3479**	**3.7962**	**5.0715**	**3.8665**	**14.789**	**3.4746**
Observables	Corresponding Predictions at GUT scale					
$\sin^2\theta^l_{13}$	0.0223307	0.0194886	0.0218753	0.0186789	0.0253152	0.0205366
$\delta_{\rm MNS}[^\circ]$	2.41793	4.52493	6.08769	335.07	357.142	14.7651
$\alpha_1[^\circ]$	347.106	8.42838	7.64991	28.0261	14.5679	1.13126
$\alpha_2[^\circ]$	163.759	191.241	188.713	218.586	196.273	177.828
$r_R\left(\frac{m_t^2}{m_\tau}\right)$ [GeV]	1.77×10^{-10}	2.63×10^{-10}	2.50×10^{-10}	4.02×10^{-10}	7.3×10^{-11}	2.82×10^{-10}

Table 3.3: Best fit solutions for fermion masses and mixing obtained assuming the type-I seesaw dominance in the minimal SUSY $SO(10)$ model. Pulls of various observables and predictions obtained at the minimum are shown for six different data sets.

angle. Threshold corrections are significant for large $\tan\beta$ and specific cases C1, C2 achieve b-τ unification but the overall fit worsens compared to B, C, D. Unlike in the type-II case, the χ^2 value obtained here for $\tan\beta = 10$ is comparable to the corresponding value in [57]. We give the fitted parameters for the best fit solution (case C2) in Appendix B.1.

3.1.4 Tension between seesaw scale & unification scale

It is remarkable feature of the MSGUT that a constrained Yukawa sector provide a reasonably good fit and can account correctly for all the fermion masses and mixing. However, some of the parameters of the fermion mass sector are tightly constrained from the requirement of gauge unification and proton decay lifetime. From the systematic survey of the parameter space, it is found that the MSGUT is incompatible with the generic type-I and type-II seesaw mechanisms [61, 62, 63, 64]. Such an incompatibility of the seesaw

mechanisms are also confirmed by [57, 65]. The main conclusions of these studies are

- For the generic as well as the special values of MSGUT couplings and Yukawa couplings taken from the generic type-II seesaw fit, it implies that type-II is highly sub-dominant to type-I seesaw in most of the parameter space of the MSGUT.

- The maximal values of the type-I seesaw masses attainable in the MSGUT fall at least an order or two of magnitude short of those required by atmospheric neutrino oscillation.

In very simple words, both of these seesaw mechanisms arise due to $U(1)_{B-L}$ and are inversely proportional to M_{B-L}. In MSGUT, supersymmetric unification forces $M_{B-L} \sim M_{GUT}$ which gives the neutrino mass scale smaller than the required by the atmospheric neutrino oscillation.

This problem of over suppression of seesaw mechanisms can also be seen from the results of the generic fit presented in Table 3.2 and 3.3. The overall scale of neutrino mass $r_L(r_R)$ in the case of type-II (type-I) seesaw can be fixed by using the atmospheric scale as normalization. The resulting values are displayed in Table 3.2 and 3.3. As discussed earlier, $r_L(r_R)$ arise from the VEVs of the components of $\overline{126}_H$ transforming as $(3,1,-2)$ $((1,3,-2))$ under the $SU(2)_L \times SU(2)_R \times U(1)_{B-L}$. In particular, $\langle(1,3,-2)\rangle_{\overline{126}_H}$ sets the scale of the $B-L$ breaking and is directly determined from the fits to fermion masses in the type-I scenario. From Eqs. (3.10),

$$\langle(1,3,-2)\rangle_{\overline{126}_H} \approx r_R^{-1} v s_m \cos\beta \ , \tag{3.11}$$

where s_m gives the mixing of the light H_d in the doublet part of $\overline{126}_H$ and $v \approx 174$ GeV. r_R is roughly independent of the input data set and for the value $r_R \approx 2.6 \times 10^{-10} m_\tau/m_t^2$ GeV, Eq. (3.11) gives

$$\langle(1,3,-2)\rangle_{\overline{126}_H} \approx 3.7 \times 10^{15} s_m \cos\beta \ \text{ GeV}$$

Thus the $B - L$ breaking scale in the type-I seesaw can be close to the GUT scale for $s_m \cos\beta \sim \mathcal{O}(1)$. It would however be significantly lower for large values of $\tan\beta$ and would conflict with the constraints from the gauge coupling unification. The determination of the $B - L$ breaking scale in the type-II dominated scenario is dependent on the details of the superpotential. Earlier [57, 62] analysis in the minimal model has shown that this scale cannot easily be lifted to the GUT scale and pauses a problem with the gauge coupling unification in the minimal scenario both for the type-I and type-II seesaw dominance [57]. Thus the problem persists for these new fits also and one does need to go beyond the minimal model.

3.2 The non-minimal model with $10 + \overline{126} + 120$ Higgs

In the last section we investigated in detail the correlations among the Yukawa couplings in the minimal SUSY $SO(10)$ model. We have seen that the consistent neutrino masses demand a seesaw scale significantly lower than the GUT scale which unfortunately spoils the gauge coupling unification of the MSSM. As a result of this, the minimal model is turns out to be over constrained and it needs suitable extensions. An obvious attempt to loosen the corset of the minimal theory is to add the 120-plet of scalars [66, 67, 68, 69]. As we have seen in the previous chapter, 120_H can couple to the matter fields at the renormalizable level and can contribute in the fermion mass sector. In this section, we investigate the viability of such scenario with the realistic fermion mass spectrum as we did in the case of the minimal model.

3.2.1 Extension of the minimal model with additional 120 Higgs

Adding a 120-plet Higgs is perhaps the simplest possible way to extend the minimal model to overcome from its over constrained parameter space. The

antisymmetric nature of the Yukawa structure coming from an additional 120_H brings the minimal number of new parameters. It also introduce additional 4 complex parameters in the Higgs superpotential. An important feature of 120_H is that it cannot participate in the spontaneous symmetry breaking of the $SO(10)$ symmetry and thus the presence of both the 210_H and 126_H is necessary (Recently, an alternative model is also proposed in [70] where 210_H is replaced by $45_H \oplus 54_H$). The Higgs part of superpotential of this model can be written as

$$\begin{aligned} W_H &= W_{\min} + m_{120} 120_H^2 + \frac{\gamma}{4!} 10_H 120_H 210_H \\ &+ \frac{\eta'}{4!} 210_H 120_H 120_H + \frac{1}{4!} 210_H 120_H (\alpha' 126_H + \beta' \overline{126}_H) \end{aligned} \quad (3.12)$$

where $W_{\min}$ is a Higgs superpotential of the minimal model given by Eq. (3.1). Since 120_H does not contribute to $SO(10)$ breaking, one may assume that the same breaking pattern like the minimal SUSY $SO(10)$ is achieved (see Section 3.1.1 for details).

3.2.2 Yukawa sector & assumption of spontaneous CP violation

The Yukawa part of the superpotential of the model under consideration is given by

$$W_Y = 16_F^i (Y_{10}^{ij} 10_H + Y_{126}^{ij} \overline{126}_H + Y_{120}^{ij} 120_H) 16_F^j \quad (3.13)$$

where, as we have already seen, Y_{10}^{ij} and Y_{126}^{ij} are symmetric matrices and Y_{120}^{ij} is an antisymmetric matrix in generation space. An important feature of the 120-dimensional representation of $SO(10)$ is its $SU(2)_L$ doublet contents. Unlike 10_H or $\overline{126}_H$, 120_H contains two copies of the $SU(2)_L \times SU(2)_R$ bi-doublets residing in the components with Pati-Salam quantum numbers (1, 2, 2) and (15, 2, 2). Since 210_H mixes 126_H, $\overline{126}_H$, as well as 120_H, with 10_H one expects that all the color singlet $SU(2)_L$ doublets mix to give the two

light Higgs doublets of MSSM, leaving the remaining states heavy. After the electroweak symmetry breaking, the above Yukawa interactions result into the following effective sum-rules for fermion mass matrices.

$$\begin{aligned} M_d &= v_d^{10} Y_{10} + v_d^{126} Y_{126} + (v_d^{120} + \tilde{v}_d^{120}) Y_{120} \\ M_u &= v_u^{10} Y_{10} + v_u^{126} Y_{126} + (v_u^{120} + \tilde{v}_u^{120}) Y_{120} \\ M_l &= v_d^{10} Y_{10} - 3 v_d^{126} Y_{126} + (v_d^{120} - 3\tilde{v}_d^{120}) Y_{120} \\ M_D &= v_u^{10} Y_{10} - 3 v_u^{126} Y_{126} + (v_u^{120} - 3\tilde{v}_u^{120}) Y_{120} \end{aligned} \tag{3.14}$$

Since the 120_H does not contribute in the Majorana masses of the neutrinos, the matrices M_L and M_R will maintain there form of Eq. (3.5). The light neutrino mass matrix after the seesaw mechanism is given by the same expression of Eq. (3.6). The above sum-rules can suitably be rewritten as

$$\begin{aligned} M_d &= H + F + iG \ , \\ M_u &= r(H + sF + it_u \ G \ ), \\ M_l &= H - 3F + \ it_l \ G \ , \\ M_D &= r(H - 3sF + it_D \ G \ ), \\ M_L &= r_L F \ , \\ M_R &= r_R^{-1} F. \end{aligned} \tag{3.15}$$

where (G) H, F are complex (anti)symmetric matrices. $r,\ s,\ t_l,\ t_u,\ t_D,\ r_L,\ r_R$ are dimensionless complex parameters of which $r,\ r_L,\ r_R$ can be chosen real without lose of generality. In this case, the most general model assuming type-II (type-I) dominance has 29 (31) independent parameters after rotating to basis with a real and diagonal H. One needs to make additional assumptions in order to reduce the parameter space. Considerable reduction in number of parameters is achieved assuming parity symmetry [71] or equivalently spontaneous CP violation [72]. This leads to Hermitian Dirac mass matrices. In our notation, this corresponds to taking all the parameters in Eq. (3.15) to be real, see [72, 73] for details. Such a model has only 17 parameters in case of

the type-II dominance, two less than in case of the minimal model. In spite of the reduction in number of parameters the allowed fermionic structure is analytically argued [56, 71, 74] to help in reducing tension in obtaining correct CP violating phase or fitting the first generation masses.

Numerical fits depend on whether type-II or type-I seesaw mechanism is used. Comparison of various models in case of the type-II seesaw dominance is made in [75]. All the models in this category give a very good fit to data with a significantly lower χ^2 than in case of the minimal model. The assumption of the type-I dominance leads to better fits compared to the type-II case. Moreover, unlike the type-II dominance, one does not need intermediate scale [66, 72, 73, 76] for reproducing the correct neutrino mass scale. This is a welcome feature from the point of view of obtaining the gauge coupling unification. All these works are based on the use of quark masses derived in [58] at $\tan\beta = 10$. We shall re-examine the non-minimal model with a different set of input which include the finite threshold corrections.

3.2.3 Fermion masses and mixing: Numerical analysis

We now check the viability of Eq. (3.15) by detailed numerical analysis. As before, the parameters r and $r_R(r_L)$ respectively determine the m_t and overall scale of neutrino masses in type-I (type-II) seesaw dominated scenarios. Our choice of 14 observables is the same as in the previous section. But they are now determined from the more general expression with non-zero G. H can be made diagonal without loss of generality. The mass matrices M_u, M_d, M_l, M_D, M_R and M_L are expressed in terms of 16 real parameters (3 in H, 6 in F, 3 in G, s, t_l, t_u, and t_D) which determine 14 observables P_i defined before.

Results of numerical analysis carried out separately for the type-II and type-I dominated seesaw mechanisms are shown in Table 3.4 and Table 3.5 respectively. The parameters obtained for the best fit solutions are given in Appendix B.1 and B.1. The following remarks are in order in connection with the results presented in these tables. As discovered in earlier numerical analysis [73, 75], the introduction of the 120_H leads to remarkable improvement

	A	**B**	**C**	**D**	**C1**	**C2**
Observables	Pulls obtained for best fit solution					
(m_u/m_c)	0.00196316	0.019005	−0.026015	−0.00109589	−0.00812155	0.0000225717
(m_c/m_t)	0.000750815	−0.114469	0.0964863	0.296526	−0.0278823	−0.00413523
(m_d/m_s)	0.0547314	0.618531	0.0606721	−1.14305	0.0271889	0.00312586
(m_s/m_b)	0.0565403	0.473347	−1.30774	0.675173	0.0105556	0.0361755
(m_e/m_μ)	0.0114456	−0.0155357	0.0482971	−0.00371258	0.00167012	0.000128709
(m_μ/m_τ)	−0.00279654	−0.66999	0.111235	−0.0605957	0.00155096	−0.00249006
(m_b/m_τ)	−0.171035	−0.301056	−0.381508	1.57926	0.0514536	−0.048487
$\left(\frac{\Delta m^2_{sol}}{\Delta m^2_{atm}}\right)$	0.00833338	−0.297416	0.191515	0.2129	0.00050834	−0.00412658
$\sin\theta^q_{12}$	−0.0106839	−0.0145213	−0.0420229	0.0809603	−0.00715584	0.0000538731
$\sin\theta^q_{23}$	−0.00295777	−0.058218	0.301593	0.341191	0.0120366	−0.000633901
$\sin\theta^q_{13}$	−0.00466345	−0.661544	0.381317	−0.632744	−0.137308	0.00650479
$\sin^2\theta^l_{12}$	0.0106277	−0.194399	0.333404	0.399294	0.00217496	−0.0043514
$\sin^2\theta^l_{23}$	−0.0198083	1.08433	−0.472589	−0.885401	0.0314484	0.00752103
$\delta_{\rm CKM}[^\circ]$	−0.00915099	0.168633	−0.520071	0.246618	−0.0314877	−0.0382519
χ^2_{min}	**0.0364**	**2.9315**	**2.7639**	**5.921**	**0.0254**	**0.0038**
Observables	Corresponding Predictions at GUT scale					
$\sin^2\theta^l_{13}$	0.0215726	0.0312498	0.03568	0.0214329	0.0289663	0.0069694
$\delta_{\rm MNS}[^\circ]$	34.3864	5.21955	89.5	315.898	355.507	75.6953
$\alpha_1[^\circ]$	6.26083	76.0772	289.921	80.1968	60.3609	240.526
$\alpha_2[^\circ]$	161.011	253.288	76.0613	283.63	220.306	34.4702
$r_L m_\tau$[GeV]	1.27×10^{-9}	9.57×10^{-10}	6.82×10^{-10}	1.56×10^{-9}	2.36×10^{-9}	3.68×10^{-9}

Table 3.4: Best fit solutions for fermion masses and mixing obtained assuming the type-II seesaw dominance in the non-minimal SUSY $SO(10)$ model. Pulls of various observables and predictions obtained at the minimum are shown for six different data sets.

in numerical fits in the type-II case. This mainly arises because the near maximality θ^l_{23} is not directly connected to the the b-τ unification. Thus the cases B, C, D which do not have the b-τ unification also lead to very good fits in contrast to the minimal case. The fits in cases (A, C1, C2) which have b-τ unification are even better and all the observables are fitted almost exactly in these cases. These include the low $\tan\beta$ inputs and cases with large $\tan\beta$ and threshold corrections. As the results of Table 3.5 show, the fits obtained assuming the type-I seesaw dominance are uniformly better compared to the corresponding type-II results and show significantly improvement over the minimal model with type-I dominance, Table 3.3.

One important difference compared to the minimal case is the overall $B-L$ scale determined from the neutrino masses. Unlike the minimal case, the values of r_R^{-1} in Table 3.5 are strongly dependent on the input data set and in some cases are quite large although each data set appear to give very good fit to fermion masses. For example, one obtains in case (A) from Eq. (3.11) and

	A	**B**	**C**	**D**	**C1**	**C2**
Observables	Pulls obtained for best fit solution					
(m_u/m_c)	-0.0151499	0.0262493	-0.0019449	-0.00461056	0.00542513	-0.000078
(m_c/m_t)	-0.0003845	0.0008125	0.0002582	0.004616	-0.003040	0.00490
(m_d/m_s)	-0.0778857	-0.0653974	-0.0053692	0.0272334	0.00701785	0.00147573
(m_s/m_b)	-0.052311	0.0706689	0.0726379	0.0830354	0.0120634	0.0296307
(m_e/m_μ)	0.00127584	0.00152407	0.00164957	0.0268034	-0.00722174	-0.0003495
(m_μ/m_τ)	-0.0553488	-0.0188764	-0.0212797	-0.0282999	-0.00866254	-0.008754
(m_b/m_τ)	-0.0103881	0.0214596	0.0260868	0.0498589	0.00493891	0.00967378
$\left(\frac{\Delta m^2_{sol}}{\Delta m^2_{atm}}\right)$	0.0324886	0.00926157	0.00312614	-0.00630473	-0.00302065	0.000653399
$\sin\theta^q_{12}$	0.0159112	-0.0140628	-0.000195379	0.00791696	-0.0171517	-0.000184021
$\sin\theta^q_{23}$	0.0375281	-0.00674466	-0.00216987	0.00501282	0.0100126	0.00590551
$\sin\theta^q_{13}$	0.0309917	0.0571306	0.175888	0.0213394	-0.131639	-0.00184989
$\sin^2\theta^l_{12}$	0.00539037	-0.0176765	0.00577816	-0.013618	0.0092152	0.000404734
$\sin^2\theta^l_{23}$	0.0332756	0.0143127	0.0125096	0.0200216	0.00356131	0.00026684
$\delta_{\rm CKM}[^\circ]$	-0.0585649	-0.00882152	-0.0406312	-0.0292954	-0.0291351	-0.0310722
χ^2_{min}	**0.0204**	**0.0150**	**0.0392**	**0.0137**	**0.0191**	**0.0011**
Observables	Corresponding Predictions at GUT scale					
$\sin^2\theta^l_{13}$	0.0122064	0.0168745	0.0146633	0.0359278	0.0246489	0.030277
$\delta_{\rm MNS}[^\circ]$	87.6747	22.8731	330.351	282.035	272.186	84.0238
$\alpha_1[^\circ]$	5.82048	167.229	192.077	286.062	352.828	329.804
$\alpha_2[^\circ]$	339.846	331.88	34.5585	336.358	17.6585	325.182
$r_R\left(\frac{m_t^2}{m_\tau}\right)$ [GeV]	6.56×10^{-15}	1.22×10^{-12}	1.34×10^{-12}	3.03×10^{-15}	5.0×10^{-14}	1.40×10^{-13}

Table 3.5: Best fit solutions for fermion masses and mixing obtained assuming the type-I seesaw dominance in the non-minimal SUSY $SO(10)$ model. Pulls of various observables and predictions obtained at the minimum are shown for six different data sets.

Table 3.5,

$$\langle(1,3,-2)\rangle_{\overline{126}_H} \approx 1.5\times10^{20} s_m \cos\beta \text{ GeV}$$

Thus reproducing neutrino masses in this case would require fine tuning $s_m \sim 10^{-4}$ if the $B-L$ breaking scale is to be close to M_{GUT}. In contrast, in case C2 with $\tan\beta = 38$, Table 3.5 gives

$$\langle(1,3,-2)\rangle_{\overline{126}_H} \approx 1.8\times10^{17} s_m \text{ GeV}$$

which is close to the GUT scale.

3.3 Conclusions

In this chapter, we have undertaken an exhaustive analysis of some attractive class of SUSY $SO(10)$ models. Using several different data sets as input, we have numerically determined viability of these models in reproducing the

fermion spectrum. We used data corresponding to different values of $\tan\beta$ and with or without appreciable finite threshold correction. Comparison of different set clearly brings out some interesting features.

- In the minimal model with type-II seesaw dominance, the b-τ unification appears to be a key ingredient. The cases without such unification cannot explain the entire fermion spectrum. In particular, the case of very low $\tan\beta$ showing this unification works much better than the previously studied data set with $\tan\beta = 10$.

- In the non-minimal model with type-II seesaw dominance, one gets good fits compared the minimal model and the b-τ unification is not necessarily required. However, the presence of b-τ unification improves the fit.

- This connection is not required if neutrinos obtain their masses from the type-I seesaw mechanism. In this case one can obtain very good fits in the minimal model almost for every data set used.

- In the case of type-I seesaw dominance, the $B-L$ breaking scale inferred from neutrino masses also lies closer to the GUT scale compared to the type-II seesaw mechanism. The situation becomes better when a 120-plet of Higgs field is added to the model. Here one can get excellent fits to fermion masses in both the type-I and type-II seesaw mechanisms.

Chapter 4

Viability of The Exact Tribimaximal Lepton Mixing in $SO(10)$

The observed mixing pattern among leptons is remarkably close to the tribimaximal mixing (TBM) [77].

$$O_{TBM} = \begin{pmatrix} \sqrt{\frac{2}{3}} & \frac{1}{\sqrt{3}} & 0 \\ -\frac{1}{\sqrt{6}} & \frac{1}{\sqrt{3}} & -\frac{1}{\sqrt{2}} \\ -\frac{1}{\sqrt{6}} & \frac{1}{\sqrt{3}} & \frac{1}{\sqrt{2}} \end{pmatrix} \tag{4.1}$$

This possibly indicates underlying flavour symmetries several of which have been identified and studied, see [78] for a review. Incorporating such symmetries or the tribimaximal mixing into grand unified theories, particularly based on the $SO(10)$ gauge group is quite challenging, see [79, 80] for some examples. Since all fermions in a given generation are unified into a single 16 dimensional irreducible representation of $SO(10)$, imposition of the TBM structure on the leptonic mass matrices also constrains the quark mass matrices. It is not clear if the requirement of the exact tri-bimaximal mixing among leptons would be consistent with a precise description of the quark masses and mixing. In this chapter, we try to address this issue by checking the viability of the exact tribi-

maximal mixing in the non-minimal SUSY $SO(10)$ model. First, we device a general method of incorporating the exact TBM structure within $SO(10)$ and then we use it to obtain quantitative description of the fermion masses and mixing in the model of our interest.

4.1 Leptonic mixing matrices and tribimaximal mixing

We shall derive general forms for the neutrino mass matrix M_ν and the left handed charged lepton mixing matrix U_l which lead in the flavour basis to a neutrino mass matrix $\mathcal{M}_{\nu f}$ exhibiting the TBM structure. We define the TBM structure for $\mathcal{M}_{\nu f}$ as follows:

$$\mathcal{M}_{\nu f} = \frac{1}{3}\begin{pmatrix} 2f_1+f_2 & f_2-f_1 & f_2-f_1 \\ f_2-f_1 & \frac{1}{2}(f_1+2f_2+3f_3) & \frac{1}{2}(f_1+2f_2-3f_3) \\ f_2-f_1 & \frac{1}{2}(f_1+2f_2-3f_3) & \frac{1}{2}(f_1+2f_2+3f_3) \end{pmatrix} , \qquad (4.2)$$

where $f_{1,2,3}$ are complex neutrino masses. This matrix is diagonalized by

$$U_{PMNS} = O_{TBM} Q \ , \qquad (4.3)$$

where Q is a diagonal phase matrix.

A more general definition of TBM structure would be to replace $\mathcal{M}_{\nu f}$ and U_{PMNS} above by $P_l \mathcal{M}_{\nu f} P_l$ and $P_l^* U_{PMNS}$, where P_l denotes a diagonal phase matrix. Since P_l can be rotated away by redefining the charged lepton fields, we shall refer to TBM structure as the one defined by Eqs. (4.2,4.3).

It is known [81, 82] that $\mathcal{M}_{\nu f}$ in Eq. (4.2) is invariant under a $Z_2 \times Z_2$ symmetry. The elements of the $Z_2 \times Z_2$ are defined as

$$S_2 = \frac{1}{3}\begin{pmatrix} -1 & 2 & 2 \\ 2 & -1 & 2 \\ 2 & 2 & -1 \end{pmatrix} \quad \text{and} \quad S_3 = \begin{pmatrix} 1 & 0 & 0 \\ 0 & 0 & 1 \\ 0 & 1 & 0 \end{pmatrix} . \qquad (4.4)$$

and satisfy

$$S_{2,3}^T \mathcal{M}_{\nu f} S_{2,3} = \mathcal{M}_{\nu f} \tag{4.5}$$

We shall exploit this $Z_2 \times Z_2$ invariance in arriving at the structure of U_l. As noted in [75], one can always choose a specific basis in which M_ν exhibits the TBM structure and is thus invariant under $Z_2 \times Z_2$:

$$S_{2,3}^T M_\nu S_{2,3} = M_\nu \tag{4.6}$$

If M'_ν in an arbitrary basis is not invariant under $Z_2 \times Z_2$ then one can go to a new basis with $M_\nu = U^T M'_\nu U$ and choose U in such a way that

$$U_\nu^T M_\nu U_\nu = D_\nu \ , \tag{4.7}$$

with D_ν a diagonal matrix with real positive elements and

$$U_\nu \equiv O_{TBM} P \ . \tag{4.8}$$

P being a general diagonal phase matrix. Let U_l denote the mixing matrix among the left handed charged leptons in a basis in which M_ν is $Z_2 \times Z_2$ symmetric. If such a defined U_l itself is $Z_2 \times Z_2$ symmetric, *i.e.* satisfies

$$S_{2,3}^T U_l S_{2,3} = U_l \tag{4.9}$$

then $\mathcal{M}_{\nu f}$ will also satisfy Eq. (4.5) and thus would exhibit the TBM structure of Eq. (4.2). This follows trivially from the definition

$$\mathcal{M}_{\nu f} = U_l^T M_\nu U_l \ , \tag{4.10}$$

after using Eqs. (4.6,4.9). Thus the $Z_2 \times Z_2$ invariance of U_l is sufficient to ensure the TBM for $\mathcal{M}_{\nu f}$.

Above equation allows us to determine TBM preserving class of U_l in a basis with M_ν satisfying Eq. (4.6). S_3 invariance corresponds to imposing the

μ-τ interchange symmetry on U_l. The S_2 invariance further requires $U_l^T = U_l$ and that the sum of elements in each of its raw must be equal. Such a U_l can be parameterized as

$$U_l = e^{i\alpha} P_l \tilde{U}_l P_l \ , \tag{4.11}$$

where $P_l = \text{diag.}(1, e^{i\beta}, e^{i\beta})$ is a diagonal phase matrix and

$$\tilde{U}_l = \begin{pmatrix} c_\theta & \frac{s_\theta}{\sqrt{2}} & \frac{s_\theta}{\sqrt{2}} \\ \frac{s_\theta}{\sqrt{2}} & -\frac{1}{2}(c_\theta + e^{i\delta}) & -\frac{1}{2}(c_\theta - e^{i\delta}) \\ \frac{s_\theta}{\sqrt{2}} & -\frac{1}{2}(c_\theta - e^{i\delta}) & -\frac{1}{2}(c_\theta + e^{i\delta}) \end{pmatrix} , \tag{4.12}$$

with $\tan\theta = -2\sqrt{2}\cos\beta$. U_l is thus fully determined by three phases α, β and δ.

The form of U_l as given above is the most general one required in order to obtain TBM in the basis with M_ν satisfying Eq. (4.6). The generality is proved by noticing that the $Z_2 \times Z_2$ invariance of U_l is also necessary if $\mathcal{M}_{\nu f}$ is to exhibit the TBM structure. This follows in a straightforward manner. Assume that $\mathcal{M}_{\nu f}$ has TBM structure of Eq. (4.2). The U_{PMNS} matrix in this case can be chosen to have the form in Eq. (4.3). Since $U_l = U_\nu U_{PMNS}^\dagger$, it has the following form in the basis specified by Eq. (4.8):

$$\begin{aligned} U_l &= O_{TBM} P Q^* O_{TBM}^T \ , \\ &= \frac{1}{3} \begin{pmatrix} 2p_1 + p_2 & p_2 - p_1 & p_2 - p_1 \\ p_2 - p_1 & \frac{1}{2}(p_1 + 2p_2 + 3p_3) & \frac{1}{2}(p_1 + 2p_2 - 3p_3) \\ p_2 - p_1 & \frac{1}{2}(p_1 + 2p_2 - 3p_3) & \frac{1}{2}(p_1 + 2p_2 + 3p_3) \end{pmatrix} , \end{aligned} \tag{4.13}$$

where p_i denote the elements of the diagonal phase matrix PQ^*. Interestingly, the above U_l is obtained from the general TBM $\mathcal{M}_{\nu f}$ Eq. (4.2), by replacing the neutrino masses with the phases p_i and like $\mathcal{M}_{\nu f}$ such a U_l is automatically $Z_2 \times Z_2$ symmetric. Thus Eq. (4.9) also becomes necessary for the $Z_2 \times Z_2$ invariance of $\mathcal{M}_{\nu f}$. Eq. (4.13) provides an alternative parametrization of U_l.

It reduces to the earlier parametrization in Eq. (4.12) with the definition

$$\begin{aligned} p_1 &= -e^{i(\alpha+\beta-\eta)}, \\ p_2 &= e^{i(\alpha+\beta+\eta)}, \\ p_3 &= -e^{i(\alpha+2\beta+\delta)}, \end{aligned} \tag{4.14}$$

with $\cos\eta = -3c_\theta \cos\beta$ and $\sin\eta = -c_\theta \sin\beta$.

We note that the U_ν and U_l in Eqs. (4.8,4.11) are defined up to a simultaneous redefinition $U_\nu \to UU_\nu$ and $U_l \to UU_l$. In addition, U_l can also be multiplied by an arbitrary phase matrix from the right. Since P_l is arbitrary, the U_l in some model may not appear to have the $Z_2 \times Z_2$ invariance even in a basis with U_ν chosen as in Eq. (4.8). But the above exercise shows that U_l can always be chosen to have the TBM form by appropriate rephasing of the charged lepton fields.

The above reasoning can be applied to more general patterns of mixing and not just to TBM. The key role in this construction is played by the fact that one can always choose a basis in which M_ν is $Z_2 \times Z_2$ symmetric. This follows from the fact that the $Z_2 \times Z_2$ symmetry does not put any restrictions on the neutrino masses but only on the structure of mixing. As long as the neutrino mass matrices obey such "mass-independent" symmetries, the above construction of determining the most general U_l can be carried through. One can indeed define [81, 82] an appropriate $Z_2 \times Z_2$ symmetry corresponding to every mixing pattern and then impose this symmetry on U_l to obtain the desired mixing structure in the flavour basis.

4.2 Obtaining the exact TBM in $SO(10)$ model

We now integrate the above leptonic structures into an $SO(10)$ model discussed in the previous chapter *i.e.* the supersymmetric $SO(10)$ model with the Higgs transforming as $10, \overline{126}, 120$ representations of $SO(10)$. For simplicity, we assume that the dominant contribution to M_ν is a type-II seesaw, *i.e.*

linear in the $\overline{126}$ Yukawa coupling. The last assumption with its attractive consequences is made in a number of $SO(10)$ models [51, 71, 73, 74, 75]. But it is also realized [70, 83] that its justification requires a non-minimal Higgs sector.

The fermion mass relations in this case after electroweak symmetry breaking are already shown in Eq. (3.15) and the light neutrino mass matrix is given by Eq. (3.6). The first term proportional to F denotes type-II seesaw contribution. In the numerical analysis that follows, we shall assume that M_ν is entirely given by this term and subsequently analyze the effect of a small type-I corrections on the numerical solution found.

We can always rotate the 16-plet fermions in generation space in such a way that $M_\nu \propto F$ is diagonalized by the TBM matrix.

$$F \to R^T F R = F_{TBM} \equiv O_{TBM}\ \text{Diag.}(f_1, f_2, f_3)\ O_{TBM}^T \tag{4.15}$$

where f_i are now real eigenvalues of F and the O_{TBM} is given by Eq. (4.1). The matrix $(G)H$ maintains its (anti)symmetric form in such basis and we use the same label for them in the rotated basis. In case of type-II seesaw dominance, the light neutrino mass matrix $M_\nu = r_L F_{TBM}$ has the form given on the RHS of Eq. (4.2). The model has altogether 17 independent real parameters (3 in F_{TBM}, 6 in H, 3 in G, r, s, t_u, t_l and r_L) which determine the entire 22 low energy observables of the fermion mass spectrum. Some of these parameters can be fixed by the known values of observables directly. As noted in [84], the $SO(10)$ relation for the charged lepton mass matrix in Eq. (3.15) can be rewritten as

$$H + i t_l G = V_l D_l V_l^\dagger + 3 F_{TBM}\ , \tag{4.16}$$

where D_l is a diagonal charged lepton mass matrix. Since H and G are real, the real and imaginary parts of the RHS separately determine H and $t_l G$ in terms of the charged lepton masses, parameters of F_{TBM} and V_l. V_l is a unitary matrix that diagonalizes M_l and contains nine free parameters in the most general situation. One can suitably write $V_l = \tilde{V}_l P$ where P is diagonal

phase matrix and $\tilde{V}_l$ contains six real parameters. From Eq. (4.16), it is easy to see that the phase matrix P does not play any role in determining H and G and can be removed. So the nine real parameters of LHS can be related to six real parameters of $\tilde{V}_l$, three charged lepton masses and parameters of F_{TBM} in Eq. (4.16). This fixing helps us in numerical analysis as we will see in the next subsection.

4.3 Numerical analysis

We perform a numerical analysis to study the viability of Eq. (3.15) with the experimentally observed values of fermion masses and mixing angles. We shall present numerical analysis in two different cases. (A) Corresponding to the most general V_l (B) with $V_l = U_l$ given as in Eqs. (4.11,4.12). The case (A) has already been studied numerically in [75, 83, 84]. Since our numerical procedure is somewhat different, we repeat this analysis and use it as a benchmark with which to compare the case (B) which leads to the exact TBM at M_{GUT}. We use the same χ^2 fitting procedure used in the previous chapter to fit the model with the data. To make consistent comparison of this scenario with other existing models analyzed in [75] we use the same input values of quark and lepton masses and mixing angles as used in [75]. In this data set, the charged fermion masses at the GUT scale are [58] obtained from the low energy values using MSSM and $\tan\beta = 10$. The effect of the RG evolution on the quark mixing angles is known to be negligible. This is also true for the lepton mixing angles in case of the hierarchical neutrino spectrum. We assume such hierarchy in neutrino masses and therefore the input values of the quark mixing angles, CP phase and neutrino parameters we use correspond to their values at low energy. The lepton mixing angles and solar and atmospheric squared mass differences are taken from [85]. We reproduce all these input values in Table 4.1 for convenience of the reader.

GUT scale values with propagated uncertainty			
m_d(MeV)	1.24 ± 0.41	$\Delta m^2_{sol}(\text{eV}^2)$	$(7.65 \pm 0.23) \times 10^{-5}$
m_s(MeV)	21.7 ± 5.2	$\Delta m^2_{atm}(\text{eV}^2)$	$(2.40 \pm 0.12) \times 10^{-3}$
m_b(GeV)	$1.06^{+0.14}_{-0.09}$	$\sin\theta^q_{12}$	0.2243 ± 0.0016
m_u(MeV)	0.55 ± 0.25	$\sin\theta^q_{23}$	0.0351 ± 0.0013
m_c(GeV)	0.210 ± 0.021	$\sin\theta^q_{13}$	0.0032 ± 0.0005
m_t(GeV)	$82.4^{+30.3}_{-14.8}$	$\sin^2\theta^l_{12}$	0.304 ± 0.022
m_e(MeV)	0.3585 ± 0.0003	$\sin^2\theta^l_{23}$	0.50 ± 0.07
m_μ(MeV)	75.672 ± 0.058	$\sin^2\theta^l_{13}$	$< 0.04(3\sigma)$
m_τ(GeV)	1.2922 ± 0.0013	J_{CP}	$(2.2 \pm 0.6) \times 10^{-5}$

Table 4.1: Input values for quark and leptonic masses and mixing angles in the MSSM extrapolated at $M_{GUT} = 2 \times 10^{16}$ GeV for $\tan\beta = 10$ which we use in our numerical analysis.

4.3.1 The most general lepton mixing

We fit the above data to the fermion mass relations (3.15) predicted in the model by numerically minimizing the χ^2 function. As already mentioned above, this exercise has been done in [75] and a very good fit corresponding to $\chi^2_{min} = 0.127$ is found. We repeat the same analysis because of the following differences in our fitting procedure:

- Compared to other observables, the charged lepton masses are known very precisely with extremely small errors in their measurements. Instead of fitting them through χ^2 minimization, we use their central values as inputs on the RHS of Eq. (4.16). Because of this, our definition of the χ^2 function in Eq. (A.5) does not include the charged lepton masses in it.

- We also use the central value of the solar to the atmospheric mass squared difference ratio as an input and use it to fix f_3 through the following relation:

$$f_3 = f_2 \left(\frac{\Delta m^2_{atm}}{\Delta m^2_{sol}} + \left(1 - \frac{\Delta m^2_{atm}}{\Delta m^2_{sol}}\right) \left(\frac{f_1}{f_2}\right)^2 \right)^{1/2} . \qquad (4.17)$$

After obtaining the solution, the overall scale of neutrino masses r_L at

the minimum is determined by using the atmospheric scale as a normalization.

- In [75], the reactor angle θ_{13}^l is included in the χ^2 function and fitted to its value $\sin^2\theta_{13}^l = 0.01 \pm 0.016$ obtained from the global fits to neutrino oscillation data. We do not include θ_{13}^l in the definition of χ^2 function but do the minimization with a constrain $\sin^2\theta_{13}^l \leq 0.04$ which is the present 3σ upper bound on it [85].

As a result of these simplifications, the χ^2 function in our approach includes only 12 observables, 6 quark masses, 3 quark mixing angles, a CKM phase and 2 lepton mixing angles. These are complex nonlinear functions of 12 real parameters (2 in F_{TBM}, 6 in V_l, r, s, t_l and t_u). This χ^2 is numerically minimized as discussed in Appendix A.2. The results of our analysis are shown in column A in Table 4.2.

We obtain an excellent fit corresponding to $\chi^2_{min} = 0.035$ which is slightly better than $\chi^2_{min} = 0.127$ obtained in [75]. Parameters obtained for the best fit solutions are shown in Appendix B.2. All the observables are fitted within the 0.1σ deviation from their central values. The solution at its minimum predicts large reactor mixing angle $\sin^2\theta_{13}^l \approx 0.039$ near to its present upper bound.

4.3.2 The exact tribimaximal lepton mixing

After discussion of the above general case, we now specialize to the case of the exact TBM. This case is of considerable theoretical interest since it can point to some underlying symmetry existing at M_{GUT}. We can implement the exact TBM in a model independent way by choosing $V_l = U_l$ in Eq. (4.16). With this choice, all the leptonic mixing angles get fixed to their TBM values. Also the central value of the ratio of the solar to the atmospheric (mass)^2 differences is used as input and a parameter r_L is determined at the minimum by using the atmospheric scale. Thus the χ^2 function in Eq. (A.5) now involves only observables in the quark sector. As already discussed, U_l in Eqs. (4.11,4.12)

	Case A		**Case B1**		**Case B2**	
Observables	Fitted value	Pull	Fitted value	Pull	Fitted value	Pull
m_d[MeV]	1.19851	−0.101205	1.22098	−0.0463899	1.02686	−0.519852
m_s[MeV]	22.1374	0.0841145	21.9922	0.0561874	22.0058	0.058806
m_b[GeV]	1.05103	−0.0996223	1.16345	0.738942	1.2842	1.60145
m_u[MeV]	0.550206	0.000824013	0.550234	0.000936368	0.550787	0.00314771
m_c[GeV]	0.209956	−0.00208935	0.209952	−0.00230315	0.210481	0.0229054
m_t[GeV]	82.6175	0.00717855	82.5855	0.00612198	81.7487	−0.0440052
m_e[MeV]	0.3585	–	0.3585	–	0.3585	–
m_μ[MeV]	75.672	–	75.672	–	75.672	–
m_τ[GeV]	1.2922	–	1.2922	–	1.2922	–
$\left(\frac{\Delta m^2_{sol}}{\Delta m^2_{atm}}\right)$	0.031875	–	0.031875	–	0.031875	–
$\sin\theta^q_{12}$	0.224299	−0.0007232	0.2243	0.0002182	0.224303	0.0019076
$\sin\theta^q_{23}$	0.0350871	−0.0099165	0.0350951	−0.0038047	0.0351294	0.022597
$\sin\theta^q_{13}$	0.00317877	−0.0424606	0.00319436	−0.0112796	0.0031749	−0.0502087
$\sin^2\theta^l_{12}$	0.303622	−0.0171641	**0.3333**	–	**0.3333**	–
$\sin^2\theta^l_{23}$	0.501109	0.015842	**0.5**	–	**0.5**	–
$\sin^2\theta^l_{13}$	**0.0394**	–	**0**	–	**0**	–
J_{CP}	2.24×10^{-5}	0.0732629	2.21×10^{-5}	0.0194165	2.25×10^{-5}	0.0845729
δ_{MNS}	**273.934**	–	–	–	–	–
α_1	**186.801**	–	**160.829**	–	**180**	–
α_2	**70.8178**	–	**318.593**	–	**0**	–
r_L	6.62×10^{-10}	–	9.82×10^{-10}	–	3.53×10^{-9}	–
χ^2_{min}		**0.0351**		**0.5519**		**2.8510**

Table 4.2: Best fit solutions for fermion masses and mixing obtained assuming type-II seesaw dominance in the SUSY $SO(10)$ model with $10 + \overline{126} + 120$ Higgs. Various observables and their pulls at the minimum are shown for three different cases correspond to (A) the general (non TBM) leptonic mixing, (B1) Exact TBM leptonic mixing with U_l of Eqs. (4.11,4.12) and (B2) Exact TBM leptonic mixing with diagonal M_l and $t_l = 0$ (See the discussions in the text for more details). The predictions of different approaches are shown in boldface.

is parameterized by three phase angles α, β and δ. An overall phase α is irrelevant for the physical observables and can be removed. This leaves only 8 real parameters (2 in F_{TBM}, 2 in U_l, r, s, t_l and t_u) which are fitted to the 10 observables in the quark sector by minimizing the χ^2. The results are shown in column B1 in Table 4.2. The obtained fit corresponds to $\chi^2_{min} = 0.552$ (χ^2_{min}/d.o.f. = 0.276). Only the fitted value of m_b deviates slightly from the central value with a 0.74σ pull. All the remaining observables are fitted within 0.06σ. A set of parameters obtained for this solutions are shown in Appendix B.2. The fit obtained here is not significantly different from the general case discussed before showing that all the fermion masses and mixing angles can be nicely reproduced along with the exact TBM within the $SO(10)$ framework discussed here.

Before we discuss possible perturbations in TBM pattern, let us discuss

a very special case corresponding to a diagonal M_l. This corresponds to U_l coinciding with an identity matrix and is a special case of Eqs. (4.11,4.12) with $\beta = \frac{\pi}{2}$ and $\delta = 0$. Since M_l is real and diagonal in this case, $t_l G$ must vanish in Eq. (4.16). If $G = 0$ then the quark mass matrices also become real and there is no room for CP violation. The viable scenario must therefore have nonzero G and hence $t_l = 0$. As a result, unlike before, the three parameters in G do not get determined from M_l, see, Eq. (4.16) and remain free. They can be fitted from the quark sector observables. We carried out a separate numerical analysis for this particular case and the results are shown in column B2 in Table 4.2. The fit obtained gives relatively large $\chi^2_{min} = 2.85$ (χ^2_{min}/d.o.f. = 1.43) with more than 1σ deviation in the bottom quark mass. Although the obtained χ^2_{min} is statistically acceptable at 90% confidence level, it is not as good as the previous one and we shall not consider this case with $U_l = I$ any further.

4.4 Perturbations to the tribimaximal mixing

The TBM is an ideal situation and various perturbations to this can arise in the model. We need to analyze these perturbations in order to distinguish this case from the generic case without the built in TBM. A deviation from tri-bimaximality can arise due to

1. renormalization group evolution (RGE) from M_{GUT} to M_Z.

2. small contribution from the sub dominant type-I seesaw term in Eq. (3.6).

3. the breaking of the $Z_2 \times Z_2$ symmetry in U_l which ensured TBM.

The effect of (1) is known to be negligible [86, 87] in case of the hierarchical neutrino mass spectrum which we obtain here. We quantitatively discuss the implications of the other two scenarios via detailed numerical analysis in the following subsections.

4.4.1 Perturbation from type-I seesaw

Depending on the GUT symmetry breaking pattern and parameters in the superpotential of the theory, a type-I seesaw contribution can be dominant or sub dominant compared to type-II but it is always present and can generate deviations in an exact TBM mixing pattern in general. In the approach pursued here it is assumed that such contribution remains sub dominant and generates a small perturbation in dominant type-II spectrum. Eq. (3.6) can be rewritten as

$$M_\nu = r_L(F - \xi M_D F^{-1} M_D^T) \tag{4.18}$$

where $\xi = r_R/r_L$ determine the relative contribution of type-I term in the neutrino mass matrix.

The second term in Eq. (3.6) brings in two new parameters ξ and t_D present in the definition of M_D in Eq. (3.9). These parameters however affect only the neutrino sector. We isolate the effect of type-I contribution by choosing other parameters at the χ^2 minimum found in Section 4.3.2. ξ and t_D remain unconstrained at this minimum and their values do not change the χ^2 obtained earlier since the latter contains only the observables in the quark sector. The ξ, t_D however generate departure from the exact TBM. We randomly vary the parameters ξ and t_D and evaluate the neutrino masses and mixing angles. While doing this, we take care that all these observables remain within their present 3σ [85] limits. Such constrains allow very small values of $|\xi| \leq 10^{-7}$. The correlations between different leptonic mixing angles found from such analysis are shown in Fig. 4.1.

It is seen from Fig. 4.1 that the perturbation induced by type-I term cannot generate considerable deviation in the reactor angle if the other two mixing angles are to remain within their 3σ range. In particular, requiring that $\sin^2\theta_{12}^l$ remains within the 3σ range puts an upper bound $\sin^2\theta_{13}^l \leq 0.0002$. Moreover, the model predicts interesting correlations between the solar and the atmospheric mixing angles. The present 1σ range of the solar mixing angle prefers the range $0.45 - 0.5$ for $\sin^2\theta_{23}^l$ and this range will become narrower

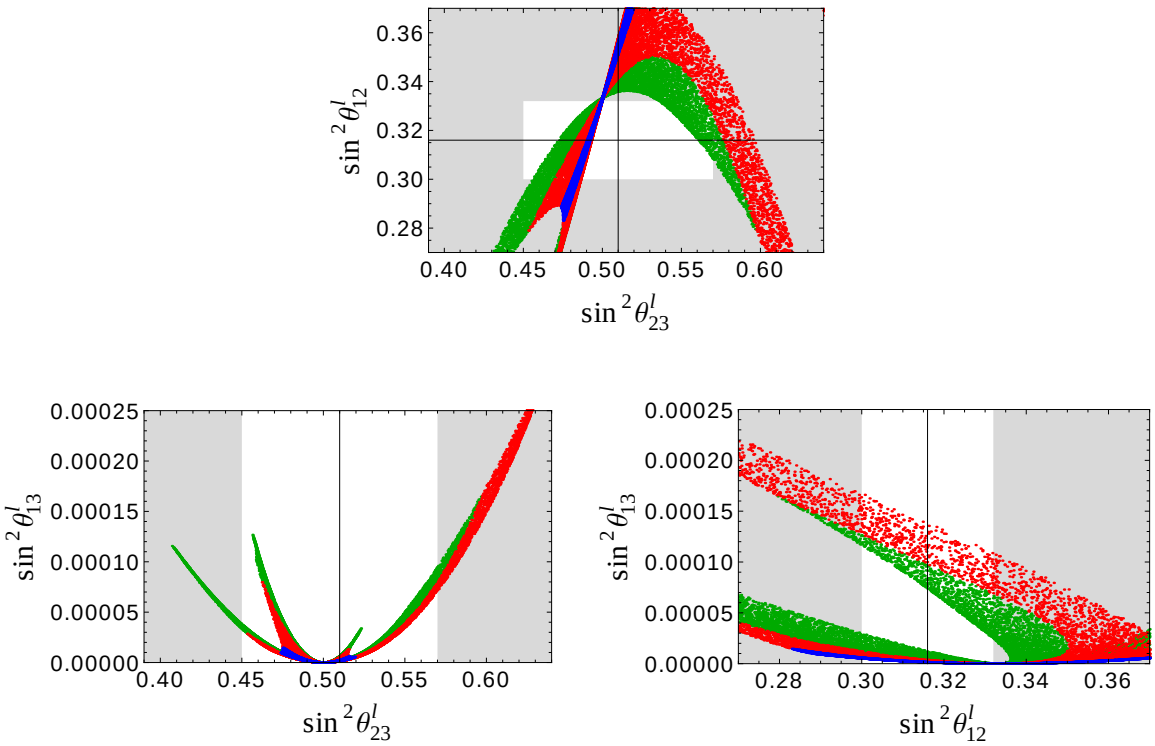

Figure 4.1: Correlations among the lepton mixing angles when two real parameters ξ and t_D are varied randomly. The points with different colors correspond to $|t_D| < 1$ (blue), $1 \leq |t_D| < 5$ (red) and $5 \leq |t_D| < 10$ (green). The black lines are the updated central values of $\sin^2\theta^l_{12}$ and $\sin^2\theta^l_{23}$ obtained by the global fits on neutrino oscillation data [85]. The unshaded and the shaded regions correspond to 1σ and 3σ bounds respectively.

with more precise measurements of θ^l_{12}.

4.4.2 Perturbation from the charged lepton mixing

A different class of perturbation to TBM arise when U_l deviates from its $Z_2 \times Z_2$ symmetric form given in Eq. (4.11). In this case, the neutrino mass matrix has TBM structure but the charged lepton mixing leads to departure from it. This case has been considered in the general context (for examples, see [88] and references therein) as well as in $SO(10)$ context [75]. Within our approach, we can systematically look at the perturbations which change the values of any one or more angles from the TBM value. Alternative possibility is to simultaneously perturb all three mixing angles and look at the quality of fit compared to the exact TBM case. We follow this approach. For this we

choose U_l to be a general unitary matrix and go back to the analysis in Section III-A. There, we have fitted the solar and the atmospheric mixing angles to their low energy values given in Table 4.1. Here, we modify the definition of χ^2 and pin down a specific value o_i of the mixing angles p_i by adding a term

$$\chi^2_{lm} = \sum_i \left(\frac{p_i - o_i}{0.01 o_i} \right)^2 \tag{4.19}$$

to χ^2_q that contains all the observables of the quark sector. Sum in Eq. (4.19) runs over the three lepton mixing angles. The $\chi^2 = \chi^2_q + \chi^2_{lm}$ is then numerically minimized to fit the 13 observables determined in terms of 12 real parameters as mentioned in Section 4.3.1. Artificially introduced small errors in Eq. (4.19) fix the value o_i for p_i at the minimum of the χ^2. We then look at the quantity

$$\bar{\chi}^2_{min} \equiv \chi^2|_{min} - \chi^2_{lm}|_{min} \tag{4.20}$$

which represents the fit to the quark spectrum when the lepton mixing angles p_i are pinned down to values o_i. We repeat such analysis by randomly varying o_i within the allowed 3σ ranges of lepton mixing angles [85]. The results are displayed in Fig. 4.2.

We plot the correlations among the lepton mixing angles and show the corresponding values of $\bar{\chi}^2_{min}$ in three different regions. The points corresponding to $\bar{\chi}^2_{min} < 1$ (green) represent very good fit in which all the observables are fitted within 1σ. The obtained fit shown by the points corresponding to $1 \leq \bar{\chi}^2_{min} < 4$ (blue) is not as good as the previous one but it is statistically acceptable. The points for $\bar{\chi}^2_{min} > 4$ (red) represent poor fit and can be ruled out at 95% confidence level. Fig. 4.2 shows definite correlations between θ^l_{23} and θ^l_{13}. It is seen that the region $\bar{\chi}^2_{min} < 4$ falls largely above $\sin^2\theta^l_{13} > 0.005$ for $\sin^2\theta^l_{23} = 0.5$ which may be regarded as an approximate lower bound on θ^l_{13}. Such a lower bound on θ^l_{13} increases with atmospheric mixing angle if $\sin^2\theta^l_{23} > 0.5$. This is to be contrasted with the previous case where perturbation from type-I seesaw term led to an upper bound. The bounds obtained

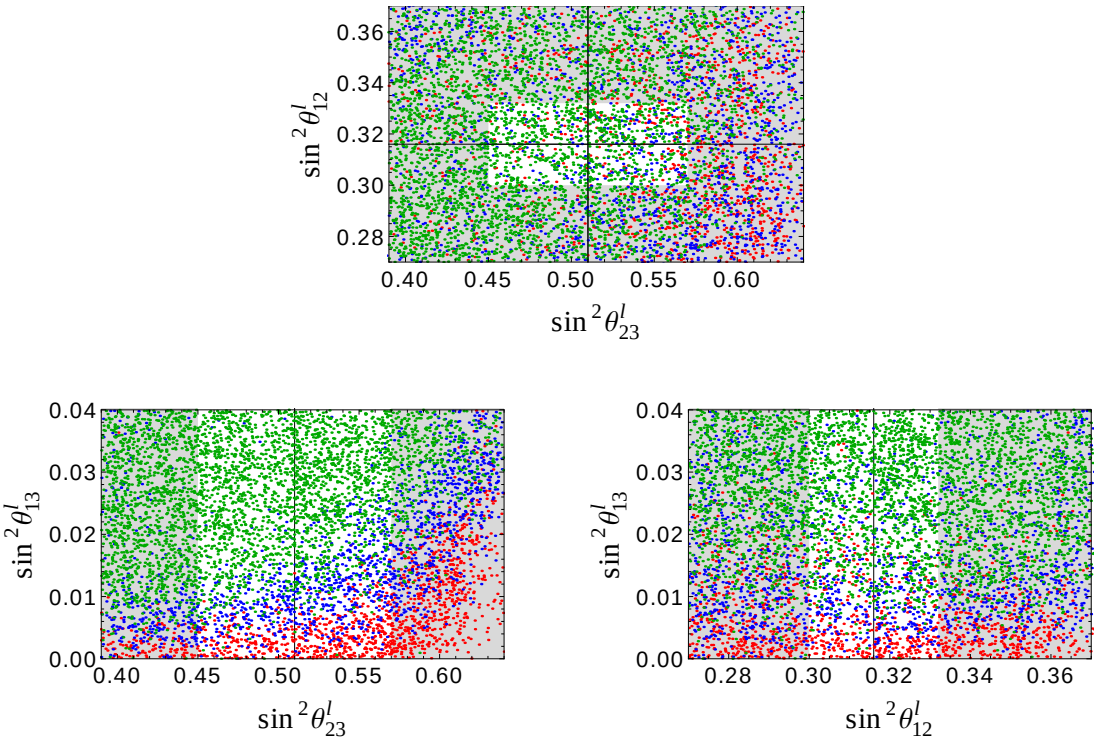

Figure 4.2: Correlations among the lepton mixing angles in case of the most general charged lepton mixing matrix U_l. The points with different colors correspond to $\bar{\chi}^2_{min} < 1$ (green), $1 \leq \bar{\chi}^2_{min} < 4$ (blue) and $\bar{\chi}^2_{min} \geq 4$ (red). The black lines are the updated central values of $\sin^2\theta^l_{12}$ and $\sin^2\theta^l_{23}$ obtained by the global fits on neutrino oscillation data [85]. The unshaded and the shaded regions correspond to 1σ and 3σ bounds respectively.

numerically would allow us to clearly distinguish the case of the exact TBM at M_{GUT} in comparison to the one in which the charged leptons lead to departures from the tribimaximality. Unlike in the previous case, we do not find any clear correlation among the solar and atmospheric mixing angles in this case. The situation here is qualitatively different from the perturbation due to type-I term.

4.5 Conclusions & outlook

We have analyzed the viability of the exact tribimaximal mixing in a larger context of the grand unified $SO(10)$ theory taking a specific model as an example. The TBM structure for the neutrino mass matrix is a matter of choice of the basis [75]. Thus the existence of TBM is linked to the structure of

the charged lepton mixing matrix U_l in this basis. All the related studies in this context [75, 88] assume that U_l deviates slightly from identity and discuss the breaking of the TBM pattern through such U_l. We have shown that it is possible to construct a class of non-trivial U_l quite different from identity which preserve the TBM structure of M_ν when transformed to the flavour basis. Identification of such non-trivial U_l becomes crucial in the context of $SO(10)$ and allows us to obtain a viable fit to fermion spectrum keeping TBM intact. The quality of fit obtained in this case is excellent as shown in Table 4.2 and differs only marginally from a general situation without imposing the TBM structure at the outset.

The existence of TBM at the GUT scale may be inferred by considering its breaking which can arise in the model and the reactor mixing angle is a good pointer to this. The quantum corrections are known [86, 87] to lead to very small θ_{13}^l for the hierarchical neutrinos. Similarly, corrections coming from type-I seesaw term imply an upper bound, $\sin^2\theta_{13}^l \leq 0.0002$ as discussed in Section 4.3.1. These two cases are in sharp contrast to a situation in which one does not impose the TBM at M_{GUT} and determined U_l from a detailed fits to fermion masses as done here and in [75]. Requiring that one gets an acceptable fit, one is lead to an approximate lower bound $\sin^2\theta_{13}^l \geq 0.005$ in this case. θ_{13}^l can thus provide a good way of determining the existence or otherwise of the exact TBM at M_{GUT} in the specific model considered here.

Very recently, the observations of $\nu_e - \nu_\mu$ oscillation by T2K [89] and MINOS [90] experiments and their combined effect on global fits [91, 92] of neutrino oscillation data have indicated that θ_{13}^l is nonzero at 3σ. If confirmed, these results disfavor the exact TBM pattern in the lepton mixing. Taking this into the consideration, we have updated our numerical analysis and its results are reported in [93]. It is found that the quantum corrections and corrections coming from type-I seesaw term can be ruled out by relatively large value of θ_{13}^l as indicated by the observations from T2K and MINOS. However, the perturbations from the charged lepton mixing can provide the large θ_{13}^l consistent with the detailed description of all the fermion masses and mixing angles.

Chapter 5

Supersymmetric $SO(10)$ Models with Flavour Symmetries

The two major elements of the flavor puzzle in the SM are: (i) strong mass hierarchy in the quark and charged lepton sector in contrast to the weak mass hierarchy for neutrinos; (ii) large lepton mixing angles *i.e.* $\theta_{23}^{l} = 45^{o}$ and $\theta_{12}^{l} = 35^{o}$ as against small quark mixing angles $\theta_{23}^{q} = 2.5^{o}$ and $\theta_{12}^{q} = 12^{o}$ and some empirical relations between some of the mixing angles and the fermion masses. In generic bottom-up pictures where quarks and leptons are treated as different species of particles with no particular relation between them, this problem is not so serious since one can simply focus on each sector separately, as is often done for neutrinos [11, 78, 94, 95]. In this kind of approaches, a suitable flavour symmetry, applied on the quark and lepton sector separately, can lead to the understanding of (i) and/or (ii). However all these approaches fail in explaining the origin of differences between quark and lepton sector. Since grand unified theories not only unify different gauge couplings at a high scale but also unify quarks and leptons within a single framework, they have often been thought of as an attractive venue for unraveling this puzzle. However, in grand unified theories where the quarks and leptons unify at a very high scale, one would naively expect that their masses and mixings would exhibit a similar pattern. Therefore a major challenge in such frameworks is to find out a suitable flavor symmetry which uniquely determines the observed differences

in the flavor patterns of quarks and leptons. This makes it highly nontrivial to understand all the details of flavor puzzle although many attempts have been made (see [11, 78] for examples and references therein).

In this chapter, we propose and study some similar models in which the suitable flavor symmetries are integrated in the SUSY $SO(10)$ GUT framework. The consequences of such integrations are unique and very interesting. For example, we discuss the μ-τ symmetric $SO(10)$ in the first section of this chapter which explain the observed differences between quark and lepton mixing angles. In the second section, we propose a specific ansatz followed by a flavor symmetry that leads to the quasidegenerate neutrinos which is generally opposed in the GUTs because of the quark-lepton unification. In the last section, we discuss an $SO(10)$ GUT model with a discrete family symmetry which predicts several interesting relations between the observables of quark and lepton sectors.

5.1 Fermion masses and mixing in μ-τ symmetric $SO(10)$

5.1.1 μ-τ symmetry

There exist variety of theoretical frameworks/specific models [94, 95] which try, to account for the large atmospheric mixing angle observed more than a decade ago. One class of theories attribute the maximal atmospheric mixing to the presence of some underlying flavour symmetry. This would be a preferred alternative if the deviation of the atmospheric mixing angle from maximality is constrained to be very small. The simplest of such flavour symmetries is the μ-τ symmetry [96, 97, 98, 99, 100, 101, 102] which exchanges the μ and τ fields. The light neutrino mass matrix M_ν is restricted to have the following

form in the presence of this symmetry:

$$M_\nu = \begin{pmatrix} X & A & A \\ A & B & C \\ A & C & B \end{pmatrix} \tag{5.1}$$

If it is assumed to be true in the flavour basis, this form leads to a maximal atmospheric mixing and comes with an additional prediction that one of the three leptonic mixing angles namely, θ_{13}^l must be zero. In the same basis, the charged lepton mass matrix is diagonal and consequently, it is not invariant under the μ-τ symmetry which would have implied $m_\mu = m_\tau$.

μ-τ symmetry is predictive and simple but it appears to have two shortcomings. Successful predictions follow only if it is an effective symmetry of the neutrino mass matrix in specific basis corresponding to a diagonal charged lepton mass matrix. The underlying flavour symmetry in general may not pick up this basis. Secondly, μ-τ symmetry has been proposed with a view of explaining the mixing angles in the leptonic sector alone. It would be more desirable to have a symmetry providing overall understanding of complete fermionic mass spectrum. This can be done using the grand unified theory as the underlying framework. Various alternatives within such theories to simultaneously obtain small mixing in the quark sector and large mixing among leptons have already been proposed [11, 51, 103].

5.1.2 μ-τ symmetric $SO(10)$

If μ-τ symmetry is to be integrated with grand unification then a more general symmetry which exchanges the second and third generations of fermions should be imposed. Consequences of this generalization were first considered in [98, 99, 100]. It was subsequently noted [101] that this generalization automatically leads to understanding of why Cabibbo angle is larger than other two angles and a mild breaking of this symmetry was shown to lead to a correct description of the quark mixing angles and masses. Most of these works did not use the

grand unified framework. Here, we consider a model based on the $SO(10) \otimes Z_2^{\mu-\tau} \otimes Z_2^P$. The first Z_2 corresponds to the generalized μ-τ symmetry. The second Z_2 symmetry called [71] "parity" interchanges two components of the 16_F field transforming as $(4,2,1)$ and $(\overline{4},1,2)$ under the Pati-Salam group decomposition (2.17).

We use the non-minimal SUSY $SO(10)$ model discussed in Chapter 3 as a basic framework. As already shown in Section 3.2, the model predicts the Yukawa sum-rules (3.14) which can be suitably written as:

$$\begin{aligned} M_d &= H + F + i\, G\ , \\ M_u &= rH + sF + i\, t_u G\ , \\ M_l &= H - 3F + i\, t_l\, G\ , \\ M_D &= rH - 3sF + i\, t_D\, G\ , \\ M_L &= r_L F\ , \\ M_R &= r_R^{-1} F. \end{aligned} \tag{5.2}$$

The generalized parity symmetry Z_2^P makes the matrices H, F and G real. In addition, if all VEVs and (hence r, s, t, p, q, r_L, r_R) are real then all the Dirac masses in Eq. (5.2) are Hermitian and M_L, M_R are real. We assume that the 10_H and $\overline{126}_H$ fields are invariant under the generalized μ-τ symmetry while the 120_H changes sign. This assumption allows spontaneous breaking of the μ-τ symmetry. The resulting structures for H, F, G are given by

$$H = \begin{pmatrix} h_{11} & h_{12} & h_{12} \\ h_{12} & h_{22} & h_{23} \\ h_{12} & h_{23} & h_{22} \end{pmatrix};\quad F = \begin{pmatrix} f_{11} & f_{12} & f_{12} \\ f_{12} & f_{22} & f_{23} \\ f_{12} & f_{23} & f_{22} \end{pmatrix};\quad G = \begin{pmatrix} 0 & g_{12} & -g_{12} \\ -g_{12} & 0 & g_{23} \\ g_{12} & -g_{23} & 0 \end{pmatrix} \tag{5.3}$$

All the coefficients in these matrices are real. They satisfy

$$S^T(H, F, G)S = (H, F, -G)\ , \tag{5.4}$$

where

$$S = \begin{pmatrix} 1 & 0 & 0 \\ 0 & 0 & 1 \\ 0 & 1 & 0 \end{pmatrix} \tag{5.5}$$

exchanges the second and the third generations. The effective neutrino mass matrix M_ν (3.6) for the three light neutrinos is a combination of type-I and type-II seesaw mechanisms which we rewrite here for convincingness.

$$M_\nu = r_L F - r_R M_D F^{-1} M_D^T \equiv M_\nu^{II} + M_\nu^I \tag{5.6}$$

In general, both contributions are present but one may dominate over the other. We shall be considering two separate cases corresponding to the type-II and type-I dominance respectively.

The relations $\theta_{23}^l = \frac{\pi}{4}$ and $\theta_{13}^l = 0$ are major predictions and motivation for imposing the μ-τ symmetry. These can arise if the effective neutrino mass matrix $\mathcal{M}_{\nu f}$ in flavour basis possesses a μ-τ symmetry. Let us see how this can come about in our approach. It is easy to see that the fermionic mass matrices in our model satisfy:

$$S^{-1} M_f S = M_f^* \ , \tag{5.7}$$

$$S^{-1} M_\nu^{II} S = M_\nu^{II} \ , \tag{5.8}$$

$$S^{-1} M_\nu^{I} S = M_\nu^{I*} \ . \tag{5.9}$$

$f = u, d, l, D$ label the (Dirac) fermionic mass matrices. The $M_\nu^{I,II}$ correspond to the type-I and II contributions to the light neutrino mass matrix, Eq. (3.6). Let us note that

- Eq. (5.8) implies an exact μ-τ symmetry for M_ν^{II}.

- Eqs. (5.7,5.9) correspond to an invariance under the generalized CP

transformation defined [97, 104, 105] as

$$f_\alpha \to iS_{\alpha\beta}\gamma^0 C\overline{f_\beta}^T \tag{5.10}$$

- If Eq. (5.8) represents the neutrino masses in flavour basis then one obtains the predictions $\theta_{23}^l = \frac{\pi}{4}$ and $\theta_{13}^l = 0$.

- If Eq. (5.9) holds in the flavour basis then only the θ_{23}^l is maximal with definite correlations of θ_{13}^l with the CP violating phase δ_{PMNS} [104, 105].

- M_l is not diagonal here and hence these predictions do not follow immediately. It is still possible to recover these predictions even with a non-diagonal M_l.

Define

$$U_l^\dagger M_l U_l = D_l \ , \tag{5.11}$$

where D_l is the diagonal mass matrix for the charged leptons. By factoring out a diagonal phase matrix P_l, the U_l can be written as:

$$U_l \equiv \tilde{U}_l P_l \tag{5.12}$$

The neutrino mass matrix in the flavour basis is then given by

$$\mathcal{M}_{\nu f} = P_l^\dagger \tilde{U}_l^\dagger M_\nu \tilde{U}_l^* P_l^* \equiv P_l^\dagger \tilde{\mathcal{M}}_{\nu f} P_l^* \tag{5.13}$$

The predictions of the μ-τ symmetry are recovered if $\tilde{\mathcal{M}}_{\nu f}$ is μ-τ invariant. This does not require a diagonal M_l. A general μ-τ symmetric $\tilde{U}_l$ satisfying $S^{-1}\tilde{U}_l S = \tilde{U}_l$ will do the job in case of the type-II dominance. This makes it possible to recover the predictions of the μ-τ symmetry for a non-diagonal M_l and obtain reasonably good fits to other fermion masses and mixing.

It is known [97, 104, 105] that with appropriate choice of P_l, $\tilde{U}_l$ can be cast

into the following form if M_l satisfies Eq. (5.7):

$$\tilde{U}_l = \begin{pmatrix} u_{1l} & u_{2l} & u_{3l} \\ w_{1l} & w_{2l} & w_{3l} \\ w^*_{1l} & w^*_{2l} & w^*_{3l} \end{pmatrix} , \tag{5.14}$$

with real u_{il}. A unitary matrix with this form can be parametrized in terms of two angles and a phase.

$$\tilde{U}_l = P_\eta \begin{pmatrix} c_1 & s_1 c_2 & s_1 s_2 \\ \frac{s_1}{\sqrt{2}} & -\frac{1}{\sqrt{2}}(c_1 c_2 - i\epsilon s_2) & -\frac{1}{\sqrt{2}}(c_1 s_2 + i\epsilon c_2) \\ \frac{s_1}{\sqrt{2}} & -\frac{1}{\sqrt{2}}(c_1 c_2 + i\epsilon s_2) & -\frac{1}{\sqrt{2}}(c_1 s_2 - i\epsilon c_2) \end{pmatrix} , \tag{5.15}$$

where $\epsilon = \pm 1, s_{1,2} \equiv \sin\theta_{1,2}$, $c_{1,2} = \cos\theta_{1,2}$. c_2 and s_2 can be chosen positive with appropriate choice of P_l in Eq. (5.12).

$$P_\eta = \text{Diag.}(1, e^{-i\eta}, e^{i\eta})$$

is a diagonal phase matrix. The above $\tilde{U}_l$ becomes μ-τ symmetric if $s_2 = c_2$ and $\eta = 0$. This defines a one parameter family of the leptonic mass matrices which lead to the prediction of the μ-τ symmetry in case of the type-II dominance. We will use this form subsequently in our numerical analysis.

There is an important but unwelcome feature associated with the generalized CP invariance of the mass matrices in Eq. (5.7). The CKM matrix in this case turns out to be real. To see this explicitly, we note that just as in case of U_l, the matrices $U_{u,d}$ diagonalizing the up and down quark masses can be written as $\tilde{U}_{u,d}P_{u,d}$. $\tilde{U}_{u,d}$ have the same form as the RHS of Eq. (5.14) with the replacement of u_{il} with $u_{iu,id}$ and w_{il} with $w_{iu,id}$. The phase matrices $P_{u,d}$ can be absorbed in redefining the quark fields and the remaining part of the CKM matrix is given by

$$V_{ij} \equiv (\tilde{U}_u^\dagger \tilde{U}_d)_{ij} = u_{iu}u_{jd} + 2Re(w_{iu}w^*_{jd})$$

which is real since $u_{iu,id}$ are real.

One can generate CP violation in the model by breaking the generalized CP invariance of the mass matrices. This can be done in two ways. Either one allows complex VEV for some of the Higgs doublets as in [72, 76] or one retains the real VEV but allows breaking of the μ-τ symmetry in the Yukawa couplings. In the following, we will discuss the second alternative.

5.1.3 Numerical analysis

We now discuss the numerical implications of this model in detail. As already mentioned, we assume that either the type-I or the type-II term in the neutrino mass matrix dominates and carry out analysis separately in each of these two cases. The free parameters in the model are r, s, t, p, q, r_L, r_R, Eq. (5.2) and the real elements of the matrices G, H, F, Eq. (5.3). Parameter q is absent in the type-II case. An overall rotation R on G, H, F: $(G, H, F) \to R^T(G, H, F)R$ amounts to a choice of initial basis for the 16-plet of fermions. We can use this freedom to set say, $h_{12} = 0$. This is done with a specific choice $R = R_{23}^T(\frac{\pi}{4})R_{12}(\theta_{12}^h)R_{23}(\frac{\pi}{4})$. Here $R_{ij}(\theta)$ denotes rotation in the ij^{th} plane by an angle θ and

$$\tan 2\theta_{12}^h = \frac{2\sqrt{2}h_{12}}{h_{11} - h_{22} - h_{23}} \ .$$

This rotation amounts to redefinition of elements of F and G which still retain the same form as in Eq. (5.3). We continue to use the same notation for the parameters of the redefined F, G. With the choice $h_{12} = 0$, we have 14 (15) input parameters in case of type-II (type-I) seesaw dominance. These input parameters together generate 12 fermion masses and six mixing angles. As already remarked, the exact μ-τ symmetric H, F, G are not able to generate CP violation. We introduce this CP violation by adding a small μ-τ breaking difference between the 22 and 33 elements in H. This one additional parameter now leads to four CP violating phases, one in the CKM matrix and three in the PMNS matrix.

We use the same χ^2 technique discussed in the Appendix A to fit the

fermion mass spectrum on the model. Our choice of the input values of the physical observables are same as given in Table 4.1 of the previous chapter, except for the values of light quarks m_d, m_s and m_u which are obtained by taking their low-energy values from [106] and scaling them to M_{GUT}. We reproduce all these input values in Table 5.1 for convenience. While fitting, we

GUT scale values with propagated uncertainty			
m_d(MeV)	1.03 ± 0.41	$\Delta m^2_{sol}(\text{eV}^2)$	$(7.9 \pm 0.3) \times 10^{-5}$
m_s(MeV)	19.6 ± 5.2	$\Delta m^2_{atm}(\text{eV}^2)$	$(2.50^{+0.20}_{-0.25}) \times 10^{-3}$
m_b(GeV)	$1.06^{+0.14}_{-0.09}$	$\sin\theta^q_{12}$	0.2243 ± 0.0016
m_u(MeV)	0.45 ± 0.15	$\sin\theta^q_{23}$	0.0351 ± 0.0013
m_c(GeV)	0.210 ± 0.021	$\sin\theta^q_{13}$	0.0032 ± 0.0005
m_t(GeV)	$82.4^{+30.3}_{-14.8}$	$\sin^2\theta^l_{12}$	0.31 ± 0.025
m_e(MeV)	0.3585 ± 0.0003	$\sin^2\theta^l_{23}$	0.50 ± 0.065
m_μ(MeV)	75.6715 ± 0.058	$\sin^2\theta^l_{13}$	$< 0.0155(1\sigma)$
m_τ(GeV)	1.2922 ± 0.0013	J_{CP}	$(2.2 \pm 0.6) \times 10^{-5}$

Table 5.1: Input values for quark and leptonic masses and mixing angles in the MSSM extrapolated at $M_{GUT} = 2 \times 10^{16}$ GeV for $\tan\beta = 10$ which we use in our numerical analysis.

omit the parameters r_R, r_L which define the overall scales of neutrino masses in case of the type-I and type-II seesaw respectively. The ratio of the solar and atmospheric mass scales and neutrino mixing parameters are independent of these overall scales and are used in our definition of χ^2 function instead of the individual neutrino masses. In addition, we assume Δm^2_{atm} to be positive corresponding to the normal neutrino mass hierarchy. Parameters r_R, r_L are fixed subsequent to minimization using the atmospheric scale.

Numerical analysis: Type-II seesaw

We perform the minimization in three physically different cases.

(A) In this case, we impose the conditions $\theta^l_{23} = \frac{\pi}{4}$ and $\theta^l_{13} = 0$ using a μ-τ symmetric $\tilde{U}_l$. As discussed in the earlier section, this is done using parametrization in Eq. (5.15) with $s_2 = c_2 = \frac{1}{\sqrt{2}}$. The charged lepton mass matrix is then determined completely in terms of three masses and the angle θ_1.

Using the third of Eq. (5.2), the real and imaginary parts of M_l can be used to determine respectively elements of H in terms of that of F and elements of G in terms of p, the charged lepton masses and θ_1. f_{12} also gets determined in terms of these parameters because of the choice $h_{12} = 0$. Thus $f_{22}, f_{23}, f_{11}, r, s, t, p, \theta_1$ are the only free parameters which determine the 11 remaining observables - six quark masses, three angles of the CKM matrix, the solar angle and the solar to atmospheric mass ratio. The result of the minimization are shown in Table 5.2. The parameters obtained at the minimum are shown in Appendix B.3. One obtains a reasonably good fit to all observables except the down and bottom quark masses which are respectively $\sim 1.5\sigma$ and $\sim 2.5\sigma$ away from their respective mean values. All other observables are reproduced correctly with very small pulls as seen in the Table 5.2.

	A	*B*	*C*
Quantity	**Pull**	**Pull**	**Pull**
m_d	-1.47532	0.167255	0.0620115
m_s	-0.8225	0.271662	-0.0545523
m_b	-2.52388	1.68787	1.72811
m_u	0.274609	-0.00446626	-0.00184452
m_c	-0.0125887	0.000159604	0.00744292
m_t	0.00190476	0.00901941	-0.0199522
m_e	0	-0.000951761	0.000179815
m_μ	0	0.0176266	-0.000749102
m_τ	0	-0.0192274	-0.017642
$\frac{\Delta m^2_{sol}}{\Delta m^2_{atm}}$	0.679035	-0.169337	-0.0544521
$\sin\theta^q_{12}$	-0.0116059	0.00250491	-0.00412383
$\sin\theta^q_{23}$	0.155231	-0.00717926	0.0402861
$\sin\theta^q_{13}$	-0.0705362	0.0000163982	0.0163964
$\sin^2\theta^l_{12}$	0.112082	-0.111783	-0.00578002
$\sin^2\theta^l_{23}$	0	0.129873	-0.141465
$\delta_{\rm CKM}$	–	–	-0.0364271
χ^2	9.80473	3.00957	3.02019
	Predictions	**Predictions**	**Predictions**
$\sin^2\theta^l_{23}$	0.5	–	–
$\sin^2\theta^l_{13}$	0	0.000471537	0.000226908
$\delta_{\rm CKM}$	0°	0°	–
$\delta_{\rm PMNS}$	0°	0°	-12.759°
α_1	180°	180°	169.80°
α_2	0°	0°	-9.445°
r_L	2.8714×10^{-10}	1.8183×10^{-9}	1.8645×10^{-9}

Table 5.2: Best fit solutions for fermion masses and mixing obtained assuming the type-II seesaw dominance. Various observables and their pulls obtained at the minimum are shown in three cases (A)-(C) defined in the text.

(B) In this case, we do not impose the maximality of θ^l_{23} but include $\sin^2\theta^l_{23}$ in the χ^2 to be minimized. $\sin^2\theta^l_{13}$ is not included in the definition of χ^2 but we require it to be ≤ 0.0155 during the minimization. r, s, t, p and elements of H, F, G are now treated as free and the χ^2 definition now includes the charged lepton masses as well. This results in significant improvement in the fit and one is able to fit 15 observables in terms of 13 parameters with $\chi^2 = 3.01$. The fit to the bottom and the down quark masses also improves. δ_{CKM} remains zero in this case.

(C) For this case, we depart from the exact 23 symmetry and take h_{22} different from h_{33}. As already discussed, this breaks the generalized CP and results in a non-trivial CKM phase. Remarkably, a very small ($\sim 8\%$) breaking of the 23 symmetry is able to generate a non-trivial CKM phase and $\chi^2_{min} = 3.02$ with 2 degrees of freedom. Bottom quark mass is the only variable which deviates from its central value considerably.

Some of the observables are not part of the χ^2 and their values get fixed at the minimum. These are shown as predictions in Table 5.2. These include the CP violating Dirac phase δ_{PMNS} and the Majorana phases $\alpha_{1,2}$. These are trivial for the cases (A) and (B) due to the generalized CP invariance but one obtains non-zero values displayed in the Table 5.2 in case (C).

Before going into the more detailed predictions, let us underline some important points connected with the above fits.

- Detailed fits to fermion masses have been considered in a number of papers with [72, 76] or without [57, 65] the addition of the 120-plet to the minimal $10 + \overline{126}$ Higgs fields. The minimal model without the 120-plet but not imposing reality of the coupling has more parameters than the present case but the fit is not better compared to here, *e.g.* the fit in pure type-II case [57] with 18 parameters and 15 data points gives a minimum χ^2 around 14.5.

- The best fit solutions in cases (B) and (C) give θ^l_{23} close to maximal and θ^l_{13} close to zero as seen from Table 5.2.

- We have fixed the overall scale of neutrino mass r_L in Eq. (5.6) by using the atmospheric scale as normalization. The resulting values are displayed in Table 5.2. In all three cases, r_L comes close to 10^{-10}. r_L is related to the mass of the left handed triplet residing in the $\overline{126}$ representation and to other parameters in the superpotential. Detailed analysis [38, 39, 48, 49, 57, 63, 64, 65] has shown that one needs this triplet mass to be at an intermediate scale $\sim 10^{12}$ GeV if the overall neutrino mass scale is to be correctly reproduced. The presence of such light triplet conflicts with the gauge coupling unification. An additional 120-plet does not qualitatively alter the situation. One possible solution suggested [83] in the literature is to add a 54-plet of Higgs and allow $SO(10)$ to break first to $SU(5)$ leaving a complete 15-plet of Higgs light at around 10^{12} GeV. Other solution corresponds to having split supersymmetry breaking [65]. Third possibility is to allow type-I seesaw dominance [66, 67, 68, 69]. We shall look at this in the next subsection in the present context.

We now turn to predictions in the neutrino sector. As it has been already discussed in Section 4.4.2 in the previous chapter, the firm predictions of the scheme can be obtained by checking the variation of χ^2 with the values of various observables. We do the similar analysis here and check the predictions of the model for (1) deviations in θ_{23} from its maximal value (2) the reactor angel and (3) Dirac CP violating phase in the lepton sector. The results are displayed in Figs. 5.1, 5.2, 5.3.

Fig. 5.1 shows the variation of $\bar{\chi}^2_{min}$ for various pinned downed values of $\sin^2\theta^l_{23}$. It is seen that the minimum occurs when $\sin^2\theta^l_{23}$ is fixed to around 0.46 rather than the value 0.5 obtained in the fits shown in Table 5.2. The variation of $\bar{\chi}^2_{min}$ is not drastic and all values in the range $0.3 - 0.7$ are allowed at 90%CL. In comparison, variation of $\bar{\chi}^2_{min}$ with $\sin^2\theta^l_{13}$ shown in Fig. 5.2 is little more significant. There is a preference for values close to zero but values up to 0.008 cannot be ruled out at 90% confidence level. Fig. 5.3 shows the prediction for the PMNS phase in the leptonic mixing matrix. Clear prediction is the negative values for the $\sin\delta_{PMNS}$. However, all negative

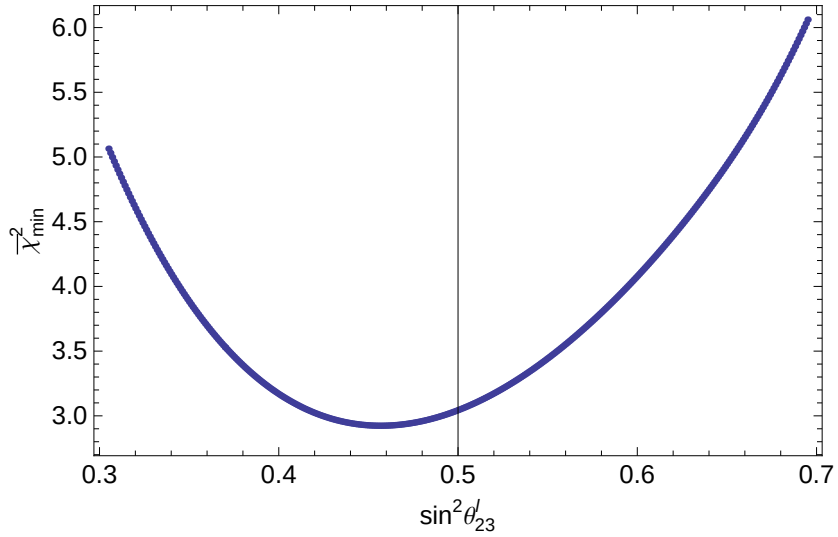

Figure 5.1: Variation of $\bar{\chi}^2_{min}$ with $\sin^2\theta^l_{23}$ in Type-II seesaw.

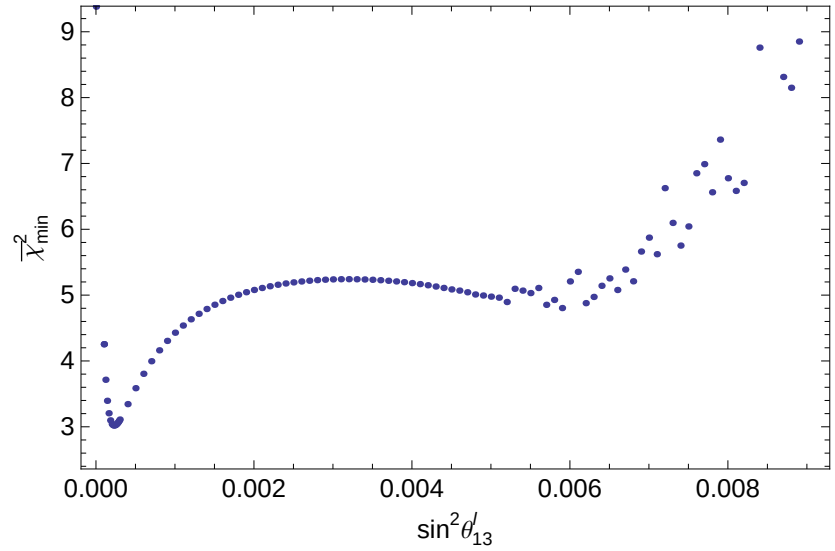

Figure 5.2: Variation of $\bar{\chi}^2_{min}$ with $\sin^2\theta^l_{13}$ in Type-II seesaw.

values are allowed within the 90% confidence limit.

Numerical analysis: Type-I seesaw

The structure of the neutrino mass matrix in the type-I case is qualitatively different compared to the type-II case. Unlike M_ν^{II}, M_ν^I is not μ-τ invariant in general. But it can be made approximately μ-τ symmetric if either 120 contribution or the $10+\overline{126}$ dominates in M_D, see Eq. (5.2). We discuss below fits in three qualitatively different cases as done for the type-II dominance.

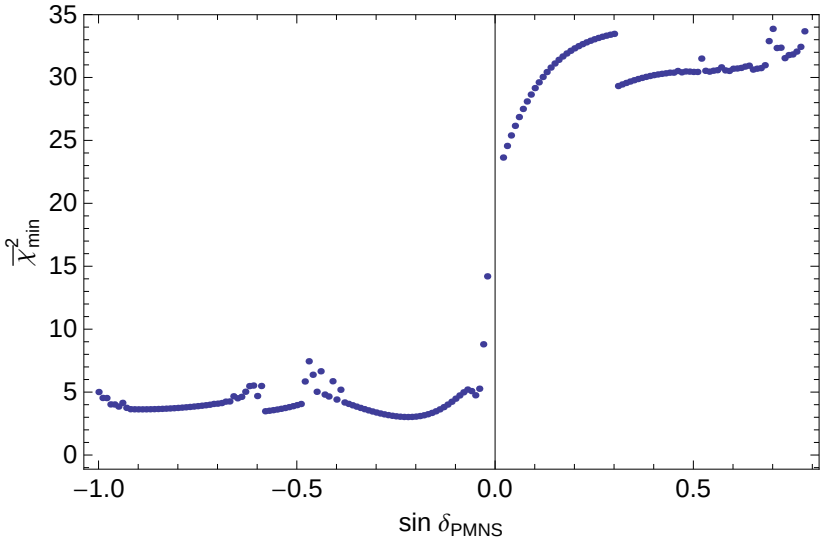

Figure 5.3: Variation of $\bar{\chi}^2_{min}$ with $\sin\delta_{PMNS}$ in Type-II seesaw.

(A) Here we impose the exact μ-τ symmetry for M_ν^I by hand, i.e. by choosing $q = 0$ in M_D. As before, U_l is also chosen μ-τ symmetric. The input parameters and observables are the same as in the case (A) of type-II seesaw. The results of the fits are displayed in the first column of the Table 5.3. The total χ^2 involves 11 observables and is determined by 8 parameters . The minimum value is ~ 13. While most observables can be fitted nicely, the top quark mass deviate by 3.6σ from the central value. Enforcing the exact μ-τ symmetry does not appear to be a very good choice.

(B) In this case, we do not take $q = 0$. M_ν^I now satisfies Eq. (5.9) and is not symmetric under μ-τ symmetry. θ_{23}^l is not fixed to be maximal but is included in the definition of χ^2. As in the earlier case (B), χ^2 is defined by 15 observables and is determined in terms of 14 parameters. The CP violating phases are zero in this case and the CKM phase is therefore not included in χ^2. Experimental bound on θ_{13}^l shown in Table 4.1 is imposed during the minimization. One now gets excellent fit to all the included variables with $\chi^2_{min} = 0.017$.

(C) In this case we introduce a small explicit μ-τ symmetry breaking by assuming $h_{22} \neq h_{33}$ in Eq. (5.2). This allows CP violation. χ^2 definition now includes all 16 observables and depends on 15 parameters. Bound on θ_{13}^l is

Quantity	A **Pull**	B **Pull**	C **Pull**
m_d	-0.31569	0.0346007	-0.379829
m_s	0.473034	-0.0483779	-0.0717277
m_b	-0.108264	-0.113763	-0.114314
m_u	0.50263	0.00026323	0.00344698
m_c	-0.151225	-0.000606809	-0.00938266
m_t	-3.60744	-0.0193107	0.0122663
m_e	0	-4.874×10^{-6}	0.0000348858
m_μ	0	0.000480511	0.00078371
m_τ	0	0.00254153	-0.0106065
$\frac{\Delta m^2_{sol}}{\Delta m^2_{atm}}$	-0.00977627	-0.00192856	0.0125218
$\sin\theta^q_{12}$	0.0218205	-0.00061312	0.00761817
$\sin\theta^q_{23}$	0.00289271	0.00129946	0.0284214
$\sin\theta^q_{13}$	-0.238953	-0.00823361	0.0366413
$\sin^2\theta^l_{12}$	-0.0129712	0.000590904	-0.00265193
$\sin^2\theta^l_{23}$	0	-0.00544523	0.0289959
$\delta_{\rm CKM}$	–	–	-0.120278
χ^2	13.6821	0.0169632	0.180526
	Predictions	**Predictions**	**Predictions**
$\sin^2\theta^l_{23}$	0.5	–	–
$\sin^2\theta^l_{13}$	0	0.0135605	0.013505
$\delta_{\rm CKM}$	0°	0°	–
$\delta_{\rm PMNS}$	0°	0°	-0.287748°
α_1	180°	0°	2.156°
α_2	0°	0°	2.616°
r_R	4.1143×10^{-11}	5.2329×10^{-18}	5.0093×10^{-18}

Table 5.3: Best fit solutions for fermion masses and mixing obtained assuming the type-I seesaw dominance. Various observables and their pull obtained at the minimum are shown in three cases (A)-(C) defined in the text.

imposed during minimization. Once again we get an excellent fit to all the observables with $\chi^2_{min} = 0.18$. CP violating phases in the PMNS matrix come as predictions.

Noteworthy features of the fits in (B) and (C) cases above are the following:

- The overall neutrino mass scale is determined to be around $r_R \sim 5 \times 10^{-18}$. r_R is related to the ratio of the VEV of the doublet and the RH triplet components in $\overline{126}$. The values of r_R obtained here are similar to the values obtained in [72] which assume $\overline{126}$ RH triplet VEV to be at the GUT scale. Thus one does not need an intermediate scale in order to fit the neutrino masses and one can obtain the gauge coupling unification. This is consistent with observations in [68, 69, 72, 76].

- Maximality of θ_{23}^l is not imposed. But it is fixed to be very close to $\frac{\pi}{4}$ at the minimum in both the cases. The departure from the μ-τ symmetry results in θ_{13}^l being non-zero and is fixed around the upper bound at the minimum as seen from the Table 5.2.

- Although an explicit breaking of the μ-τ symmetry is introduced in case (C), the amount of the breaking required in order to obtain the large CP violating phase is extremely tiny,

$$\frac{h_{22} - h_{33}}{h_{22} + h_{33}} \sim 0.0045 \ . \tag{5.16}$$

- The exact μ-τ symmetry is known [103] to lead to the unwanted predictions $V_{ub} = V_{cb} = \sin^2 \theta_{23}^l = 0$. Here we have two sources of breaking this symmetry, spontaneous through the VEV of the 120-plet and explicit through Eq. (5.16) which allows one to reproduce the mixing angles correctly. In spite of the μ-τ breaking, the final fermion mass matrices display a remarkably good μ-τ symmetry. We make this explicit by giving the quark and lepton mass matrices in the case (C) above in Appendix B.3. $M_{u,d,l}$ and M_ν^I are seen to be nearly μ-τ symmetric. There is an order of magnitude difference in the imaginary parts of the 12 and 13 elements of M_ν^I. But these imaginary parts are much smaller than the corresponding μ-τ symmetric real parts. The only source of the large μ-τ breaking occurs as a difference between the 12 and 13 elements of the Dirac neutrino mass matrix M_D. This results from the spontaneous breakdown and rather large value of the parameter q.

- As in [72, 76] we have concentrated here in obtaining generic fits to fermion masses rather than considering the entire parameter space of the theory given by the Yukawa couplings and basic parameters in the superpotential. Parameters in fermion mass matrices are related to the strengths of the light Higgs components in various $SO(10)$ Higgs representations. These are determined by the fine tuning conditions and

the full superpotential. Grimus and Kühböck [76] have laid down consistency constraints on these parameters following from these fine tuning relations and from the requirement that the Yukawa couplings stay in the perturbative regime. We have checked that these conditions are satisfied by the parameters given in the Appendix B.3.

We follow a similar procedure of the type-II case to obtain possible predictions on the neutrino mixing variables. Variations of $\bar{\chi}^2_{min}$ obtained at different local minima are shown as scattered plots in Fig. 5.4, 5.5, 5.6.

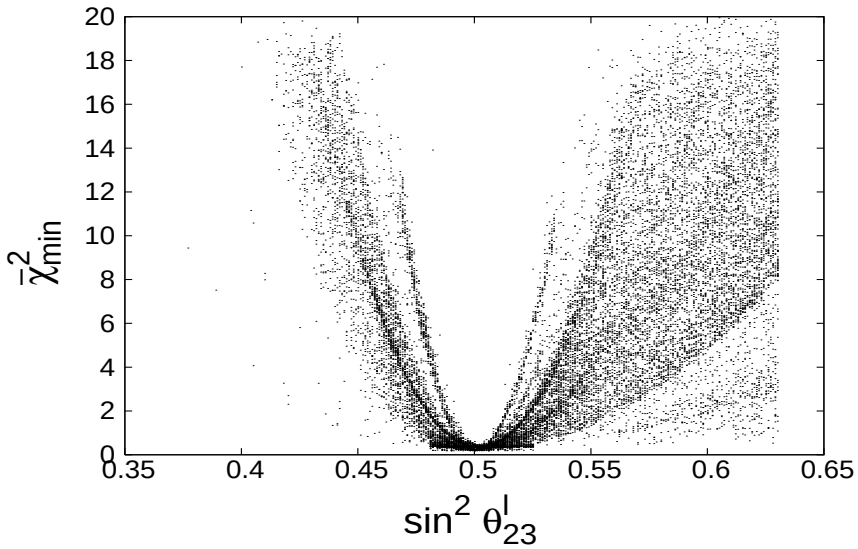

Figure 5.4: Variation of $\bar{\chi}^2_{min}$ with $\sin^2\theta^l_{23}$ in Type-I seesaw.

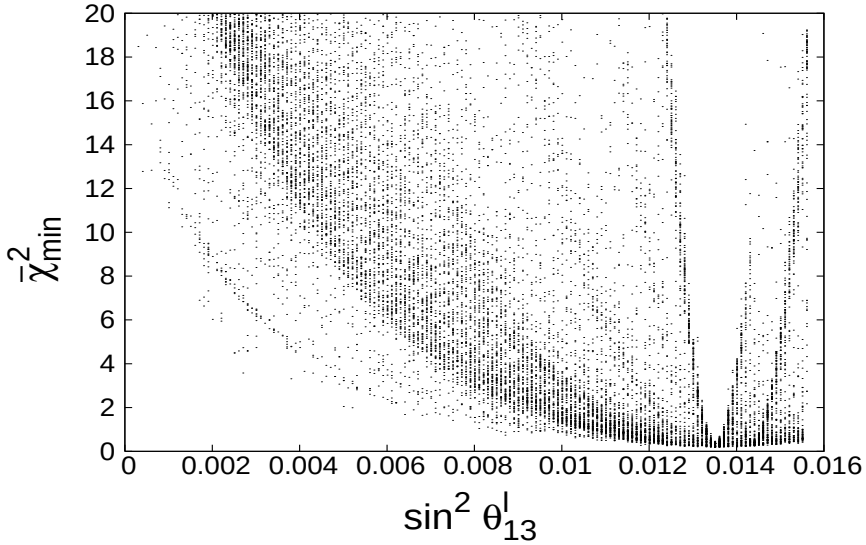

Figure 5.5: Variation of $\bar{\chi}^2_{min}$ with $\sin^2\theta^l_{13}$ in Type-I seesaw.

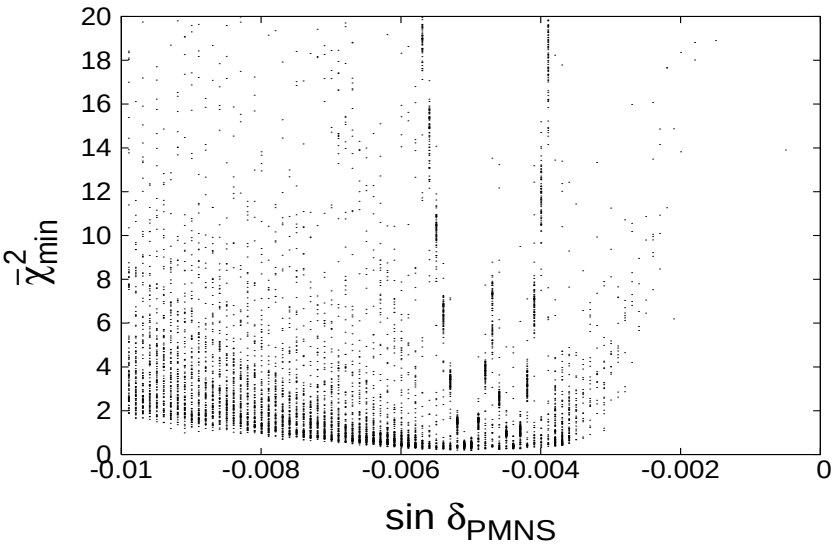

Figure 5.6: Variation of $\bar{\chi}^2_{min}$ with $\sin\delta_{PMNS}$ in Type-I seesaw.

Clear predictions emerge unlike in the type-II case. As Fig. 5.4 shows, the $\sin^2\theta^l_{23}$ is preferentially restricted near 0.5 and one obtains the limit $\sim 0.42 - 0.63$ at the 90% CL. Fig. 5.5 shows similar variation with respect to $\sin^2\theta^l_{13}$. Here, the preferred values occur near the present limit and one obtains $\sin^2\theta^l_{13} > 0.005$ at 90% CL. The predicted values for $\sin\delta_{PMNS}$ are displayed in Fig. 5.6. These are negative but very small.

We end this section with a comment on the specific μ-τ symmetry defined by S used in Eq. (5.5). Definition of S is basis-dependent. One could change the original basis of the 16-plet through an arbitrary rotation R. The structure of the Yukawa couplings and the resulting fermionic mass matrices would look different in the new basis. The new Yukawa couplings would still satisfy the same equation as (5.4) but now with a rotated S: $S_R \equiv R^T S R$. Thus the μ-τ symmetry may appear to look different with different choices of R. Specifically, if R corresponds to a rotation by $\frac{\pi}{4}$ in the 23 plane then the S_R assumes the form

$$S_R = \begin{pmatrix} 1 & 0 & 0 \\ 0 & -1 & 0 \\ 0 & 0 & 1 \end{pmatrix} . \tag{5.17}$$

This is nothing but the Z_2 symmetry imposed in [76] which is thus equivalent to the generalized μ-τ symmetry considered here if both remain unbroken.

Difference arises after these symmetries are broken. Ref. [76] uses complex VEV to achieve Z_2 breaking as a result of which analogue of Eqs. (5.7-5.8) do not hold in their case. In our approach, we introduce small explicit breaking of μ-τ symmetry in H. The model in [76] has 20 free parameters compared to 15 used here.

Note that the explicit breaking of the μ-τ symmetry is technically natural in the supersymmetric context. Alternatively, one can achieve such breaking by introducing an additional 10-plet of the Higgs field which changes sign under the μ-τ symmetry. Combined contributions of these two 10-plets would then give an explicitly μ-τ non-invariant H.

5.2 Quasidegenerate neutrinos in $SO(10)$

As we already noted in the beginning of this chapter,

1. Two of the neutrino mixing angles are large as opposed to the small quark mixing angles.

2. Neutrino mass hierarchy is milder compared to quarks and extreme case of all neutrinos being quasidegenerate is still an allowed possibility.

Several independent reasons have been advanced [11, 51, 103] to understand feature (1) of the fermion spectrum but it may be that its answer lies in (2). Large mixing angles become quite natural if neutrinos are almost degenerate. They remain undefined in the exact degenerate limit. A small perturbation which leads to differences in neutrino masses can also stabilize all or some of the mixing angles to large values. Thus theory which predicts quasidegeneracy has built in mechanism to explain large mixing angles.

The stringent constraints on the degenerate mass m_0 comes from cosmology. Depending on which data set one uses and method of analysis, $3m_0$ can vary between 0.9-1.7 eV or 2-3 eV [107], the latter limit is based solely on the information from the cosmological microwave background studies. All the neutrinos having a quasidegenerate mass in the range 0.3-1 eV is thus an al-

lowed possibility. It is non-trivial to accommodate this possibility within the conventional pictures of neutrino mass generation. Indeed, unified treatment of all fermion masses tend to generate hierarchical masses for neutrinos as well. For example, the light neutrino masses are related to the Dirac neutrino mass matrix M_D in type I seesaw model [11] and generically follow the hierarchical patterns as many grand unified framework predicts $M_D \sim M_u$ where M_u is a mass matrix for up-type of quarks. We present an $SO(10)$ based unified description of fermion masses and mixing leading to hierarchical charged fermions and quasidegenerate neutrino masses. We propose a specific ansatz for the structure of Yukawa matrices in $SO(10)$ models which differ from this generic expectations and lead to quasidegenerate neutrinos through the type-I seesaw mechanism. Consistency of this ansatz is demonstrated through a detailed fits to fermion masses and mixing angles all of which can be explained with reasonable accuracy in a model which uses the Higgs fields transforming as $10, 120$ and $\overline{126}$ representations of $SO(10)$. The proposed ansatz is shown to follow from an extended model based on the three generations of the vector like fermions and an $O(3)$ flavour symmetry.

5.2.1 Ansatz & phenomenology

We use supersymmetric $SO(10)$ as our basic framework and consider its most general Yukawa sector. The fermion masses arise in renormalizable through their couplings to Higgs fields transforming as 10, $\overline{126}$ and 120 representations. As already discussed in the previous chapters, all three Higgs fields are not necessarily required to construct viable models and can either choose a valid minimal Higgs fields or can invoke additional symmetries to reduce the number of free parameters in the theory. In our context, we find that all the three Higgs representations are needed to obtain satisfactory and viable fits to fermion masses and mixing angles. As noted earlier, the final fermion mass matrices (3.14) obtained after $SO(10)$ and $SU(2)_L \times U(1)$ breaking can be parametrized

as:

$$\begin{aligned} M_d &= H + F + G, \\ M_u &= r(H + s\ F + t_u\ G), \\ M_l &= H - 3\ F + \ t_l\ G, \\ M_D &= r(H - 3s\ F + t_D\ G), \\ M_L &= r_L\ F, \\ M_R &= r_R^{-1}\ F. \end{aligned} \tag{5.18}$$

where the matrices H and F are complex symmetric and G is an anti-symmetric matrix in generation space. $r,\ s,\ t_u,\ t_l,\ t_D,\ r_L,\ r_R$ are complex parameters determined by the ratios of VEVs and mixing among various Higgs doublets. The light neutrino mass matrix is given by Eq. (5.6). It is known that the above fermion mass structure allows different mixing patterns for quarks and neutrinos if type-II seesaw mechanism dominates [63]. Consider the limit in which the contribution of the 10-plet H dominates. In this limit, all the charged fermions are diagonalized by the same matrix and the CKM matrix becomes proportional to identity. In the same limit, neutrino mixing with the type-II dominance is governed by F in Eq. (5.6) leading to non-trivial leptonic mixing. In fact, if only H dominates the charged fermion masses then one can obtain b-τ unification which in turn drives the large atmospheric mixing [63]. The existing fits [56, 57, 74] to fermion masses and mixing with type-II dominance are for the hierarchical neutrino masses. Degenerate neutrino spectrum can be obtained in this approach with an additional assumption:

$$F = c_0 I \tag{5.19}$$

I denoting a 3×3 identity matrix. The sub-dominant type-I contribution can then lead to the quark mixing and neutrino mass differences.

As noted in Section 3.1.4, the realization of the attractive type-II dominated scenario was found difficult in the context of the minimal model [48, 56, 57, 63,

74]. This motivates us to study degenerate neutrinos in the context of a purely type-I seesaw mechanism. A general framework to obtain quasidegenerate neutrinos in type-I seesaw was recently discussed in [108]. It was shown in this approach that M_R has the following form in an effective theory invariant under a specific flavour symmetry:

$$M_R \approx M_D^T M_D + \dots \ . \tag{5.20}$$

This form leads to degenerate neutrinos to the lowest order.

An equivalent description at the $SO(10)$ level can be obtained by imposing the following ansatz:

$$F = aH^2 \ , \tag{5.21}$$

Since H is a symmetric matrix it can be diagonalized by a unitary matrix $U^T\ H\ U = D_H$, where D_H is a diagonal matrix with real elements. Without loss of generality, we can express the mass matrices in (5.18) in an $SO(10)$ basis with a diagonal H. This basis are obtained from Eq. (5.18) by the replacement $H \to D_H$ and

$$F \longrightarrow U^T\ F\ U = a(U^T H U\ U^\dagger U^*\ U^T H U) = a\ D_H V^* D_H \ . \tag{5.22}$$

G retains its antisymmetric form and we use the same notation for it and for various mass matrices in the new basis. From now on, we will work in this rotated basis. $V = U^T U$ in Eq. (5.22) is a symmetric unitary matrix which can be parametrized [109] as

$$V = P R_{23}^T(\phi) U_{12}(\theta, \alpha) R_{23}(\phi) P \ , \tag{5.23}$$

with

$$R_{23}(\phi) = \begin{pmatrix} 1 & 0 & 0 \\ 0 & \cos\phi & \sin\phi \\ 0 & \sin\phi & -\cos\phi \end{pmatrix}; \quad U_{12}(\theta,\alpha) = \begin{pmatrix} \cos\theta & \sin\theta & 0 \\ \sin\theta & -\cos\theta & 0 \\ 0 & 0 & e^{i\alpha} \end{pmatrix} \tag{5.24}$$

and $P = \text{Diag.}(e^{i\beta_1}, e^{i\beta_2}, 1)$ is a diagonal phase matrix (One phase in P is absorbed in the complex parameter a in Eq. (5.22)).

Before we present the detailed fits let us look at the implications of the ansatz Eq. (5.21) qualitatively.

- Correct b-τ unification and second generation masses are obtained if dominant contribution to the charged fermion masses come from the 10-plet, i.e. from H with a sub-dominant contribution from $\overline{126}, 120$ fields. Retaining only the H contribution, the ansatz, Eq. (5.21) implies that

$$M_\nu^I = -r_R M_D F^{-1} M_D^T \approx -\frac{r^2 r_R}{a} V + \ldots , \tag{5.25}$$

  where the ... terms arise from the $\overline{126}$ and 120 contribution to the Dirac mass matrix M_D. CKM matrix is unity in this limit while the neutrino mixing is determined from V. Diagonalization of V leads [109] to $\theta_{23} = \phi$, $\theta_{12} = \frac{\theta}{2}$ and $\theta_{13} = 0$ where the angles θ_{ij} are angles defined in the standard parametrization of the leptonic mixing matrix in which θ_{12} drives the solar and θ_{23} the atmospheric neutrino oscillations. Thus ansatz in Eq. (5.21) can lead to correct description of the quark and leptonic mixing angles to zeroth order without requiring the type-II dominance as is commonly done.

- If H in the original basis was real then V entering Eq. (5.22) would be unity. In this case, all the fermion mixing vanish in the absence of the 120 contribution. Thus complex couplings and CP violation proves to be important in understanding large neutrino mixing within this approach. Numerically, we find that even after including 120 contribution,

one cannot get the correct mixing pattern with a real H.

The mixing angles obtained at zeroth order with H dominance get corrected by the contributions from $\overline{126}$ and 120-plets. They induce non-zero quark mixing angles and perturb Eq. (5.25):

$$M_\nu^I = -\frac{r_R r^2}{a}(V - 6saD_H + t_D(GD_H^{-1}V - VD_H^{-1}G)) + \mathcal{O}(s^2, t_D^2)) \qquad (5.26)$$

The above neutrino mass matrix corresponds to an effective dimension five operator induced after integration of the right handed neutrino fields. Assuming that the heavy mass scale is close to the GUT scale and neglecting the effect of the Dirac neutrino couplings in the renormalization group (RG) evolution one can obtain [11] the low scale neutrino mass matrix as follows. Define the neutrino mass matrix $\mathcal{M}_{\nu f}(M_X)$ in the flavour basis as

$$\mathcal{M}_{\nu f}(M_X) = U_l^\dagger M_\nu(M_X) U_l^* \ , \qquad (5.27)$$

where U_l diagonalizes the charged lepton mass matrix M_l. The radiatively corrected neutrino mass matrix is then given by [11]

$$\mathcal{M}_{\nu f}(M_Z) = I_\tau \mathcal{M}_{\nu f}(M_X) I_\tau^\dagger \ , \qquad (5.28)$$

where $I_\tau \approx Diag(1, 1, 1 + \epsilon_\tau)$ and $\epsilon_\tau \approx -\frac{1}{\cos^2\beta}\frac{m_\tau^2}{16\pi^2 v^2}\ln\frac{M_X}{M_Z}$. More detailed treatment then presented here would need to include threshold corrections due to right handed neutrinos and ruining between the GUT and the right handed neutrino mass scale etc.

5.2.2 Numerical analysis

We now discuss the fits to the fermion masses and mixing angles based on the ansatz (5.21) and (5.19) which leads to degenerate neutrino spectrum in case of type-I and type-II seesaw dominance respectively. We use the same

χ^2 technique used before. We use as our input the quark and lepton masses obtained at M_X in the MSSM for $\tan\beta = 10$, $M_{SUSY} = 1$TeV and $M_{GUT} = 2 \times 10^{16}$GeV. These input values of the charged fermion masses and quark mixing are same as used in the previous section and are given in a Table 5.1. Unlike in the previous works, the neutrino mixing angles are susceptible to change by the RG evolution due to quasidegenerate nature of neutrinos. We include this effect as follows. Using the charged lepton mass matrix at M_X, we numerically determine the neutrino mass matrix in the flavour basis at M_X through Eq. (5.27). Neglecting running of the mixing angles in U_l, the low scale neutrino mass matrix in Eq. (5.28) is numerically determined and used to obtain the observable neutrino masses and mixing angles. For neutrino masses and lepton mixings, we use the updated low energy values given in [60].

Numerical Fits: Type-I seesaw

We first do the fitting for the ansatz (5.21) and the fermion mass matrices, Eq. (5.18) that leads to quasidegenerate neutrino spectrum if type-I seesaw contribution dominates over type-II in Eq. (5.6). In this case we have total 25 real parameters (3 in D_H, 5 in V, 6 in G, real r, complex $s,\ a,\ t_u,\ t_l,\ t_D$) which are fitted over 16 observables (9 charged fermion masses, 4 CKM parameters, 2 leptonic mixing angles and $\Delta m^2_{sol}/\Delta m^2_{atm}$). Lepton mixings and $\Delta m^2_{sol}/\Delta m^2_{atm}$ are independent of the overall neutrino mass ($m_0 = |\frac{r_R r^2}{a}|$) appearing in Eq. (5.26). m_0 sets the overall neutrino mass scale and can be determined from the fit using the observed value of Δm^2_{atm}. Our definition of χ^2 allows only the solution with $\Delta m^2_{sol}\cos 2\theta > 0$ as required by experiments. We also set $r = \frac{m_t}{m_b}$ and minimize χ^2 with respect to the remaining 24 parameters. The results of the minimization are displayed as solutions (1) and (2) in Table 5.4.

We obtained the best fit value of $\chi^2 = 2.038$ corresponding to the solution 1 for which all the observables are fitted within $\lesssim 0.9\sigma$. Solution 2 is also acceptable which fits all observables within $\lesssim 0.7\sigma$ with exception of down

		Type-I: Solution 1		**Type-I: Solution 2**		**Type-II**	
No.	Observables	Fitted value	Pull	Fitted value	Pull	Fitted value	Pull
1	m_d[MeV]	0.653677	−0.917861	0.207819	**-2.00532**	0.868041	−0.395023
2	m_s[MeV]	17.5885	−0.386821	21.6923	0.402361	12.2829	**-1.40714**
3	m_b[GeV]	1.11131	0.418721	1.05832	−0.046348	1.25634	**1.69141**
4	m_u[MeV]	0.462718	0.0847896	0.450825	0.005499	0.450489	0.0032611
5	m_c[GeV]	0.210603	0.0136849	0.211727	0.0695654	0.210393	0.00324503
6	m_t[GeV]	63.6891	−0.832404	67.6155	−0.658038	102.325	0.883371
7	m_e[MeV]	0.358503	0.009696	0.358506	0.0206782	0.358502	0.00503107
8	m_μ[MeV]	75.6719	0.00734514	75.6711	−0.0083064	75.6709	−0.0111809
9	m_τ[GeV]	1.29219	−0.008144	1.29223	0.0218404	1.29217	−0.0244576
10	$\frac{\Delta m^2_{sol}}{\Delta m^2_{atm}}$	0.0303514	0.050109	0.0303237	0.0377877	0.0302538	0.00659421
11	m_0[eV]	**0.31**	–	**0.17**	–	**0.36**	–
12	$\sin\theta^q_{12}$	0.224205	−0.0592102	0.224306	0.00359473	0.224154	−0.0913125
13	$\sin\theta^q_{23}$	0.0351308	0.023704	0.0350426	−0.0441173	0.0351436	0.033571
14	$\sin\theta^q_{13}$	0.003193	−0.0132867	0.0031588	−0.0825897	0.00326199	0.123983
15	$\sin^2\theta^l_{12}$	0.319801	−0.0619079	0.321124	0.0187774	0.321168	0.0214673
16	$\sin^2\theta^l_{23}$	0.481942	0.313909	0.436492	−0.178126	0.439779	−0.14255
17	$\sin^2\theta^l_{13}$	**0.01953**	–	**0.00288**	–	**0.03568**	–
18	$\delta_{CKM}[^\circ]$	67.7227	0.247333	56.4935	−0.134071	49.7146	−0.429864
19	$\delta_{PMNS}[^\circ]$	**53.98**	–	**-66.99**	–	**-25.33**	–
20	$\alpha_1[^\circ]$	**146.55**	–	**-59.31**	–	**137.71**	–
21	$\alpha_2[^\circ]$	**-89.88**	–	**162.41**	–	**-33.44**	–
	χ^2		2.038		4.684		6.0

Table 5.4: Best fit solutions for fermion masses and mixing obtained assuming the type-I seesaw dominance (solutions (1) and (2)) and type-II seesaw dominance (solution(3)). Various observables and their pulls obtained at the minimum are shown (See text for details). The bold faced quantities are predictions of the respective solutions.

quark mass m_d. We also include in table the values of the Majorana phases obtained at the minimum. The fits obtained here are better than the one obtained by Bertolini *et al.* [56, 57, 74] in case of the minimal model with complete type-II seesaw dominance and hierarchical neutrinos. Unlike here, their fits have several observables which are > 1 or 2σ away from the central values.

The values of input parameters determined from χ^2 minimization in case of solution 1 of Table 5.4 are the following.

$$D_H = \text{Diag.}(0.00033658, 0.0149966, -0.757334) \tag{5.29}$$

$$G_{12} = (0.00167{+}0.00154i)\ ;\ G_{13} = (0.0108{+}0.0101i)\ ;\ G_{23} = (0.191{+}0.033i)\ . \tag{5.30}$$

$$\begin{aligned} a &= -(5.24 - 9.34i)\text{GeV}^{-1}; t_l = 0.15 - 1.05i; t_u = 0.551 - 0.084i; \\ s &= (-3.21 + 3.32i) \times 10^{-4}; t_D = -(2.56 + 0.43i) \times 10^{-4}; \\ \phi &= 50.65^\circ; \theta = -56.9^\circ; \alpha = 0.20^\circ; \beta_1 = -39.55^\circ; \beta_2 = 83.79^\circ \end{aligned} \quad (5.31)$$

Elements of D_H and G are expressed in GeV units. Note that ϕ and $\theta/2$ respectively determine the atmospheric and the solar mixing angles at M_X in the absence of perturbation. These values get stabilized at M_X to $\phi \approx 40.4^\circ$; $\theta \approx -61.0^\circ$ once the perturbations from $\overline{126}_H$, 120_H couplings are added. RG running changes them to the required values displayed in Table 5.4. θ_{13} has not been included in our definition of χ^2 and its initial value was zero. This becomes non-zero but remains small in both the solutions displayed. However, almost the entire allowed range in θ_{13} is compatible with reasonable fits to other fermion masses as shown by both the solutions. Unlike the solar and atmospheric mixing angles, the ratio $\Delta m^2_{sol}/\Delta m^2_{atm}$ changes appreciably from 0.09 at M_X to 0.03 at M_Z by the RG effects. All these solutions predict large CP violating leptonic phase.

Noteworthy outcome of the fits is the values of m_0 determined using the observed value of Δm^2_{atm}. Values of m_0^2 in table are seen to be $\gg \Delta m^2_{atm}$ showing the consistency of our ansatz. This arises as a result of Eq. (5.26) and smallness of s, t_D. The m_0 in turn determine the heaviest RH neutrino mass scale (see Eq. (5.18) and ansatz (5.21))

$$M_3 \approx r_R^{-1}|a|m_b^2 \approx \frac{r^2}{m_0} m_b^2 \approx 1.3 \times 10^{13}\text{GeV} \ ,$$

in case of solution 1. Here we used, $m_0 = \frac{r_R r^2}{|a|}$. Thus the RH neutrino mass falls below the GUT scale for this particular solution.

Numerical Fits: Type-II seesaw

We now turn to the numerical discussion of the ansatz (5.19) in which the contribution of $\overline{126}$ to fermion masses is assumed to be degenerate. Such an ansatz for the type-II contribution was considered [110, 111] in the specific

context of $SO(10)$. Detailed fits to fermion masses with recent data are however not presented in these works. We do this essentially following the same procedure as the one adopted in purely type-I case. We assume H, G to have the most general form. One could choose to work in a basis with a diagonal H. In this basis, Eq. (5.19) gets changed to

$$F = c_0 V \ , \tag{5.32}$$

where V is a unitary symmetric matrix defined in Eq. (5.23). In this basis, the charged fermion mass matrices can be obtained from Eq. (5.18) by replacing H with diagonal D_H, and F with $c_0 V$. The neutrino mass matrix, Eq. (5.6) can be written in the same basis as

$$M_\nu = m_0 \left(V - \epsilon \ M_D V^* M_D^T \right) \tag{5.33}$$

The parameter ϵ controls the contribution from type-I seesaw which induces splittings in neutrino masses.

We use these equations to fit all the fermion masses and mixing using the previous procedure. Results corresponding to the minimal case are displayed in Table 5.4. The best fit solution we obtained here corresponds to $\chi^2 = 6.0$ which is acceptable for 16 data points from statistical point of view and all the observables except m_b and m_s are fitted within 1σ. The obtained fit in the type-II case is however not as good as in the case of pure type-I seesaw combined with the ansatz (5.21). As before, the m_0 sets the overall neutrino mass scale which is determined to be ~ 0.36 eV using the atmospheric scale and fits shown in the Table 5.4. Numerical fits also lead to $\epsilon \approx 2 \times 10^{-6} \text{GeV}^{-2}$. Since the scale of M_D is set by the top mass the type-I contribution relative to the type II is given by $\epsilon m_t^2 \sim 10^{-2}$ and type II contribution dominates as assumed. Now the overall scale of the RH neutrino mass is given by (see Eq. (5.18 and ansatz (5.19))

$$M_3 \approx \frac{1}{m_0 \epsilon} \approx 1.1 \times 10^{15} \text{GeV}$$

is close to the GUT scale unlike the minimal models with type-II dominance but hierarchical neutrinos [48, 56, 57, 63, 74]. Increase in M_3 here is linked to degeneracy of neutrinos. The atmospheric neutrino mass scale in models with type-II seesaw and hierarchical neutrinos is typically given by

$$\Delta m^2_{atm} \sim \frac{v^4}{M_3^2}.$$

While in the present case it arises from the combination of type-I and type-II contributions and is scaled by

$$\Delta m^2_{atm} \sim m_0 \frac{v^2}{M_3}$$

leading to a higher M_3 compared to purely type-II dominated scenario.

5.2.3 An $SO(10)\times O(3) \times U(1)$ model for quasidegenerate neutrinos

In this subsection, we illustrate how the ansatz (5.21) can be obtained in a model from a flavour symmetry. A simple flavour symmetry to be used is $O(3)$ under which three generation of the 16_F transform as triplets. The $O(3)$ breaking is introduced through a complex flavon field η transforming as spin 2. We need to introduce three generations of vector-like multiplets $16_V + \overline{16}_V$ transforming as $(16, 3) + (\overline{16}, 3)$ under $SO(10) \times O(3)$ and a $U(1)_X$ symmetry in order to realize Eq. (5.21). The X-charges of $(16_F, 16_V, \overline{16}_V, \eta, 10_H, \overline{126}_H)$ are chosen respectively as $(x, y, -y, 1/2(y-x), -(x+y), -2y)$ with $x \neq y$.

The general super potential invariant under $SO(10) \times O(3) \times U(1)_X$ can be written as:

$$W = M\overline{16}_V 16_V + \beta 16_V 16_V \overline{126}_H + \gamma 16_V 16_F 10_H + \frac{\delta}{M_P}\overline{16}_V \eta^2 16_F + \frac{\delta'}{M_P}\overline{16}_V (Tr\eta^2) 16_F \tag{5.34}$$

The $O(3)$ and $U(1)_X$ breaking originates in the above super potential only from the Planck scale effects through the VEV of the flavon field η. The last

two terms are the only terms which determine both the 10 and $\overline{126}$ Yukawa couplings once the heavy vector like fields are integrated out. The dotted terms correspond to terms suppressed by M_P^2. Here, the mass M of the vector like pair and the scale of the VEV of η lie above the GUT scale. The effective theory after integration of the vector like field is represented by

$$W_{eff} \approx \beta 16_F \xi^2 16_F \overline{126}_H + \gamma 16_F \xi 16_F 10_H \ , \tag{5.35}$$

where

$$\xi_{ab} \equiv \frac{\delta}{M M_P}(\eta_{ab}^2 + \frac{\delta'}{\delta} Tr\eta^2 \delta_{ab})$$

and $a, b = 1, 2, 3$ refer to the $O(3)$ index. This effective super-potential is also $SO(10) \times O(3) \times U(1)_X$ invariant. The Yukawa coupling H is proportional to the $\langle \xi \rangle$ and is a general complex symmetric matrix. The F is related to the square of H and satisfies the ansatz in Eq. (5.21). The coupling to the 120_H field can be generated by introducing a flavon field χ with the $U(1)_X$ charge $-2x$ and transforming as a triplet of $O(3)$. This leads to the Yukawa coupling matrix G through the coupling

$$16_F \frac{\chi}{M_P} 16_F 120_H$$

A detailed model along this line will require study of the details of the vacuum structure of the potential involving η, χ and possibly additional fields for generating the right structure of the Yukawa couplings H, G.

For type-II dominated degenerate neutrino spectrum, the ansatz (5.19) if the contribution of $\overline{126}$ to fermion masses is assumed to be $O(3)$ invariant. The $O(3)$ breaking arises from the H and G contributions which lead to departure from degeneracy through the type-I seesaw.

5.3 Quark-lepton complementarity in $SO(10)$

As it has been already mentioned in the beginning of this chapter, two of the three leptonic mixing angles are large. In contrast, the observed quark mixing angles are small and hierarchical. It has been observed long ago [112] that there exists an interesting empirical relation between quark and lepton mixing angles.

$$\theta_{12}^{l} + \theta_{12}^{q} \sim \frac{\pi}{4} \tag{5.36}$$

The above relation is known as Quark-Lepton Complementarity [112, 113, 114, 115, 116, 117, 118] and still favored by the present experimental data within their measurement errors. It is also possible to write similar relation between 23 angles of quark and lepton mixing.

$$\theta_{23}^{l} + \theta_{23}^{q} \sim \frac{\pi}{4} \tag{5.37}$$

If such relations are not accidental, they strongly suggest the common roots between quarks and leptons [113, 114, 115, 116, 117, 118]. Clearly it is very hard to realize such relations in ordinary bottom-up approaches where the quarks and leptons are treated separately with no specific connections between them. So one requires top-down approaches like the grand unified theories which sometime also unify quarks and leptons and provide a framework to construct a model in which QLC relation can be embedded in a natural way.

5.3.1 QLC & Grand unification

The general conditions under which QLC relation (5.36) can be realized from quark-lepton unification are thoroughly discussed in [113, 114]. We describe one such possibility here. Assume that the structure of neutrino and quark mass matrices at high scale are such that the PMNS matrix is exact bimaximal $V_{PMNS} = U_{BM}$ whereas the CKM matrix is an identity matrix to a leading

order.

$$U_{BM} = \begin{pmatrix} \frac{1}{\sqrt{2}} & -\frac{1}{\sqrt{2}} & 0 \\ \frac{1}{2} & \frac{1}{2} & -\frac{1}{\sqrt{2}} \\ \frac{1}{2} & \frac{1}{2} & \frac{1}{\sqrt{2}} \end{pmatrix} \tag{5.38}$$

Both the mixing matrices get corrected by $\mathcal{O}(\theta_C)$ terms coming from the next leading order where the down quark and charged lepton mass matrices are equal (or nearly so). In this scenario, a QLC relation can emerge from quark-lepton unification at high scale. Construction of a realistic GUT model in which all fermion masses and mixing angles are correctly reproduced along with QLC is highly non-trivial. In fact several models [115, 116, 117, 118] proposed to explain QLC are based on a smaller gauge group, namely Pati-Salam $SU(4)_c \times SU(2)_L \times SU(2)_R$ group. A complete and realistic model based on $SO(10)$ GUT has not been proposed so far. The original proposal [114] was based on $SU(5)$ relation $M_e = M_d^T$ but detailed explanation of the fermionic spectrum was not developed. Here we present a predictive $SO(10)$ based unified description of fermion masses and mixing in which QLC relation can be naturally realized.

We consider three families of 16-dimensional fermions obtaining their masses from renormalizable couplings to four Higgs multiplates, three of them (denoted by $10_H, 10'_H$ and $10''_H$) transforming as 10 and the other ($\overline{126}_H$) as $\overline{126}$ dimensional representations under $SO(10)$. Like the minimal model discussed in the previous chapter, the $SO(10)$ breaking can be achieved with $210_H + 54_H + 126_H + \overline{126}_H$ [39, 42, 49, 83]. The Yukawa interactions of the model can be written as

$$W_Y = 16_F[Y_{10}10_H + Y_{\overline{126}}\overline{126}_H + Y_{10'}10'_H + Y_{10''}10''_H]16_F \tag{5.39}$$

where Y_i are symmetric Yukawa coupling matrices. As noted in Chapter 2, 10_H and $\overline{126}_H$ have two MSSM doublets in each of them. Assuming the fine-tuning condition for MSSM like light Higgs doublets, the fermion mass matrices after

the electroweak symmetry breaking can be suitably written as

$$\begin{aligned} M_d &= H + F + t\ H' + H''; \\ M_u &= r\ H + s\ F + H' + p\ H''; \\ M_e &= H - 3F + t\ H' + H''; \\ M_D &= r\ H - 3s\ F + H' + p\ H''; \\ M_L &= r_L\ F; \\ M_R &= r_R^{-1}\ F. \end{aligned} \tag{5.40}$$

where H, F, H' and H'' are obtained by multiplying electroweak VEVs and Higgs mixing parameters with Yukawa coupling matrices $Y_{10}, Y_{\overline{126}}, Y_{10'}$ and $Y_{10''}$ respectively. r, s, t, p, r_L are r_R are dimensionless parameters determined by the Clebsch-Gordan coefficients, ratios of VEVs, and mixing among Higgs fields.. M_D denotes neutrino Dirac mass matrix. $M_L(M_R)$ is the Majorana mass matrix for left-(right-)handed neutrinos which receives a contribution only from the VEV of $\overline{126}_H$ field. In generic $SO(10)$ models of this type, the effective neutrino mass matrix M_ν for the three light neutrinos has both the type-I and type-II contributions and given by Eq. (5.6). In general, both contributions are present and they depend on two different parameters so one may dominate over the other. It has been shown in several references [39, 42, 49, 83] that it is possible to have symmetry breaking pattern in $SO(10)$ where type-II term dominates over the type-I contributions. The equations (5.40) and (5.6) are the key equations that provide basic platform to construct a model in which the QLC relation (5.36) can be realized.

5.3.2 An $SO(10)$ ansatz for QLC

We propose following ansatz which leads to relation (5.36).

$$
\begin{aligned}
H &= \frac{1}{2}\begin{pmatrix} 0 & 0 & 0 \\ 0 & h & h \\ 0 & h & h \end{pmatrix}; \quad F = \begin{pmatrix} b+c & \sqrt{2}a & 0 \\ \sqrt{2}a & b+c & 0 \\ 0 & 0 & b-c \end{pmatrix}; \\
H' &= \begin{pmatrix} 0 & 0 & \sqrt{2}a' \\ 0 & 0 & 0 \\ \sqrt{2}a' & 0 & 0 \end{pmatrix}; \quad H'' = x\ I
\end{aligned} \tag{5.41}
$$

where I is 3×3 identity matrix. To do the simple analytical study of such ansatz we assume that all the above parameters are real. Without loss of generality, we can express the above matrices in a basis with diagonal H. Such basis are obtained by rotating the 16-dimensional fermion fields in 2-3 plane by an angle $\pi/4$. The matrices in (5.41) will be redefined in new basis as

$$
(H, F, H', H'') \to R_{23}\left(\frac{\pi}{4}\right)(H, F, H', H'')R_{23}^{T}\left(\frac{\pi}{4}\right) \tag{5.42}
$$

and can be rewritten as

$$
\begin{aligned}
H &= \begin{pmatrix} 0 & 0 & 0 \\ 0 & 0 & 0 \\ 0 & 0 & h \end{pmatrix}; \quad F = \begin{pmatrix} b+c & a & a \\ a & b & c \\ a & c & b \end{pmatrix}; \\
H' &= \begin{pmatrix} 0 & -a' & a' \\ -a' & 0 & 0 \\ a' & 0 & 0 \end{pmatrix}; \quad H'' = x\ I
\end{aligned} \tag{5.43}
$$

Before we present the detailed analysis let us look at some immediate implications of the above ansatz. The dominant 10-Higgs coupling matrix H has rank-1. As it was pointed out in [119, 120] this can simultaneously explain both the observed hierarchy of quark masses as well as the origin of large lepton mixings if the light neutrino masses are generated through type-II seesaw

mechanism. Assuming only one 10-Higgs contribution in charged fermion mass matrices, we get at zeroth order,

$$m_b = m_\tau = \frac{1}{r} m_t;\ V_{CKM} = I;\ V_{PMNS} = U_{BM}. \tag{5.44}$$

Correct b-τ unification and large lepton mixings (bimaximal) are obtained with no mixings between quarks. The charged fermions of first two generations are massless in this case. Further, the contributions coming from other Higgs coupling matrices F, H' and H'' make the model realistic by giving nonzero masses to first two fermion generations as well as by perturbing both the mixing matrices which reproduce observed mixing patterns for both the quark and lepton sectors.

We now present the detailed analysis of ansatz (5.43). Substituting it in Eq. (5.40) and (5.6), we get

$$\begin{aligned}
M_u &= \begin{pmatrix} s(b+c)+x' & sa-a' & sa+a' \\ sa-a' & sb+x' & sc \\ sa+a' & sc & rh+sb+x' \end{pmatrix}; \\
M_d &= \begin{pmatrix} b+c+x & a-ta' & a+ta' \\ a-ta' & b+x & c \\ a+ta' & c & h+b+x \end{pmatrix}; \\
M_e &= \begin{pmatrix} -3(b+c)+x & -3a-ta' & -3a+ta' \\ -3a-ta' & -3b+x & -3c \\ -3a+ta' & -3c & h-3b+x \end{pmatrix}; \\
M_\nu &= r_L\ F
\end{aligned} \tag{5.45}$$

where $x' = px$. Since each mass matrix is real symmetric, it can be diagonalized by a rotation matrix parameterized (in the standard parameterization) by three angles.

$$\begin{aligned}
R_f^T M_f R_f &= \text{Diag.}(m_{f1}, m_{f2}, m_{f3}); \\
R_f &= R_{23}(\theta_{23}^f) R_{13}(\theta_{13}^f) R_{12}(\theta_{12}^f)
\end{aligned} \tag{5.46}$$

where $f = d, u, e, \nu$ and R_{ij} is a rotation matrix in ij plane. The charged fermion mass matrices are hierarchical ($h \gg b, c \gg a, a' \gg x, x'$) and can be approximately diagonalized by Jacobi rotation. The results obtained from such diagonalization for the quark sector are displayed below.

$$\begin{aligned} m_b &\approx h + b + x + \mathcal{O}\left(\frac{c^2}{h}\right); \\ m_s &\approx b + x + \frac{(a - ta')^2}{b}\left(1 - \frac{x}{b}\right) + \mathcal{O}\left(\frac{c^2}{h}\right); \\ m_d &\approx b + c + x - \frac{(a - ta')^2}{b}\left(1 - \frac{x}{b}\right) + \mathcal{O}\left(\frac{a^2}{h}\right). \end{aligned} \tag{5.47}$$

$$\begin{aligned} m_t &\approx rh + sb + x' + \mathcal{O}\left(\frac{s^2c^2}{rh}\right); \\ m_c &\approx sb + x' + \frac{(sa - a')^2}{sb}\left(1 - \frac{x'}{sb}\right) + \mathcal{O}\left(\frac{s^2c^2}{rh}\right); \\ m_u &\approx s(b + c) + x' - \frac{(sa - a')^2}{sb}\left(1 - \frac{x'}{sb}\right) + \mathcal{O}\left(\frac{s^2a^2}{rh}\right). \end{aligned} \tag{5.48}$$

$$\theta_{12}^d \approx -\frac{a - ta'}{b}\left(2 + \frac{c - x}{b}\right); \quad \theta_{23}^d \approx -\frac{c}{h}; \quad \theta_{13}^d \approx -\frac{a + ta'}{h}\left(1 + \frac{c}{h}\right). \tag{5.49}$$

$$\theta_{12}^u \approx -\frac{sa - a'}{sb}\left(2 + \frac{sc - x'}{sb}\right); \quad \theta_{23}^u \approx -\frac{sc}{rh}; \quad \theta_{13}^u \approx -\frac{sa + a'}{rh}\left(1 + \frac{sc}{rh}\right) \tag{5.50}$$

Let us underline some important points in connection with above relations.

- The six real parameters h, b, x, r, s, x' can be approximated from the six quark masses. m_b and m_s determine the parameters h and b. It is easy to see that $r \approx m_t/m_b$ and $s \approx m_c/m_s$ are required to obtain the masses of heavy quarks m_t and m_c. Further, m_d and m_u fix the values of x and x'. Since $b, c \gg x$, we require $c \sim -b$ to obtain small masses of first generation fermions.

- Let us assume that $a' \approx sa$ in order to keep $\theta_{12}^u \ll \theta_{12}^d$. Also note that

$\theta^u_{23} \approx (s/r)\theta^d_{23} \ll \theta^d_{23}$ and $\theta^u_{13} \sim (s/r)\theta^d_{13} \ll \theta^d_{13}$. In this limit, the quark mixing matrix takes the form

$$V_{CKM} = U_u^\dagger U_d \approx U_d \approx R_{23}(\theta^d_{23}) R_{13}(\theta^d_{13}) R_{12}(\theta^d_{12}) \tag{5.51}$$

- The elements of the CKM matrix fix some more parameters as follows.

$$c \sim -V_{cb}\ h; \quad a - ta' \sim -V_{us}\ b; \quad a + ta' \sim -V_{ub}\ h. \tag{5.52}$$

An interesting relationship between V_{us} and V_{ub} can be found in the limit $t \sim 0$.

$$V_{ub} \approx V_{us} \frac{m_s}{m_b} + \mathcal{O}\left(\frac{m_s^2}{m_b^2}\right) \tag{5.53}$$

We will show later in this section that $t \sim 0$ is a necessary requirement to obtain QLC relation(5.36).

- Our assumption of real parameters makes the theory CP invariant. The observed CP violation in the quark sector can be accommodated by making some parameters complex.

It is interesting to note that all the parameters are fixed in terms of the observables of the quark sector. Hence the entire lepton sector emerges as the prediction of the model. Let us first derive the predictions for the charged leptons.

$$\begin{aligned}
m_\tau &\approx h - 3b + x + \mathcal{O}\left(\frac{c^2}{h}\right); \\
m_\mu &\approx -3b + x - \frac{(3a + ta')^2}{3b}\left(1 + \frac{x}{3b}\right) + \mathcal{O}\left(\frac{c^2}{h}\right); \\
m_e &\approx -3(b + c) + x + \frac{(3a + ta')^2}{3b}\left(1 + \frac{x}{3b}\right) + \mathcal{O}\left(\frac{a^2}{h}\right).
\end{aligned} \tag{5.54}$$

$$\theta^e_{12} \approx -\frac{3a+ta'}{3b}\left(2+\frac{3c+x}{3b}\right); \quad \theta^e_{23} \approx \frac{3c}{h}; \quad \theta^e_{13} \approx \frac{3a-ta'}{h}\left(1+\frac{c}{h}\right). \quad (5.55)$$

Noteworthy features of the above relations are the following,

- It predicts $m_\tau \approx m_b$ and $m_\mu \approx -3m_s$.
- For $b = -c$, $m_e \approx m_d$ which is viable with observed values of m_e and m_d extrapolated at the GUT scale within 3σ deviations [58]. However for $b \neq -c$, any desired value of m_d/m_e can be obtained.
- For $t \sim 0$, $\theta^e_{12} \approx \theta_C$, $\theta^e_{23} \approx -3\theta_{cb}$ and $\theta^e_{13} \approx -3\theta_{ub}$.

The light neutrino mass matrix in Eq. (5.45) has the most general form which can be diagonalized by bimaximal matrix U_{BM}. The mass eigenvalues are,

$$m_1 = m_0(b+c+\sqrt{2}a);\ m_2 = m_0(b+c-\sqrt{2}a);\ m_3 = m_0(b-c) \quad (5.56)$$

Interestingly, for $b = -c$ (which can now also be written as $V_{cb} \approx m_s/m_b$), we get the partial degenerate neutrino mass spectrum $m_1 = -m_2 \ll m_3$ which leads to vanishing solar (mass)^2 difference ($\Delta m^2_{sol} = m_2^2 - m_1^2 = 0$) at high scale. We performed numerical study and found that the radiative corrections to the original neutrino mass matrix are unable to generate the required splitting between m_1 and m_2. Another way to induce non zero value of Δm^2_{sol} is to allow type-I contribution to the original type-II seesaw neutrino mass matrix. However such contribution is highly hierarchical (like M_l^2) and it largely contributes to the 33 element of neutrino mass matrix which ultimately spoils the nice symmetry of neutrino mass matrix and hence the bimaximality of neutrino mixings. This forces us to consider the case where $V_{cb} \neq m_s/m_b$. In this case we obtain the following expression for the ratio of the solar to atmospheric squared mass difference.

$$\frac{\Delta m^2_{sol}}{\Delta m^2_{atm}} \approx \sqrt{2} V_{us} \left(\frac{m_s/m_b}{V_{cb}} \left(1 + \frac{m_s}{m_b} \right) - 1 \right) \tag{5.57}$$

Note that one requires $m_s/m_b \sim 1.08\ V_{cb}$ to obtain the observed value of $\Delta m^2_{sol}/\Delta m^2_{atm} (\sim 0.031)$ and it implies that $V_{cb} < m_s/m_b$ which is not favored by their present observed values extrapolated at the GUT scale. However as argued in [120], the threshold corrections to $b - s$ quark mass mixing from gluino and wino exchange via one-loop diagrams can give desired value of V_{cb}. The required deviation from $b = -c$ is quantified by

$$b + c \approx m_s \left(1 - \frac{V_{cb}}{m_s/m_b} \right) \lesssim 0.08\ m_s$$

which is small and of order of first generation fermion masses and hence allows the correct m_d in Eq. (5.47).

The leptonic mixing matrix can be seen as dominant bimaximal mixing resulting from neutrino mass matrix and then corrected by $\mathcal{O}(\theta_C)$ terms coming from the unitary matrix U_e which diagonalize charged lepton mass matrix.

$$V_{PMNS} \equiv U_e^\dagger U_\nu = U_e^T U_{BM} \tag{5.58}$$

where $U_e = R_{23}(-3\theta_{cb}) R_{13}(-3\theta_{ub}) R_{12}(\theta_C)$. The resulting neutrino mixing parameters are the following.

$$\begin{aligned} U_{e2} &\equiv (V_{PMNS})_{12} \approx -\frac{1}{\sqrt{2}} + \frac{(V_{us} - 3V_{ub})}{2}; \\ U_{\mu 3} &\equiv (V_{PMNS})_{23} \approx -\frac{1}{\sqrt{2}} (1 + 3V_{cb}); \\ U_{e3} &\equiv (V_{PMNS})_{13} \approx -\frac{1}{\sqrt{2}} (V_{us} + 3V_{ub}). \end{aligned} \tag{5.59}$$

The correction of $\mathcal{O}(\theta_C)$ from charged lepton generates correct solar mixing angle which follows QLC relation (5.36). The atmospheric mixing angle gets considerable deviation $\theta^l_{23} \approx \frac{\pi}{4} + 3\theta_{cb}$ in this model unlike the standard QLC relation for 23 mixing angle of quark and lepton given in Eq. (5.37). The

model also predicts large value of $U_{e3} \approx 0.16$ which can be tested in planned long baseline experiments.

Note that Eq. (5.59) holds at GUT scale which might be changed by RGE corrections in principle. However it is known that running of the Cabibbo angle is negligibly small in MSSM even with large value of tanβ. Running of leptonic mixing angle depends on the type of mass spectrum of light neutrinos. For $b \neq -c$, neutrino mass spectrum follows normal hierarchy $m_1 < m_2 \ll m_3$. The effect of RGE corrections are known to be negligible [86, 87] in this case and Eq. (5.59) holds at low scale also.

5.3.3 An explicit numerical example

We now provide an example of values of the parameters of Eq. (5.43) which successfully generate entire fermion mass spectrum as well as mixing patterns for both quark and lepton sector. The required CP violation in the quark sector is incorporated by making a' complex. In the limit $t \sim 0$, a' contributes only to the up quark mass matrix and does not change the other predictions of ansatz given in Eq. (5.43). One more parameter x' is made complex to reproduce m_u correctly. The numerical values of parameters are

$$\begin{aligned} h &= 1.7 \text{ GeV};\ b = 0.0243 \text{ GeV};\ c = -0.022113 \text{ GeV};\ a = -0.0052 \text{ GeV}; \\ a' &= (0.0344247 - 0.028885i) \text{ GeV};\ x' = (0.0233596 - 0.00293374i) \text{ GeV}; \\ x &= 0.00325 \text{ GeV};\ r = 55.88;\ s = -8.64198;\ t = 0. \end{aligned} \tag{5.60}$$

Substituting these numbers in Eq. (5.45), we get

$$\begin{aligned} &m_t = 94.8 \text{ GeV}; \quad m_c = 0.19 \text{ GeV}; \quad m_u = 0.65 \text{ MeV}; \\ &m_b = 1.73 \text{ GeV}; \quad m_s = 28.5 \text{ MeV}; \quad m_d = 4.21 \text{ MeV}; \\ &m_\tau = 1.63 \text{ GeV}; \quad m_\mu = 75.4 \text{ MeV}; \quad m_e = 0.35 \text{ MeV}. \end{aligned} \tag{5.61}$$

$$\begin{array}{llll} \sin\theta_{us} = 0.222; & \sin\theta_{cb} = 0.015; & \sin\theta_{ub} = 0.005; & \delta_{CKM} = 60.9^{\circ}; \\ \sin^2\theta^l_{12} = 0.368; & \sin^2\theta^l_{23} = 0.527; & \sin^2\theta^l_{13} = 0.024; & \frac{\Delta m^2_{sol}}{\Delta m^2_{atm}} = 0.030. \end{array} \tag{5.62}$$

The obtained spectrum is in good agreement with the data extrapolated at the GUT scale. For example, we compare our results with the charged fermion masses obtained at the GUT scale in the MSSM for tanβ=55, $M_{SUSY} = 1$ TeV and $M_{GUT} = 2 \times 10^{16}$ GeV given in Table 5 of reference [58]. All charged fermion masses (except m_d) obtained here fits with the data within 1σ. Our ansatz predicts larger value of m_d. The quark mixing angles θ_{cb} is small ($< m_s/m_b$) as required by Eq. (5.57). The reproduced values of lepton mixing angles and $\Delta m^2_{sol}/\Delta m^2_{atm}$ are also in accordance with their updated low energy values (within 3σ measurement errors) given in [60].

5.3.4 An $SO(10) \times S_4 \times Z_n$ model of QLC

In this section, we will illustrate how the ansatz (5.41) can be obtained in a model from flavor symmetry. We use discrete flavor symmetry based on the group S_4 which is a group of permutation of four distinct objects. It has 24 distinct elements filled in five conjugate classes and hence five irreducible representations of dimensions $\mathbf{3_2}, \mathbf{3_1}, \mathbf{2}, \mathbf{1_2}$ and $\mathbf{1_1}$. A singlet representation with subscript "2" changes sign under transformation involving the odd number of permutations of S_4. More details on the group theory of S_4, its multiplication rules and the Clebsch-Gordan (CG) coefficients are reported in Appendix C.

Our model follows the same line as model constructed in [120] and uses the same symmetry group. However it differs at some places since the ansatz required here is different from their ansatz. The basic matter fields and Higgs fields content of the model is the same as discussed in Section 5.3.1. In addition to this we use five flavon fields which are singlets under $SO(10)$ and two pair of vector-like fermion fields which transform like $16 \oplus \overline{16}$ under $SO(10)$. We impose the S_4 symmetry together with Z_n symmetry to get desired structure

of Yukawa matrices. Three matter fields 16_F are assigned as $\mathbf{3_2}$ dimensional representation of S_4 while five flavon fields χ, ϕ, η, σ and σ' form $\mathbf{3_1}, \mathbf{3_2}, \mathbf{3_1}, \mathbf{1_1}$ and $\mathbf{1_2}$ representations of S_4 respectively. The other fields are singlet ($\mathbf{1_1}$ or $\mathbf{1_2}$) under S_4. An additional Z_n symmetry is required to allow/forbid interactions between particular fields. The Z_n charges of various fields are listed in Table 5.5 where $\omega = e^{i(2\pi/n)}$.

	16_F	10_H	$10'_H$	$10''_H$	$\overline{126}_H$	χ	ϕ	η	σ	σ'	16_{V1}	$\overline{16}_{V1}$	16_{V2}	$\overline{16}_{V2}$
SO(10)	16	10	10	10	$\overline{126}$	$\mathbf{1}$	$\mathbf{1}$	$\mathbf{1}$	$\mathbf{1}$	$\mathbf{1}$	16	$\overline{16}$	16	$\overline{16}$
S_4	$\mathbf{3_2}$	$\mathbf{1_1}$	$\mathbf{1_2}$	$\mathbf{1_1}$	$\mathbf{1_1}$	$\mathbf{3_1}$	$\mathbf{3_2}$	$\mathbf{3_1}$	$\mathbf{1_1}$	$\mathbf{1_2}$	$\mathbf{1_1}$	$\mathbf{1_1}$	$\mathbf{1_2}$	$\mathbf{1_2}$
Z_n	1	ω^{-2m}	$\omega^{-(p+q)}$	ω^{-2q}	ω^{-2k}	ω^k	ω^m	ω^p	ω^k	ω^q	ω^m	ω^{-m}	ω^k	ω^{-k}

Table 5.5: Various fields and their representations under $SO(10) \times\ S_4 \times Z_n$.

Let us consider a theory above GUT scale which is invariant under the symmetry group $SO(10) \times S_4 \times Z_n$. The Yukawa superpotential allowed by such symmetry can be written as

$$\begin{aligned} W &= (\phi 16_F)\overline{16}_{V1} + \lambda 16_{V1} 16_{V1} 10_H + M_1 16_{V1}\overline{16}_{V1} \\ &+ (\chi 16_F)\overline{16}_{V2} + \lambda' 16_{V2} 16_{V2} \overline{126}_H + M_2 16_{V2}\overline{16}_{V2} \\ &+ \sum_i \frac{\alpha_i}{\Lambda^2}(\chi^2 16_F 16_F)_i \overline{126}_H + \frac{\beta}{\Lambda^2}\sigma(\chi 16_F 16_F)\overline{126}_H + \frac{\gamma}{\Lambda^2}\sigma^2(16_F 16_F)\overline{126}_H \\ &+ \frac{\alpha'}{\Lambda^2}\sigma'(\eta 16_F 16_F)10'_H + \frac{\alpha''}{\Lambda^2}\sigma'^2(16_F 16_F)10''_H \end{aligned} \tag{5.63}$$

where Λ is the Planck scale up to which the theory is valid. The S_4 singlet contraction of flavor index is indicated with bracket. $\alpha_i, \alpha', \alpha'', \beta, \gamma, \lambda$, and λ' are coefficients of $\mathcal{O}(1)$. The term $(\chi^2 16_F 16_F)$ represents all the different S_4 contractions which can be constructed as follows:

$$
\begin{aligned}
(\chi^2 16_F 16_F)_i \;\equiv\; & ((\chi\chi)_{\mathbf{1_1}}(16_F 16_F)_{\mathbf{1_1}}), ((\chi\chi)_{\mathbf{2}}(16_F 16_F)_{\mathbf{2}}), \\
& ((\chi\chi)_{\mathbf{3_1}}(16_F 16_F)_{\mathbf{3_1}}), ((\chi\chi)_{\mathbf{3_2}}(16_F 16_F)_{\mathbf{3_2}}), \\
& ((\chi 16_F)_{\mathbf{1_2}}(\chi 16_F)_{\mathbf{1_2}}), ((\chi 16_F)_{\mathbf{2}}(\chi 16_F)_{\mathbf{2}}), \\
& ((\chi 16_F)_{\mathbf{3_1}}(\chi 16_F)_{\mathbf{3_1}}), ((\chi 16_F)_{\mathbf{3_2}}(\chi 16_F)_{\mathbf{3_2}})
\end{aligned}
\tag{5.64}
$$

where $(...)_R$ indicates the representation R under S_4. Now consider a theory below the scale of $M_{1,2}$ and at the GUT scale. The effective superpotential after integrating out heavy vector-like fields is given by,

$$
\begin{aligned}
W_{eff} \;=\; & \frac{\lambda}{M_1^2}(\phi 16_F)(\phi 16_F)10_H + \frac{\lambda'}{M_2^2}(\chi 16_F)(\chi 16_F)\overline{126}_H \\
+ \; & \sum_i \frac{\alpha_i}{\Lambda^2}(\chi^2 16_F 16_F)_i \overline{126}_H + \frac{\beta}{\Lambda^2}\sigma(\chi 16_F 16_F)\overline{126}_H + \frac{\gamma}{\Lambda^2}\sigma^2(16_F 16_F)\overline{126}_H \\
+ \; & \frac{\alpha'}{\Lambda^2}\sigma'(\eta 16_F 16_F)10'_H + \frac{\alpha''}{\Lambda^2}\sigma'^2(16_F 16_F)10''_H
\end{aligned}
\tag{5.65}
$$

where first two terms allow the desired rank-1 structure of Yukawa matrices. Note that effective Yukawa superpotential still has the symmetry $SO(10) \times S_4 \times Z_n$. This symmetry will be broken to $SO(10)$ by VEVs of the flavon fields. In order to get the desired structure of Yukawa couplings, we will choose particular vacuum alignment of the flavon fields as given below.

$$
\langle\phi\rangle = \begin{pmatrix} 0 \\ 1 \\ 1 \end{pmatrix} v_\phi;\;\; \langle\chi\rangle = \begin{pmatrix} 0 \\ 0 \\ 1 \end{pmatrix} v_\chi;\;\; \langle\eta\rangle = \begin{pmatrix} 0 \\ 1 \\ 0 \end{pmatrix} v_\eta;
$$

$$
\langle\sigma\rangle = v_\sigma;\;\; \langle\sigma'\rangle = v_{\sigma'} \tag{5.66}
$$

These VEVs of flavon fields break flavor symmetry S_4 at the GUT scale and

generate following structure of various Yukawa couplings.

$$Y_{10} = \frac{\lambda v_\phi^2}{M_1^2} \begin{pmatrix} 0 & 0 & 0 \\ 0 & 1 & 1 \\ 0 & 1 & 1 \end{pmatrix} \tag{5.67}$$

$$\begin{aligned} Y_{126} &= \frac{\lambda' v_\chi^2}{M_2^2} \begin{pmatrix} 0 & 0 & 0 \\ 0 & 0 & 0 \\ 0 & 0 & 1 \end{pmatrix} + \frac{v_\chi^2}{\Lambda^2} \begin{pmatrix} \tilde{\alpha} & 0 & 0 \\ 0 & \tilde{\alpha} & 0 \\ 0 & 0 & \tilde{\alpha_0} \end{pmatrix} \\ &+ \frac{\beta v_\chi v_\sigma}{\Lambda^2} \begin{pmatrix} 0 & 1 & 0 \\ 1 & 0 & 0 \\ 0 & 0 & 0 \end{pmatrix} + \frac{\gamma v_\sigma^2}{\Lambda^2} I \end{aligned} \tag{5.68}$$

$$Y_{10'} = \frac{\alpha' v_{\sigma'} v_\eta}{\Lambda^2} \begin{pmatrix} 0 & 0 & 1 \\ 0 & 0 & 0 \\ 1 & 0 & 0 \end{pmatrix} \tag{5.69}$$

$$Y_{10''} = \frac{\alpha'' v_{\sigma'}^2}{\Lambda^2} I \tag{5.70}$$

where all non-relevant CG coefficients are suitably absorbed. $\tilde{\alpha}$ and $\tilde{\alpha_o}$ are linear combinations of different α_i. The Yukawa matrices derived from the super potential can successfully explain the ansatz given in Eq. (5.41). Note that $M_2 \ll \Lambda$ which implies $b + c \ll b - c$ (or $b \approx -c$) in Eq. (5.41). Further, the assumption $M_1 \ll M_2$ leads to $h \gg b, c$.

It is very important to show that the required vacuum structure of flavon fields (5.66) is allowed by flavon superpotential. This point has already been discussed in great details in reference [120]. Since our model has the same kind of flavon structure as theirs, we simply use their results. Note that due to non-trivial Z_n charges, bilinear terms which correspond to masses of flavon

fields are not allowed. As a result of this the model requires doubling of flavon fields to allow Dirac type mass terms. The new flavon fields have the same S_4 representations but opposite Z_n charges. It has been shown in [120] that all the desired vacua of Eq. (5.66) are present in the model.

5.4 Conclusions & outlook

Aim of the first section of this chapter was to integrate the successful μ-τ symmetry within the $SO(10)$ framework in order to obtain a constrained picture of fermion masses and theoretical understanding of the largeness of the atmospheric mixing angle. The explicit model discussed here provides this integration rather well as shown by the detailed fits to fermion masses presented in Tables 5.2 and 5.3. Interestingly, mass matrices obtained in the model under consideration display a generalized CP invariance if Yukawa couplings are taken to be μ-τ symmetric. Small explicit breaking of this symmetry is sufficient to generate the required CP violating phase. The best scenario is obtained in the type-I seesaw model with very tiny explicit μ-τ symmetry breaking. This scenario is characterized by the predictions $\sin^2\theta^l_{23} \sim 0.42 - 0.63$, $\sin^2\theta^l_{13} > 0.005$ and negligible CP violation in neutrino oscillations. Final quark, the charged lepton and the light neutrino mass matrices respect μ-τ symmetry to a very good approximation indicating that this symmetry provides a good description of the entire fermion spectrum rather than being restricted to the neutrino sector alone.

Quasidegenerate neutrino is an experimentally allowed possibility. Considering the popular mechanisms for neutrino mass generation, it is challenging to obtain quasidegenerate masses for neutrinos. This becomes more challenging in GUTs since quarks do not share this properties. In this chapter, we have shown that it is indeed possible to obtain such a description starting from the fermionic mass structure, Eq. (5.18) that can arise in a general $SO(10)$ model. We considered two distinct possibilities based on purely type-I and the other based on the mixture of type-I and type-II seesaw mechanisms. Both these

possibilities can lead to quasidegenerate spectrum if they are supplemented respectively with ansatz (5.21) and (5.19). We have shown through the detailed numerical analysis that these ansatz are capable of explaining the entire fermionic spectrum and not just the quasidegenerate neutrinos. Moreover, the origin of large leptonic mixing here is linked to the quasidegenerate structure of the neutrino mass matrix providing yet another reason why quark and leptonic mixing angles are so different in spite of underlying unified mass structure.

In the last section of this chapter, we have discussed a possible way to realize QLC relation (5.36) between the Cabibbo angle and solar mixing angle in realistic quark-lepton unification theory based on $SO(10)$ gauge group. All the previous attempts in this direction are based either in the context of the Pati-Salam or $SU(5)$ symmetric theories. Ours is the first complete model which achieves QLC relation in $SO(10)$ model. We have shown here that it is indeed possible to obtain such relation starting from the fermionic mass structure (5.40) if they are supplemented with ansatz (5.41) and assuming that only type-II seesaw mechanism is responsible for light neutrino masses. One necessary ingredient for QLC is bimaximal mixing pattern from the neutrino sector which has been obtained through specific ansatz. Our ansatz also makes use of recently proposed [119] rank-1 strategy which naturally explains charged fermions mass hierarchy as well as origin of hierarchical quark mixing angles as opposed to the large lepton mixing angles. We have shown through the detailed analysis that this ansatz is capable of explaining the entire fermionic spectrum and not just the QLC relation. Moreover, the various predictions made by such ansatz are in agreement with observations. We have shown that the proposed ansatz can be obtained in a model from a discrete flavor symmetry group S_4 together with an additional Z_n symmetry. A generic prediction of our approach is $\theta^l_{13} \approx \theta_C/\sqrt{2}$ which is near to its current experimental upper bound. The atmospheric mixing angle gets considerable deviation from maximality ($\theta^l_{23} \approx \pi/4 + 3\theta_{cb}$) in this approach. These predictions can be confirmed or excluded by the current generation of neutrino oscillations experiments.

Chapter 6

Fermion Masses in Non-supersymmetric $SO(10)$ Models

Most of the attention in recent years has been focused on the supersymmetric versions of grand unified theories because of the facts that (i) low energy supersymmetry controls the gauge hierarchy and (ii) perhaps more importantly, it leads to the successful gauge coupling unification. While (i) provides very good motivations to integrate supersymmetry with GUTs, (ii) does not forbid completely the possibilities of constructing the viable nonsupersymmetric GUTs. It is well known that the gauge couplings do not unify without low-energy supersymmetry in the minimal $SU(5)$ theory. The problem is the following: while the color and weak gauge couplings meet at around 10^{16} GeV, an ideal scale from the point of view of the proton stability and perturbativity, the $U(1)$ coupling meets the $SU(2)_L$ coupling at around 10^{13} GeV in the absence of low energy supersymmetry. Most interestingly, $SO(10)$ GUT does not need supersymmetry for a successful unification of gauge couplings. On the contrary, the failure of ordinary $SU(5)$ tells us that in the absence of supersymmetry there is necessarily an intermediate scale such as the left-right symmetry breaking scale M_R. In this case the $SU(2)_L$ and $SU(3)_c$ couplings run as in the standard model or with a tiny change depending whether or not there are additional

Higgs multiplets at M_R. However, the $U(1)$ coupling is strongly affected by the embedding in $SU(2)_R$ above M_R. The large contributions of the right-handed gauge bosons makes the $U(1)$ coupling increase much slower and helps it meet the other two couplings at the same point. The scale M_R typically lies between 10^{10} GeV and 10^{14} GeV, which fits very nicely with the seesaw mechanisms.

Another motivation to study the nonsupersymmetric GUTs comes from the failure of the minimal supersymmetric $SO(10)$ model. As discussed in detail in Chapter 3 (Section 3.1.4), there is an inherent tension between the need for a relatively large atmospheric mass-squared difference in the neutrino sector (implying an upper bound on M_{BL} quite below M_{GUT}) and the requirements of the gauge coupling convergence (preferring M_{BL} close to M_{GUT}). This issue is absent in the nonsupersymmetric case because then the separation between the GUT scale and intermediate scale(s) is essential for a successful gauge unification. In fact, a minimal non-supersymmetric $SO(10)$ model has been revived in recent studies [121, 122] and it is shown that successful gauge coupling unification and consistent breaking of $SO(10)$ upto the SM can be achieved with one or two intermediate symmetry breaking scales. It is observed that the minimal non-SUSY $SO(10)$ is more economical then the corresponding supersymmetric case as far the choice of Higgs representation is concerned.

Any such viable constructions must be also accountable for the realistic fermion mass spectrum and this is the principle motivation behind the studies carried out in this chapter. We do the detailed investigations of three different cases for the viable fermion mass spectrum. These three cases correspond to three different choices of the Higgs fields $(1)10_H + \overline{126}_H$, $(2)120_H + \overline{126}_H$ and $(3)10_H + 120_H + \overline{126}_H$ which are responsible to generate fermion masses at the renormalizable level. In this chapter, we discuss the viability of each case and derive its possible predictions for the lepton mixing observables.

6.1 Minimal model with $10 + \overline{126}$ Higgs

The minimal choice of Higgs content plays a crucial role in the construction of any predictive and phenomenologically relevant GUT models. We have already seen in Chapter 3 some nice examples of SUSY GUT models constructed demanding the minimality of Higgs sector. A similar approach is also followed in the case of non-supersymmetric $SO(10)$ theory. Like other GUTs, here also the choice of the Higgs representation is subject to two main requirements, (1) a consistent $SO(10)$ breaking up to the SM and (2) realistic fermion mass spectrum. We will discuss the minimal Higgs content needed to meet both these requirements.

6.1.1 Symmetry breaking & intermediate scales

A full breaking of the $SO(10)$ GUT symmetry down to the SM can be achieved via a pair of Higgs multiplets: one 45-dimensional adjoint representation, 45_H and one $\overline{126}$-dimensional tensor representation $\overline{126}_H$. Note that $\overline{126}_H$ can also be replaced by a smaller representation $\overline{16}_H$. However we stick to the choice of $\overline{126}_H$ because it also contributes in the fermion masses (essentially for the seesaw mechanisms) at the renormalizable level. The explicit decomposition of the 45 and $\overline{126}$ representations under the Pati-Salam gauge group are given in Eqs. (2.17). We rewrite them here for the convenience.

$$\begin{aligned} \overline{126} &= (15,\ 2,\ 2) \oplus (\overline{10},\ 3,\ 1) \oplus (10,\ 1,\ 3) \oplus (6,\ 1,\ 1) \\ 45 &= (15,\ 1,\ 1) \oplus (6,\ 2,\ 2) \oplus (1,\ 3,\ 1) \oplus (1,\ 1,\ 3) \end{aligned} \tag{6.1}$$

A SM preserving breaking pattern is controlled by the following two 45_H VEVs and one $\overline{126}_H$ VEV.

$$\omega_Y \equiv \langle (15,\ 1,\ 1)_{45} \rangle; \quad \omega_R \equiv \langle (1,\ 1,\ 3)_{45} \rangle; \quad \chi_{B-L} \equiv \langle (\overline{10},\ 3,\ 1)_{\overline{126}} \rangle \tag{6.2}$$

Different VEV configurations trigger the spontaneous breakdown of the $SO(10)$

symmetry into the following subgroups. For $\chi_{B-L} = 0$ one finds

$$\begin{aligned}
&\omega_R = 0, \quad \omega_Y \neq 0 \quad \Rightarrow \quad SU(3)_c \times SU(2)_L \times SU(2)_R \times U(1)_{B-L} \\
&\omega_R \neq 0, \quad \omega_Y = 0 \quad \Rightarrow \quad SU(4)_c \times SU(2)_L \times U(1)_R \\
&\omega_R \neq 0, \quad \omega_Y \neq 0 \quad \Rightarrow \quad SU(3)_c \times SU(2)_L \times U(1)_R \times U(1)_{B-L} \\
&\omega_R = +(-)\omega_Y \neq 0 \quad \Rightarrow \quad \text{standard (flipped)} SU(5) \times U(1)
\end{aligned} \tag{6.3}$$

and all these intermediate symmetries are spontaneously broken down to the SM symmetry when $\chi_{B-L} \neq 0$. Remarkably enough, a consistent $SO(10)$ gauge symmetry breaking in the usual low-scale supersymmetric context requires minimally $45_H + 54_H$ [17] or 210_H [47], in addition to $126_H + \overline{126}_H$. A series of studies in the early 1980's of the non-SUSY $SO(10)$ models [123, 124, 125, 126] indicated that the requirement of the gauge coupling unification, even without proton decay limits, excludes any intermediate $SU(5)$ symmetry stages and so the last option in Eq. (6.3) is not viable. Recently, similar analysis has been carried out using the updated values of the gauge coupling constants in [121]. According to this analysis, the phenomenologically favored scenarios allowed by gauge coupling unification correspond to a two-step breaking along one of the following directions (labeled as chain VII and XII in Ref. [121]):

$$\begin{aligned}
SO(10) \;&\longrightarrow\; SU(3)_c \times SU(2)_L \times SU(2)_R \times U(1)_{B-L} \;\longrightarrow\; \mathrm{S}M \\
SO(10) \;&\longrightarrow\; SU(4)_C \times SU(2)_L \times U(1)_R \;\longrightarrow\; \mathrm{S}M
\end{aligned} \tag{6.4}$$

where the first breaking stage is driven by the VEVs of 45_H, while the breaking to the SM at the intermediate scale M_I is controlled by the VEV of $\overline{126}_H$. One of the two 45_H VEVs may also contribute to the second step (see [121] for details).

It was shown about 30 years ago that while the above chains (6.4) are the only ones which are compatible with the non-SUSY unification constraints, they seem to be disfavored by the detailed Higgs sector dynamics [123, 124, 125, 126] due to the emergence of tachyons within the corresponding vacua.

This is due to the fact that a detailed analysis of the classical (tree level) Higgs potential [123, 124, 125, 126] reveals a pair of scalar multiplets with the SM level masses given by the following relation.

$$\frac{M^2(1,3,0)_{45}}{M^2(8,1,0)_{45}} = -\frac{(\omega_Y + 2\omega_R)}{(\omega_R + 2\omega_Y)} \tag{6.5}$$

It is clear that at least one of the scalar multiplets develops a negative mass-squared in the majority of the parametric space (unless $-2 < \omega_Y/\omega_R < -1/2$). This leads to the instability in the vacuum configuration. Consequently, all stable settings exhibit an intermediate flipped $SU(5) \times U(1)$ stage which is problematic with the gauge coupling unification as mentioned before. Recently, it is argued in [122] that this old result is an artifact of the tree level Higgs potential and it is shown that quantum corrections have a dramatic impact. The minimization of the one-loop effective potential in the $\chi_{B-L} = 0$ limit shows that the simplest non-SUSY $SO(10)$ model with a $45_H + \overline{126}_H$ (or $\overline{16}_H$) Higgs sector allows breaking through the intermediate symmetry patterns available. In particular, the chains shown in Eq. (6.3) are supported. This result generally applies to any Higgs sector where the vacuum is dominated by the 45_H VEVs. This observation has opened the option of reconsidering the non-SUSY $SO(10)$ model as a reference framework for model building. However as argued earlier, any realistic model must produce the viable fermion mass sector and it requires the extension of Higgs sector to include 10_H and/or 120_H.

6.1.2 The Yukawa sector and global $U(1)_{PQ}$ symmetry

At the renormalizable level, the most general Yukawa Higgs sector can contain 10_H, 120_H and $\overline{126}_H$ representations which generate the masses for matter fields once the electroweak symmetry breaks. As noted earlier, all three Higgs are not needed in general and one can select at least two of them to construct the realistic theory of fermion masses. The $\overline{126}_H$ is required for $B-L$ symmetry breaking and hence for the renormalizable versions of the seesaw mechanisms, so it is indispensable. As we already discussed in Chapter 3, the SUSY version

with $10_H + \overline{126}_H$ scalars has been studied in the great details and found to be consistent with low energy observations of fermion masses and mixing angles (accept the fact that it cannot account for the observed atmospheric scale). Thus, a first obvious possibility in non-SUSY $SO(10)$ is to address the model with $10_H + \overline{126}_H$, and to see whether or not it can continue to be realistic. Unlike the SUSY case, there is no systematic and complete three generation analysis of fermion masses within non-supersymmetric models. Various issues involved are summarized in a recent paper [127] which contains analytic discussion of the simplified two generation case.

In the absence of SUSY, both the real and the imaginary parts of 10_H can independently couple to fermions, this would mean additional Yukawa couplings. So the most economical possibility for fermion masses and mixing in non-supersymmetric model would be to choose a real 10_H. It is argued [127] that a $\overline{126}_H$ and a real 10_H cannot fit even two generation case and leads to wrong prediction like $m_b = m_t$. Thus one needs a complex 10_H. As noted in Chapter 2, it introduces an extra set of Yukawa couplings which makes the model less predictive. This can be avoided by assigning a Peccei-Quinn (PQ) charge to 10_H. Consider the following general definition of the PQ symmetry:

$$16_F \to e^{i\alpha} 16_F;\ 10_H \to e^{-2i\alpha} 10_H;\ \overline{126}_H \to e^{-2i\alpha} \overline{126}_H. \tag{6.6}$$

The most general Yukawa interactions allowed by this symmetry can be written as

$$-\mathcal{L}_Y \ = \ 16_F^i (Y_{10}^{ij} 10_H + Y_{126}^{ij} \overline{126}_H) 16_F^j + h.c. \tag{6.7}$$

which is similar to Yukawa interactions in the MSGUT (3.3). The 10_H and $\overline{126}_H$ contain respectively bi-doublets (1,2,2) and (15,2,2). They need to mix in order to finally generate the standard model doublet(s) simultaneously containing the 10_H and $\overline{126}_H$ components. This can be achieved by fine tuning. For example, the mixing between bi-doublets is achieved through the following

term

$$V \sim \chi_{ij}\chi_{kl}\Sigma_{ijklm}\phi_m \tag{6.8}$$

which couples 45_H (χ) to $\overline{126}_H$ (Σ) and 10_H (ϕ). This mixes two bi-doublets when component of 45_H transforming as singlet under the $SU(3)_c \times SU(2)_L \times SU(2)_R \times U(1)_{B-L}$ acquires a VEV. Then through fine tuning one can keep one of the two bi-doublets in 10_H and $\overline{126}_H$ at the intermediate scale. Subsequent breaking to SM is achieved through the $(1, 1, 3)$ component of $\overline{126}_H$. Eq. (6.8) provides this way the required mixing between doublets in $\overline{126}_H$ and 10_H.

After the electroweak symmetry breaking, Eq. (6.7) reduces to the same mass matrices relations Eqs. (3.4, 3.5) obtained in the case of MSGUT. We rewrite them here for the convenience of the reader.

$$\begin{aligned} M_d &= H + F, \\ M_u &= r(H + sF), \\ M_l &= H - 3F, \\ M_D &= r(H - 3sF), \\ M_L &= r_L F\ , \\ M_R &= r_R^{-1} F. \end{aligned} \tag{6.9}$$

and the light neutrino mass matrix after the seesaw mechanism is given by

$$M_\nu \equiv M_\nu^{II} + M_\nu^I = M_L - M_D M_R^{-1} M_D^T \tag{6.10}$$

Thus formally both SUSY and non-SUSY cases look alike. But there is an important difference. The renormalization group running of the Yukawa couplings is different in these two cases. Moreover the non-supersymmetric case has intermediate scales. Thus input values and consequently the resulting fits would be quite different in these two cases.

6.1.3 Fermion masses and mixing: Numerical analysis

We now check the viability of Eqs. (6.9, 6.10) through χ^2 fitting. Minimization of χ^2 is performed based on the input values of the charged fermion masses obtained by running quark and lepton masses up to the GUT scale with m_H=140 GeV [128]. We use the updated low energy values of quark mixing angles, CP phase and neutrino parameters since the effect of RG is known to be negligible for hierarchical neutrino spectrum. We reproduce all the input values in Table 6.1 for convenience. As before, we take M_d and M_l as independent and express the remaining matrices in terms of them and r, s as in Eqs. (3.10). Since the masses of the charged leptons are known precisely, we go to the basis with a diagonal M_l and use them as fixed input. Thus we have 15 real parameters (12 in M_d, complex s and real r) which determine remaining 13 observables shown in Table 6.1. The χ^2 function is defined in terms of these parameters.

GUT scale values with propagated uncertainty			
m_d(MeV)	$1.14^{+0.51}_{-0.48}$	$\Delta m^2_{sol}(\mathrm{eV}^2)$	$(7.59 \pm 0.20) \times 10^{-5}$
m_s(MeV)	22^{+7}_{-6}	$\Delta m^2_{atm}(\mathrm{eV}^2)$	$(2.51 \pm 0.12) \times 10^{-3}$
m_b(GeV)	1.00 ± 0.04	$\sin\theta^q_{12}$	0.2246 ± 0.0011
m_u(MeV)	$0.48^{+0.20}_{-0.17}$	$\sin\theta^q_{23}$	0.0420 ± 0.0013
m_c(GeV)	$0.235^{+0.035}_{-0.034}$	$\sin\theta^q_{13}$	0.0035 ± 0.0003
m_t(GeV)	$74.0^{+4.0}_{-3.7}$	$\sin^2\theta^l_{12}$	0.3208 ± 0.0164
m_e(MeV)	$0.469652046 \pm 0.000000041$	$\sin^2\theta^l_{23}$	$0.4529^{+0.0924}_{-0.0484}$
m_μ(MeV)	99.1466226 ± 0.0000089	$\sin^2\theta^l_{13}$	$< 0.049(3\sigma)$
m_τ(GeV)	1.68558 ± 0.00019	δ_{CKM}	$69.63^\circ \pm 3.3^\circ$

Table 6.1: Input values for quark and leptonic masses and mixing angles in the non-supersymmetric standard model extrapolated at $M_{GUT} = 2 \times 10^{16}$ GeV.

Results of numerical analysis carried out separately for type-I and type-II dominated seesaw mechanisms are shown in Table 6.2. Parameters obtained for the best fit solutions are shown in Appendix B.4. It is evident that the type-II mechanism fails completely in reproducing the spectrum. Once again this is linked to the complete absence of the b-τ unification in non-supersymmetric theories. Neither the atmospheric mixing nor the b quark mass can be repro-

duced correctly in this fit. In contrast, the type-I seesaw works quite well. In fact, the quality of fit in this case is much better than the minimal supersymmetric model with type-I seesaw, Table 3.3.

	Type-I		Type-II	
Observables	Fitted value	pull	Fitted value	pull
m_d	0.000810163	-0.687161	0.00101285	-0.264898
m_s	0.0208099	-0.198354	0.0225915	0.0844982
m_b	0.999667	-0.00831657	1.08201	2.05031
m_u	0.000495023	0.0751133	0.000507336	0.13668
m_c	0.237348	0.0670883	0.237096	0.0598882
m_t	73.9427	-0.0154941	74.3006	0.075144
m_e	0.000469652	–	0.000469652	–
m_μ	0.0991466	–	0.0991466	–
m_τ	1.68558	–	1.68558	–
$\left(\frac{\Delta m^2_{sol}}{\Delta m^2_{atm}}\right)$	0.030526	0.127968	0.0297114	-0.235285
$\sin\theta^q_{12}$	0.224651	0.0464044	0.224499	-0.0916848
$\sin\theta^q_{23}$	0.0420499	0.0392946	0.0421308	0.103004
$\sin\theta^q_{13}$	0.00349369	-0.0974312	0.00353053	0.0389979
$\sin^2\theta^l_{12}$	0.323245	0.148134	0.3108	-0.610792
$\sin^2\theta^l_{23}$	0.435096	-0.369178	0.113306	-7.02461
$\sin^2\theta^l_{13}$	**0.0244287**	–	**0.0176863**	–
$\delta_{\rm CKM}[^\circ]$	69.5262	-0.0314447	69.2051	-0.128759
$\delta_{\rm MNS}[^\circ]$	**318.465**	–	**14.5386**	–
$\alpha_1[^\circ]$	**21.5053**	–	**345.645**	–
$\alpha_2[^\circ]$	**215.128**	–	**141.905**	–
$r_{R(L)}$	$\mathbf{5.62 \times 10^{-14}}$	–	$\mathbf{2.09 \times 10^{-10}}$	–
χ^2		**0.710777**		**54.1197**

Table 6.2: Best fit solutions for fermion masses and mixing obtained assuming the type-I and type-II seesaw dominance in the minimal non-SUSY $SO(10)$ model. Various observables and their pulls at the minimum are shown. All the masses shown are in GeV units. The bold faced quantities are predictions of the respective solutions.

As before the r_R gets determined from the atmospheric neutrino mass scale. Assuming, that only one standard model survives at the electroweak scale one has,

$$\langle(1,3,-2)\rangle_{\overline{126}_H} \approx r_R^{-1} s_m v$$

r_R in Table 6.2 gives

$$\langle(1,3,-2)\rangle_{\overline{126}_H} \approx 3 \times 10^{15} s_m \text{GeV} \ . \tag{6.11}$$

Unlike the supersymmetric model, one would like to have this scale at an intermediate value 10^{11} GeV [121] in order to achieve the gauge coupling unification. This will require substantial fine tuning. The exact value of the required intermediate scale for the gauge coupling unification would depend on threshold effects not included in the analysis in [121]. This would need a detailed study of the scalar potential minimization and the scalar sector of the theory.

The leptonic parameters θ_{13} and three CP violating phases $\alpha_{1,2}$ and δ_{MNS} get fixed at the minimum and are shown in Table 6.2. The firm predictions on these observables in the scheme can be obtained by checking the variation of χ^2 with the values of various observables. As already explained in Chapter 4 (Section 4.4), we pin down a specific value p_0 of an observable P by adding a term

$$\chi^2_P = \left(\frac{P - p_0}{0.01\ p_0}\right)^2$$

to χ^2 and then minimizing

$$\hat{\chi}^2 \equiv \chi^2 + \chi^2_P\ .$$

If P happens to be one of the observables used in defining χ^2, then its contribution is removed from there. Artificially introduced small error fixes the value p_0 for P at the minimum of the $\hat{\chi}^2$. We then look at the variation of

$$\bar{\chi}^2_{min} \equiv (\hat{\chi}^2 - \chi^2_P)|_{min} \tag{6.12}$$

with p_0. The results of such analysis carried out for the observables $\sin^2\theta^l_{23}$ and $\sin^2\theta^l_{13}$ are displayed in Fig. 6.1 and Fig. 6.2 respectively. $\sin^2\theta^l_{23}$ can assume value in large range and the 90% confidence level bound corresponding to $\Delta\chi^2 = 4.61$ covers its entire 3σ range $0.33 - 0.64$. In contrast, a clear prediction emerges for the angle $\sin^2\theta^l_{13}$ which preferentially lies in the range $0.015 - 0.03$.

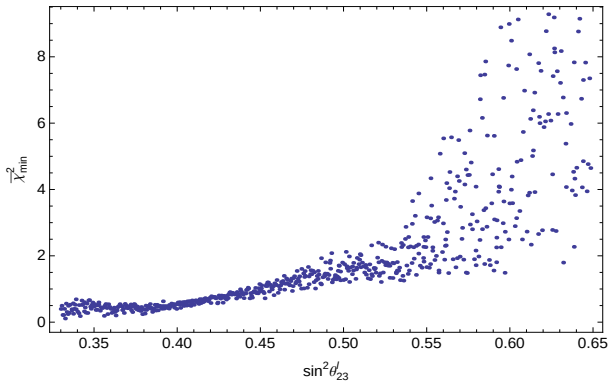

Figure 6.1: Variation of $\bar{\chi}^2_{min}$ with $\sin^2\theta^l_{23}$ in the minimal non-susy $SO(10)$ model with Type-I seesaw.

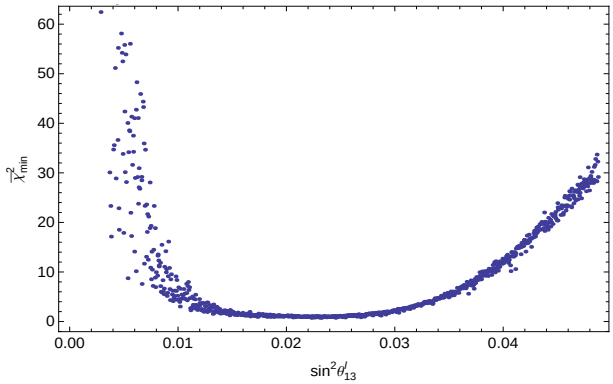

Figure 6.2: Variation of $\bar{\chi}^2_{min}$ with $\sin^2\theta^l_{13}$ in the minimal non-susy $SO(10)$ model with Type-I seesaw.

6.1.4 Yukawa matrices and underlying flavour structure

Numerical analysis presented in the previous subsection has demonstrated viability of the minimal non-SUSY $SO(10)$ model in explaining the fermion masses and mixing. In the process, it has also provided us with specific structure of fermion mass matrices which can be used to obtain some insight into the underlying flavour structure. In this subsection, we discuss the observed flavor structure of the model in detail.

At the $SO(10)$ level, Yukawa couplings H, F, G determine the flavour structure of various mass matrices, Eqs. (6.9). Thus any underlying flavour symmetry if it exists should get reflected in the structure of these matrices. Specific structures for the Yukawa coupling matrices have been used to predict relations between the (hierarchical) quark masses and (small) quark mixing, see for ex-

ample [59, 129, 130, 131]. In a large class of such models, the observed masses and mixing patterns among quarks are reproduced when elements of the quark mass matrices are expressed as powers of one or two expansion parameters. Following this, we try to look for a similar parameterization for the underlying matrices F, H in case of the minimal non-supersymmetric model. We choose the Cabibbo angle $\lambda = 0.2246$ as a convenient parameter. Elements of F and H in this case are then found to have the following hierarchical structure in the basis with a diagonal M_l:

$$
\begin{aligned}
H &= 1.088e^{0.435i}\ \text{GeV} \begin{pmatrix} 0.513e^{1.659i}\lambda^4 & 0.361e^{-1.257i}\lambda^3 & 0.685e^{0.843i}\lambda^2 \\ 0.361e^{-1.257i}\lambda^3 & 0.119e^{1.143i}\lambda^2 & 0.490e^{-2.123i}\lambda \\ 0.685e^{0.843i}\lambda^2 & 0.490e^{-2.123i}\lambda & 1 \end{pmatrix}, \\
F &= 0.278e^{2.561i}\ \text{GeV} \begin{pmatrix} 0.802e^{-0.226i}\lambda^4 & 0.470e^{2.90i}\lambda^3 & 0.892e^{-1.283i}\lambda^2 \\ 0.470e^{2.90i}\lambda^3 & 2.359e^{0.515i}\lambda^2 & 0.639e^{2.034i}\lambda \\ 0.892e^{-1.283i}\lambda^2 & 0.639e^{2.034i}\lambda & 1 \end{pmatrix}
\end{aligned} \tag{6.13}
$$

The 33 element turns out to be largest both for F and H and we have normalized other elements by its value in writing the above structure. Most coefficients in powers of λ are roughly $\mathcal{O}(1)$ except for the 22 elements.

The above structure determined numerically here is suggestive of an underlying $U(1)$ symmetry used [132] in the Froggatt Nielsen (FG) approach. Indeed a simple $U(1)$ can explain the occurrence of various powers of λ in Eq. (6.13). Consider a $U(1)$ symmetry with the $U(1)$ charges $2, 1, 0$ assigned respectively to three generations of 16_F-plet. Both 10_H and $\overline{126}_H$ are assumed neutral under this symmetry. In this case, the 33 elements of F, H arise from the renormalizable couplings $16_{3F}16_{3F}\phi_H \quad (\phi = 10, \overline{126})$. The 23 and 32 elements follow from the couplings $16_{2F}16_{3F}\phi_H\frac{\eta}{M}$. Likewise, the two, three and four powers of η respectively generate $\mathcal{O}(\lambda^2, \lambda^3, \lambda^4)$ terms in Eq. (6.13) where $\lambda = \frac{\langle\eta\rangle}{M}$, M being some underlying scale above the $U(1)$ breaking scale $\langle\eta\rangle$ and η is assumed to carry the $U(1)$ charge -1. The quark mass matrices resulting from the above F, H also follow this simple pattern as in Eq. (6.13):

$$M_d = 0.9708e^{0.6809i}\ \text{GeV} \begin{pmatrix} 0.800e^{1.481i}\lambda^4 & 0.539e^{-1.503i}\lambda^3 & 1.024e^{0.597i}\lambda^2 \\ 0.539e^{-1.503i}\lambda^3 & 0.699e^{2.204i}\lambda^2 & 0.733e^{-2.370i}\lambda \\ 1.024e^{0.597i}\lambda^2 & 0.733e^{-2.370i}\lambda & 1 \end{pmatrix},$$

$$M_u = 72.639e^{0.523i}\ \text{GeV} \begin{pmatrix} 0.609e^{1.585i}\lambda^4 & 0.419e^{-1.359i}\lambda^3 & 0.796e^{0.741i}\lambda^2 \\ 0.419e^{-1.359i}\lambda^3 & 0.281e^{1.981i}\lambda^2 & 0.570e^{-2.225i}\lambda \\ 0.796e^{0.741i}\lambda^2 & 0.570e^{-2.225i}\lambda & 1 \end{pmatrix}$$

This structure is already proposed and studied in [130] as a possible explanation of quark and neutrino mixing and masses. Here it follows from a detailed analysis of this specific $SO(10)$ model. As shown in [130], such a form can reproduce the observed mixing and mass patterns for quarks. The expansion parameter chosen in [130] is somewhat larger, $\lambda = 0.26$. The Dirac neutrino mass matrix on the other hand is given by

$$M_D = 86.240e^{0.210i}\ \text{GeV} \begin{pmatrix} 0.253e^{1.795i}\lambda^4 & 0.201e^{-0.959i}\lambda^3 & 0.382e^{1.140i}\lambda^2 \\ 0.201e^{-0.959i}\lambda^3 & 0.567e^{-0.222i}\lambda^2 & 0.273e^{-1.825i}\lambda \\ 0.382e^{1.140i}\lambda^2 & 0.273e^{-1.825i}\lambda & 1 \end{pmatrix} \tag{6.14}$$

The coefficients in front of various elements are anomalously small and thus M_D does not really share the same symmetry as the underlying Yukawa matrices. The M_D and $M_R \sim F$ conspire to produce a neutrino mass matrix which has an interesting form

$$M_\nu = 0.087e^{-0.898i} r_R r^2\ \text{GeV} \begin{pmatrix} 1.339e^{2.543i}\lambda^3 & 0.878e^{-0.662i}\lambda^2 & 1.753e^{1.529i}\lambda \\ 0.878e^{-0.662i}\lambda^2 & 0.800e^{-2.646i} & 1.062e^{-1.458i} \\ 1.753e^{1.529i}\lambda & 1.062e^{-1.458i} & 1 \end{pmatrix} \tag{6.15}$$

Since we are working in a basis with a diagonal M_l, the above matrix determines physical neutrino mixing and allows us to understand the leptonic mixing structure analytically. Firstly, the 23 block has all elements of $\mathcal{O}(1)$

which results in the large atmospheric angle and hierarchy in neutrino masses. Secondly, the 11 and 12 elements are zero to leading order in λ. In the approximation of neglecting higher powers of λ, the M_ν has two-zero texture (classified as A1 in [133]). The presence of the zeros leads to a firm prediction of the third mixing angle [133]

$$\sin^2\theta^l_{13} \approx \left(\frac{\Delta m^2_{sol}}{\Delta m^2_{atm}}\right) \frac{\sin^2\theta^l_{12}\cos^2\theta^l_{12}}{\cos 2\theta^l_{12}\tan^2\theta^l_{23}} \ . \tag{6.16}$$

This analytic relation is in very good agreement with the numerical values. Evaluation of the RHS using the best fit values of parameters in Table 6.2 leads to $\sin^2\theta^l_{13} \approx 0.0245$ in agreement with the numerical prediction. Even away from the minimum χ^2, one would get $\sin^2\theta^l_{13}$ around 0.02 as long as two zero structure and hence Eq. (6.16) holds approximately. This is born out quite well in Fig. 6.2.

The simple $U(1)$ symmetry used to explain the structure of F, H may appear to have two shortcomings. Firstly, the specific structures are found in a basis with a diagonal M_l Secondly, the coefficients of powers of λ in F, H are not strictly $\mathcal{O}(1)$, notably in the 22 elements. In general, the definition of symmetry and resulting texture of Yukawa matrices are basis dependent. Basis with a diagonal M_l are very special basis and it would be more desirable to find a basis in which M_l also has a structure similar to the F, H, M_d, M_u. One can indeed find a class of unitary rotations which bring the diagonal M_l to the form as in Eq. (6.13) and at the same time retain the forms of F, H albeit with a different set of coefficients. The $U(1)$ symmetry leads to the following general form of the Yukawa matrices:

$$(F,H) = a^{F,H}_{33} \begin{pmatrix} a^{F,H}_{11}\lambda^4 & a^{F,H}_{12}\lambda^3 & a^{F,H}_{13}\lambda^2 \\ a^{F,H}_{12}\lambda^3 & a^{F,H}_{22}\lambda^2 & a^{F,H}_{23}\lambda \\ a^{F,H}_{13}\lambda^2 & a^{F,H}_{23}\lambda & 1 \end{pmatrix} \ . \tag{6.17}$$

F, H as given above can be diagonalized with high accuracy by rotation $R_{F,H}$ consisting of three successive rotations in 2-3, 1-3 and 1-2 plane with the mixing

angles [130]

$$\begin{aligned} \sin\theta_{23}^{F,H} &\approx a_{23}^{F,H}\ \lambda, \\ \sin\theta_{13}^{F,H} &\approx a_{13}^{F,H}\ \lambda^2, \\ \tan 2\theta_{12}^{F,H} &\approx 2\lambda\ \frac{a_{12}^{F,H} - a_{23}^{F,H} a_{13}^{F,H}}{a_{22}^{F,H} - (a_{23}^{F,H})^2 + \mathcal{O}(\lambda^2)} \end{aligned} \tag{6.18}$$

The eigenvalues of F, H are $\mathcal{O}(1, \lambda^2, \lambda^4)$. The eigenvalues of M_l are roughly of similar order-though the coefficient for the electron mass is somewhat small. Thus M_l can be put to the form as in (6.13) by rotating the diagonal M_l with a rotation matrix V_l with angles as in Eq. (6.18) but with a different set of coefficients a_{ij}^l. It is easy to see that when F, H are expressed in new basis their forms do not change to leading order in λ but now coefficients in front of powers of λ are different say, $a_{ij}^{\prime F,H}$. They depend on $a_{ij}^{F,H}$ and a_{ij}^l. Thus symmetry in question may manifest itself in more general basis than the specific diagonal basis provided $a_{ij}^{\prime F,H}$ are also $\mathcal{O}(1)$.

Let us consider a simple example. Rotate F, H and diagonal M_l with a common rotation V_l defined as

$$V_l = \begin{pmatrix} 1 & 0 & 0 \\ 0 & 1 - 1/2\lambda^2 & \lambda e^{i\beta} \\ 0 & -\lambda e^{-i\beta} & 1 - 1/2\lambda^2 \end{pmatrix}$$

β can be chosen such that the coefficient of various powers of λ in elements of $F' = V_l^T F V_l$ and $H' = V_l H V_l$ are near to 1. The best fit value of β turns out to be $\beta = 1.055$ and for this one gets

$$\begin{aligned} |F'| &= 0.278\ \text{GeV} \begin{pmatrix} 0.802\lambda^4 & 0.772\lambda^3 & 0.892\lambda^2 \\ 0.772\lambda^3 & 1.12\lambda^2 & 1.638\lambda \\ 0.892\lambda^2 & 1.638\lambda & 1 \end{pmatrix} \\ |H'| &= 1.088\ \text{GeV} \begin{pmatrix} 0.513\lambda^4 & 0.593\lambda^3 & 0.685\lambda^2 \\ 0.593\lambda^3 & 0.939\lambda^2 & 0.876\lambda \\ 0.685\lambda^2 & 0.876\lambda & 1 \end{pmatrix} \end{aligned} \tag{6.19}$$

Unlike in Eq. (6.13), all the coefficients of various elements in the above equation are now $\mathcal{O}(1)$. M_l is non-diagonal in this basis and is given by

$$|M_l| = 1.685\text{GeV} \begin{pmatrix} 0.109\lambda^4 & 0 & 0 \\ 0 & 1.06\lambda^2 & 1.006\lambda \\ 0 & 1.006\lambda & 1 \end{pmatrix} . \tag{6.20}$$

Hence, the Yukawa coupling matrices obtained numerically in this case display interesting structure which can be understood from a very simple symmetry imposed at a high scale. These features coupled with its economy makes the minimal non supersymmetric model an attractive choice to unify basic gauge and Yukawa interactions.

6.2 Model with $\overline{126} + 120$ Higgs

We now consider an alternative model obtained by replacing 10_H with 120_H in the minimal model discussed before. This model is argued to be quite attractive and predictive when restricted to the second and the third generations [127]. It is thus interesting to see if the model works in more realistic case with three generations which require explanation of several new observables.

In the presence of 120_H together with $10_H + \overline{126}_H$ and $U(1)_{PQ}$ symmetry, the most general effective Yukawa sum-rules are given by Eq. (3.14). With $Y_{10} = 0$, they reduce to the mass relations of the present model and can be suitably written as:

$$\begin{aligned} M_d &= F + G, \\ M_u &= s(F + t_u F), \\ M_l &= -3F + t_l G, \\ M_D &= s(-3F + t_D G), \\ M_L &= r_L F \ , \\ M_R &= r_R^{-1} F. \end{aligned} \tag{6.21}$$

where (G) F is a complex (anti)symmetric matrix and s, r_L, r_R, t_l, t_u and t_D are the complex parameters in general out of which the parameters s, r_L and r_R can be made real without loss of generality.

6.2.1 Outlines of two generation analysis

A simple two generation study was carried out in the context of the above mass relations in [127]. It was found out that the above relations seem to lead to three main predictions. We briefly outline the main points and predictions of their analysis here before we begin the full three generation analysis. In the basis where F is diagonal with real and positive elements, the most general charged fermion mass matrix can be written as [127]:

$$M_f = \mu_f \begin{pmatrix} \sin^2\theta & i(\sin\theta\cos\theta+\epsilon_f) \\ -i(\sin\theta\cos\theta+\epsilon_f) & \cos^2\theta \end{pmatrix} \tag{6.22}$$

where $f = u, d, l$ stands for charged fermions, $|\mu_f| \approx m_{3f}$, $|\epsilon_f| \approx m_{2f}/m_{3f}$ and m_{2f} and m_{3f} correspond to second and third generation masses of f type fermions respectively. It is also evident from Eqs. (6.21) and seesaw formula of neutrino mass matrix (6.10) that in the limit of $t_D \to 0$,

$$M_\nu^I \propto M_\nu^{II} \propto F \tag{6.23}$$

Eq. (6.22) and (6.23) leads to the following predictions.

1. For the neutrino masses, it gives the relation

$$\frac{m_3^2 - m_2^2}{m_3^2 + m_2^2} = \frac{\cos 2\theta_A}{1 - \sin^2 2\theta_A/2} + \mathcal{O}(\epsilon) \tag{6.24}$$

The above relation predicts the relation between the degeneracy of neutrino masses and the maximality of atmospheric mixing angle θ_A. For $\Delta m^2_{atm} = m_3^2 - m_2^2 \approx 2.5\times10^{-3}$ eV^2 and $\theta_A = 45^o$, the above relation puts a lower bound on $m_2 > 0.03$ eV. Further, this lower bound decreases (*i.e.* neutrinos becomes more hierarchical) with increasing deviation from the

maximality for the atmospheric mixing.

2. The model predicts

$$\frac{m_\tau}{m_b} \approx 3 + 3\sin 2\theta_A \mathrm{Re}[\epsilon_l - \epsilon_d] + \mathcal{O}(\epsilon^2) \tag{6.25}$$

We will see later that this relation holds approximately true also in the full three generation study. However it kills the model because the extrapolation of m_b and m_τ at the GUT scale leads to $m_\tau \approx 1.6 m_b$.

3. It was also shown that Eq. (6.22) leads to the following relation between quark mixing V_{cb} and the atmospheric mixing angle θ_A.

$$|V_{cb}| \approx |\mathrm{Re}\xi - i\cos 2\theta_A \mathrm{Im}\xi| + \mathcal{O}(\epsilon^2) \tag{6.26}$$

where $\xi = \cos 2\theta_A(\epsilon_d - \epsilon_u)$.

It is important to note that all three predictions, particularly (1) and (3), are very sensitive to the corrections arise due to the inclusion of first generation. In the next subsection we carry out complete three generation analysis of Eqs. (6.21). We will see there that none of the predictions (1) and (3) holds in three generation case while (2) survives but it is found inconsistent with the fermion masses extrapolated at the GUT scale given in Table 6.1.

6.2.2 Full three generation study: Numerical analysis

In Eqs. (6.21), F can be made real diagonal without loss of generality. M_l is not diagonal and the charged lepton masses are included in the χ^2 function unlike the previous case of the minimal model where they were set as input. Since the errors in the charged lepton masses are extremely small, the numerical optimization algorithm we use is unable to converge to the solution in finite time. Thus we set 10% error in charged lepton masses and minimize the χ^2 with respect to 16 (3 in F, 6 in G, real s and complex t_l, t_u, t_D) real parameters.

	Type-I		Type-II	
Observables	Fitted value	pull	Fitted value	pull
m_d	0.000186192	-1.9871	0.000223284	-1.90982
m_s	0.00267758	-3.2204	0.00296063	-3.17323
m_b	0.844022	-3.89946	0.836471	-4.08822
m_u	0.00048096	0.00480131	0.000483412	0.0170595
m_c	0.23454	-0.0135291	0.237869	0.0819818
m_t	74.053	0.0132566	73.891	-0.0294532
m_e	0.000467656	-0.0424983	0.000475465	0.123771
m_μ	0.0964545	-0.271534	0.101839	0.271587
m_τ	2.61149	5.49314	2.60147	5.43367
$\left(\frac{\Delta m^2_{sol}}{\Delta m^2_{atm}}\right)$	0.0303749	0.0605819	8.59×10^{-7}	-13.4841
$\sin\theta^q_{12}$	0.224581	-0.0172464	0.224591	-0.00790894
$\sin\theta^q_{23}$	0.0419722	-0.0218756	0.0420623	0.0490417
$\sin\theta^q_{13}$	0.00354561	0.0948516	0.00353062	0.0393252
$\sin^2\theta^l_{12}$	0.321216	0.0243762	0.320612	-0.0124452
$\sin^2\theta^l_{23}$	0.450311	-0.0544896	0.0375094	-8.59228
$\delta_{\rm CKM}$	69.5526	-0.0234639	69.5794	-0.0153481
χ^2		**59.7934**		**315.705**

Table 6.3: Best fit solutions for fermion masses and mixing obtained assuming the type-I and type-II seesaw dominance in non-SUSY $SO(10)$ model with $120+\overline{126}$ Higgs. All the masses shown are in GeV units. Various observables and their pulls at the minimum are shown.

Results of numerical analysis carried out separately for type-I and type-II dominated seesaw scenarios are shown in Table 6.3. The detailed fits are quite different in two cases showing that a simple proportionality (6.23) of the type-II and type-I contribution observed in the two generation study [127] does not hold in general. The model fails badly in reproducing the fermion mass spectrum in either case. Analytic study of the two generations lead in the model to a relation $m_\tau \approx 3m_b$. This is born out in the detailed numerical study with three generations as well. But this relation becomes one of the causes of the failure of the model as is clearly seen in the Table 6.3. Likewise, the numerical fits lead to nearly vanishing solar scale at the minimum in the type-II case. This becomes an added cause of very poor fits. It appears from the results that the renormalizable model with $45_H+120_H+\overline{126}_H$ Higgs fields is not a good candidate to obtain even fermion mass spectrum.

6.3 Model with $10 + \overline{126} + 120$ Higgs

As we have already discussed in Section 6.1, the minimal case works quite well and provides realistic fermion mass spectrum and there is no real motivation to go to the non-minimal case with $10_H + \overline{126}_H + 120_H$. However we carry out such analysis for completeness and find that this case works even better than the minimal case as far as the fermion masses are concerned.

6.3.1 Extension with additional 120 Higgs

The minimal model discussed in Section 6.1 is extended by adding 120_H field which transforms as

$$120_H \to e^{-2i\alpha} 120_H$$

under the global $U(1)_{PQ}$ symmetry. Like in the SUSY case, here also, 120_H do not play any major role in $SO(10)$ symmetry breaking and the entire symmetry breaking is governed by 45_H and $\overline{126}_H$. However 120_H contributes in the fermion masses through its two SM like doublets. Assuming that the CP is violated maximally and spontaneously (or equivalent Z_2 parity defined in [83]), we obtain the same fermion mass relations Eqs. (3.15) as we obtained in the SUSY case. We rewrite these relations again for convenience.

$$\begin{aligned}
M_d &= H + F + iG\ , \\
M_u &= r(H + sF + it_u\ G\ ), \\
M_l &= H - 3F + \ it_l\ G\ , \\
M_D &= r(H - 3sF + it_D\ G\ ), \\
M_L &= r_L F\ , \\
M_R &= r_R^{-1} F. \qquad (6.27)
\end{aligned}$$

where (G) H, F are real (anti)symmetric matrices. r, s, t_l, t_u, t_D, r_L, r_R are dimensionless real parameters. We carry out the numerical analysis of the above relations to check their consistency with the data given in Table 6.1.

6.3.2 Numerical analysis of fermion masses & mixing

We select a basis in which H is diagonal in Eqs. (6.27). M_l is not diagonal in this basis and we parameterize it as $M_l = U_l D_l U_l^\dagger$ with U_l being a general unitary matrix expressed in terms of three angles and six phases and D_l is a diagonal matrix for the charged lepton masses. One can rewrite M_l in Eqs. (3.9) as

$$3F - it_l G = H - U_l D_l U_l^\dagger$$

Since F and G are real, the real and imaginary parts of the RHS separately determine F and $t_l G$ in terms of the charged lepton masses and parameters of H and U_l which are put back in Eqs. (3.9). The remaining fermion mass matrices can be expressed in terms of 17 (3 in H, 9 in U_l, real r, s, t_l, t_u, t_D) real parameters in the case of type-I seesaw dominance which determine 16 observables P_i shown in Table 6.1. One parameter t_D becomes irrelevant for the type-II seesaw case. We do the numerical analysis for this case and results are shown in Table 6.4.

Parameters obtained for the best fit solutions in type-I case are shown in Appendix B.4. Unlike the supersymmetric case, the presence of 120_H does not help in improving the fits in the type-II seesaw dominated case. But the fits obtained for the type-I scenario are considerably better compared to the corresponding supersymmetric as well as the minimal non-supersymmetric case. Pulls in all observables are practically zero in this case.

The predictions of the model for the observables $\sin^2\theta_{23}^l$ and $\sin^2\theta_{13}^l$ are displayed in Fig. 6.3 and Fig. 6.4 respectively. Once again a clear prediction$\sin^2\theta_{13} \gtrsim 0.015$ emerges in this case.

6.4 Conclusions & outlook

In this chapter, we carried out a detailed analysis of the fermion masses in non-supersymmetric models. The minimal non-supersymmetric $SO(10)$ model with $45_H + 10_H + \overline{126}_H$ is quite economical and is argued recently [121, 122]

	Type-I		Type-II	
Observables	Fitted value	pull	Fitted value	pull
m_d	0.00113968	-0.000676838	0.00108711	-0.110189
m_s	0.0219909	-0.00150966	0.0142689	-1.28852
m_b	1.	0.0000376219	1.19665	4.9162
m_u	0.000480133	0.000666686	0.000486627	0.0331338
m_c	0.235007	0.000211758	0.240819	0.166268
m_t	73.9997	-0.0000888053	77.4295	0.857367
m_e	0.000469652	0	0.000469652	0
m_μ	0.0991466	0	0.0991466	0.220249
m_τ	1.68558	0	1.68558	0.000124065
$\left(\frac{\Delta m^2_{sol}}{\Delta m^2_{atm}}\right)$	0.0302402	0.000545016	0.0260106	-1.88556
$\sin\theta^q_{12}$	0.224601	0.00105776	0.224567	-0.0304356
$\sin\theta^q_{23}$	0.0420001	0.0000431604	0.0431393	0.897068
$\sin\theta^q_{13}$	0.00351992	-0.000308192	0.00338234	-0.509862
$\sin^2\theta^l_{12}$	0.320821	0.000292661	0.278093	-2.6052
$\sin^2\theta^l_{23}$	0.453034	0.000947066	0.343286	-2.26804
$\sin^2\theta^l_{13}$	**0.0306736**	–	**0.00538748**	–
$\delta_{\rm CKM}[^\circ]$	69.6278	-0.000660788	72.7155	0.935014
$\delta_{\rm MNS}[^\circ]$	**355.719**	–	**46.8148**	–
$\alpha_1[^\circ]$	**60.079**	–	**60.6202**	–
$\alpha_2[^\circ]$	**214.691**	–	**250.978**	–
$r_{R(L)}$	$\mathbf{1.56\times10^{-15}}$	–	$\mathbf{3.43\times10^{-10}}$	–
χ^2		$\sim\mathbf{10^{-6}}$		**44.0801**

Table 6.4: Best fit solutions for fermion masses and mixing obtained assuming the type-I and type-II seesaw dominance in the non-supersymmetric $SO(10)$ model with $10+\overline{126}+120$ Higgs. Various observables and their pulls at the minimum are shown. All the masses shown are in GeV units. The bold faced quantities are predictions of the respective solutions.

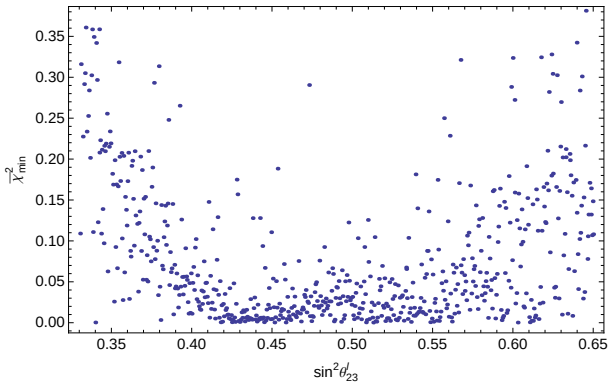

Figure 6.3: Variation of $\bar{\chi}^2_{min}$ with $\sin^2\theta^l_{23}$ in the extended model with Type-I seesaw.

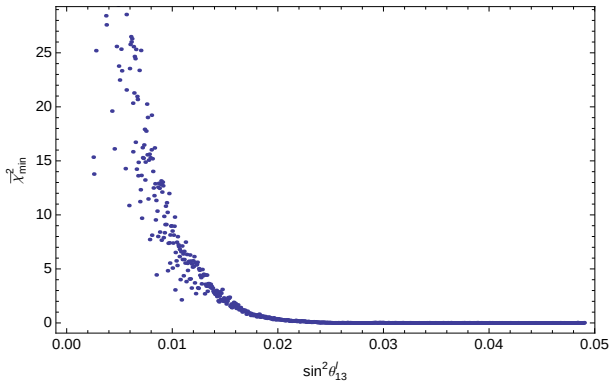

Figure 6.4: Variation of $\bar{\chi}^2_{min}$ with $\sin^2\theta^l_{13}$ in the extended model with Type-I seesaw.

to be a viable candidate for the gauge coupling unification. As shown here it also provides a very good description of fermion masses as well. Some of the interesting outcomes of this study are the following.

- Unlike the supersymmetric case, the extrapolated values of bottom quark mass and tau lepton mass at the GUT scale do not unify. Thus type-II models in this category fail completely, namely, they predict very small atmospheric mixing angle $\theta^l_{23} \sim \mathcal{O}(V_{cb})$.

- Intermediate scale $\sim 10^{11}$ GeV is required in this model in order to obtain the unification of gauge coupling [121]. The scale preferred from the fits to fermion masses presented in the minimal model is somewhat larger. This scale can be reduced if the admixture of the light doublet in the doublet component of $\overline{126}_H$ is very small, see Eq. (6.11).

- The Yukawa coupling matrices obtained numerically in this case display interesting structure which can be understood from a very simple symmetry imposed at a high scale.

- Based on simplified two generation study, a model with $120_H + \overline{126}_H$ was argued to be potential candidate for the viable fermion spectrum. As it is shown here through complete three generations study, this model fails in explaining the fermion spectrum and hence can be ruled out.

- The non minimal model with $10_H + \overline{126}_H + 120_H$ also provides an excellent fit to the fermion masses and mixing angles.

In particular, the minimal model with type-I seesaw emerges as best viable scenario based on which a complete non-SUSY $SO(10)$ model can be constructed. Consistency of the parameter space provided by fermion mass fitting as well as simultaneous analysis of the constraint from the gauge coupling unification will depend on the detailed analysis of the scalar sector of the theory. Such analysis will provide the playground for exploring the possibility of a realistic and predictive GUT, along the lines of the recent efforts in the supersymmetric context.

Chapter 7

Summary & Outlook

An understanding of the fermion mass spectrum and their peculiar mixing patterns is one of the major goals of the particle physics beyond the standard model. Because of the virtue of quark-lepton unification, the grand unified theories can play an important role in revealing the origin of similarities and contrasts between the quarks and leptons masses and mixing patterns observed in nature. On the other hand, eventhough the idea of the grand unification is as old as the standard model, it is still an "idea" because most of its smoking gun signals lie in the domain beyond our experimental reach. As a result, one has to rely either on its predictions of ultra-weak interactions like nucleon decay or some of its indirect evidences like the unification of the gauge couplings. Most importantly, it is recently understood that the fermion masses and mixing can also provide a testing ground for GUTs at least when they are constructed on the principle of minimality. The precisely known values of fermion masses and mixing angles can provide a crucial viability test for any such GUT framework. We have examples of beautiful models such as the minimal SUSY $SU(5)$ model (in Chapter 2) and minimal SUSY $SO(10)$ model (in Chapter 3) which are consistent with other constraints but which failed in explaining the observed fermion mass spectrum.

In this thesis, we have concentrated on studies of the implied fermion mass spectrum within otherwise successful GUT models based on an $SO(10)$ gauge symmetry. The choice of $SO(10)$ based models is naturally motivated due

to their economy and ability to incorporate neutrino masses. A complete unification of a fermion family leads to very interesting consequences which otherwise are impossible to achieve in ordinary bottom-up approaches. We have outlined some of these features of $SO(10)$ GUTs and their advantages over the standard model in the first two chapters of the thesis. Particularly in the second chapter, we disuses the origin of fermion masses and connections between quark and lepton spectra in $SU(5)$ and $SO(10)$ based GUTs. Many qualitative comparisons have been drawn in order to understand the relevance of $SO(10)$ GUT which is quantitatively studied in the subsequent chapters. We have already summarized the detailed results and their major implications at the end of each chapter. Here we briefly discuss the main outcomes of each study.

As argued earlier, the minimality sometimes leads to predictive frameworks which can be tested through their viability in reproducing the fermion mass spectrum. In Chapter 3, we study two such models built on the SUSY $SO(10)$ gauge theories. One of them is the minimal SUSY $SO(10)$ model which was studied earlier in great details and found inconsistent due to the conflict between the position of the seesaw scale and the requirements of gauge couplings unification. However all these studies were based on the fermion mass data which do not include the supersymmetric threshold corrections. Such SUSY threshold corrections play significant role in changing some of the observables of fermion mass spectrum extrapolated at the GUT scale. For example, the viability of type-II seesaw mechanism in the minimal model crucially depends on the precise b-τ unification at the GUT scale which is sensitive to SUSY threshold corrections. We show that the type-II seesaw mechanism in the minimal model can provide reasonable fits only in the cases where b-τ unification is achieved with/without including the threshold corrections. A small departure from b-τ unification results into the small atmospheric mixing angle which is disfavored by the neutrino oscillation experiments. On the other hand, type-I seesaw works uniformly well and does not require b-τ unification. We also confirm the existing conflict between seesaw scale and unification scale from

our fitted parameters. The extension of the minimal model is also studied. It is found that in this model, one obtains reasonable improvements over the minimal model and both type-I and type-II cases work well. In the case of type-II seesaw dominance, the b-τ unification is not necessary to obtain the good fits unlike in the minimal model. However its presence improves the fit. As a result, the non-minimal model which correctly accounts for the realistic fermion mass spectrum can be considered as the potential candidate for the new minimal GUT model. However its ultimate fate depend on the consistency of the fitted parameters with the other constraints coming from the scalar potential minimization, proton decay etc.

In Chapter 4 and 5, we tried to understand the origin of difference between the quark and lepton mixing patterns. In the quark-lepton unified frameworks, one naively expects that the quark and lepton mixing patterns would be identical. However this is not the case and we know that the lepton mixing angles are large when compared to the quark mixing angles. The lepton mixing angles seem to follow a particular mixing pattern known as tribimaximal mixing. It is not even known that such large lepton mixing are compatible with the small and hierarchical quark mixing together with fermion masses. In Chapter 4, we address this question by checking the viability of the exact tribimaximal lepton mixing with the remaining fermion mass spectrum. We first find out the most general condition under which the exact tribimaximal lepton mixing pattern can exist and then we numerically investigate the viability of an entire fermion mass spectrum subject to this condition in a non-minimal SUSY $SO(10)$ model. It is found that the exact TBM pattern in the lepton mixing is a viable scenario and it is consistent with the entire fermion spectrum.

We study some flavor symmetric models built on SUSY $SO(10)$ framework in Chapter 5 which can account for the observed differences between quark and lepton flavor mixing patterns. Flavor symmetry constraints the parameter space in a given model by establishing the horizontal relations between different families of fermions. This sometimes leads to an understanding of specific flavor mixing pattern. In a grand unified framework, such symmetries

must uniquely determine the flavor mixing pattern of quarks and leptons treating them identically at the GUT scale. We provide three candidate $SO(10)$ GUT models of flavor symmetries which do this job in different ways. The spontaneously broken μ-τ symmetry in an $SO(10)$ model simultaneously accounts for the small quark mixing and large lepton mixing being consistent with fermion masses. One gets similar patterns in fermion mass matrices irrespective of type-I or type-II seesaw dominance. In the second part of Chapter 5, we propose an $SO(10)$ model based on a continuous $O(3)$ symmetry which leads to quasidegenerate neutrinos. The large lepton mixing angles are the natural consequences of quasidegenerate neutrinos. Consistency of quasidegenerate neutrino spectrum with hierarchical charged fermions is shown through detailed numerical analysis. In the last section of Chapter 5, we consider an S_4 symmetric $SO(10)$ model which establishes many interesting connections between the observables of the quark and lepton sector. It predicts relations like quark-lepton complementarity, Georgi-Jarlskog relations which were empirically known since long ago. The largeness of lepton mixing angles can be understood in terms of type-II seesaw dominance.

The non-supersymmetric $SO(10)$ GUTs have emerged as natural alternatives to SUSY GUTs because an intermediate seesaw scale required for neutrino masses is a necessary ingredient of this model if gauge couplings are to unify. In order to construct a realistic model based on non-SUSY $SO(10)$, one needs to decide a suitable Higgs content which can account for consistent symmetry breaking and viable fermion mass spectrum. In Chapter 6, we address the second requirements through detailed investigations of different Higgs content and checking their viability with respect to observed fermion spectrum. We find that the minimal model based on the scalar content $10_H + \overline{126}_H + 45_H$ and with a global $U(1)_{PQ}$ symmetry can precisely reproduce entire fermion spectrum if type-I seesaw dominates. Also an extension with 120_H works well while a replacement of 10_H by 120_H fails in explaining the observed fermion masses. It is shown that type-II seesaw mechanism in all these models is disfavored by the b-τ non-unification at the GUT scale. Our results strongly favor the scalar

sector which includes $10_H + \overline{126}_H + 45_H$ as the best candidate for the minimal non-SUSY $SO(10)$ model. However, one has to test the consistency of the $10_H + \overline{126}_H + 45_H$ vacuum against gauge unification. If the vacuum turned out to be compatible with the phenomenological requirements it would be then important to perform an accurate estimate of the proton decay branching ratios. As a matter of fact non-supersymmetric GUTs offer the possibility of making definite predictions for proton decay where the main theoretical uncertainty lies in the mass of the leptoquark vector bosons, subject to gauge unification constraints.

Appendix A

Extraction of the observables and fitting procedure

In this Appendix, we discuss our method of extracting the physical observables from the fermion mass matrices predicted in the different models. We also briefly explain the χ^2 method through which we fit the model on the fermion mass data extrapolated at the GUT scale.

A.1 Extraction of the physical observables

From the given mass matrices of fermions, we extract the physically relevant quantities as the following. First we diagonalize the mass matrices by biunitary transformations:

$$U_{f_L}^{\dagger} M_f U_{f_R} = \text{Diag.}(m_{f_1}, m_{f_2}, m_{f_3}) \equiv D_f \tag{A.1}$$

where $f = u, d, l, \nu$ stands for up-, down-type quarks, charged leptons and neutrinos respectively. In practice, the U_{f_L} (U_{f_R}) is constructed from the eigenvectors of a Hermitian matrix $M_f M_f^{\dagger}$ ($M_f^{\dagger} M_f$). In the most of the cases we studied in the thesis, M_f is either complex symmetric or Hermitian. In these special cases, one obtains $U_{f_R} = U_{f_L}^*$ or $U_{f_R} = U_{f_L}$ respectively. Basically, $U_{f_{L,R}}$ are the unitary rotations which relate the flavor eigenstates to the physical

eigenstates (denoted by $f'_{L,R}$) by the following transformation:

$$f_{L,R} = U_{f_{L,R}} f'_{L,R} \tag{A.2}$$

As a result, the charged-current interactions (1.26) couple to the physical fermions $f'_{L,R}$ with couplings given by

$$\begin{aligned} V_{CKM} &\equiv U^{\dagger}_{u_L} U_{d_L} \\ V_{PMNS} &\equiv U^{\dagger}_{l_L} U_{\nu_L} \end{aligned} \tag{A.3}$$

where V_{CKM} is Cabibbo-Kobayashi-Maskawa [134, 135] matrix which mixes the quark flavors while an analogous mixing in the lepton sector is characterized by the Pontecorvo-Maki-Nakagawa-Sakata [136, 137] mixing matrix, namely V_{PMNS}. In the case of three fermionic generations, each of the above matrix is a 3×3 unitary matrix and can be parametrized by three mixing angles and a CP-violating phase [106]. In the popular "standard parametrization", it can be written as

$$V = P_L \begin{pmatrix} c_{12}c_{13} & s_{12}c_{13} & s_{13}e^{-i\delta} \\ -s_{12}c_{23} - c_{12}s_{23}s_{13}e^{i\delta} & c_{12}c_{23} - s_{12}s_{23}s_{13}e^{i\delta} & s_{23}c_{13} \\ s_{12}s_{23} - c_{12}c_{23}s_{13}e^{i\delta} & -c_{12}s_{23} - s_{12}c_{23}s_{13}e^{i\delta} & c_{23}c_{13} \end{pmatrix} P_R \tag{A.4}$$

where $s_{ij} = \sin\theta_{ij}$ and $c_{ij} = \cos\theta_{ij}$. $P_L = \text{Diag.}(e^{i\beta_1}, e^{i\beta_2}, e^{i\beta_3})$ and $P_R = \text{Diag.}(e^{i\frac{\alpha_1}{2}}, e^{i\frac{\alpha_2}{2}}, 1)$ are diagonal phase matrices. In the quark sector, both P_L and P_R can be rotated away by redefining the quark fields u_L and d_L respectively and thus none of them is physical. However, in the lepton sector, P_R cannot be rotated away if neutrinos are Majorana fields. This keeps α_1 and α_2 physically relevant and they are known as the Majorana phases [106].

From Eqs. (A.1) and (A.4), we have total 22 physical observables (12 fermion masses + 3 quark mixing angles + CP phase in the quark sector + 3 lepton mixing angles + 3 CP phases in the lepton sector) which can be probed in the low energy experiments. Out of these 22 observables, 17 have already

been measured (9 charged fermion masses, Δm^2_{sol}, Δm^2_{atm}, 4 CKM parameters, θ^l_{23} and θ^l_{12} mixing angles in the lepton sector). There exists upper bound on the reactor angle θ^l_{13} in the lepton sector while the remaining 3 phases and the absolute mass of neutrinos are not known. Recently, the T2K and MINOS experiments have indicated nonzero θ^l_{13}. We have also taken this into account wherever required.

A.2 Fitting procedure

The different $SO(10)$ scenarios discussed in the thesis predict the fermion mass matrices M_f as functions of finite number of free parameters x_α. In order to check the viability of these predictions and further to determine the best fit values of parameters x_α, we carry out the χ^2 fitting in the thesis wherever it is needed. For this, we construct a χ^2 function defined as

$$\chi^2(x_\alpha) = \sum_i \left(\frac{P_i(x_\alpha) - O_i}{\sigma_i} \right)^2 . \tag{A.5}$$

where the sum runs over different observables. P_i denote the theoretical values of physical observables which are extracted from the fermion mass matrices M_f as discussed above. The O_i are the experimental values of the same observable extrapolated to the GUT scale and σ_i denote the 1σ errors in O_i.

The data of the fermion masses and mixing angles are fitted by minimizing the $\chi^2(x_\alpha)$ with respect to the free parameters x_α. Note that the $\chi^2(x_\alpha)$ is highly non-linear and complex function in general which cannot be minimized by any known analytical technique. Thus it is minimized using an algorithm based on the numerical optimization technique, the simplex method [138]. To implement this method, we use the function minimization tool MINUIT [139] developed by the CERN library. The simplex method does not use the first derivatives of function to locate the minima. As a result, it is rather robust with respect to gross fluctuations in the function value and hence considered to be most suitable method of optimization for extremely non-linear and complex

functions. However, it gives no reliable information about the parameter errors. Moreover, it cannot be expected to converge accurately to the minimum in a finite time. It is also important to note that considering the non-linearity and complexity of the problem here, the algorithm is not guaranteeing the global minimum. In this case, it is difficult to rule out the existence of still lower minima if it exist which may improve the solutions. To increase the chance of getting global minimum we run the program for long enough time to scan all the possible minimum which may exist in the parameter space.

Appendix B

Parameters obtained for the best fit solutions

In this Appendix, we show the parameter values obtained from our fitting procedure for some of the best fitted models that we have analyzed. The fitted parameters are shown in each case and all the fermion mass matrices can be constructed from these parameters using the mass relations predicted by respective models.

B.1 The supersymmetric $SO(10)$ models

The minimal model with type-II seesaw

The best fit ($\chi^2 = 6.9367$) is obtained for $\tan\beta = 1.3$ in this case. The results are given in column A of Table 3.2. The values of parameters obtained at the minimum of χ^2 are:

$$
\begin{aligned}
M_l &= m_\tau \begin{pmatrix} 0.000285653 & 0 & 0 \\ 0 & 0.0593651 & 0 \\ 0 & 0 & 1. \end{pmatrix} \\
M_d &= m_\tau \begin{pmatrix} 0.001190 + 0.000816i & -0.001425 - 0.003735i & -0.044221 - 0.009033i \\ -0.001425 - 0.003735i & -0.0193451 + 0.013953i & 0.081325 + 0.095024i \\ -0.044221 - 0.009033i & 0.081325 + 0.095024i & 1.00871 - 0.133436i \end{pmatrix} \\
s &= 0.0963194 + 0.158168i
\end{aligned}
\tag{B.1}
$$

The minimal model with type-I seesaw

The best fit ($\chi^2 = 3.4746$) is obtained for $\tan\beta = 38$ in this case. The results are given in column C2 of Table 3.3. The values of parameters obtained at the minimum of χ^2 are:

$$\begin{aligned}
M_l &= m_\tau \begin{pmatrix} 0.00025867 & 0 & 0 \\ 0 & 0.0540358 & 0 \\ 0 & 0 & 1. \end{pmatrix} \\
M_d &= m_\tau \begin{pmatrix} 0.001800i & 0.005386 - 0.000214i & 0.034807 + 0.031733i \\ 0.005386 - 0.000215i & -0.009305 - 0.018381i & 0.097663 - 0.104384i \\ 0.034807 + 0.031733i & 0.097663 - 0.104384i & 0.945297 - 0.052779i \end{pmatrix} \\
s &= 0.467643 - 0.124332i
\end{aligned} \tag{B.2}$$

The non-minimal model with type-II seesaw

The best fit ($\chi^2 = 0.0038$) is obtained for $\tan\beta = 38$ in this case. The results are given in column C2 of Table 3.4. The values of parameters obtained at the minimum of χ^2 are:

$$\begin{aligned}
H &= m_\tau \begin{pmatrix} -0.000251755 & 0 & 0 \\ 0 & -0.00357438 & 0 \\ 0 & 0 & -0.98908 \end{pmatrix} \\
F &= m_\tau \begin{pmatrix} -0.000423953 & 0.000552908 & 0.00210575 \\ 0.000552908 & -0.00692301 & -0.00563144 \\ 0.00210575 & -0.00563144 & -0.00837315 \end{pmatrix} \\
G &= m_\tau \begin{pmatrix} 0 & 0.000948193 & 0.00669678 \\ -0.000948193 & 0 & -0.0227847 \\ -0.00669678 & 0.0227847 & 0 \end{pmatrix} \\
(s,\ t_u,\ t_l) &= (-0.82278,\ 0.123789,\ -8.02413)
\end{aligned} \tag{B.3}$$

The non-minimal model with type-I seesaw

The best fit ($\chi^2 = 0.0011$) is obtained for $\tan\beta = 38$ in this case. The results are given in column C2 of Table 3.5. The values of parameters obtained at the minimum of χ^2 are:

$$
\begin{aligned}
H &= m_\tau \begin{pmatrix} -0.000124146 & 0 & 0 \\ 0 & -0.00336696 & 0 \\ 0 & 0 & 0.998283 \end{pmatrix} \\
F &= m_\tau \begin{pmatrix} 0.00107671 & -0.00155537 & -0.00259023 \\ -0.00155537 & 0.0136525 & -0.0253916 \\ -0.00259023 & -0.0253916 & 0.00144251 \end{pmatrix} \\
G &= m_\tau \begin{pmatrix} 0 & -0.00116384 & 0.00106055 \\ 0.00116384 & 0 & 0.00165029 \\ -0.00106055 & -0.00165029 & 0 \end{pmatrix} \\
(s,\ t_u,\ t_l,\ t_D) &= (\ 0.0817661,\ -0.242018,\ -10.8351,\ 565.082)
\end{aligned}
\tag{B.4}
$$

B.2 The tribimaximal mixing in $SO(10)$

TBM in $SO(10)$: The most general V_l

The parameter values corresponding to the best fit solution shown in column A in Table 4.2 are the following.

$$
\begin{aligned}
H &= \begin{pmatrix} 0.0023206 & 0.000117224 & -0.0219357 \\ 0.000117224 & 0.0438213 & 0.121791 \\ -0.0219357 & 0.121791 & 1.06669 \end{pmatrix} \text{GeV} \\
F &= \begin{pmatrix} -0.00289886 & -0.00526436 & -0.00526436 \\ -0.00526436 & -0.0411171 & 0.0329539 \\ -0.00526436 & 0.0329539 & -0.0411171 \end{pmatrix} \text{GeV} \\
G &= \begin{pmatrix} 0 & 0.003501 & 0.00758655 \\ -0.003501 & 0 & 0.0435519 \\ -0.00758655 & -0.0435519 & 0 \end{pmatrix} \text{GeV} \\
(r,\ s,\ t_u,\ t_l) &= (77.6714,\ 0.545681,\ 0.214621,\ 7.64053)
\end{aligned}
\tag{B.5}
$$

TBM in $SO(10)$: Exact TBM lepton mixing ($V_l = U_l$)

The parameter values corresponding to the best fit solution shown in column B1 in Table 4.2 are the following.

$$
\begin{aligned}
H &= \begin{pmatrix} 0.00111546 & 0.000428794 & -0.020097 \\ 0.000428794 & 0.0188148 & 0.0639684 \\ -0.020097 & 0.0639684 & 1.17731 \end{pmatrix} \text{GeV} \\
F &= \begin{pmatrix} -0.0016484 & -0.00375321 & -0.00375321 \\ -0.00375321 & -0.0276748 & 0.0222732 \\ -0.00375321 & 0.0222732 & -0.0276748 \end{pmatrix} \text{GeV} \\
G &= \begin{pmatrix} 0 & -0.00278749 & -0.0378996 \\ 0.00278749 & 0 & -0.0820076 \\ 0.0378996 & 0.0820076 & 0 \end{pmatrix} \text{GeV} \\
(r,\ s,\ t_u,\ t_l) &= (70.5742,\ 0.526782,\ 0.551405,\ 2.15986)
\end{aligned} \tag{B.6}
$$

B.3 The μ-τ symmetric $SO(10)$

μ-τ symmetric $SO(10)$: type-II seesaw

The parameter values corresponding to the best fit solution obtained for the case C in Table 5.2 are the following.

$$
\begin{aligned}
H &= \begin{pmatrix} -0.818923 & 0 & 0 \\ 0 & -701.354 & -32.0485 \\ 0 & -32.0485 & -598.783 \end{pmatrix} \text{MeV} \\
F &= \begin{pmatrix} -0.343138 & -2.07269 & -2.07269 \\ -2.07269 & 11.2606 & -14.3836 \\ -2.07269 & -14.3836 & 11.2606 \end{pmatrix} \text{MeV} \\
G &= \begin{pmatrix} 0 & 4.19817 & -4.19817 \\ -4.19817 & 0 & 617.845 \\ 4.19817 & -617.845 & 0 \end{pmatrix} \text{MeV} \\
(r,\ s,\ t_u,\ t_l) &= (61.1056,\ -121.664,\ 65.9824,\ -0.980791)
\end{aligned} \tag{B.7}
$$

μ-τ symmetric $SO(10)$: type-I seesaw

The parameter values corresponding to the best fit solution obtained for the case C in Table 5.3 are the following.

$$
\begin{aligned}
H &= \begin{pmatrix} 35.0178 & 0 & 0 \\ 0 & 556.777 & 554.429 \\ 0 & 554.429 & 551.775 \end{pmatrix} \text{MeV} \\
F &= \begin{pmatrix} -15.716 & 20.8951 & 20.8951 \\ 20.8951 & -29.4636 & -29.5305 \\ 20.8951 & -29.5305 & -29.4636 \end{pmatrix} \text{MeV} \\
G &= \begin{pmatrix} 0 & 2.79728 & -2.79728 \\ -2.79728 & 0 & -3.21385 \\ 2.79728 & 3.21385 & 0 \end{pmatrix} \text{MeV} \\
(r,\ s,\ t_u,\ t_l,\ t_D) &= (83.7973,\ 178.571,\ 0.011244,\ 1.0715,\ 4537.34) \qquad \text{(B.8)}
\end{aligned}
$$

We also give the fermion mass matrices obtained from eq.(5.2) using the best fit values of the parameters given above.

$$
\begin{aligned}
M_d &= \begin{pmatrix} 19.3018 & 20.8951 + 2.79728i & 20.8951 - 2.79728i \\ 20.8951 - 2.79728i & 527.314 & 524.898 - 3.21385i \\ 20.8951 + 2.79728i & 524.898 + 3.21385i & 522.311 \end{pmatrix} \text{MeV} \\
M_u &= \begin{pmatrix} 127.971 & 3731.25 + 2.99727i & 3731.25 - 2.99727i \\ 3731.25 - 2.99727i & 41395.1 & 41186.3 - 3.44363i \\ 3731.25 + 2.99727i & 41186.3 + 3.44363i & 40975.9 \end{pmatrix} \text{MeV} \\
M_l &= \begin{pmatrix} 82.1659 & -62.6852 + 0.0314526i & -62.6852 - 0.0314526i \\ -62.6852 - 0.0314526i & 645.168 & 643.02 - 0.0361365i \\ -62.6852 + 0.0314526i & 643.02 + 0.0361365i & 640.166 \end{pmatrix} \text{MeV} \\
M_\nu^I &= \begin{pmatrix} -0.0242264 & -0.0143681 + 0.0004742i & -0.0143657 - 0.0000756i \\ -0.0143681 + 0.0004742i & -0.012829 + 0.0067828i & -0.016311 + 0.0002142i \\ -0.0143657 - 0.0000756i & -0.016311 + 0.0002142i & -0.0127693 - 0.0062952i \end{pmatrix} \text{GeV} \qquad \text{(B.9)}
\end{aligned}
$$

B.4 The non-supersymmetric $SO(10)$ models

The minimal non-SUSY $SO(10)$ model with type-I seesaw

The values of fitted parameters corresponding to the best fit solution obtained for type-I seesaw in Table 6.2 are the following.

$$
\begin{aligned}
M_l &= \begin{pmatrix} 0.000469652 & 0 & 0 \\ 0 & 0.0991466 & 0 \\ 0 & 0 & 1.68558 \end{pmatrix} \text{GeV} \\
M_d &= \begin{pmatrix} -0.001101 + 0.001641i & 0.004037 - 0.004345i & 0.014501 + 0.048008i \\ 0.00403 - 0.004345i & -0.033107 + 0.008704i & -0.018711 - 0.158707i \\ 0.014501 + 0.048008i & -0.018711 - 0.158707i & 0.754282 + 0.611126i \end{pmatrix} \text{GeV} \\
(r,\ s) &= (69.1739,\ 0.362941 - 0.0463175i)
\end{aligned}
\tag{B.10}
$$

The non-minimal non-SUSY $SO(10)$ model with type-I seesaw

The values of fitted parameters corresponding to the best fit solution obtained for type-I seesaw in Table 6.4 are the following.

$$
\begin{aligned}
H &= \begin{pmatrix} 0.00158452 & 0 & 0 \\ 0 & 0.0407501 & 0 \\ 0 & 0 & -0.330398 \end{pmatrix} \text{GeV} \\
F &= \begin{pmatrix} -0.00116221 & -0.000145513 & 0.0130876 \\ -0.000145513 & -0.0224155 & -0.00121344 \\ 0.0130876 & -0.00121344 & -0.667509 \end{pmatrix} \text{GeV} \\
G &= \begin{pmatrix} 0 & -0.00670763 & 0.00612927 \\ 0.00670763 & 0 & -0.0437162 \\ -0.00612927 & 0.0437162 & 0 \end{pmatrix} \text{GeV} \\
(r,\ s,\ t_l,\ t_u,\ t_D) &= (-52.4173,\ 1.61949,\ 3.1751,\ 0.0413014,\ -11.7339)
\end{aligned}
\tag{B.11}
$$

Appendix C

The S_4 group theory: Representations and invariants

C.1 The S_4 group

The group S_4 is the permutation group of four distinct objects. It is isomorphic to the symmetry group of a regular octahedron and so well-known in solid state physics. Its order is 24, i.e. it has 24 distinct elements. S_4 has five conjugate classes and therefore contains five irreducible representations which are all real. Among these are two one-dimensional ones, the identity (i.e. the representation being invariant under all transformations of S_4, also called the symmetric representation) and the anti-symmetric one (i.e. the one changing sign under odd permutations, also called alternating). In the following we will denote the identity one with $\mathbf{1_1}$ and the anti-symmetric one with $\mathbf{1_2}$. There is one two-dimensional representation called $\mathbf{2}$ and two three-dimensional ones, $\mathbf{3_1}$ and $\mathbf{3_2}$. Out of these five irreducible representations only the two three-dimensional ones are faithful. Their characters χ, i.e. the traces of their representation matrices, are given in the character table, see Table C.1. There we use the following notations: $\mathcal{C}_i$ with $i = 1, ..., 5$ are the five classes of the group, $^\circ\mathcal{C}_i$ is the order of the i^{th} class, i.e. the number of distinct elements contained in this class, $^\circ\mathrm{h}_{\mathcal{C}_i}$ is the order of the elements R in the class $\mathcal{C}_i$, i.e. the smallest integer (> 0) for which the equation $R^{\,^\circ\mathrm{h}_{\mathcal{C}_i}} = \mathbf{1}$ holds.

	classes				
	$\mathcal{C}_1$	$\mathcal{C}_2$	$\mathcal{C}_3$	$\mathcal{C}_4$	$\mathcal{C}_5$
G	$\mathbf{1}$	A^2	AB^2	B	A
$^\circ\mathcal{C}_i$	1	3	6	8	6
$^\circ h_{\mathcal{C}_i}$	1	2	2	3	4
$\mathbf{1_1}$	1	1	1	1	1
$\mathbf{1_2}$	1	1	-1	1	-1
$\mathbf{2}$	2	2	0	-1	0
$\mathbf{3_1}$	3	-1	1	0	-1
$\mathbf{3_2}$	3	-1	-1	0	1

Table C.1: Character table of the group S_4. see text for details

Furthermore the table contains one representative for each class $\mathcal{C}_i$ given as product of the generators A and B of the group.

From the generators A and B all other elements of S_4 can be formed by multiplication. They ought to fulfill the following relations [140] :

$$A^4 = \mathbf{1} \ , \ B^3 = \mathbf{1} \quad \text{and} \quad AB^2A = B \ , \ ABA = BA^2B \, . \tag{C.1}$$

We show one possible choice of generators in the next section. Using them we calculate the Clebsch Gordan coefficients for all the Kronecker products.

S_4 is the smallest group containing one-, two- and three-dimensional representations together with the group T'.

S_4 can be embedded into $SO(3)$ as well as in $SU(3)$ (where it is isomorphic to the group $\Delta(24)$ [141]) and therefore gives the opportunity to embed our discrete flavor symmetry into a continuous one which is broken at a high energy scale.

In our model the group S_4 is broken completely at the electroweak scale, however this breaking could also occur in two steps such that S_4 breaks to one of its subgroups which is then completely broken. The non-abelian subgroups of S_4 turn out to be already well-known as flavor symmetries: they are S_3 (which is isomorphic to D_3), D_4 and A_4. Correlation tables containing the corresponding breaking sequences for the representations of S_4 can be found

in [142].

C.2 Representation matrices

The representation matrices fulfilling Eq.(C.1) can be chosen as:

$$\mathrm{A} = \begin{pmatrix} -1 & 0 \\ 0 & 1 \end{pmatrix} \quad \text{and} \quad \mathrm{B} = -\frac{1}{2}\begin{pmatrix} 1 & \sqrt{3} \\ -\sqrt{3} & 1 \end{pmatrix} \quad \text{for} \quad \mathbf{2}\,,$$

$$\mathrm{A} = \begin{pmatrix} -1 & 0 & 0 \\ 0 & 0 & -1 \\ 0 & 1 & 0 \end{pmatrix} \quad \text{and} \quad \mathrm{B} = \begin{pmatrix} 0 & 0 & 1 \\ 1 & 0 & 0 \\ 0 & 1 & 0 \end{pmatrix} \quad \text{for} \quad \mathbf{3_1}$$

and

$$\mathrm{A} = \begin{pmatrix} 1 & 0 & 0 \\ 0 & 0 & 1 \\ 0 & -1 & 0 \end{pmatrix} \quad \text{and} \quad \mathrm{B} = \begin{pmatrix} 0 & 0 & 1 \\ 1 & 0 & 0 \\ 0 & 1 & 0 \end{pmatrix} \quad \text{for} \quad \mathbf{3_2}\,.$$

These matrices can be found in [140].

C.3 Kronecker products

The Kronecker products can be calculated from the above given character table [143].

$$\begin{aligned}
\mathbf{1_i} \times \mathbf{1_j} &= \mathbf{1}_{(\mathrm{i+j}) \bmod 2 +1} \quad \forall\, \mathrm{i \text{ and } j} \\
\mathbf{2} \times \mathbf{1_i} &= \mathbf{2} \quad \forall\, \mathrm{i} \\
\mathbf{3_i} \times \mathbf{1_j} &= \mathbf{3}_{(\mathrm{i+j}) \bmod 2 +1} \quad \forall\, \mathrm{i \text{ and } j} \\
\mathbf{3_i} \times \mathbf{2} &= \mathbf{3_1} + \mathbf{3_2} \quad \forall\, \mathrm{i} \\
\mathbf{3_1} \times \mathbf{3_2} &= \mathbf{1_2} + \mathbf{2} + \mathbf{3_1} + \mathbf{3_2}
\end{aligned}$$

$$[\mathbf{2} \times \mathbf{2}] = \mathbf{1_1} + \mathbf{2}\,, \quad \{\mathbf{2} \times \mathbf{2}\} = \mathbf{1_2} \quad \text{and}$$

$$\left[\mathbf{3_i} \times \mathbf{3_i}\right] = \mathbf{1_1} + \mathbf{2} + \mathbf{3_1} \ , \quad \left\{\mathbf{3_i} \times \mathbf{3_i}\right\} = \mathbf{3_2} \quad \forall \, \mathrm{i}$$

where we introduced the notation $[\mu \times \mu]$ for the symmetric and $\{\mu \times \mu\}$ for the anti-symmetric part of the product $\mu \times \mu$.

Note that $\nu \times \mu = \mu \times \nu$ for all representations μ and ν.

C.4 Clebsch Gordan coefficients

The Clebsch Gordan coefficients can be calculated [144] with the given representation matrices for

$$A, A' \sim \mathbf{1_1} \quad , \quad B, B' \sim \mathbf{1_2} \quad , \quad \begin{pmatrix} a_1 \\ a_2 \end{pmatrix}, \begin{pmatrix} a_1' \\ a_2' \end{pmatrix} \sim \mathbf{2} \ ,$$

$$\begin{pmatrix} b_1 \\ b_2 \\ b_3 \end{pmatrix}, \begin{pmatrix} b_1' \\ b_2' \\ b_3' \end{pmatrix} \sim \mathbf{3_1} \quad \text{and} \quad \begin{pmatrix} c_1 \\ c_2 \\ c_3 \end{pmatrix}, \begin{pmatrix} c_1' \\ c_2' \\ c_3' \end{pmatrix} \sim \mathbf{3_2} \ .$$

Since we choose all the representation matrices to be real, it also holds:

$$A^\star \sim \mathbf{1_1} \ , \quad B^\star \sim \mathbf{1_2} \ , \quad \begin{pmatrix} a_1^\star \\ a_2^\star \end{pmatrix} \sim \mathbf{2} \ , \quad \begin{pmatrix} b_1^\star \\ b_2^\star \\ b_3^\star \end{pmatrix} \sim \mathbf{3_1} \quad \text{and} \quad \begin{pmatrix} c_1^\star \\ c_2^\star \\ c_3^\star \end{pmatrix} \sim \mathbf{3_2} \ .$$

The Clebsch Gordan coefficients for the one-dimensional representations are trivial:

$$A\,A' \sim \mathbf{1_1} \quad , \quad A\,B \sim \mathbf{1_2} \quad , \quad B\,A \sim \mathbf{1_2} \quad , \quad B\,B' \sim \mathbf{1_1}$$

as well as the products $\mathbf{1_1} \times \mu$ of any representation μ with the total singlet $\mathbf{1_1}$:

$$\begin{pmatrix} A\,a_1 \\ A\,a_2 \end{pmatrix} \sim \mathbf{2} \quad , \quad \begin{pmatrix} A\,b_1 \\ A\,b_2 \\ A\,b_3 \end{pmatrix} \sim \mathbf{3_1} \quad , \quad \begin{pmatrix} A\,c_1 \\ A\,c_2 \\ A\,c_3 \end{pmatrix} \sim \mathbf{3_2} \ .$$

And here are the ones for $\mathbf{1_2} \times \mu$ of any representation μ:

$$\begin{pmatrix} -B\,a_2 \\ B\,a_1 \end{pmatrix} \sim \mathbf{2} \quad , \quad \begin{pmatrix} B\,b_1 \\ B\,b_2 \\ B\,b_3 \end{pmatrix} \sim \mathbf{3_2} \quad , \quad \begin{pmatrix} B\,c_1 \\ B\,c_2 \\ B\,c_3 \end{pmatrix} \sim \mathbf{3_1} \; .$$

The Clebsch Gordan coefficients for $\mu \times \mu$ have the form:

for $\mathbf{2}$

$$a_1 a'_1 + a_2 a'_2 \sim \mathbf{1_1}$$
$$-a_1 a'_2 + a_2 a'_1 \sim \mathbf{1_2}$$
$$\begin{pmatrix} a_1 a'_2 + a_2 a'_1 \\ a_1 a'_1 - a_2 a'_2 \end{pmatrix} \sim \mathbf{2}$$

for $\mathbf{3_1}$

$$\sum_{j=1}^{3} b_j b'_j \sim \mathbf{1_1}$$
$$\begin{pmatrix} \frac{1}{\sqrt{2}}(b_2 b'_2 - b_3 b'_3) \\ \frac{1}{\sqrt{6}}(-2b_1 b'_1 + b_2 b'_2 + b_3 b'_3) \end{pmatrix} \sim \mathbf{2}$$
$$\begin{pmatrix} b_2 b'_3 + b_3 b'_2 \\ b_1 b'_3 + b_3 b'_1 \\ b_1 b'_2 + b_2 b'_1 \end{pmatrix} \sim \mathbf{3_1} \; , \quad \begin{pmatrix} b_3 b'_2 - b_2 b'_3 \\ b_1 b'_3 - b_3 b'_1 \\ b_2 b'_1 - b_1 b'_2 \end{pmatrix} \sim \mathbf{3_2}$$

for $\mathbf{3_2}$

$$\sum_{j=1}^{3} c_j c'_j \sim \mathbf{1_1}$$

$$\begin{pmatrix} \frac{1}{\sqrt{2}}(c_2c'_2 - c_3c'_3) \\ \frac{1}{\sqrt{6}}(-2c_1c'_1 + c_2c'_2 + c_3c'_3) \end{pmatrix} \sim \mathbf{2}$$

$$\begin{pmatrix} c_2c'_3 + c_3c'_2 \\ c_1c'_3 + c_3c'_1 \\ c_1c'_2 + c_2c'_1 \end{pmatrix} \sim \mathbf{3_1} \ , \quad \begin{pmatrix} c_3c'_2 - c_2c'_3 \\ c_1c'_3 - c_3c'_1 \\ c_2c'_1 - c_1c'_2 \end{pmatrix} \sim \mathbf{3_2} \quad .$$

Note here that the parts belonging to the symmetric part of the product $\mu \times \mu$ are symmetric under the interchange of unprimed and primed whereas the ones belonging to the anti-symmetric part change sign, i.e. are anti-symmetric.

Note also that for our choice of generators the Clebsch Gordan coefficients for $\mathbf{3_1} \times \mathbf{3_1}$ and $\mathbf{3_2} \times \mathbf{3_2}$ turn out to be the same. For the coupling $\mathbf{2} \times \mathbf{3_1}$ the Clebsch Gordan coefficients are

$$\begin{pmatrix} a_2b_1 \\ -\frac{1}{2}(\sqrt{3}a_1b_2 + a_2b_2) \\ \frac{1}{2}(\sqrt{3}a_1b_3 - a_2b_3) \end{pmatrix} \sim \mathbf{3_1}$$

$$\begin{pmatrix} a_1b_1 \\ \frac{1}{2}(\sqrt{3}a_2b_2 - a_1b_2) \\ -\frac{1}{2}(\sqrt{3}a_2b_3 + a_1b_3) \end{pmatrix} \sim \mathbf{3_2} \tag{C.2}$$

and for $\mathbf{2} \times \mathbf{3_2}$

$$\begin{pmatrix} a_1c_1 \\ \frac{1}{2}(\sqrt{3}a_2c_2 - a_1c_2) \\ -\frac{1}{2}(\sqrt{3}a_2c_3 + a_1c_3) \end{pmatrix} \sim \mathbf{3_1}$$
$$\begin{pmatrix} a_2c_1 \\ -\frac{1}{2}(\sqrt{3}a_1c_2 + a_2c_2) \\ \frac{1}{2}(\sqrt{3}a_1c_3 - a_2c_3) \end{pmatrix} \sim \mathbf{3_2}.$$
(C.3)

And for $\mathbf{3_1} \times \mathbf{3_2}$ one finds the following combinations:

$$\sum_{j=1}^{3} b_jc_j \sim \mathbf{1_2}$$
$$\begin{pmatrix} \frac{1}{\sqrt{6}}(2b_1c_1 - b_2c_2 - b_3c_3) \\ \frac{1}{\sqrt{2}}(b_2c_2 - b_3c_3) \end{pmatrix} \sim \mathbf{2}$$
$$\begin{pmatrix} b_3c_2 - b_2c_3 \\ b_1c_3 - b_3c_1 \\ b_2c_1 - b_1c_2 \end{pmatrix} \sim \mathbf{3_1} \ , \quad \begin{pmatrix} b_2c_3 + b_3c_2 \\ b_1c_3 + b_3c_1 \\ b_1c_2 + b_2c_1 \end{pmatrix} \sim \mathbf{3_2} \quad .$$
(C.4)

Bibliography

[1] S. L. Glashow, Nucl. Phys. **22**, 579-588 (1961).

[2] A. Salam, J. C. Ward, Phys. Lett. **13**, 168-171 (1964).

[3] S. Weinberg, Phys. Rev. Lett. **19**, 1264-1266 (1967).

[4] R. P. Feynman, M. Gell-Mann, Phys. Rev. **109**, 193-198 (1958).

[5] E. C. G. Sudarshan, R. e. Marshak, Phys. Rev. **109**, 1860-1860 (1958).

[6] H. Fritzsch, M. Gell-Mann, [hep-ph/0208010].

[7] H. Fritzsch, M. Gell-Mann, H. Leutwyler, Phys. Lett. **B47**, 365-368 (1973).

[8] D. J. Gross, F. Wilczek, Phys. Rev. Lett. **30**, 1343-1346 (1973).

[9] H. D. Politzer, Phys. Rev. Lett. **30**, 1346-1349 (1973).

[10] H. Nishino *et al.* [Super-Kamiokande Collaboration], Phys. Rev. Lett. **102**, 141801 (2009). [arXiv:0903.0676 [hep-ex]].

[11] R. N. Mohapatra *et al.*, Rept. Prog. Phys. **70**, 1757-1867 (2007). [hep-ph/0510213].

[12] P. Langacker, Phys. Rept. **72**, 185 (1981).

[13] H. Georgi, S. L. Glashow, Phys. Rev. Lett. **32**, 438-441 (1974).

[14] S. Dimopoulos, H. Georgi, Nucl. Phys. **B193**, 150 (1981).

[15] N. Sakai, Z. Phys. **C11**, 153 (1981).

[16] J. Hisano, T. Moroi, K. Tobe and T. Yanagida, Phys. Lett. B **342** (1995) 138 [arXiv:hep-ph/9406417].

[17] C. S. Aulakh, B. Bajc, A. Melfo, A. Rasin and G. Senjanovic, Nucl. Phys. B **597**, 89 (2001) [arXiv:hep-ph/0004031].

[18] S. Wiesenfeldt, Ph.D. thesis on "Proton decay in supersymmetric grand unified theories".

[19] T. Goto, T. Nihei, Phys. Rev. **D59**, 115009 (1999). [hep-ph/9808255].

[20] H. Murayama, A. Pierce, Phys. Rev. **D65**, 055009 (2002). [hep-ph/0108104].

[21] B. Bajc, P. Fileviez Perez, G. Senjanovic, Phys. Rev. **D66**, 075005 (2002). [hep-ph/0204311].

[22] B. Bajc, P. Fileviez Perez, G. Senjanovic, [hep-ph/0210374].

[23] D. Emmanuel-Costa, S. Wiesenfeldt, Nucl. Phys. **B661**, 62-82 (2003). [hep-ph/0302272].

[24] I. Dorsner, P. Fileviez Perez, Nucl. Phys. **B723**, 53-76 (2005). [hep-ph/0504276].

[25] I. Dorsner, P. Fileviez Perez and R. Gonzalez Felipe, Nucl. Phys. B **747**, 312 (2006) [arXiv:hep-ph/0512068].

[26] B. Bajc and G. Senjanovic, JHEP **0708**, 014 (2007) [arXiv:hep-ph/0612029].

[27] B. Bajc, M. Nemevsek and G. Senjanovic, Phys. Rev. D **76**, 055011 (2007) [arXiv:hep-ph/0703080].

[28] R. Foot, H. Lew, X. G. He, G. C. Joshi, Z. Phys. **C44**, 441 (1989).

[29] E. Ma, Phys. Rev. Lett. **81**, 1171-1174 (1998). [hep-ph/9805219].

[30] H. Georgi, in Particles and Fields (edited by C. E. Carlson), A.I.P., 1975.

[31] H. Fritzsch, P. Minkowski, Annals Phys. **93**, 193-266 (1975).

[32] J. C. Pati, A. Salam, Phys. Rev. **D10**, 275-289 (1974).

[33] R. N. Mohapatra, Phys. Rev. **D34**, 3457-3461 (1986).

[34] R. N. Mohapatra, Berlin, Germany: Springer (1986) 309 P. (Contemporary Physics).

[35] R. N. Mohapatra and B. Sakita, Phys. Rev. D **21**, 1062 (1980).

[36] F. Wilczek and A. Zee, Phys. Rev. D **25**, 553 (1982).

[37] P. Nath and R. M. Syed, Phys. Lett. B **506**, 68 (2001) [Erratum-ibid. B **508**, 216 (2001)] [arXiv:hep-ph/0103165].

[38] C. S. Aulakh and A. Girdhar, Int. J. Mod. Phys. A **20**, 865 (2005) [arXiv:hep-ph/0204097].

[39] T. Fukuyama, A. Ilakovac, T. Kikuchi, S. Meljanac and N. Okada, J. Math. Phys. **46**, 033505 (2005) [arXiv:hep-ph/0405300].

[40] R. Slansky, Phys. Rept. **79**, 1-128 (1981).

[41] R. N. Mohapatra, [hep-ph/9310265].

[42] T. Fukuyama, A. Ilakovac, T. Kikuchi, S. Meljanac and N. Okada, Eur. Phys. J. C **42**, 191 (2005) [arXiv:hep-ph/0401213];

[43] T. Fukuyama, A. Ilakovac, T. Kikuchi, S. Meljanac, N. Okada, JHEP **0409**, 052 (2004). [hep-ph/0406068].

[44] B. Dutta, Y. Mimura, R. N. Mohapatra, Phys. Rev. Lett. **94**, 091804 (2005). [hep-ph/0412105].

[45] T. E. Clark, T. K. Kuo and N. Nakagawa, Phys. Lett. B **115**, 26 (1982).

[46] C. S. Aulakh and R. N. Mohapatra, Phys. Rev. D **28**, 217 (1983).

[47] C. S. Aulakh, B. Bajc, A. Melfo, G. Senjanovic and F. Vissani, Phys. Lett. B **588**, 196 (2004) [arXiv:hep-ph/0306242].

[48] B. Bajc, A. Melfo, G. Senjanovic and F. Vissani, Phys. Rev. D **70**, 035007 (2004) [arXiv:hep-ph/0402122].

[49] C. S. Aulakh and A. Girdhar, Nucl. Phys. B **711**, 275 (2005) [arXiv:hep-ph/0405074].

[50] K. S. Babu and R. N. Mohapatra, Phys. Rev. Lett. **70**, 2845 (1993) [arXiv:hep-ph/9209215].

[51] B. Bajc, G. Senjanovic and F. Vissani, Phys. Rev. Lett. **90**, 051802 (2003) [arXiv:hep-ph/0210207].

[52] B. Bajc, G. Senjanovic and F. Vissani, Phys. Rev. D **70**, 093002 (2004) [arXiv:hep-ph/0402140].

[53] H. S. Goh, R. N. Mohapatra and S. P. Ng, Phys. Lett. B **570**, 215 (2003) [arXiv:hep-ph/0303055].

[54] H. S. Goh, R. N. Mohapatra and S. P. Ng, Phys. Rev. D **68**, 115008 (2003) [arXiv:hep-ph/0308197].

[55] K. S. Babu and C. Macesanu, Phys. Rev. D **72**, 115003 (2005) [arXiv:hep-ph/0505200].

[56] S. Bertolini and M. Malinsky, Phys. Rev. D **72**, 055021 (2005) [arXiv:hep-ph/0504241].

[57] S. Bertolini, T. Schwetz and M. Malinsky, Phys. Rev. D **73**, 115012 (2006) [arXiv:hep-ph/0605006].

[58] C. R. Das and M. K. Parida, Eur. Phys. J. C **20**, 121 (2001) [arXiv:hep-ph/0010004].

[59] G. Ross and M. Serna, Phys. Lett. B **664**, 97 (2008) [arXiv:0704.1248 [hep-ph]].

[60] M. C. Gonzalez-Garcia, M. Maltoni and J. Salvado, JHEP **1004**, 056 (2010) [arXiv:1001.4524 [hep-ph]].

[61] C. S. Aulakh, Phys. Rev. D **72**, 051702 (2005) [arXiv:hep-ph/0501025].

[62] C. S. Aulakh, arXiv:hep-ph/0506291.

[63] B. Bajc, A. Melfo, G. Senjanovic and F. Vissani, Phys. Lett. B **634**, 272 (2006) [arXiv:hep-ph/0511352].

[64] C. S. Aulakh and S. K. Garg, Nucl. Phys. B **757**, 47 (2006) [arXiv:hep-ph/0512224].

[65] B. Bajc, I. Dorsner and M. Nemevsek, JHEP **0811**, 007 (2008) [arXiv:0809.1069 [hep-ph]].

[66] C. S. Aulakh, [hep-ph/0602132].

[67] C. S. Aulakh, S. K. Garg, [hep-ph/0612021].

[68] C. S. Aulakh, Phys. Lett. B **661**, 196 (2008) [arXiv:0710.3945 [hep-ph]].

[69] C. S. Aulakh and S. K. Garg, arXiv:0807.0917 [hep-ph].

[70] A. Melfo, A. Ramirez and G. Senjanovic, Phys. Rev. D **82**, 075014 (2010) [arXiv:1005.0834 [hep-ph]].

[71] B. Dutta, Y. Mimura and R. N. Mohapatra, Phys. Lett. B **603**, 35 (2004) [arXiv:hep-ph/0406262].

[72] W. Grimus, H. Kuhbock, Eur. Phys. J. **C51**, 721-729 (2007). [hep-ph/0612132].

[73] A. S. Joshipura, B. P. Kodrani and K. M. Patel, Phys. Rev. D **79**, 115017 (2009) [arXiv:0903.2161 [hep-ph]].

[74] S. Bertolini, M. Frigerio, M. Malinsky, Phys. Rev. **D70**, 095002 (2004). [hep-ph/0406117].

[75] G. Altarelli, G. Blankenburg, JHEP **1103**, 133 (2011). [arXiv:1012.2697 [hep-ph]].

[76] W. Grimus, H. Kuhbock, Phys. Lett. **B643**, 182-189 (2006). [hep-ph/0607197].

[77] P. F. Harrison, D. H. Perkins, W. G. Scott, Phys. Lett. **B530**, 167 (2002). [hep-ph/0202074].

[78] G. Altarelli and F. Feruglio, Rev. Mod. Phys. **82**, 2701 (2010) [arXiv:1002.0211 [hep-ph]].

[79] S. Morisi, M. Picariello, E. Torrente-Lujan, Phys. Rev. **D75**, 075015 (2007). [hep-ph/0702034].

[80] F. Bazzocchi, M. Frigerio, S. Morisi, Phys. Rev. **D78**, 116018 (2008). [arXiv:0809.3573 [hep-ph]].

[81] C. S. Lam, Phys. Rev. Lett. **101**, 121602 (2008). [arXiv:0804.2622 [hep-ph]].

[82] C. S. Lam, Phys. Rev. **D78**, 073015 (2008). [arXiv:0809.1185 [hep-ph]].

[83] H. S. Goh, R. N. Mohapatra, S. Nasri, Phys. Rev. **D70**, 075022 (2004). [hep-ph/0408139].

[84] A. S. Joshipura, K. M. Patel, Phys. Rev. **D83**, 095002 (2011). [arXiv:1102.5148 [hep-ph]].

[85] T. Schwetz, M. Tortola and J. W. F. Valle, arXiv:1103.0734 [hep-ph].

[86] A. Dighe, S. Goswami, W. Rodejohann, Phys. Rev. **D75**, 073023 (2007). [hep-ph/0612328].

[87] T. Araki, C. -Q. Geng, Z. -z. Xing, Phys. Lett. **B699**, 276-280 (2011). [arXiv:1012.2970 [hep-ph]].

[88] D. Meloni, F. Plentinger and W. Winter, Phys. Lett. B **699**, 354 (2011) [arXiv:1012.1618 [hep-ph]].

[89] K. Abe *et al.* [T2K Collaboration], Phys. Rev. Lett. **107**, 041801 (2011) [arXiv:1106.2822 [hep-ex]].

[90] P. Adamson *et al.* [MINOS Collaboration], arXiv:1108.0015 [hep-ex].

[91] G. L. Fogli, E. Lisi, A. Marrone, A. Palazzo and A. M. Rotunno, Phys. Rev. D **84**, 053007 (2011) [arXiv:1106.6028 [hep-ph]].

[92] T. Schwetz, M. Tortola and J. W. F. Valle, New J. Phys. **13**, 109401 (2011) [arXiv:1108.1376 [hep-ph]].

[93] A. S. Joshipura and K. M. Patel, JHEP **1109**, 137 (2011) [arXiv:1105.5943 [hep-ph]].

[94] G. Altarelli, F. Feruglio, New J. Phys. **6**, 106 (2004). [hep-ph/0405048].

[95] R. N. Mohapatra and A. Y. Smirnov, Ann. Rev. Nucl. Part. Sci. **56**, 569 (2006) [arXiv:hep-ph/0603118].

[96] T. Fukuyama and H. Nishiura, arXiv:hep-ph/9702253.

[97] P. F. Harrison and W. G. Scott, Phys. Lett. B **547**, 219 (2002) [arXiv:hep-ph/0210197].

[98] Y. Koide, H. Nishiura, K. Matsuda, T. Kikuchi and T. Fukuyama, Phys. Rev. D **66**, 093006 (2002) [arXiv:hep-ph/0209333].

[99] K. Matsuda, H. Nishiura, Phys. Rev. **D69**, 053005 (2004). [hep-ph/0309272].

[100] A. Datta and P. J. O'Donnell, Phys. Rev. D **72**, 113002 (2005) [arXiv:hep-ph/0508314].

[101] A. S. Joshipura, Eur. Phys. J. C **53**, 77 (2008) [arXiv:hep-ph/0512252].

[102] H. Nishiura, K. Matsuda and T. Fukuyama, Int. J. Mod. Phys. A **23**, 4557 (2008) [arXiv:0804.4515 [hep-ph]].

[103] A. S. Joshipura and A. Y. Smirnov, Nucl. Phys. B **750**, 28 (2006) [arXiv:hep-ph/0512024].

[104] W. Grimus and L. Lavoura, Phys. Lett. B **579**, 113 (2004) [arXiv:hep-ph/0305309].

[105] W. Grimus and L. Lavoura, Acta Phys. Polon. B **34**, 5393 (2003) [arXiv:hep-ph/0310050].

[106] W. M. Yao *et al.* [Particle Data Group], J. Phys. G **33**, 1 (2006).

[107] J. Lesgourgues and S. Pastor, Phys. Rept. **429**, 307 (2006) [arXiv:astro-ph/0603494].

[108] A. S. Joshipura, K. M. Patel and S. K. Vempati, Phys. Lett. B **690**, 289 (2010) [arXiv:0911.5618 [hep-ph]].

[109] G. C. Branco, M. N. Rebelo and J. I. Silva-Marcos, Phys. Rev. Lett. **82**, 683 (1999) [arXiv:hep-ph/9810328].

[110] A. Ioannisian and J. W. F. Valle, Phys. Lett. B **332**, 93 (1994) [arXiv:hep-ph/9402333].

[111] D. G. F. Lee and R. N. Mohapatra, Phys. Lett. B **329**, 463 (1994) [arXiv:hep-ph/9403201].

[112] A. Y. Smirnov, arXiv:hep-ph/0402264.

[113] H. Minakata and A. Y. Smirnov, Phys. Rev. D **70**, 073009 (2004) [arXiv:hep-ph/0405088].

[114] M. Raidal, Phys. Rev. Lett. **93**, 161801 (2004) [arXiv:hep-ph/0404046].

[115] P. H. Frampton and R. N. Mohapatra, JHEP **0501**, 025 (2005) [arXiv:hep-ph/0407139].

[116] S. Antusch, S. F. King and R. N. Mohapatra, Phys. Lett. B **618**, 150 (2005) [arXiv:hep-ph/0504007].

[117] S. F. King, JHEP **0508**, 105 (2005) [arXiv:hep-ph/0506297].

[118] R. de Adelhart Toorop, F. Bazzocchi and L. Merlo, JHEP **1008**, 001 (2010) [arXiv:1003.4502 [hep-ph]].

[119] B. Dutta, Y. Mimura and R. N. Mohapatra, Phys. Rev. D **80**, 095021 (2009) [arXiv:0910.1043 [hep-ph]].

[120] B. Dutta, Y. Mimura and R. N. Mohapatra, JHEP **1005**, 034 (2010) [arXiv:0911.2242 [hep-ph]].

[121] S. Bertolini, L. Di Luzio, M. Malinsky, Phys. Rev. **D80**, 015013 (2009). [arXiv:0903.4049 [hep-ph]].

[122] S. Bertolini, L. Di Luzio, M. Malinsky, Phys. Rev. **D81**, 035015 (2010). [arXiv:0912.1796 [hep-ph]].

[123] M. Yasue, Phys. Rev. **D24**, 1005 (1981).

[124] M. Yasue, Phys. Lett. **B103**, 33 (1981).

[125] G. Anastaze, J. P. Derendinger, F. Buccella, Z. Phys. **C20**, 269-273 (1983).

[126] K. S. Babu, E. Ma, Phys. Rev. **D31**, 2316 (1985).

[127] B. Bajc, A. Melfo, G. Senjanovic, F. Vissani, Phys. Rev. **D73**, 055001 (2006). [hep-ph/0510139].

[128] Z. -z. Xing, H. Zhang, S. Zhou, Phys. Rev. **D77**, 113016 (2008). [arXiv:0712.1419 [hep-ph]].

[129] R. G. Roberts, A. Romanino, G. G. Ross, L. Velasco-Sevilla, Nucl. Phys. **B615**, 358-384 (2001). [hep-ph/0104088].

[130] I. Dorsner, A. Y. .Smirnov, Nucl. Phys. **B698**, 386-406 (2004). [hep-ph/0403305].

[131] A. Y. Smirnov, Phys. Rev. D **48**, 3264 (1993) [arXiv:hep-ph/9304205].

[132] C. D. Froggatt, H. B. Nielsen, Nucl. Phys. **B147**, 277 (1979).

[133] P. H. Frampton, S. L. Glashow, D. Marfatia, Phys. Lett. **B536**, 79-82 (2002). [hep-ph/0201008].

[134] N. Cabibbo, Phys. Rev. Lett. **10**, 531-533 (1963).

[135] M. Kobayashi, T. Maskawa, Prog. Theor. Phys. **49**, 652-657 (1973).

[136] B. Pontecorvo, Sov. Phys. JETP **26**, 984-988 (1968).

[137] Z. Maki, M. Nakagawa, S. Sakata, Prog. Theor. Phys. **28**, 870-880 (1962).

[138] See for instance, W. H. Press et al., Numerical Recipes in FORTRAN: The Art of Scientific Computing, Cambridge University Press 1992.

[139] http://seal.web.cern.ch/seal/work-packages/mathlibs/minuit/home.html

[140] J. S. Lomont, *Applications of Finite Groups*, Acad. Press (1959) 346 p.

[141] W. Grimus, P. O. Ludl, J. Phys. A **A43**, 445209 (2010). [arXiv:1006.0098 [hep-ph]].

[142] S. Califano, *Vibrational States*, Wiley, London (1976) 365 p.

[143] M. Hamermesh, *Group Theory and Its Application to Physical Problems*, "Reading, Mass.:Addison-Wesley (1962) 509 p.

[144] J. F. Cornwell, *Group Theory in Physics: An Introduction*, San Diego, USA: Academic (1997) 349 p.

Publications attached with the thesis

1. **"Quasi-degenerate neutrinos in** $SO(10)$**"**

   A. S. Joshipura and K. M. Patel

   Phys. Rev. D **82** (Rapid Communication), 031701 (2010) [arXiv:1005.0045 [hep-ph]]

2. **"An** $SO(10) \times S_4$ **Model of Quark-Lepton Complementarity"**

   K. M. Patel

   Phys. Lett. B **695**, 225 (2011) [arXiv:1008.5061 [hep-ph]]

PHYSICAL REVIEW D **82,** 031701(R) (2010)

Quasidegenerate neutrinos in $SO(10)$

Anjan S. Joshipura* and Ketan M. Patel†

Physical Research Laboratory, Navarangpura, Ahmedabad 380 009, India

(Received 14 May 2010; published 19 August 2010)

We propose a specific ansatz for the structure of Yukawa matrices in $SO(10)$ models that lead to quasidegenerate neutrinos through the type-I seesaw mechanism. Consistency of this ansatz is demonstrated through detailed fits to fermion masses and mixing angles, all of which can be explained with reasonable accuracy in a model that uses the Higgs fields transforming as 10, 120, and $\overline{126}$ representations of $SO(10)$. The proposed ansatz is shown to follow from an extended model based on the three generations of the vectorlike fermions and an $O(3)$ flavor symmetry. Successful numerical fits are also discussed in earlier proposed models, which used a combination of the type-I and type-II seesaw mechanisms for obtaining quasidegenerate neutrinos. Large neutrino mixing angles emerge as a consequence of neutrino mass degeneracy in both these cases.

DOI: 10.1103/PhysRevD.82.031701 PACS numbers: 12.10.−g, 12.10.Kt, 12.15.Ff, 14.60.Pq

I. INTRODUCTION

Experiments over the years have revealed the following:

(1) Two of the neutrino mixing angles are large as opposed to the small quark mixing angles.
(2) Neutrino mass hierarchy is milder compared to quarks, and the extreme case of all neutrinos being quasidegenerate is still an allowed possibility.

Several independent reasons have been advanced [1–3] to understand feature (1) of the fermion spectrum but it may be that its answer lies in (2). Large mixing angles become quite natural if neutrinos are almost degenerate. They remain undefined in the exact degenerate limit. A small perturbation that leads to differences in neutrino masses can also stabilize all or some of the mixing angles to large values. Such theory, which predicts quasidegeneracy, has a built-in mechanism to explain large mixing angles. We present an $SO(10)$-based unified description of fermion masses and mixing leading to hierarchical charged fermions and quasidegenerate neutrino masses.

$SO(10)$ models provide a natural framework for understanding neutrino masses because of the seesaw mechanisms [1] inherent in them. Neutrino masses arise in these models from two separate sources either from the vacuum expectation value of the left-handed triplet (type-II) or from the right-handed triplet (type-I) Higgs. It was pointed out [4,5] long ago that the combination of these two sources provides an interesting framework for understanding quasidegeneracy of neutrinos. In this approach, some flavor symmetry leads to a degenerate type-II contribution, and its breaking in the Dirac neutrino masses then leads to departure from degeneracy through the type-I contribution. This is realizable if the type-II contribution dominates over the type-I, which is not always the case [6,7]. An alternative possibility is that both degeneracy and its breaking arise from a single source, namely, the type-I seesaw mechanism. This, however, requires a peculiar structure for the right-handed (RH) neutrino mass matrix M_R. It has been pointed out that the required structure can arise from the "Dirac screening" [8] or more generally from the application of the minimal flavor violation [9] hypothesis to the leptonic sector [10].

While these possibilities are known, there does not exist a detailed study of all fermion masses and mixing in the context of realistic $SO(10)$ models with quasidegenerate neutrinos, and we address this question using (A) a type-I mechanism alone and (B) a combination of type-I and type-II mechanisms.

We use supersymmetric $SO(10)$ as our basic framework. Fermion masses arise in renormalizable $SO(10)$ models through their couplings to Higgs fields transforming as 10, $\overline{126}$, and 120 representations. One needs at least two of these fields to get fermion mixing, and the minimal model with 10 and $\overline{126}$ has attracted a lot of attention [2,6,7,11]. There have been studies of models with an additional 120 also [12–14]. In our context, we find that all three Higgs representations are needed to obtain satisfactory fits to fermion masses and mixing. Starting with a supersymmetric $SO(10)$, an effective minimal supersymmetric standard model (MSSM) is obtained by assuming fine-tuning, which keeps only two Higgs doublets lights. The final fermion mass matrices obtained after $SO(10)$ and $SU(2)_L \times U(1)$ breaking can be parametrized as [13,14]

$$M_d = H + F + G, \qquad M_u = r(H + sF + t_u G),$$
$$M_l = H - 3F + t_l G, \qquad M_D = r(H - 3sF + t_D G),$$
$$M_L = r_L F, \qquad M_R = r_R^{-1} F, \tag{1}$$

where the matrices H and F are complex symmetric and G

*anjan@prl.res.in
†kmpatel@prl.res.in

is an antisymmetric matrix in generation space. We follow the same conventions as used in [14]. H, F, and G arise from the fermionic Yukawa couplings to the 10, $\overline{126}$, and 120 Higgs fields, respectively. r, s, t_u, t_l, t_D, r_L, and r_R are complex parameters. The light neutrino mass matrix is given by

$$\mathcal{M}_\nu = r_L F - r_R M_D F^{-1} M_D^T \equiv \mathcal{M}_\nu^{II} + \mathcal{M}_\nu^I. \quad (2)$$

It is known that the above fermion mass structure allows different mixing patterns for quarks and neutrinos if a type-II seesaw mechanism dominates [2,11]. Consider the limit in which the contribution of the 10-plet H dominates. In this limit, all the charged fermions are diagonalized by the same matrix and the Cabibbo-Kobayashi-Maskawa (CKM) matrix becomes proportional to identity. In the same limit, neutrino mixing with the type-II dominance is governed by F in Eq. (2) leading to nontrivial leptonic mixing. In fact, if only H dominates the charged fermion masses, then one can obtain b-τ unification, which in turn drives the large atmospheric mixing [2]. The existing fits [7,14] to fermion masses and mixing with type-II dominance are for the hierarchical neutrino masses. A degenerate neutrino spectrum can be obtained in this approach with an additional assumption:

$$F = c_0 I, \quad (3)$$

with I denoting a 3×3 identity matrix. The subdominant type-I contribution can then lead to the quark mixing and neutrino mass differences.

The realization of the attractive type-II dominated scenario was found difficult in the context of the minimal model [6,7]. It was found that parameter space favored by the overall fit to fermion masses suppresses the type-II contribution compared to the type-I. This motivates us to study degenerate neutrinos in the context of a purely type-I seesaw mechanism. A general framework to obtain quasi-degenerate neutrinos in a type-I seesaw was recently discussed [10] and following it we impose

$$F = aH^2. \quad (4)$$

Since H is a symmetric matrix it can be diagonalized by a unitary matrix: $U^T H U = D_H$, where D_H is a diagonal matrix with real elements. Without loss of generality, we can express the mass matrices in (1) in an $SO(10)$ basis with a diagonal H. This basis is obtained from Eq. (1) by the replacement $H \rightarrow D_H$ and

$$H^2 \rightarrow D_H V^* D_H, \quad (5)$$

where D_H is a diagonal matrix with real elements. G retains its antisymmetric form, and we use the same notation for it and for various mass matrices in the new basis. $V = U^T U$ in Eq. (5) is a symmetric unitary matrix that can be parametrized [15] in terms of two angles and three phases.

Before we present the detailed fits, let us look at the implications of the ansatz Eq. (4) qualitatively.

(i) Correct b-τ unification and second generation masses are obtained if a dominant contribution to the charged fermion masses comes from H with a subdominant contribution from F and G. Retaining only the H contribution, the ansatz, Eq. (4) implies that

$$\mathcal{M}_\nu^I = -r_R M_D F^{-1} M_D^T \approx -\frac{r^2 r_R}{a} V + \cdots, \quad (6)$$

where the $\cdots$ terms arise from the $\overline{126}$ and 120 contributions to the Dirac mass matrix M_D. The CKM matrix is unity in this limit while the neutrino mixing is determined from V. The diagonalization of V leads [15] to $\theta_{23} = \phi$, $\theta_{12} = \frac{\theta}{2}$, and $\theta_{13} = 0$ where the angles θ_{ij} are angles defined in the standard parametrization of the leptonic mixing matrix and ϕ, θ enter into the definition of V [15]. Thus ansatz in Eq. (4) can lead to a correct description of the quark and leptonic mixing angles to zeroth order without requiring the type-II dominance as is commonly done.

(ii) If H in the original basis was real, then V entering Eq. (5) would be unity. In this case, all the fermion mixing vanish in the absence of the 120 contribution. Thus complex couplings and CP violation prove to be important in understanding large neutrino mixing within this approach.

The contributions from $\overline{126}$ and 120-plets induce nonzero quark mixing angles and perturb Eq. (6):

$$\mathcal{M}_\nu^I(M_X) = -\frac{r_R r^2}{a}(V - 6saD_H + t_D(GD_H^{-1}V - VD_H^{-1}G) + \mathcal{O}(s^2, t_D^2)). \quad (7)$$

$\mathcal{M}_\nu^I(M_X)$ corresponds to an effective dimension five operator induced after integration of the right-handed neutrino fields. Assuming that the heavy mass scale is close to the grand unified theory (GUT) scale and neglecting the effect of the Dirac neutrino couplings in the renormalization group (RG) evolution, the radiatively corrected low scale neutrino mass matrix is given by [1]

$$\mathcal{M}_{\nu f}(M_Z) = I_\tau \mathcal{M}_{\nu f}(M_X) I_\tau^\dagger, \quad (8)$$

where $I_\tau \approx \mathrm{Diag}(1, 1, 1 + \epsilon_\tau)$, $\epsilon_\tau \approx -\frac{1}{\cos^2\beta}\frac{m_\tau^2}{16\pi^2 v^2}\ln\frac{M_X}{M_Z}$, and $\mathcal{M}_{\nu f}$ denotes the neutrino mass matrix in the flavor basis.

II. NUMERICAL FITS: TYPE-I SEESAW

We now discuss detailed fits to fermion masses and mixing based on the ansatz (4) and the fermion mass matrices, Eq. (1). The latter are defined at the GUT scale M_X. We use as our input the quark and lepton masses

obtained at M_X in the MSSM for $\tan\beta = 10$, $M_{\rm SUSY} = 1$ TeV, and $M_{\rm GUT} = 2 \times 10^{16}$ GeV. The input values in the quark sector are given in [14,16]. We include the RG evolution in neutrino mass matrix as follows. Using the charged lepton mass matrix at M_X, we numerically determine $\mathcal{M}_{\nu f}(M_X)$. The low scale neutrino mass matrix in Eq. (8) is then numerically determined and used to obtain the observable neutrino masses and mixing angles. For neutrino masses and lepton mixings, we use the updated low energy values given in [17].

We do the χ^2 fitting to check the viability of the model as previously done in [7,13,14]. In this case we have a total of 25 real parameters (3 in D_H, 5 in V, 6 in G, real r, complex s, a, t_u, t_l, and t_D), which are fitted over 16 observables (9 charged fermion masses, 4 CKM parameters, 2 leptonic mixing angles, and $\Delta m^2_{\rm sol}/\Delta m^2_{\rm atm}$). Lepton mixings and $\Delta m^2_{\rm sol}/\Delta m^2_{\rm atm}$ are independent of the overall neutrino mass ($m_0 = |\frac{r_R r^2}{a}|$) appearing in Eq. (7). m_0 sets the overall neutrino mass scale and can be determined from the fit using the observed value of $\Delta m^2_{\rm atm}$. Our definition of χ^2 allows only the solution with $\Delta m^2_{\rm sol}\cos 2\theta > 0$ as required by experiments. We also set $r = \frac{m_t}{m_b}$ and minimize χ^2 with respect to the remaining 24 parameters. The results of the minimization are displayed as solutions (1) and (2) in Table I. We obtained the best fit value of $\chi^2 = 2.038$ corresponding to the solution (1) for which all the observables are fitted within $\lesssim 0.9\sigma$. Solution (2) is also acceptable, which fits all observables within $\lesssim 0.7\sigma$ with the exception of the down quark mass m_d. We also include in Table I the values of the Majorana phases obtained at the minimum.

θ_{13} has not been included in our definition of χ^2 and its initial value was zero. This becomes nonzero but remains small in both the solutions displayed. However, almost the entire allowed range in θ_{13} is compatible with reasonable fits to other fermion masses as shown by both the solutions. All the solutions displayed in Table I predict large CP violating leptonic phase.

The values of m_0 determined using the observed value of $\Delta m^2_{\rm atm}$ are seen from Table I to be $\gg \Delta m^2_{\rm atm}$ showing the consistency of our ansatz. This arises as a result of Eq. (7) and the smallness of s, t_D. The m_0 in turn determine the heaviest RH neutrino mass scale [see Eq. (1) and ansatz (4)],

$$M_3 \approx r_R^{-1}|a|m_b^2 \approx \frac{r^2}{m_0}m_b^2 \approx 1.3 \times 10^{13}\ \text{GeV},$$

in case of solution (1). Here we used, $m_0 = \frac{r_R r^2}{|a|}$. Thus the RH neutrino mass falls below the GUT scale for this particular solution.

Let us now illustrate how the ansatz (4) can be obtained in a model from a flavor symmetry. A simple flavor symmetry to be used is $O(3)$ under which three generations of the 16-plet ψ transform as triplets. The $O(3)$ breaking is introduced through a complex flavon field η transforming as spin 2. We need to introduce three generations of vectorlike multiplets $\Psi_V + \Psi_{\bar V}$ transforming as $(16, 3) + (\overline{16}, 3)$ under $SO(10) \times O(3)$ and a $U(1)_X$ symmetry in order to realize Eq. (4). The X charges of $(\psi, \Psi_V, \Psi_{\bar V}, \eta, \phi_{10}, \phi_{\overline{126}})$ are chosen, respectively, as $(x, y, -y, 1/2(y-x), -(x+y), -2y)$ with $x \neq y$. The general superpotential invariant under $SO(10) \times O(3) \times U(1)_X$ can be written as

$$W = M\Psi_{\bar V}\Psi_V + \beta\Psi_V\Psi_V\phi_{\overline{126}} + \gamma\Psi_V\psi\phi_{10} + \frac{\delta}{M_P}\Psi_{\bar V}\eta^2\psi + \frac{\delta'}{M_P}\,\mathrm{Tr}\eta^2\Psi_{\bar V}\psi + \cdots. \quad (9)$$

The $O(3)$ and $U(1)_X$ breaking originates in the above superpotential only from the Planck scale effects through the vacuum expectation value (vev) of the flavon field η. The last two terms are the only terms that determine both the 10 and $\overline{126}$ Yukawa couplings once the heavy vectorlike fields are integrated out. The dotted terms correspond to terms suppressed by M_P^2. Here, the mass M of the vectorlike pair and the scale of the vev of η lie above the GUT scale. The effective theory after integration of the vectorlike field is represented by

$$W_{\rm eff} \approx \beta\psi\xi^2\psi\phi_{\overline{126}} + \gamma\psi\xi\psi\phi_{10}, \quad (10)$$

where

$$\xi_{ab} \equiv \frac{\delta}{MM_P}\left(\eta^2_{ab} + \frac{\delta'}{\delta}Tr\eta^2\delta_{ab}\right)$$

and $a, b = 1, 2, 3$ refer to the $O(3)$ index. This effective superpotential is also $SO(10) \times O(3) \times U(1)_X$ invariant. The Yukawa coupling H is proportional to the $\langle\xi\rangle$ and is a general complex symmetric matrix. The F is related to the square of H and satisfies the ansatz in Eq. (4). The coupling to the 120 field can be generated by introducing a flavon field χ with the $U(1)_X$ charge $-2x$ and transforming as a triplet of $O(3)$. This leads to the Yukawa coupling matrix G through the coupling

$$\psi\frac{\chi}{M_P}\psi\phi_{120}.$$

A detailed model along this line will require study of the details of the vacuum structure of the potential involving η, χ, and possibly additional fields for generating the right structure of the Yukawa couplings H, G.

III. NUMERICAL FITS: TYPE-II SEESAW

We now turn to the numerical discussion of the ansatz (3) in which the contribution of $\overline{126}$ to fermion masses is assumed to be $O(3)$ invariant. The $O(3)$ breaking arises from the H and G contributions, which lead to departure from degeneracy through the type-I seesaw. We shall not specify how this breaking occurs [18]. Such an ansatz for the type-II contribution was considered [5] in the specific context of $SO(10)$. Detailed fits to fermion masses with

TABLE I. Best fit solutions for fermion masses and mixing obtained assuming the type-I seesaw dominance [solutions (1) and (2)] and type-II seesaw dominance [solution (3)]. Various observables and their pulls obtained at the minimum are shown (see text for details). Notations and conventions used here are the same as in [14]. The boldfaced quantities are predictions of the respective solutions.

No.	Observables	Sol. 1 Fitted value	Sol. 1 Pull	Sol. 2 Fitted value	Sol. 2 Pull	Sol. 3 Fitted value	Sol. 3 Pull
1	m_d [MeV]	0.653 677	−0.917 861	0.207 819	**−2.005 32**	0.868 041	−0.395 023
2	m_s [MeV]	17.5885	−0.386 821	21.6923	0.402 361	12.2829	**−1.407 14**
3	m_b [GeV]	1.111 31	0.418 721	1.058 32	−0.046 348	1.256 34	**1.691 41**
4	m_u [MeV]	0.462 718	0.084 789 6	0.450 825	0.005 499 32	0.450 489	0.003 261 1
5	m_c [GeV]	0.210 603	0.013 684 9	0.211 727	0.069 565 4	0.210 393	0.003 245 03
6	m_t [GeV]	63.6891	−0.832 404	67.6155	−0.658 038	102.325	0.883 371
7	m_e [MeV]	0.358 503	0.009 696 91	0.358 506	0.020 678 2	0.358 502	0.005 031 07
8	m_μ [MeV]	75.6719	0.007 345 14	75.6711	−0.008 306 4	75.6709	−0.011 180 9
9	m_{τ_2} [GeV]	1.292 19	−0.008 144 29	1.292 23	0.021 840 4	1.292 17	−0.024 457 6
10	$\frac{\Delta m^2_{\rm sol}}{\Delta m^2_{\rm atm}}$	0.030 351 4	0.050 109	0.030 323 7	0.037 787 7	0.030 253 8	0.006 594 21
11	m_0 [eV]	**0.31**	⋯	**0.17**	⋯	**0.36**	⋯
12	$\sin\theta^q_{12}$	0.224 205	−0.059 210 2	0.224 306	0.003 594 73	0.224 154	−0.091 312 5
13	$\sin\theta^q_{23}$	0.035 130 8	0.023 704	0.035 042 6	−0.044 117 3	0.035 143 6	0.033 571
14	$\sin\theta^q_{13}$	0.003 193 36	−0.013 286 7	0.003 158 71	−0.082 589 7	0.003 261 99	0.123 983
15	$\sin^2\theta^l_{12}$	0.319 801	−0.061 907 9	0.321 124	0.018 777 4	0.321 168	0.021 467 3
16	$\sin^2\theta^l_{23}$	0.481 942	0.313 909	0.436 492	−0.178 126	0.439 779	−0.142 55
17	$\sin^2\theta^l_{13}$	**0.019 526 6**	⋯	**0.002 881 76**	⋯	**0.035 683 6**	⋯
18	$\delta_{\rm CKM}$ [°]	67.7227	0.247 333	56.4935	−0.134 071	49.7146	−0.429 864
19	$\delta_{\rm PMNS}$ [°]	**53.98**	⋯	**−66.99**	⋯	**−25.33**	⋯
20	α_1 [°]	**146.55**	⋯	**−59.31**	⋯	**137.71**	⋯
21	α_2 [°]	**−89.88**	⋯	**162.41**	⋯	**−33.44**	⋯
	χ^2		2.038		4.684		6.0

recent data are, however, not presented in these works. We assume H, G to have the most general form and choose to work in a basis with a diagonal H. In this basis, Eq. (3) gets changed to

$$F = c_0 V, \tag{11}$$

where V is a unitary symmetric matrix. In this basis, the charged fermion mass matrices can be obtained from Eq. (1) by replacing H with diagonal D_H, and F with $c_0 V$. The neutrino mass matrix, Eq. (2) can be written in the same basis as

$$M_\nu = m_0(V - \epsilon M_D V^* M_D^T). \tag{12}$$

The parameter ϵ controls the contribution from a type-I seesaw, which induces splittings in neutrino masses.

We use these equations to fit all the fermion masses and mixing using the previous procedure. Results corresponding to the minimal case are displayed as solution (3) in Table I. The best fit solution we obtained here corresponds to $\chi^2 = 6.0$, which is acceptable for 16 data points from a statistical point of view and all the observables except m_b and m_s are fitted with less than 1σ accuracy. The obtained fit in the type-II case is, however, not as good as in the case of a pure type-I seesaw combined with the ansatz (4). As before, the m_0 sets the overall neutrino mass scale, which is determined to be ∼0.36 eV, using the atmospheric scale and fits shown in Table I. Numerical fits also lead to $\epsilon \approx 2 \times 10^{-6}$ GeV^{-2}. Since the scale of M_D is set by the top mass, the type-I contribution relative to the type-II is given by $\epsilon m_t^2 \sim 10^{-2}$, and the type-II contribution dominates as assumed. Now the overall scale of the RH neutrino mass is given by [see Eq. (1) and ansatz (3)]

$$M_3 \approx \frac{1}{m_0 \epsilon} \approx 1.1 \times 10^{15}\ \text{GeV},$$

which is close to the GUT scale, unlike the minimal models with type-II dominance but hierarchical neutrinos [6,7]. The increase in M_3 here is linked to the degeneracy of neutrinos. The atmospheric neutrino mass scale in models with type-II seesaw and hierarchical neutrinos is typically given by

$$\Delta m^2_{\rm atm} \sim \frac{v^4}{M_3^2},$$

while in the present case it arises from the combination of type-I and type-II contributions and is scaled by

$$\Delta m^2_{\rm atm} \sim m_0 \frac{v^2}{M_3},$$

leading to a higher M_3 compared to a purely type-II dominated scenario.

IV. SUMMARY

Obtaining a unified description of vastly different patterns of quark and lepton spectra is a challenging task. This becomes more so if neutrinos are quasidegenerate. We have shown here that it is indeed possible to obtain such a description starting from the fermionic mass structure, Eq. (1) that can arise in a general $SO(10)$ model. We considered two distinct possibilities based on purely type-I and the other based on the mixture of type-I and type-II seesaw mechanisms. Both these possibilities can lead to quasidegenerate spectra if they are supplemented, respectively, with ansatz (4) and (3). We have shown through the detailed numerical analysis that these ansatz are capable of explaining the entire fermionic spectrum and not just the quasidegenerate neutrinos. Moreover, the origin of large leptonic mixing here is linked to the quasidegenerate structure determined by the matrix V, providing yet another reason why quark and leptonic mixing angles are so different in spite of underlying unified mass structure.

[1] R. N. Mohapatra *et al.*, Rep. Prog. Phys. **70**, 1757 (2007); G. Altarelli and F. Feruglio, New J. Phys. **6**, 106 (2004).

[2] B. Bajc, G. Senjanovic, and F. Vissani, Phys. Rev. Lett. **90**, 051802 (2003); H. S. Goh, R. N. Mohapatra, and S. P. Ng, Phys. Lett. B **570**, 215 (2003).

[3] A. S. Joshipura and A. Y. Smirnov, Nucl. Phys. **B750**, 28 (2006).

[4] D. O. Caldwell and R. N. Mohapatra, Phys. Rev. D **48**, 3259 (1993); A. S. Joshipura, Z. Phys. C **64**, 31 (1994); Phys. Rev. D **51**, 1321 (1995); S. T. Petcov and A. Y. Smirnov, Phys. Lett. B **322**, 109 (1994).

[5] A. Ioannisian and J. W. F. Valle, Phys. Lett. B **332**, 93 (1994); D. G. Lee and R. N. Mohapatra, Phys. Lett. B **329**, 463 (1994).

[6] B. Bajc, A. Melfo, G. Senjanovic, and F. Vissani, Phys. Rev. D **70**, 035007 (2004); Phys. Lett. B **634**, 272 (2006); C. S. Aulakh and S. K. Garg, Nucl. Phys. **B757**, 47 (2006).

[7] S. Bertolini, M. Frigerio, and M. Malinský, Phys. Rev. D **70**, 095002 (2004); S. Bertolini and M. Malinský, Phys. Rev. D **72**, 055021 (2005); S. Bertolini, T. Schwetz, and M. Malinsky, Phys. Rev. D **73**, 115012 (2006); B. Bajc, I. Dorsner, and M. Nemevsek, J. High Energy Phys. 11 (2008) 007.

[8] M. Lindner, M. A. Schmidt, and A. Y. Smirnov, J. High Energy Phys. 07 (2005) 048.

[9] G. D'Ambrosio, G. F. Giudice, G. Isidori, and A. Strumia, Nucl. Phys. **B645**, 155 (2002).

[10] A. S. Joshipura, K. M. Patel, and S. K. Vempati, Phys. Lett. B **690**, 289 (2010).

[11] K. S. Babu and R. N. Mohapatra, Phys. Rev. Lett. **70**, 2845 (1993); C. S. Aulakh, B. Bajc, A. Melfo, G. Senjanovic, and F. Vissani, Phys. Lett. B **588**, 196 (2004); H. S. Goh, R. N. Mohapatra, and S. P. Ng, Phys. Rev. D **68**, 115008 (2003); C. S. Aulakh and A. Girdhar, Int. J. Mod. Phys. A **20**, 865 (2005); Nucl. Phys. **B711**, 275 (2005); K. Matsuda, Y. Koide, and T. Fukuyama, Phys. Rev. D **64**, 053015 (2001); K. Matsuda, Y. Koide, T. Fukuyama, and H. Nishiura, Phys. Rev. D **65**, 033008 (2002); **65**, 079904(E) (2002); T. Fukuyama and N. Okada, J. High Energy Phys. 11 (2002) 011; T. Fukuyama, A. Ilakovac, T. Kikuchi, S. Meljanac, and N. Okada, J. Math. Phys. (N.Y.) **46**, 033505 (2005); Phys. Rev. D **72**, 051701(R) (2005); C. S. Aulakh, Phys. Rev. D **72**, 051702(R) (2005); B. Dutta, Y. Mimura, and R. N. Mohapatra, J. High Energy Phys. 05 (2010) 034; Phys. Rev. D **80**, 095021 (2009).

[12] N. Oshimo, Phys. Rev. D **66**, 095010 (2002); Nucl. Phys. **B668**, 258 (2003); C. S. Aulakh, arXiv:hep-ph/0602132; Phys. Lett. B **661**, 196 (2008); C. S. Aulakh and S. K. Garg, arXiv:hep-ph/0612021; arXiv:0807.0917; B. Dutta, Y. Mimura, and R. N. Mohapatra, Phys. Rev. Lett. **94**, 091804 (2005); Phys. Rev. D **72**, 075009 (2005); Phys. Lett. B **603**, 35 (2004); W. M. Yang and Z. G. Wang, Nucl. Phys. **B707**, 87 (2005).

[13] W. Grimus and H. Kuhbock, Phys. Lett. B **643**, 182 (2006); Eur. Phys. J. C **51**, 721 (2007).

[14] A. S. Joshipura, B. P. Kodrani, and K. M. Patel, Phys. Rev. D **79**, 115017 (2009).

[15] G. C. Branco, M. N. Rebelo, and J. I. Silva-Marcos, Phys. Rev. Lett. **82**, 683 (1999).

[16] C. R. Das and M. K. Parida, Eur. Phys. J. C **20**, 121 (2001).

[17] M. C. Gonzalez-Garcia, M. Maltoni, and J. Salvado, J. High Energy Phys. 04 (2010) 056.

[18] Various possibilities are considered in S. Antusch and S. F. King, Nucl. Phys. **B705**, 239 (2005).

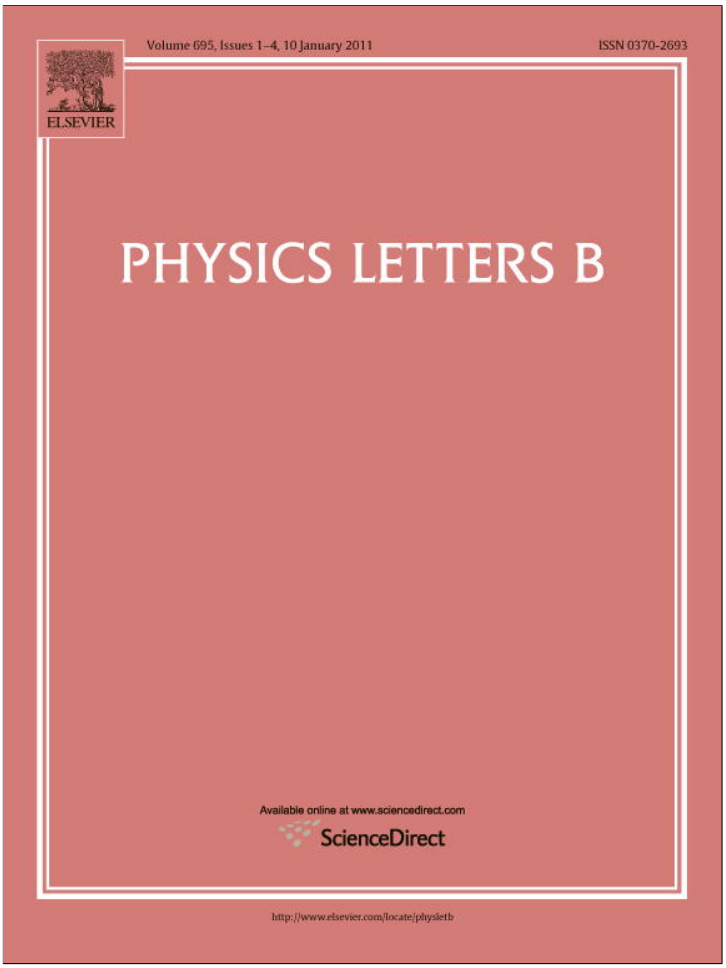

Physics Letters B 695 (2011) 225–230

Contents lists available at ScienceDirect

Physics Letters B

www.elsevier.com/locate/physletb

An $SO(10) \times S_4 \times Z_n$ model of Quark–Lepton Complementarity

Ketan M. Patel

Physical Research Laboratory, Navarangpura, Ahmedabad 380 009, India

ARTICLE INFO

Article history:
Received 6 September 2010
Received in revised form 1 November 2010
Accepted 4 November 2010
Available online 11 November 2010
Editor: M. Cvetič

Keywords:
Lepton mixing angle
Quark mixing angle
Quark lepton complementarity
Grand unified theory
Flavor symmetry

ABSTRACT

The present observations of Cabibbo angle and solar mixing angle satisfy the empirical relation called Quark–Lepton Complementarity (QLC), namely $\theta_{12}^l \sim \pi/4 - \theta_C$. It suggests the existence of correlation between quarks and leptons which is supported by the idea of grand unification. We propose a specific ansatz for the structure of Yukawa matrices in $SO(10)$ unified theory which leads to similar relation if neutrinos get masses through type-II seesaw mechanism. Viability of this ansatz is discussed through detailed analysis of fermion masses and mixing angles all of which can be explained in a model which uses three Higgs fields transforming as 10 and one transforming as $\overline{126}$ representations under $SO(10)$. It is shown that the proposed ansatz can be derived from an extended model based on the two pairs of 16-dimensional vector-like fermions and an $S_4 \times Z_n$ flavor symmetry. The model leads to the lepton mixing matrix that is dominantly bimaximal with $\mathcal{O}(\theta_C)$ corrections related to quark mixings. A generic prediction of the model is the reactor angle $\theta_{13}^l \sim \theta_C/\sqrt{2}$ which is close to its present experimental upper bound.

1. Introduction

Experiments on neutrino oscillations have revealed that two of the three leptonic mixing angles are large. One of them called the atmospheric mixing angle is almost maximal $\theta_{23}^l = 42.3^\circ\ (^{+11.4}_{-7.1})$ and the other known as the solar mixing angle $\theta_{12}^l = 34.5^\circ\ (^{+3.2}_{-2.8})$ is smaller compared to it [1]. In contrast, the observed quark mixing angles are small and hierarchical. The largest angle is the Cabibbo angle $\theta_C \equiv \theta_{us} \approx 13^\circ$ while other two are $\theta_{cb} \approx 2.4^\circ$ and $\theta_{ub} \approx 0.2^\circ$. An understanding of such wide dissimilarity between the quark and lepton mixing patterns is considered as one of the major challenges for the physics beyond the standard model. It has been observed long ago [2] that there exists an interesting empirical relation between quark and lepton mixing angles.

$$\theta_{12}^l + \theta_{us} \sim \frac{\pi}{4}. \tag{1}$$

The above relation is known as Quark–Lepton Complementarity [3–6] and still favored by the present experimental data within their measurement errors. It is also possible to write similar relation between 23 angles of quark and lepton mixing.

$$\theta_{23}^l + \theta_{cb} \sim \frac{\pi}{4}. \tag{2}$$

If such relations are not accidental, they strongly suggest the common roots between quarks and leptons [3–5]. Clearly it is very hard to realize such relations in ordinary bottom-up approaches where the quarks and leptons are treated separately with no specific connections between them. So one requires top-down approaches like the Grand Unified Theories (GUT) which sometime also unify quarks and leptons and provide a framework to construct a model in which QLC relation can be embedded in a natural way.

The general conditions under which QLC relation (1) can be realized from quark–lepton unification are thoroughly discussed in [3,4]. We describe one such possibility here. The quark mixing matrix known as Cabibbo–Kobayashi–Maskawa (CKM) matrix is defined as $V_{CKM} = U_u^\dagger U_d$ where $U_u(U_d)$ is unitary matrix that diagonalizes the up-(down-)type quark mass matrix. Corresponding leptonic mixing matrix, also called Pontecorvo–Maki–Nakagawa–Sakata (PMNS) matrix, is $V_{PMNS} = U_e^\dagger U_\nu$. Assume that the structure of neutrino and quark mass matrices at high scale are such that the PMNS matrix is exact bimaximal $V_{PMNS} = U_{BM}$ whereas the CKM matrix is an identity matrix to a leading order.

$$U_{BM} = \begin{pmatrix} \frac{1}{\sqrt{2}} & -\frac{1}{\sqrt{2}} & 0 \\ \frac{1}{2} & \frac{1}{2} & -\frac{1}{\sqrt{2}} \\ \frac{1}{2} & \frac{1}{2} & \frac{1}{\sqrt{2}} \end{pmatrix}. \tag{3}$$

Both the mixing matrices get corrected by $\mathcal{O}(\theta_C)$ terms coming from the next leading order where the down quark and charged lepton mass matrices are equal (or nearly so). In this scenario, a QLC relation can emerge from quark–lepton unification at high scale. Construction of a realistic GUT model in which all fermion

E-mail address: kmpatel@prl.res.in.

0370-2693/$ – see front matter
doi:10.1016/j.physletb.2010.11.024

masses and mixing angles are correctly reproduced along with QLC is highly non-trivial. In fact several models [5] proposed to explain QLC are based on a smaller gauge group, namely Pati–Salam $SU(4)_c \times SU(2)_L \times SU(2)_R$ group. A complete and realistic model based on $SO(10)$ GUT has not been proposed so far. The original proposal [4] was based on $SU(5)$ relation $M_e = M_d^T$ but detailed explanation of the fermionic spectrum was not developed. Here we present a predictive $SO(10)$ based unified description of fermion masses and mixing in which QLC relation can be naturally realized.

The renormalizable models based on the $SO(10)$ gauge group are quite powerful in constraining the fermion mass structure. Moreover, they provide a natural framework for understanding neutrino masses because of the seesaw mechanisms inherent in them. Fermion masses arise in these models through their couplings to Higgs fields transforming as **10**-, $\overline{\mathbf{126}}$- and **120**-dimensional representations under $SO(10)$. Neutrino masses arise from two separate sources either from the vacuum expectation value (vev) of the right-handed triplet (type-I) or from the left-handed triplet (type-II) Higgs. The minimal model with **10** and $\overline{\mathbf{126}}$ Higgs fields has attracted a lot attention [7–9]. There also exist a class of models where appropriate flavor symmetry is integrated with $SO(10)$ framework with extended Higgs sector [11–14] to construct a predictive theory which can simultaneously explain hierarchical nature of quark masses and mixing angles and large lepton mixing angles. In this Letter, we show that QLC relation follows in a specific $SO(10)$ model combined with S_4 symmetry if dominant source of neutrino mass is type-II. An additional Z_n symmetry is required in the model to get desired interactions between various fields.

The Letter is organized as follows. We describe the fermion mass relations in the model based on renormalizable supersymmetric (SUSY) $SO(10)$ GUT in the next section. In Section 3, we propose a specific ansatz which predictively interrelates various observables of quark and lepton sectors and leads to QLC relation. We also discuss the phenomenological implications of such ansatz in this section. In Section 4, we justify the proposed ansatz by a flavor symmetry group $S_4 \times Z_n$. Finally we conclude in Section 5.

2. Renormalizable SUSY $SO(10)$ model for fermion masses

We consider three families of **16**-dimensional fermions obtaining their masses from renormalizable couplings to four Higgs multiplets, three of them (denoted by Φ, Φ' and Φ'') transforming as **10** and the other ($\bar{\Sigma}$) as $\overline{\mathbf{126}}$-dimensional representations under $SO(10)$. The $SO(10)$ breaking can be achieved with either $\mathbf{210} + \mathbf{54} + \mathbf{126} + \overline{\mathbf{126}}$ [9] or $\mathbf{45} + \mathbf{54} + \mathbf{126} + \overline{\mathbf{126}} + \mathbf{120}$ [10]. The Yukawa interactions of the model can be written as

$$W_Y = Y_{10}\psi\psi\Phi + Y_{\overline{126}}\psi\psi\bar{\Sigma} + Y_{10'}\psi\psi\Phi' + Y_{10''}\psi\psi\Phi'' \qquad (4)$$

where Y_i are symmetric Yukawa coupling matrices. The representations Φ, Φ', Φ'' and $\bar{\Sigma}$ have two minimal supersymmetric standard model (MSSM) doublets in each of them. It is assumed that only one linear combination of the up-type doublets and one of the down-type doublets remain light and play the role of H_u and H_d fields. Once these light doublets acquire vacuum expectation values, they break electroweak symmetry and generate the fermion masses as well. The resulting fermion mass matrices can be suitably written as [11]

$$\begin{aligned} M_d &= H + F + tH' + H'';\\ M_u &= rH + sF + H' + pH'';\\ M_e &= H - 3F + tH' + H'';\\ M_D &= rH - 3sF + H' + pH'';\\ M_L &= r_L F;\\ M_R &= r_R^{-1} F, \end{aligned} \qquad (5)$$

where H, F, H' and H'' are obtained by multiplying electroweak vevs and Higgs mixing parameters with Yukawa coupling matrices $Y_{10}, Y_{\overline{126}}, Y_{10'}$ and $Y_{10''}$ respectively. r, s, t, p, r_L are r_R are dimensionless parameters determined by the Clebsch–Gordan coefficients, ratios of vevs, and mixing among Higgs fields (see [12] for example). M_D denotes neutrino Dirac mass matrix. $M_L(M_R)$ is the Majorana mass matrix for left- (right-)handed neutrinos which receives a contribution only from the vev of $\bar{\Sigma}$ field. In generic $SO(10)$ models of this type, the effective neutrino mass matrix $\mathcal{M}_\nu$ for the three light neutrinos has type-I and type-II contributions.

$$\mathcal{M}_\nu \equiv \mathcal{M}_\nu^{II} + \mathcal{M}_\nu^{I} = r_L F - r_R M_D F^{-1} M_D^T. \qquad (6)$$

In general, both contributions are present and they depend on two different parameters so one may dominate over the other. It has been shown in several references [9] that it is possible to have symmetry breaking pattern in $SO(10)$ where type-II term dominates over the type-I contributions. In this limit, neutrino masses and mixing are governed by F which can be written as $F \sim M_d - M_e$. It is well known that this relation establish interesting relationship between $b - \tau$ unification and large atmospheric mixing angle [8]. Eqs. (5) and (6) are the key equations that provide basic platform to construct a model in which the QLC relation (1) can be realized.

3. Ansatz

We propose following ansatz which leads to relation (1).

$$\begin{aligned} H &= \frac{1}{2}\begin{pmatrix} 0 & 0 & 0 \\ 0 & h & h \\ 0 & h & h \end{pmatrix}; \qquad F = \begin{pmatrix} b+c & \sqrt{2}a & 0 \\ \sqrt{2}a & b+c & 0 \\ 0 & 0 & b-c \end{pmatrix};\\ H' &= \begin{pmatrix} 0 & 0 & \sqrt{2}a' \\ 0 & 0 & 0 \\ \sqrt{2}a' & 0 & 0 \end{pmatrix}; \qquad H'' = xI, \end{aligned} \qquad (7)$$

where I is 3×3 identity matrix. To do the simple analytical study of such ansatz we assume that all the above parameters are real. Without loss of generality, we can express the above matrices in a basis with diagonal H. Such basis are obtained by rotating the **16**-dimensional fermion fields in 2–3 plane by an angle $\pi/4$. The matrices in (7) will be redefined in new basis as

$$\left(H, F, H', H''\right) \quad \rightarrow \quad R_{23}\left(\frac{\pi}{4}\right)\left(H, F, H', H''\right)R_{23}^T\left(\frac{\pi}{4}\right) \qquad (8)$$

and can be rewritten as

$$\begin{aligned} H &= \begin{pmatrix} 0 & 0 & 0 \\ 0 & 0 & 0 \\ 0 & 0 & h \end{pmatrix}; \qquad F = \begin{pmatrix} b+c & a & a \\ a & b & c \\ a & c & b \end{pmatrix};\\ H' &= \begin{pmatrix} 0 & -a' & a' \\ -a' & 0 & 0 \\ a' & 0 & 0 \end{pmatrix}; \qquad H'' = xI. \end{aligned} \qquad (9)$$

Before we present the detailed analysis let us look at some immediate implications of the above ansatz. The dominant **10**-Higgs coupling matrix H has rank-1. As it was pointed out in [13,14] this can simultaneously explain both the observed hierarchy of quark masses as well as the origin of large lepton mixings if the light

neutrino masses are generated through type-II seesaw mechanism. Assuming only one **10**-Higgs H contribution in charged fermion mass matrices, we get at zeroth order,

$$m_b = m_\tau = \frac{1}{r} m_t; \qquad V_{CKM} = I; \qquad V_{PMNS} = U_{BM}. \tag{10}$$

Correct b–τ unification and large lepton mixings (bimaximal) are obtained with no mixings between quarks. The charged fermions of first two generations are massless in this case. Further, the contributions coming from other Higgs coupling matrices F, H' and H'' make the model realistic by giving nonzero masses to first two fermion generations as well as by perturbing both the mixing matrices which reproduce observed mixing patterns for both the quark and lepton sectors.

We now present the detailed analysis of ansatz (9). Substituting it in Eqs. (5) and (6), we get

$$M_u = \begin{pmatrix} s(b+c)+x' & sa-a' & sa+a' \\ sa-a' & sb+x' & sc \\ sa+a' & sc & rh+sb+x' \end{pmatrix};$$

$$M_d = \begin{pmatrix} b+c+x & a-ta' & a+ta' \\ a-ta' & b+x & c \\ a+ta' & c & h+b+x \end{pmatrix};$$

$$M_e = \begin{pmatrix} -3(b+c)+x & -3a-ta' & -3a+ta' \\ -3a-ta' & -3b+x & -3c \\ -3a+ta' & -3c & h-3b+x \end{pmatrix};$$

$$M_\nu = r_L F, \tag{11}$$

where $x' = px$. Since each mass matrix is real symmetric, it can be diagonalized by a rotation matrix parameterized (in the standard parameterization) by three angles.

$$R_f^T M_f R_f = Diag(m_{f1}, m_{f2}, m_{f3});$$
$$R_f = R_{23}(\theta_{23}^f) R_{13}(\theta_{13}^f) R_{12}(\theta_{12}^f), \tag{12}$$

where $f = d, u, e, \nu$ and R_{ij} is a rotation matrix in ij plane. The charged fermion mass matrices are hierarchical ($h \gg b, c \gg a, a' \gg x, x'$) and can be approximately diagonalized by Jacobi rotation. The results obtained from such diagonalization for the quark sector are displayed below.

$$m_b \approx h + b + x + \mathcal{O}\left(\frac{c^2}{h}\right);$$
$$m_s \approx b + x + \frac{(a-ta')^2}{b}\left(1 - \frac{x}{b}\right) + \mathcal{O}\left(\frac{c^2}{h}\right);$$
$$m_d \approx b + c + x - \frac{(a-ta')^2}{b}\left(1 - \frac{x}{b}\right) + \mathcal{O}\left(\frac{a^2}{h}\right). \tag{13}$$
$$m_t \approx rh + sb + x' + \mathcal{O}\left(\frac{s^2c^2}{rh}\right);$$
$$m_c \approx sb + x' + \frac{(sa-a')^2}{sb}\left(1 - \frac{x'}{sb}\right) + \mathcal{O}\left(\frac{s^2c^2}{rh}\right);$$
$$m_u \approx s(b+c) + x' - \frac{(sa-a')^2}{sb}\left(1 - \frac{x'}{sb}\right) + \mathcal{O}\left(\frac{s^2a^2}{rh}\right). \tag{14}$$
$$\theta_{12}^d \approx -\frac{a-ta'}{b}\left(2 + \frac{c-x}{b}\right); \qquad \theta_{23}^d \approx -\frac{c}{h};$$
$$\theta_{13}^d \approx -\frac{a+ta'}{h}\left(1 + \frac{c}{h}\right). \tag{15}$$
$$\theta_{12}^u \approx -\frac{sa-a'}{sb}\left(2 + \frac{sc-x'}{sb}\right); \qquad \theta_{23}^u \approx -\frac{sc}{rh};$$
$$\theta_{13}^u \approx -\frac{sa+a'}{rh}\left(1 + \frac{sc}{rh}\right). \tag{16}$$

Let us underline some important points in connection with above relations.

- The six real parameters h, b, x, r, s, x' can be approximated from the six quark masses. m_b and m_s determine the parameters h and b. It is easy to see that $r \approx m_t/m_b$ and $s \approx m_c/m_s$ are required to obtain the masses of heavy quarks m_t and m_c. Further, m_d and m_u fix the values of x and x'. Since $b, c \gg x$, we require $c \sim -b$ to obtain small masses of first generation fermions.
- Let us assume that $a' \approx sa$ in order to keep $\theta_{12}^u \ll \theta_{12}^d$. Also note that $\theta_{23}^u \approx (s/r)\theta_{23}^d \ll \theta_{23}^d$ and $\theta_{13}^u \sim (s/r)\theta_{13}^d \ll \theta_{13}^d$. In this limit, the quark mixing matrix takes the form
$$V_{CKM} = U_u^\dagger U_d \approx U_d \approx R_{23}(\theta_{23}^d) R_{13}(\theta_{13}^d) R_{12}(\theta_{12}^d). \tag{17}$$
- The elements of the CKM matrix fix some more parameters as follows.
$$c \sim -V_{cb}\, h;$$
$$a - ta' \sim -V_{us} b; \qquad a + ta' \sim -V_{ub} h. \tag{18}$$
An interesting relationship between V_{us} and V_{ub} can be found in the limit $t \sim 0$.
$$V_{ub} \approx V_{us}\frac{m_s}{m_b} + \mathcal{O}\left(\frac{m_s^2}{m_b^2}\right). \tag{19}$$
We will show later in this section that $t \sim 0$ is a necessary requirement to obtain QLC relation (1).
- Our assumption of real parameters makes the theory CP invariant. The observed CP violation in the quark sector can be accommodated by making some parameters complex.

It is interesting to note that all the parameters are fixed in terms of the observables of the quark sector. Hence the entire lepton sector emerges as the prediction of the model. Let us first derive the predictions for the charged leptons.

$$m_\tau \approx h - 3b + x + \mathcal{O}\left(\frac{c^2}{h}\right);$$
$$m_\mu \approx -3b + x - \frac{(3a+ta')^2}{3b}\left(1 + \frac{x}{3b}\right) + \mathcal{O}\left(\frac{c^2}{h}\right);$$
$$m_e \approx -3(b+c) + x + \frac{(3a+ta')^2}{3b}\left(1 + \frac{x}{3b}\right) + \mathcal{O}\left(\frac{a^2}{h}\right). \tag{20}$$
$$\theta_{12}^e \approx -\frac{3a+ta'}{3b}\left(2 + \frac{3c+x}{3b}\right); \qquad \theta_{23}^e \approx \frac{3c}{h};$$
$$\theta_{13}^e \approx \frac{3a-ta'}{h}\left(1 + \frac{c}{h}\right). \tag{21}$$

Noteworthy features of the above relations are the following,

- It predicts $m_\tau \approx m_b$ and $m_\mu \approx -3m_s$.
- For $b = -c$, $m_e \approx m_d$ which is viable with observed values of m_e and m_d extrapolated at the GUT scale within 3σ deviations [16]. However for $b \neq -c$, any desired value of m_d/m_e can be obtained.
- For $t \sim 0$, $\theta_{12}^e \approx \theta_C$, $\theta_{23}^e \approx -3\theta_{cb}$ and $\theta_{13}^e \approx -3\theta_{ub}$.

The light neutrino mass matrix in Eq. (11) has the most general form which can be diagonalized by bimaximal matrix U_{BM}. The mass eigenvalues are,

$$m_1 = m_0\big(b + c + \sqrt{2}a\big);$$
$$m_2 = m_0\big(b + c - \sqrt{2}a\big); \qquad m_3 = m_0(b - c). \tag{22}$$

Interestingly, for $b = -c$ (which can now also be written as $V_{cb} \approx m_s/m_b$), we get the partial degenerate neutrino mass spectrum $m_1 = -m_2 \ll m_3$ which leads to vanishing solar (mass)^2 difference ($\Delta m^2_{sol} = m_2^2 - m_1^2 = 0$) at high scale. We performed numerical study and found that the radiative corrections to the original neutrino mass matrix are unable to generate the required splitting between m_1 and m_2. Another way to induce non-zero value of Δm^2_{sol} is to allow type-I contribution to the original type-II seesaw neutrino mass matrix. However such contribution is highly hierarchical (like M_l^2) and it largely contributes to the 33 element of neutrino mass matrix which ultimately spoils the nice symmetry of neutrino mass matrix and hence the bimaximality of neutrino mixings. This forces us to consider the case where $V_{cb} \neq m_s/m_b$. In this case we obtain the following expression for the ratio of the solar to atmospheric squared mass difference.

$$\frac{\Delta m^2_{sol}}{\Delta m^2_{atm}} \approx \sqrt{2} V_{us}\left(\frac{m_s/m_b}{V_{cb}}\left(1 + \frac{m_s}{m_b}\right) - 1\right). \tag{23}$$

Note that one requires $m_s/m_b \sim 1.08\ V_{cb}$ to obtain the observed value of $\Delta m^2_{sol}/\Delta m^2_{atm} (\sim 0.031)$ and it implies that $V_{cb} < m_s/m_b$ which is not favored by their present observed values extrapolated at the GUT scale. However as argued in [14], the threshold corrections to b–s quark mass mixing from gluino and wino exchange via one-loop diagrams can give desired value of V_{cb}. The required deviation from $b = -c$ is quantified by

$$b + c \approx m_s\left(1 - \frac{V_{cb}}{m_s/m_b}\right) \lesssim 0.08 m_s$$

which is small and of order of first generation fermion masses and hence allows the correct m_d in Eq. (13).

The leptonic mixing matrix can be seen as dominant bimaximal mixing resulting from neutrino mass matrix and then corrected by $\mathcal{O}(\theta_C)$ terms coming from the unitary matrix U_e which diagonalize charged lepton mass matrix.

$$V_{PMNS} \equiv U_e^\dagger U_\nu = U_e^T U_{BM} \tag{24}$$

where $U_e = R_{23}(-3\theta_{cb}) R_{13}(-3\theta_{ub}) R_{12}(\theta_C)$. The resulting neutrino mixing parameters are the following.

$$U_{e2} \equiv (V_{PMNS})_{12} \approx -\frac{1}{\sqrt{2}} + \frac{(V_{us} - 3V_{ub})}{2};$$
$$U_{\mu 3} \equiv (V_{PMNS})_{23} \approx -\frac{1}{\sqrt{2}}(1 + 3V_{cb});$$
$$U_{e3} \equiv (V_{PMNS})_{13} \approx -\frac{1}{\sqrt{2}}(V_{us} + 3V_{ub}). \tag{25}$$

The correction of $\mathcal{O}(\theta_C)$ from charged lepton generates correct solar mixing angle

$$\theta^l_{12} \approx \frac{\pi}{4} - \frac{\theta_C}{\sqrt{2}}. \tag{26}$$

Note that the correction induced in this approach is $\theta_C/\sqrt{2}$ which is small compared to exact QLC relation (1) but it is still viable with the experimental observations. The atmospheric mixing angle gets considerable deviation $\theta^l_{23} \approx \frac{\pi}{4} + 3\theta_{cb}$ in this model unlike the standard QLC relation for 23 mixing angle of quark and lepton given in Eq. (2). The model also predicts large value of $U_{e3} \approx 0.16$ which can be tested in planned long baseline experiments.

Note that Eq. (25) holds at GUT scale which might be changed by RGE corrections in principle. However it is known that running of the Cabibbo angle is negligibly small in MSSM even with large value of $\tan\beta$. Running of leptonic mixing angle depends on the type of mass spectrum of light neutrinos. For $b \neq -c$, neutrino mass spectrum follows normal hierarchy $m_1 < m_2 \ll m_3$. The effect of RGE corrections are known to be negligible in this case and Eq. (25) holds at low scale also.

We now provide an example of values of the parameters of Eq. (9) which successfully generate entire fermion mass spectrum as well as mixing patterns for both quark and lepton sector. The required CP violation in the quark sector is incorporated by making a' complex. In the limit $t \sim 0$, a' contributes only to the up quark mass matrix and does not change the other predictions of ansatz given in Eq. (9). One more parameter x' is made complex to reproduce m_u correctly. The numerical values of parameters are

$$h = 1.7\ \text{GeV}; \qquad b = 0.0243\ \text{GeV}; \qquad c = -0.022113\ \text{GeV};$$
$$a = -0.0052\ \text{GeV}; \qquad a' = (0.0344247 - 0.028885i)\ \text{GeV};$$
$$x' = (0.0233596 - 0.00293374i)\ \text{GeV}; \qquad x = 0.00325\ \text{GeV};$$
$$r = 55.88; \qquad s = -8.64198; \qquad t = 0. \tag{27}$$

Substituting these numbers in Eq. (11), we get

$$m_t = 94.8\ \text{GeV}; \quad m_c = 0.19\ \text{GeV}; \quad m_u = 0.65\ \text{MeV};$$
$$m_b = 1.73\ \text{GeV}; \quad m_s = 28.5\ \text{MeV}; \quad m_d = 4.21\ \text{MeV};$$
$$m_\tau = 1.63\ \text{GeV}; \quad m_\mu = 75.4\ \text{MeV}; \quad m_e = 0.35\ \text{MeV}. \tag{28}$$
$$\sin\theta_{us} = 0.222; \quad \sin\theta_{cb} = 0.015; \quad \sin\theta_{ub} = 0.005;$$
$$\delta_{CKM} = 60.9^\circ; \quad \sin^2\theta^l_{12} = 0.368; \quad \sin^2\theta^l_{23} = 0.527;$$
$$\sin^2\theta^l_{13} = 0.024; \quad \frac{\Delta m^2_{sol}}{\Delta m^2_{atm}} = 0.030. \tag{29}$$

The obtained spectrum is in good agreement with the data extrapolated at the GUT scale. For example, we compare our results with the charged fermion masses obtained at the GUT scale in the MSSM for $\tan\beta = 55$, $M_{SUSY} = 1$ TeV and $M_{GUT} = 2 \times 10^{16}$ GeV given in Table 5 of Ref. [16]. All charged fermion masses (except m_d) obtained here fits with the data within 1σ. Our ansatz predicts larger value of m_d. The quark mixing angles θ_{cb} is small ($< m_s/m_b$) as required by Eq. (23). The reproduced values of lepton mixing angles and $\Delta m^2_{sol}/\Delta m^2_{atm}$ are also in accordance with their updated low energy values (within 3σ measurement errors) given in [1].

4. The model

In this section, we will illustrate how the ansatz (7) can be obtained in a model from flavor symmetry. We use discrete flavor symmetry based on the group S_4 which is a group of permutation of four distinct objects. It has 24 distinct elements filled in five conjugate classes and hence five irreducible representations of dimensions $\mathbf{3_2}, \mathbf{3_1}, \mathbf{2}, \mathbf{1_2}$ and $\mathbf{1_1}$. A singlet representation with subscript "2" changes sign under transformation involving the odd number of permutations of S_4. More details on the group theory of S_4, its multiplication rules and the Clebsch–Gordan coefficients are reported in [15].

Our model follows the same line as model constructed in [14] and uses the same symmetry group. However it differs at some places since the ansatz required here is different from their ansatz. The basic matter fields and Higgs fields content of the model is

Table 1
Various fields and their representations under $SO(10) \times S_4 \times Z_n$.

	ψ	Φ	Φ'	Φ''	$\bar{\Sigma}$	χ	ϕ	η	σ	σ'	Ψ_{V1}	$\bar{\Psi}_{V1}$	Ψ_{V2}	$\bar{\Psi}_{V2}$
$SO(10)$	**16**	**10**	**10**	**10**	$\overline{\mathbf{126}}$	**1**	**1**	**1**	**1**	**1**	**16**	$\overline{\mathbf{16}}$	**16**	$\overline{\mathbf{16}}$
S_4	$\mathbf{3_2}$	$\mathbf{1_1}$	$\mathbf{1_2}$	$\mathbf{1_1}$	$\mathbf{1_1}$	$\mathbf{3_1}$	$\mathbf{3_2}$	$\mathbf{3_1}$	$\mathbf{1_1}$	$\mathbf{1_2}$	$\mathbf{1_1}$	$\mathbf{1_1}$	$\mathbf{1_2}$	$\mathbf{1_2}$
Z_n	1	ω^{-2m}	$\omega^{-(p+q)}$	ω^{-2q}	ω^{-2k}	ω^k	ω^m	ω^p	ω^k	ω^q	ω^m	ω^{-m}	ω^k	ω^{-k}

the same as discussed in Section 2. In addition to this we use five flavon fields which are singlets under $SO(10)$ and two pair of vector-like fermion fields which transform like $\mathbf{16} \oplus \overline{\mathbf{16}}$ under $SO(10)$. We impose the S_4 symmetry together with Z_n symmetry to get desired structure of Yukawa matrices. Three matter fields ψ are assigned as $\mathbf{3_2}$-dimensional representation of S_4 while five flavon fields χ, ϕ, η, σ and σ' form $\mathbf{3_1}, \mathbf{3_2}, \mathbf{3_1}, \mathbf{1_1}$ and $\mathbf{1_2}$ representations of S_4 respectively. The other fields are singlet ($\mathbf{1_1}$ or $\mathbf{1_2}$) under S_4. An additional Z_n symmetry is required to allow/forbid interactions between particular fields. The Z_n charges of various fields are listed in Table 1 where $\omega = e^{i(2\pi/n)}$.

Let us consider a theory above GUT scale which is invariant under the symmetry group $SO(10) \times S_4 \times Z_n$. The Yukawa superpotential allowed by such symmetry can be written as

$$\begin{aligned} W &= (\phi\psi)\bar{\Psi}_{V1} + \lambda\Psi_{V1}\Psi_{V1}\Phi + M_1\Psi_{V1}\bar{\Psi}_{V1} \\ &\quad + (\chi\psi)\bar{\Psi}_{V2} + \lambda'\Psi_{V2}\Psi_{V2}\bar{\Sigma} + M_2\Psi_{V2}\bar{\Psi}_{V2} \\ &\quad + \sum_i \frac{\alpha_i}{\Lambda^2}\left(\chi^2\psi\psi\right)_i\bar{\Sigma} + \frac{\beta}{\Lambda^2}\sigma(\chi\psi\psi)\bar{\Sigma} + \frac{\gamma}{\Lambda^2}\sigma^2(\psi\psi)\bar{\Sigma} \\ &\quad + \frac{\alpha'}{\Lambda^2}\sigma'(\eta\psi\psi)\Phi' + \frac{\alpha''}{\Lambda^2}\sigma'^2(\psi\psi)\Phi'' \end{aligned} \tag{30}$$

where Λ is the cut-off scale up to which the theory is valid. In renormalizable $SO(10)$ models where large dimensional Higgs fields are used, the gauge coupling hits the Landau pole soon after the unification scale and hence the cut-off scale of theory lies near to the GUT scale. For example, the Higgs fields mentioned in Table 1 together with $\mathbf{210} + \mathbf{54} + \mathbf{126}$ Higgs (required by consistent $SO(10)$ breaking) give large negative contribution to β-function which makes the gauge coupling non-perturbative just after GUT scale ($\Lambda \sim 6 \times 10^{16}$ GeV). In an alternative model [10] where **210** Higgs is replaced by $\mathbf{45} + \mathbf{120}$, cut-off scale Λ can be lifted slightly (up to $\sim 10^{17}$ GeV). In such model, the Yukawa interactions of fermions with **120**-plet Higgs field can be avoided using the $S_4 \times Z_n$ symmetry. For example, if **120** Higgs transforms as ($\mathbf{1_2}$, 1) representation of $S_4 \times Z_n$ then the renormalizable Yukawa interaction $(\psi\psi 120_H)$ is not invariant under S_4 symmetry. Further, It is easy to see that the higher-dimensional non-renormalizable Yukawa interactions mediated by flavon fields are forbidden by the Z_n symmetry. $M_{1,2}$ are mass scales of heavy vector-like fermions stay between the GUT scale and cut-off scale. Since the cut-off scale lies near the GUT scale, all these intermediate scales are very close to each other. Further, $\alpha_i, \alpha', \alpha'', \beta$, and γ small coefficients of $\mathcal{O}(\Lambda^2/M_{Pl}^2)$. The S_4 singlet contraction of flavor index is indicated with bracket. The term $(\chi^2\psi\psi)$ represents all the different S_4 contractions which can be constructed as follows:

$$\begin{aligned} \left(\chi^2\psi\psi\right)_i \equiv &\left((\chi\chi)_{\mathbf{1_1}}(\psi\psi)_{\mathbf{1_1}}\right), \left((\chi\chi)_{\mathbf{2}}(\psi\psi)_{\mathbf{2}}\right), \\ &\left((\chi\chi)_{\mathbf{3_1}}(\psi\psi)_{\mathbf{3_1}}\right), \left((\chi\chi)_{\mathbf{3_2}}(\psi\psi)_{\mathbf{3_2}}\right), \\ &\left((\chi\psi)_{\mathbf{1_2}}(\chi\psi)_{\mathbf{1_2}}\right), \left((\chi\psi)_{\mathbf{2}}(\chi\psi)_{\mathbf{2}}\right), \\ &\left((\chi\psi)_{\mathbf{3_1}}(\chi\psi)_{\mathbf{3_1}}\right), \left((\chi\psi)_{\mathbf{3_2}}(\chi\psi)_{\mathbf{3_2}}\right) \end{aligned} \tag{31}$$

where $(\cdots)_R$ indicates the representation R under S_4. Now consider a theory below the scale of $M_{1,2}$ and at the GUT scale. The effective superpotential after integrating out heavy vector-like fields is given by,

$$\begin{aligned} W_{eff} &= \frac{\lambda}{M_1^2}(\phi\psi)(\phi\psi)\Phi + \frac{\lambda'}{M_2^2}(\chi\psi)(\chi\psi)\bar{\Sigma} \\ &\quad + \sum_i \frac{\alpha_i}{\Lambda^2}\left(\chi^2\psi\psi\right)_i\bar{\Sigma} + \frac{\beta}{\Lambda^2}\sigma(\chi\psi\psi)\bar{\Sigma} \\ &\quad + \frac{\gamma}{\Lambda^2}\sigma^2(\psi\psi)\bar{\Sigma} + \frac{\alpha'}{\Lambda^2}\sigma'(\eta\psi\psi)\Phi' \\ &\quad + \frac{\alpha''}{\Lambda^2}\sigma'^2(\psi\psi)\Phi'' \end{aligned} \tag{32}$$

where first two terms allow the desired rank-1 structure of Yukawa matrices. Note that effective Yukawa superpotential still has the symmetry $SO(10) \times S_4 \times Z_n$. This symmetry will be broken to $SO(10)$ by vevs of the flavon fields. In order to get the desired structure of Yukawa couplings, we will choose particular vacuum alignment of the flavon fields as given below.

$$\begin{aligned} &\langle\phi\rangle = \begin{pmatrix}0\\1\\1\end{pmatrix}v_\phi; \qquad \langle\chi\rangle = \begin{pmatrix}0\\0\\1\end{pmatrix}v_\chi; \qquad \langle\eta\rangle = \begin{pmatrix}0\\1\\0\end{pmatrix}v_\eta; \\ &\langle\sigma\rangle = v_\sigma; \qquad \langle\sigma'\rangle = v_{\sigma'}. \end{aligned} \tag{33}$$

These vevs of flavon fields break flavor symmetry S_4 at the GUT scale and generate following structure of various Yukawa couplings.

$$Y_{10} = \frac{\lambda v_\phi^2}{M_1^2}\begin{pmatrix}0&0&0\\0&1&1\\0&1&1\end{pmatrix}; \tag{34}$$

$$\begin{aligned} Y_{126} &= \frac{\lambda' v_\chi^2}{M_2^2}\begin{pmatrix}0&0&0\\0&0&0\\0&0&1\end{pmatrix} + \frac{v_\chi^2}{\Lambda^2}\begin{pmatrix}\tilde{\alpha}&0&0\\0&\tilde{\alpha}&0\\0&0&\tilde{\alpha}_0\end{pmatrix} \\ &\quad + \frac{\beta v_\chi v_\sigma}{\Lambda^2}\begin{pmatrix}0&1&0\\1&0&0\\0&0&0\end{pmatrix} + \frac{\gamma v_\sigma^2}{\Lambda^2}I; \end{aligned} \tag{35}$$

$$Y_{10'} = \frac{\alpha' v_{\sigma'} v_\eta}{\Lambda^2}\begin{pmatrix}0&0&1\\0&0&0\\1&0&0\end{pmatrix}; \tag{36}$$

$$Y_{10''} = \frac{\alpha'' v_{\sigma'}^2}{\Lambda^2}I, \tag{37}$$

where all non-relevant Clebsch–Gordan coefficients are suitably absorbed. $\tilde{\alpha}$ and $\tilde{\alpha}_0$ are linear combinations of different α_i. The Yukawa matrices derived from the super potential can successfully explain the ansatz given in Eq. (7). Further, one has to assume $\lambda' \gg \alpha_i$ in order to achieve the relation $b \approx -c$ in Eq. (7) since there is no large hierarchy between the two scales M_2 and Λ. Note that in Eq. (30) we included only the leading order operators, linear and quadratic in flavon fields. Higher-dimensional operators with $2 + d$ ($d > 0$) flavons can generate significant corrections to the mass matrices particularly when Λ is not very far from the GUT scale. However all the operators up to some given d can be forbidden by using a Z_n with sufficiently large n and choosing carefully the Z_n charges of various fields in Table 1.

It is very important to show that the required vacuum structure of flavon fields (33) is allowed by flavon superpotential. This point has already been discussed in great details in reference [14]. Since our model has the same kind of flavon structure as theirs, we simply use their results. Note that due to non-trivial Z_n charges, bilinear terms which correspond to masses of flavon fields are not allowed. As a result of this the model requires doubling of flavon fields to allow Dirac type mass terms. The new flavon fields have the same S_4 representations but opposite Z_n charges. It has been shown in [14] that all the desired vacua of Eq. (33) are present in the model.

5. Summary

In this Letter, we have studied a possible way to realize quark–lepton complementarity between the Cabibbo angle and solar mixing angle in realistic quark–lepton unification theory based on $SO(10)$ gauge group. We have shown here that it is indeed possible to obtain such relation Eq. (26) starting from the fermionic mass structure (5) if they are supplemented with ansatz (7) and assuming that only type-II seesaw mechanism is responsible for light neutrino masses. One necessary ingredient for QLC is bimaximal mixing pattern from the neutrino sector which has been obtained through specific ansatz. Our ansatz also makes use of recently proposed [13] rank-1 strategy which naturally explains charged fermions mass hierarchy as well as origin of hierarchical quark mixing angles as opposed to the large lepton mixing angles. We have shown through the detailed analysis that this ansatz is capable of explaining the entire fermionic spectrum and not just the QLC relation. Moreover, the various predictions made by such ansatz are in agreement with observations. We have shown that the proposed ansatz can be obtained in a model from a discrete flavor symmetry group S_4 together with an additional Z_n symmetry. A generic prediction of our approach is $\theta_{13}^l \approx \theta_C/\sqrt{2}$ which is near to its current experimental upper bound. The atmospheric mixing angle gets considerable deviation from maximality ($\theta_{23}^l \approx \pi/4 + 3\theta_{cb}$) in this approach. These predictions can be confirmed or excluded by the current generation of neutrino oscillations experiments.

Acknowledgements

I thank Anjan S. Joshipura for many useful discussions, suggestions and encouragement during this work and for reading the manuscript carefully.

References

[1] M.C. Gonzalez-Garcia, M. Maltoni, J. Salvado, JHEP 1004 (2010) 056, arXiv:1001.4524 [hep-ph].
[2] A.Y. Smirnov, arXiv:hep-ph/0402264.
[3] H. Minakata, A.Y. Smirnov, Phys. Rev. D 70 (2004) 073009, arXiv:hep-ph/0405088.
[4] M. Raidal, Phys. Rev. Lett. 93 (2004) 161801, arXiv:hep-ph/0404046.
[5] P.H. Frampton, R.N. Mohapatra, JHEP 0501 (2005) 025, arXiv:hep-ph/0407139;
S. Antusch, S.F. King, R.N. Mohapatra, Phys. Lett. B 618 (2005) 150, arXiv:hep-ph/0504007;
S.F. King, JHEP 0508 (2005) 105, arXiv:hep-ph/0506297;
R.D.A. Toorop, F. Bazzocchi, L. Merlo, JHEP 1008 (2010) 001, arXiv:1003.4502 [hep-ph].
[6] J. Ferrandis, S. Pakvasa, Phys. Rev. D 71 (2005) 033004, arXiv:hep-ph/0412038;
P.H. Frampton, S.T. Petcov, W. Rodejohann, Nucl. Phys. B 687 (2004) 31, arXiv:hep-ph/0401206;
M. Lindner, M.A. Schmidt, A.Y. Smirnov, JHEP 0507 (2005) 048, arXiv:hep-ph/0505067;
C. Giunti, M. Tanimoto, Phys. Rev. D 66 (2002) 113006, arXiv:hep-ph/0209169;
K.A. Hochmuth, W. Rodejohann, Phys. Rev. D 75 (2007) 073001, arXiv:hep-ph/0607103;
F. Plentinger, W. Rodejohann, Phys. Lett. B 625 (2005) 264, arXiv:hep-ph/0507143;
W. Rodejohann, Phys. Rev. D 69 (2004) 033005, arXiv:hep-ph/0309249;
S. Antusch, S.F. King, Phys. Lett. B 631 (2005) 42, arXiv:hep-ph/0508044;
A. Dighe, S. Goswami, P. Roy, Phys. Rev. D 73 (2006) 071301, arXiv:hep-ph/0602062;
G. Altarelli, F. Feruglio, L. Merlo, JHEP 0905 (2009) 020, arXiv:0903.1940 [hep-ph];
For a review and further references, see H. Minakata, arXiv:hep-ph/0505262.
[7] K.S. Babu, R.N. Mohapatra, Phys. Rev. Lett. 70 (1993) 2845, arXiv:hep-ph/9209215;
C.S. Aulakh, B. Bajc, A. Melfo, G. Senjanovic, F. Vissani, Phys. Lett. B 588 (2004) 196, arXiv:hep-ph/0306242;
H.S. Goh, R.N. Mohapatra, S.P. Ng, Phys. Rev. D 68 (2003) 115008, arXiv:hep-ph/0308197;
B. Bajc, A. Melfo, G. Senjanovic, F. Vissani, Phys. Lett. B 634 (2006) 272, arXiv:hep-ph/0511352;
B. Dutta, Y. Mimura, R.N. Mohapatra, Phys. Rev. D 72 (2005) 075009, arXiv:hep-ph/0507319;
S. Bertolini, M. Frigerio, M. Malinský, Phys. Rev. D 70 (2004) 095002, arXiv:hep-ph/0406117;
S. Bertolini, M. Malinský, Phys. Rev. D 72 (2005) 055021, arXiv:hep-ph/0504241;
S. Bertolini, T. Schwetz, M. Malinsky, Phys. Rev. D 73 (2006) 115012, arXiv:hep-ph/0605006;
B. Bajc, I. Dorsner, M. Nemevsek, JHEP 0811 (2008) 007, arXiv:0809.1069 [hep-ph].
[8] B. Bajc, G. Senjanovic, F. Vissani, Phys. Rev. Lett. 90 (2003) 051802, arXiv:hep-ph/0210207;
H.S. Goh, R.N. Mohapatra, S.P. Ng, Phys. Lett. B 570 (2003) 215, arXiv:hep-ph/0303055.
[9] H.S. Goh, R.N. Mohapatra, S. Nasri, Phys. Rev. D 70 (2004) 075022, arXiv:hep-ph/0408139;
T. Fukuyama, A. Ilakovac, T. Kikuchi, S. Meljanac, N. Okada, Eur. Phys. J. C 42 (2005) 191, arXiv:hep-ph/0401213;
T. Fukuyama, A. Ilakovac, T. Kikuchi, S. Meljanac, N. Okada, J. Math. Phys. 46 (2005) 033505, arXiv:hep-ph/0405300;
B. Bajc, A. Melfo, G. Senjanovic, F. Vissani, Phys. Rev. D 70 (2004) 035007, arXiv:hep-ph/0402122;
C.S. Aulakh, S.K. Garg, Nucl. Phys. B 757 (2006) 47, arXiv:hep-ph/0512224;
C.S. Aulakh, A. Girdhar, Nucl. Phys. B 711 (2005) 275, arXiv:hep-ph/0405074.
[10] A. Melfo, A. Ramirez, G. Senjanovic, arXiv:1005.0834 [hep-ph].
[11] W. Grimus, H. Kuhbock, Phys. Lett. B 643 (2006) 182, arXiv:hep-ph/0607197;
W. Grimus, H. Kuhbock, Eur. Phys. J. C 51 (2007) 721, arXiv:hep-ph/0612132;
A.S. Joshipura, B.P. Kodrani, K.M. Patel, Phys. Rev. D 79 (2009) 115017, arXiv:0903.2161 [hep-ph];
A.S. Joshipura, K.M. Patel, Phys. Rev. D 82 (2010) 031701(R), arXiv:1005.0045 [hep-ph].
[12] F. Bazzocchi, M. Frigerio, S. Morisi, Phys. Rev. D 78 (2008) 116018, arXiv:0809.3573 [hep-ph];
C. Hagedorn, M.A. Schmidt, A.Y. Smirnov, Phys. Rev. D 79 (2009) 036002, arXiv:0811.2955 [hep-ph];
S.F. King, C. Luhn, Nucl. Phys. B 832 (2010) 414, arXiv:0912.1344 [hep-ph].
[13] B. Dutta, Y. Mimura, R.N. Mohapatra, Phys. Rev. D 80 (2009) 095021, arXiv:0910.1043 [hep-ph].
[14] B. Dutta, Y. Mimura, R.N. Mohapatra, JHEP 1005 (2010) 034, arXiv:0911.2242 [hep-ph].
[15] C. Hagedorn, M. Lindner, R.N. Mohapatra, JHEP 0606 (2006) 042, arXiv:hep-ph/0602244;
P.O. Ludl, arXiv:0907.5587 [hep-ph].
[16] C.R. Das, M.K. Parida, Eur. Phys. J. C 20 (2001) 121, arXiv:hep-ph/0010004.